OBLIGATE INTRACELLULAR BACTERIA: EVASION AND ADAPTATIVE TACTICS SHAPING THE HOST-PATHOGEN INTERFACE

EDITED BY: Isaura Simões, Daniel E. Voth and Luís Jaime Mota
PUBLISHED IN: Frontiers in Cellular and Infection Microbiology

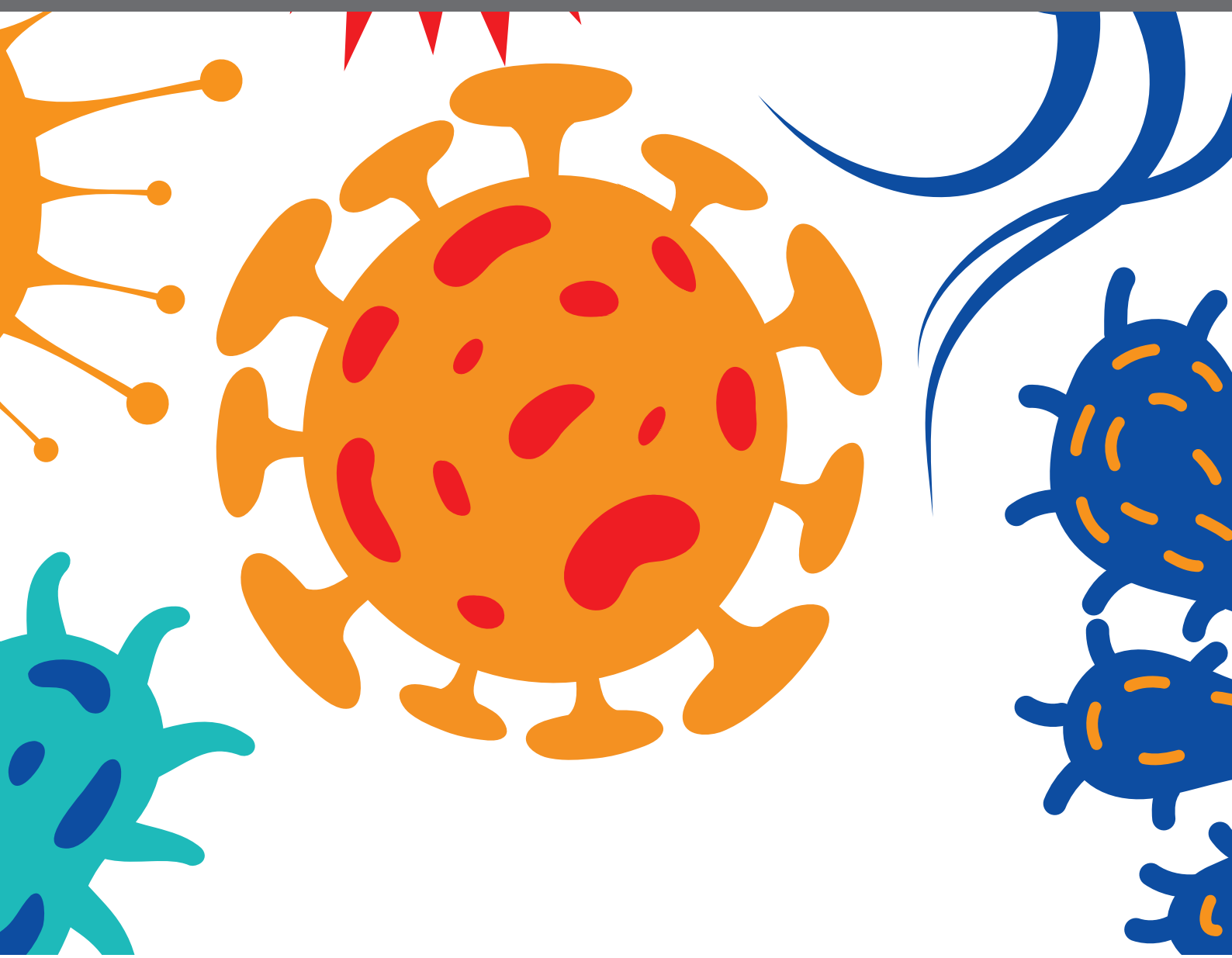

frontiers Research Topics

ISSN 1664-8714
ISBN 978-2-88976-753-3
DOI 10.3389/978-2-88976-753-3

About Frontiers

Frontiers is more than just an open-access publisher of scholarly articles: it is a pioneering approach to the world of academia, radically improving the way scholarly research is managed. The grand vision of Frontiers is a world where all people have an equal opportunity to seek, share and generate knowledge. Frontiers provides immediate and permanent online open access to all its publications, but this alone is not enough to realize our grand goals.

Frontiers Journal Series

The Frontiers Journal Series is a multi-tier and interdisciplinary set of open-access, online journals, promising a paradigm shift from the current review, selection and dissemination processes in academic publishing. All Frontiers journals are driven by researchers for researchers; therefore, they constitute a service to the scholarly community. At the same time, the Frontiers Journal Series operates on a revolutionary invention, the tiered publishing system, initially addressing specific communities of scholars, and gradually climbing up to broader public understanding, thus serving the interests of the lay society, too.

Dedication to Quality

Each Frontiers article is a landmark of the highest quality, thanks to genuinely collaborative interactions between authors and review editors, who include some of the world's best academicians. Research must be certified by peers before entering a stream of knowledge that may eventually reach the public - and shape society; therefore, Frontiers only applies the most rigorous and unbiased reviews.
Frontiers revolutionizes research publishing by freely delivering the most outstanding research, evaluated with no bias from both the academic and social point of view. By applying the most advanced information technologies, Frontiers is catapulting scholarly publishing into a new generation.

What are Frontiers Research Topics?

Frontiers Research Topics are very popular trademarks of the Frontiers Journals Series: they are collections of at least ten articles, all centered on a particular subject. With their unique mix of varied contributions from Original Research to Review Articles, Frontiers Research Topics unify the most influential researchers, the latest key findings and historical advances in a hot research area! Find out more on how to host your own Frontiers Research Topic or contribute to one as an author by contacting the Frontiers Editorial Office: frontiersin.org/about/contact

OBLIGATE INTRACELLULAR BACTERIA: EVASION AND ADAPTATIVE TACTICS SHAPING THE HOST-PATHOGEN INTERFACE

Topic Editors:
Isaura Simões, University of Coimbra, Portugal
Daniel E. Voth, University of Arkansas for Medical Sciences, United States
Luís Jaime Mota, UCIBIO, NOVA School of Science and Technology, Portugal

Citation: Simões, I., Voth, D. E., Mota, L. J., eds. (2022). Obligate Intracellular Bacteria: Evasion and Adaptative Tactics Shaping the Host-Pathogen Interface. Lausanne: Frontiers Media SA. doi: 10.3389/978-2-88976-753-3

Table of Contents

04 ***Editorial: Obligate intracellular bacteria: Evasion and adaptative tactics shaping the host-pathogen interface***
Isaura Simões, Daniel E. Voth and Luís Jaime Mota

07 ***The "Biological Weapons" of* Ehrlichia chaffeensis*: Novel Molecules and Mechanisms to Subjugate Host Cells***
Yasuko Rikihisa

18 ***Apoptosis and Autophagy: Current Understanding in Tick–Pathogen Interactions***
Xin-Ru Wang and Benjamin Cull

27 **In Vitro *Modelling of* Chlamydia trachomatis *Infection in the Etiopathogenesis of Male Infertility and Reactive Arthritis***
Simone Filardo, Marisa Di Pietro, Fabiana Diaco and Rosa Sessa

33 ***Preclinical Animal Models for Q Fever Vaccine Development***
Mahelat Tesfamariam, Picabo Binette and Carrie Mae Long

40 ***The* Chlamydia trachomatis *Early Effector Tarp Outcompetes Fascin in Forming F-Actin Bundles* In Vivo**
George F. Aranjuez, Jongeon Kim and Travis J. Jewett

52 ***The Impact of Lateral Gene Transfer in* Chlamydia**
Hanna Marti, Robert J. Suchland and Daniel D. Rockey

60 ***Cryptic Genes for Interbacterial Antagonism Distinguish* Rickettsia *Species Infecting Blacklegged Ticks From Other* Rickettsia *Pathogens***
Victoria I. Verhoeve, Tyesha D. Fauntleroy, Riley G. Risteen, Timothy P. Driscoll and Joseph J. Gillespie

76 **Chlamydia trachomatis *Requires Functional Host-Cell Mitochondria and NADPH Oxidase 4/p38MAPK Signaling for Growth in Normoxia***
Jeewan Thapa, Gen Yoshiiri, Koki Ito, Torahiko Okubo, Shinji Nakamura, Yoshikazu Furuta, Hideaki Higashi and Hiroyuki Yamaguchi

86 **Anaplasma phagocytophilum *Ankyrin A Protein (AnkA) Enters the Nucleus Using an Importin-β-, RanGTP-Dependent Mechanism***
Yuri Kim, Jianyang Wang, Emily G. Clemens, Dennis J. Grab and J. Stephen Dumler

97 **Coxiella burnetii *Affects HIF1α Accumulation and HIF1α Target Gene Expression***
Inaya Hayek, Manuela Szperlinski and Anja Lührmann

frontiers | Frontiers in Cellular and Infection Microbiology

TYPE Editorial
PUBLISHED 14 July 2022
DOI 10.3389/fcimb.2022.965554

OPEN ACCESS

EDITED AND REVIEWED BY
Joseph James Gillespie,
University of Maryland, Baltimore,
United States

*CORRESPONDENCE
Isaura Simões
isimoes@biocant.pt
Daniel E. Voth
DVoth@uams.edu
Luís Jaime Mota
ljmota@fct.unl.pt

SPECIALTY SECTION
This article was submitted to Bacteria and Host, a section of the journal Frontiers in Cellular and Infection Microbiology

RECEIVED 09 June 2022
ACCEPTED 29 June 2022
PUBLISHED 14 July 2022

CITATION
Simões I, Voth DE and Mota LJ (2022) Editorial: Obligate intracellular bacteria: Evasion and adaptative tactics shaping the host-pathogen interface.
Front. Cell. Infect. Microbiol. 12:965554.
doi: 10.3389/fcimb.2022.965554

Editorial: Obligate intracellular bacteria: Evasion and adaptative tactics shaping the host-pathogen interface

Isaura Simões[1,2]*, Daniel E. Voth[3]* and Luís Jaime Mota[4,5]*

[1]CNC - Center for Neuroscience and Cell Biology, University of Coimbra, Coimbra, Portugal, [2]III - Institute of Interdisciplinary Research, University of Coimbra, Coimbra, Portugal, [3]Department of Microbiology and Immunology, University of Arkansas for Medical Sciences, Little Rock, AR, United States, [4]Associate Laboratory i4HB - Institute for Health and Bioeconomy, NOVA School of Science and Technology, NOVA University Lisbon, Caparica, Portugal, [5]UCIBIO – Applied Molecular Biosciences Unit, Department of Life Sciences, NOVA School of Science and Technology, NOVA University Lisbon, Caparica, Portugal

KEYWORDS

obligate intracellular bacteria, host-pathogen interaction, evasion and control strategies, bacterial effector function, virulence mechanisms

Editorial on the Research Topic

Obligate Intracellular Bacteria: Evasion and Adaptative Tactics Shaping the Host-Pathogen Interface

Obligate intracellular bacteria are an important and fascinating group of microorganisms, as they are often pathogenic to humans and cause a significant clinical and public health burden worldwide. Adaptation to the obligate intracellular lifestyle implies an intimate and complex co-evolution with eukaryotic hosts over hundreds of millions of years. During this adaptation, these pathogens evolved sophisticated virulence mechanisms enabling them to grow intracellularly and resist host defences while minimizing damage to their hosts. This obligate intracellular nature is also a major research challenge, as these bacteria are typically not easy to handle and manipulate in the laboratory. However, over the last 15 years, several developments have significantly advanced understanding of the biology and virulence mechanisms of obligate intracellular bacterial pathogens. Some of these advances are covered in this Frontiers Research Topic.

Two reviews cover experimental models used to study *Chlamydia trachomatis* pathogenesis and evaluation of vaccines against Q fever (caused by *Coxiella burnetii*). Filardo et al. review the current knowledge on how *C. trachomatis* interacts with human prostate epithelial, Sertoli, and synovial cells and how studying *Chlamydia* survival and inflammatory host cell responses to infection in these cells aids elucidation of etiopathogenesis of *Chlamydia*-mediated male infertility, prostatitis, and reactive arthritis. On the importance of animal models as invaluable tools in preclinical evaluation of Q fever vaccine candidates and post-vaccination

hypersensitivity modeling, Tesfamariam et al. thoroughly review available species and their unique advantages and limitations. Consideration of non-mammalian models in vaccine development efforts are also addressed, including the need to include gender and age as important factors when choosing a model to study disease pathogenesis and vaccine efficacy.

Many important insights can be obtained from the genomic analysis of obligate intracellular bacterial pathogens. Marti et al. review the knowledge on lateral gene transfer in the *Chlamydiaceae* and how intraspecies DNA exchange occurs more frequently than previously anticipated, even crossing species. This review also highlights the impact of homologous recombination on the chlamydial genome and current knowledge of chlamydial recombination machinery, while asking open questions about the function of recombinant-associated proteins. Moreover, the authors explore homologous recombination as a potential genetic tool in *Chlamydia*.

In another example, Verhoeve et al., use bioinformatics and phylogenomics analysis to identify and characterize a novel toxin-antidote module, composed of *REIS_1424* and *REIS_1423* genes that are uniquely expressed in *Rickettsia buchneri*. This novel rCRCT/CRCA module adds to a short list of factors that might explain the mutualism between *R. buchneri* and *Ixodes scapularis* and contribute to blocking superinfection of the blacklegged tick by other *Rickettsia*. This work opens exciting avenues of research on interbacterial warfare and the role of this endosymbiont in the biology of *Ixodes scapularis*, an important vector for several infectious disease agents.

Many bacterial pathogens use specialized secretion systems to deliver effector proteins into their host cells (Galán and Waksman, 2018). Three research articles highlight advances in the understanding of effectors' functions.

Anaplasma phagocytophilum Ankyrin A (AnkA) is an important effector targeting the host cell nucleus that modifies the epigenome to promote bacterial fitness and propagation. Kim et al. investigate the AnkA nuclear import mechanism by generating mutations in N-terminal Ankyrin Repeats (ARs) to address the role of the RaDAR pathway combined with specific inhibition of the classical importin α/β pathway. Their results point toward the primacy of the importin-α/β system in AnkA nuclear localization, suggesting a supplemental or minor role for the RaDAR mechanism.

Aranjuez et al. utilize *Drosophila melanogaster* as a platform to study the impact of a *C. trachomatis* effector (Tarp) that has been associated with actin polymerization during chlamydial invasion. Here, the authors provide *in vivo* evidence that Tarp displays F-actin bundling activity and outcompetes the endogenous host bundler Fascin. This raises exciting hypotheses regarding multiple potential functions of Tarp in promoting *Chlamydia* invasion.

Ehrlichia chaffeensis is the causative agent of human monocytic ehrlichiosis, an emerging tick-borne infectious disease. *E. chaffeensis* replication within monocytes and macrophages relies on multiple proteins. Rikihisa focuses on recent findings related to the role of EtpE-C on invasion, functions of *E. chaffeensis* effectors Etf-1, -2, and -3 to facilitate intracellular replication, and *Ehrlichia* hijacking of host membrane lipids.

Another key aspect of the virulence of obligate intracellular bacteria is their ability to control host cell death. Wang and Cull highlight the current knowledge, challenges, and future perspectives regarding involvement of tick programmed cell death machinery (apoptosis and autophagy pathways) in tick-pathogen interactions. A deeper understanding of how these mechanisms and their interplay impact pathogen acquisition, replication, and transmission will ultimately identify novel approaches to controlling tick-borne diseases.

Finally, two research papers explore the importance of cellular O_2 levels and how this is perceived and explored by pathogens. To dissect the impact of O_2 concentration on growth of *Chlamydia*, Thapa et al. investigate the role of host NADPH oxidases and functional mitochondria in chlamydial growth under normoxia and hypoxia. Interestingly, their data show that *C. trachomatis* require functional mitochondria and NADPH oxidase 4/p38 MAPK signaling for growth under normoxia, opening interesting hypotheses about how *Chlamydia* might switch their energy source depending on cellular O_2 concentration.

HIF1α is an important regulator of cellular responses to hypoxia and regulates transcription of genes involved in immune responses, metabolic reprogramming, and anti-infective responses. Hayek et al., provide evidence that *C. burnetii* infection destabilizes HIF1α and alters expression of multiple HIF1α target genes. The *C. burnetti* effector(s) responsible for this destabilization and mechanistic consequences for disease outcome remain interesting open questions.

In conclusion, this Research Topic provides a diverse range of topics on host-pathogen interactions, ranging from experimental models, genomics and evolution, protein effectors and their functions, control of host programmed cell death, and the impact of O_2 concentration on infection. We thank all authors who contributed their work and all reviewers for their time and insightful comments that led to this exciting collection of articles.

Author contributions

All authors listed have made a substantial, direct, and intellectual contribution to the work and approved it for publication.

Funding

Work in IS laboratory was funded by the European Regional Development Fund (ERDF), through the COMPETE 2020 - Operational Programme for Competitiveness and Internationalisation and Portuguese national funds via FCT – Fundação para a Ciência e a Tecnologia, under project[s] POCI-01-0145-FEDER-029592 (PTDC/SAU-INF/29592/2017) (UNDOHIJACK), UIDB/04539/2020, and UIDP/04539/2020 (CIBB). Work in LJM laboratory has been supported by FCT through grants PTDC/BIA-MIC/28503/2017 (to LJM), UIDP/04378/2020 and UIDB/04378/2020 (UCIBIO), and LA/P/0140/2020 (i4HB).

Reference

Galán, J. E., and Waksman, G. (2018). Protein-injection machines in bacteria. *Cell* 172 (6), 1306–1318. doi: 10.1016/j.cell.2018.01.034

Conflict of interest

The authors declare that the research was conducted in the absence of any commercial or financial relationships that could be construed as a potential conflict of interest.

Publisher's note

frontiers in Cellular and Infection Microbiology

REVIEW
published: 14 January 2022
doi: 10.3389/fcimb.2021.830180

The "Biological Weapons" of *Ehrlichia chaffeensis*: Novel Molecules and Mechanisms to Subjugate Host Cells

Yasuko Rikihisa *

Laboratory of Molecular, Cellular, and Environmental Rickettsiology, Department of Veterinary Biosciences, College of Veterinary Medicine, Infectious Diseases Institute, The Ohio State University, Columbus, OH, United States

OPEN ACCESS

Edited by:
Daniel E. Voth, University of Arkansas for Medical Sciences, United States

Reviewed by:
Damien F. Meyer, CIRAD, UMR ASTRE CIRAD/INRAe, France
Jere W. McBride, University of Texas Medical Branch at Galveston, United States

***Correspondence:**
Yasuko Rikihisa
rikihisa.1@osu.edu

Specialty section:
This article was submitted to Bacteria and Host, a section of the journal Frontiers in Cellular and Infection Microbiology

Received: *06 December 2021*
Accepted: *20 December 2021*
Published: *14 January 2022*

Citation:
Rikihisa Y (2022) The "Biological Weapons" of Ehrlichia chaffeensis: Novel Molecules and Mechanisms to Subjugate Host Cells. Front. Cell. Infect. Microbiol. 11:830180. doi: 10.3389/fcimb.2021.830180

Ehrlichia chaffeensis is an obligatory intracellular bacterium that causes human monocytic ehrlichiosis, an emerging, potentially fatal tick-borne infectious disease. The bacterium enters human cells *via* the binding of its unique outer-membrane invasin EtpE to the cognate receptor DNase X on the host-cell plasma membrane; this triggers actin polymerization and filopodia formation at the site of *E. chaffeensis* binding, and blocks activation of phagocyte NADPH oxidase that catalyzes the generation of microbicidal reactive oxygen species. Subsequently, the bacterium replicates by hijacking/dysregulating host-cell functions using Type IV secretion effectors. For example, the *Ehrlichia* translocated factor (Etf)-1 enters mitochondria and inhibits mitochondria-mediated apoptosis of host cells. Etf-1 also induces autophagy mediated by the small GTPase RAB5, the result being the liberation of catabolites for proliferation inside host cells. Moreover, Etf-2 competes with the RAB5 GTPase-activating protein, for binding to RAB5-GTP on the surface of *E. chaffeensis* inclusions, which blocks GTP hydrolysis and consequently prevents the fusion of inclusions with host-cell lysosomes. Etf-3 binds ferritin light chain to induce ferritinophagy to obtain intracellular iron. To enable *E. chaffeensis* to rapidly adapt to the host environment and proliferate, the bacterium must acquire host membrane cholesterol and glycerophospholipids for the purpose of producing large amounts of its own membrane. Future studies on the arsenal of unique *Ehrlichia* molecules and their interplay with host-cell components will undoubtedly advance our understanding of the molecular mechanisms of obligatory intracellular infection and may identify hitherto unrecognized signaling pathways of human hosts. Such data could be exploited for development of treatment and control measures for ehrlichiosis as well as other ailments that potentially could involve the same host-cell signaling pathways that are appropriated by *E. chaffeensis*.

Keywords: *Ehrlichia chaffeensis*, invasin, ROS, type IV secretion effector, RAB5, autophagy, ferritinophagy, membrane cholesterol

1 INTRODUCTION

Ehrlichia chaffeensis is a tick-borne Gram-negative obligatory intracellular bacterium of the family *Anaplasmataceae* in the order Rickettsiales. Infection causes severe flu-like febrile disease called human monocytic ehrlichiosis (HME), which is often accompanied by hematologic abnormalities and signs similar to those of hepatitis (Dawson et al., 1991; Paddock and Childs, 2003). Tick-borne diseases are on the rise (Biggs et al., 2016; Madison-Antenucci et al., 2020; Alkishe et al., 2021). Discovered in 1986 (Maeda et al., 1987), HME is currently among the most prevalent life-threatening tick-borne zoonoses (Adams et al., 2017). HME diagnosis is challenging, as early signs and symptoms are indistinct or mimic other illnesses. No HME vaccine exists, and the only effective therapy is the broad-spectrum antibiotic doxycycline. However, treatment is often delayed (or even not initiated) owing to misdiagnosis or comorbidity with an unrelated underlying illness or injury, stress, immunosuppression, and/or co-infection with other tick-borne pathogens, which collectively can lead to severe complications or death, with a mortality rate of 1–5% among different populations (Paddock and Childs, 2003). *Ehrlichia* spp. also can negatively impact livestock agroeconomics and working and companion animals, as the various species and strains of *Ehrlichia* can cause severe and potentially fatal diseases in animals (Rikihisa, 1991).

Ehrlichia chaffeensis replicates within monocytes and macrophages, which are primary immune cells that recognize pathogen-associated molecular patterns (PAMPs) to unleash potent innate antimicrobial defenses. As a survival strategy, *E. chaffeensis* has lost genes encoding major PAMPs such as lipopolysaccharide, peptidoglycan, flagella, and common pili (Lin and Rikihisa, 2003). It has a single small (1.18 Mbp) circular genome that lacks most genes for amino-acid biosynthesis and intermediary metabolism (Dunning Hotopp et al., 2006); consequently, the bacterium depends on host cells for these molecules. Molecular and cellular research on *E. chaffeensis* has revealed unique mechanisms that mediate its parasitism. Foremost is the *E. chaffeensis* invasin EtpE (entry-triggering protein of *Ehrlichia*), which binds its cognate host-cell surface receptor DNase X, thereby inducing its internalization. This occurs without eliciting host-derived signals that normally would activate the phagocyte NADPH oxidase 2 (NOX2) complex, that catalyzes the production of microbicidal reactive oxygen species (ROS) from molecular oxygen (Mohan Kumar et al., 2013; Teymournejad et al., 2017). Once internalized, the bacterium replicates within a membrane-bound compartment (inclusion); this is also secluded from components of the NOX2 complex (Lin and Rikihisa, 2007).

Ehrlichia chaffeensis inclusions rapidly fuse with host-cell early endosomes, thereby acquiring early-endosome markers including the small GTPase RAB5 and its effectors such as early endosome antigen 1, VPS34, and Rabankyrin-5. This facilitates subsequent fusion with other early endosomes that contain transferrin receptor (TfR). Exogenous iron-loaded transferrin (Tf) enters into inclusions through the TfR-Tf endosome recycling pathway (Barnewall et al., 1997). Recent studies revealed that the inclusions have features of the early amphisome, which is the vesicular compartment formed by fusion of early endosomes with early autophagosomes, as ATG5, but not LC3 or ATG14L, was also found in inclusions (Lin et al., 2016). This review primarily focuses on recent findings pertaining to invasin, Type IV secretion system (T4SS) effectors, and host-cell membrane lipids that are acquired by *E. chaffeensis*. Readers are referred to several informative reviews for discussion of other aspects of *E. chaffeensis* (Paddock and Childs, 2003; Rikihisa, 2010; McBride and Walker, 2011; Rikihisa, 2011; Rikihisa, 2015; McClure et al., 2017; Byerly et al., 2021).

2 MOLECULES UNIQUE TO *E. CHAFFEENSIS* THAT FACILITATE ENTRY INTO HOST CELLS AND SUBSEQUENT INTRACELLULAR REPLICATION

2.1 *Ehrlichia* Entry Is Coupled With Blockade of the Activation of the NOX2 Complex

As an obligatory intracellular bacterium, *E. chaffeensis* cannot survive without entry into permissive host cells. To enter host monocytes and macrophages, *E. chaffeensis* uses the C-terminus of its unique outer-membrane protein, EtpE-C, to directly bind the host-cell DNase X (DNASE1like1), a cell-surface glycosylphosphatidylinositol-anchored receptor that senses extracellular DNA (Mohan Kumar et al., 2013) (**Figure 1**). Actin polymerization is not required for *E. chaffeensis* binding to host cells but is necessary for entry, and thus entry can be inhibited by cytochalasin D (Mohan Kumar et al., 2015).

EtpE-C-induced actin polymerization is dependent on DNase X as well as activation of the actin nucleation–promoting factor neuronal Wiskott–Aldrich Syndrome protein(N-WASP) (Mohan Kumar et al., 2015). The N-WASP inhibitor wiskostatin or overexpression of the WA domain of N-WASP, which exerts a dominant-negative effect on N-WASP, inhibits actin polymerization and *E. chaffeensis* entry (Mohan Kumar et al., 2015). How does EtpE-C binding to DNase X on the macrophage surface activate cytoplasmic signaling? EtpE-C binding to DNase X on the macrophage surface recruits three factors, namely the type I transmembrane glycoprotein CD147 (basigin/extracellular matrix metalloproteinase inducer), cytoplasmic heterogeneous nuclear ribonucleoprotein K (hnRNP-K), and N-WASP, to facilitate actin polymerization at the site of *E. chaffeensis* binding (Mohan Kumar et al., 2015) (**Figure 1**). CD147 is the key molecule to relay signals started with DNase X membrane receptor to the inside of the cell. Thus, the extracellular bone marrow–derived macrophages from *CD147$^{flox/flox}$-Lyz2-Cre* mice, in which *Cre* expression (driven by the *Lyz2* promoter) is used for myeloid cell–specific *CD147* knockout, are significantly less susceptible to *E. chaffeensis* infection (Teymournejad and Rikihisa, 2020). hnRNP-K binds N-WASP and activates the Arp2/3 complex to nucleate actin

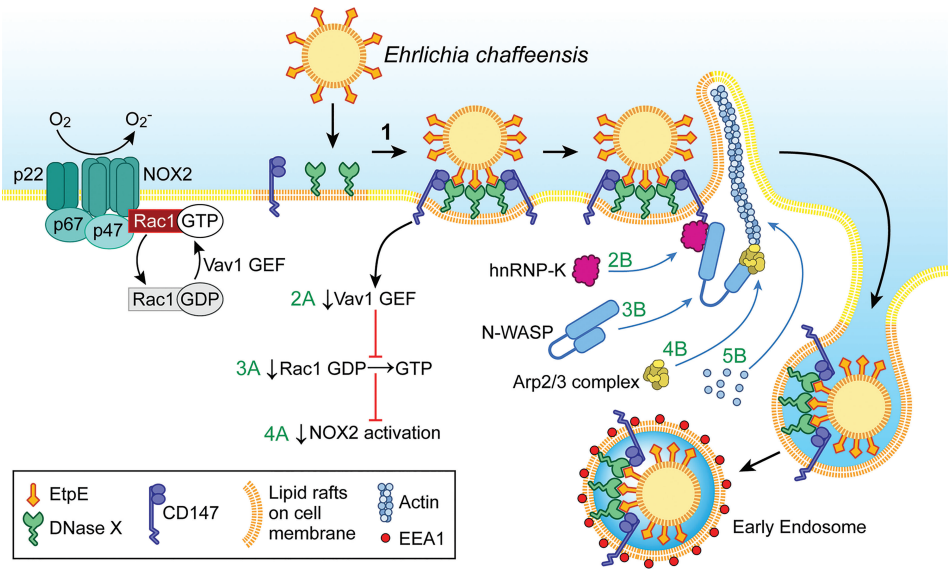

FIGURE 1 | *Ehrlichia* entry is coupled with blockade of the activation of the phagocyte NADPH oxidase (NOX2) complex. Extracellular *E. chaffeensis* uses the C-terminal region of its surface protein EtpE to bind DNase X on the host-cell surface. The consequent lateral redistribution of DNase X within dynamic lipid rafts brings CD147 into association with the EtpE–DNase X complex (1). CD147 relays the signal to downregulate Vav1 GEF (guanine-nucleotide exchange factor; 2A) that prevents Rac1 activation (3A) and consequently prevents activation of the NOX2 complex (4A). CD147 also recruits hnRNP-K to bind N-WASP, leading to activation of N-WASP (conformational change) (2B and 3B). Activated N-WASP binds the Arp2/3 actin-nucleation complex (4B), leading to spatiotemporal actin polymerization and filopodia formation to internalize *E. chaffeensis* into endosomes (5B). The drawing was modified from (Mohan Kumar et al., 2015), copyright 2015 ASM.

polymerization *in vitro* (Yoo et al., 2006), and the intracellular nanoantibody clone #47 (iAB-47), which binds and confines hnRNP-K to the nucleus (Inoue et al., 2007), potently blocks *E. chaffeensis* entry (Mohan Kumar et al., 2015). Entry requires host-cell energy but not *Ehrlichia* energy, as demonstrated by the fact that latex beads coated with recombinant EtpE-C could bind DNase X and enter phagocytes as well as non-phagocytic cells that are permissive to *E. chaffeensis* infection (Mohan Kumar et al., 2013).

Phagocytes, such as monocytes and neutrophils, produce powerful NADPH oxidase (NOX2 complex), a multicomponent enzyme composed of a membrane-bound heterodimeric cytochrome b558 component (gp91^{phox} [NOX2] and p22^{phox}), three cytoplasmic subunits (p67^{phox}, p47^{phox}, and p40^{phox}), and the small GTPase Rac1 or Rac2 (Panday et al., 2015). In resting phagocytes, these NOX2 components are dissociated and hence the enzyme is inactive. Phagocyte-activating agents such as phorbol myristate acetate (PMA), invading pathogens, or an *N*-formyl peptide can induce rapid assembly of all NOX2 components into a holoenzyme that catalyzes the production of superoxide anion (O_2^-) from molecular oxygen (Debeurme et al., 2010). O_2^- is secreted extracellularly and into the lumen of phagosomes and serves as starting material for the production of microbicidal reactive oxygen species (ROS), including hydrogen peroxide (H_2O_2), oxidized halogens, hydroxyl radicals, and singlet oxygen (Gabig and Babior, 1981). Paradoxically, *E. chaffeensis* isolated from host cells is quite sensitive to ROS, and infectivity decreases rapidly when bacteria are exposed to ROS (Lin and Rikihisa, 2007). In fact, the *E. chaffeensis* genome lacks genes encoding enzymes that facilitate ROS detoxification, free-radical scavenging, repair of ROS-induced damage, and the oxidative stress response (Dunning Hotopp et al., 2006; Lin and Rikihisa, 2007). How, then, does *E. chaffeensis* prevent or the overcome ROS assault by host macrophages? Remarkably, unlike most other bacteria, *E. chaffeensis* does not induce ROS production in human monocytes and rapidly blocks O_2^- generation induced by PMA (Lin and Rikihisa, 2007). This inhibition is specific to monocytes, as *E. chaffeensis* cannot block ROS production by PMA-stimulated neutrophils, and a host cell-surface protein is required (Lin and Rikihisa, 2007). This surface protein was later revealed to be DNase X, as inhibition of NOX2-complex activation could be initiated by the binding of EtpE-C to DNase X (Teymournejad et al., 2017) (**Figure 1**). Thus, DNase X–mediated entry and ROS blockade are coupled to ensure *E. chaffeensis* survival during entry. However, neutrophils do not express DNase X (Teymournejad et al., 2017), which is likely the primary reason why *E. chaffeensis* neither infects neutrophils nor blocks activation of the NOX2 complex. The binding of *E. chaffeensis* or of recombinant EtpE-C–coated beads to DNase X can trigger activation of N-WASP (Mohan Kumar et al., 2015). However, N-WASP activation is not involved in the blockade of ROS production initiated by *E. chaffeensis* or EtpE-C binding to DNase X (Teymournejad et al., 2017). Rac GTPases act as binary switches for the activation of NOX2 (Seifert et al., 1986; Roberts et al., 1999; Zhao et al., 2003; Bokoch and Zhao, 2006). Two Rac isoforms exist, namely Rac1 and Rac2, and Rac2 is the predominant isoform in human neutrophils, whereas Rac1 predominates in monocytes, the latter accounting for 90% of

cellular Rac (Zhao et al., 2003). For Rac activation, GTP-for-GDP exchange is facilitated by a membrane-localized, Rac-specific guanine-nucleotide exchange factor (GEF) (Bokoch et al., 1994), and Rac becomes inactivated upon GTP hydrolysis catalyzed by a GTPase-activating protein specific for Rac (Geiszt et al., 2001). Vav1 is a hemopoiesis-specific Rho/Rac guanine-nucleotide exchange factor that plays a prominent role in adhesion-mediated suppression of ROS generation in phagocytes (Zhao et al., 2003). Engagement of EtpE-C with DNase X triggers CD147-dependent suppression of the PMA-induced activation of Vav1 (Teymournejad and Rikihisa, 2020) (**Figure 1**). Consequently, *E. chaffeensis* and EtpE-C, upon binding DNase X, block Rac1 activation (Teymournejad and Rikihisa, 2020) (**Figure 1**). Actin polymerization led by Rac/wave activation is a well-known mechanism for the entry of several intracellular bacteria including *Listeria*, *Yersinia*, *Salmonella*, and *Chlamydia* into non-phagocytes (Alrutz et al., 2001; Carabeo et al., 2004; Bosse et al., 2007; Humphreys et al., 2013). However, *E. chaffeensis* does not utilize this mode of entry (Mohan Kumar et al., 2015) to colonize phagocytes, as Rac-dependent actin polymerization and entry would activate phagocyte NOX2 as well.

Immunization of mice and dogs with recombinant EtpE-C significantly inhibits *E. chaffeensis* infection *via* intraperitoneal or infected-tick challenge (Mohan Kumar et al., 2013; Budachetri et al., 2020). Thus, EtpE-C could be included in a candidate vaccine to counter tick-transmitted ehrlichiosis.

2.2 Functions of *E. chaffeensis* T4SS Effectors

The T4SS can transfer bacterial proteins or nucleoprotein complexes across the membrane of eukaryotic cells (Alvarez-Martinez and Christie, 2009). The T4SS has several ancestral lineages including the archetype *virB/virD* system of *Agrobacterium tumefaciens* and the *dot/icm* system of *Legionella pneumophila*, sometimes referred to as T4aSS and T4bSS, respectively (Alvarez-Martinez and Christie, 2009). All members of the order Rickettsiales, which includes *E. chaffeensis*, have T4aSS (Gillespie et al., 2010). T4SS functions through its effectors/substrates. To date, three T4SS effectors have been experimentally demonstrated, namely *Ehrlichia* translocated factor (Etf)-1, -2, and -3 (Liu et al., 2012; Lin et al., 2016; Yan et al., 2018; Yan et al., 2021).

Etf-1, -2, and -3 directly bind the *E. chaffeensis* T4SS coupling ATPase VirD4 and are then transferred from the bacterium into the host-cell cytoplasm by crossing three membranes (inner and outer *Ehrlichia* membranes, and inclusion membrane) (Liu et al., 2012; Lin et al., 2016; Yan et al., 2018; Yan et al., 2021). Each Etf is required for *E. chaffeensis* infection, as downregulation of any *Etf* gene by electroporation of *E. chaffeensis* with an individual *Etf*-specific antisense peptide nucleic acid significantly reduces the expression of the corresponding mRNA and hence the bacteria's ability to infect host cells (Sharma et al., 2017; Yan et al., 2018; Yan et al., 2021). This type of inhibition could be trans-complemented by ectopic expression of the corresponding GFP-coupled Etf in host cells, underscoring the critical roles of the three T4SS effectors in *E. chaffeensis* replication (Sharma et al., 2017; Yan et al., 2018; Yan et al., 2021). Characteristics of the three T4SS effectors of *E. chaffeensis* is listed in **Table 1**.

2.2.1 Etf-1 Inhibits Host-Cell Apoptosis

E. chaffeensis inhibits host-cell apoptosis to maximize bacterial proliferation inside host cells (Liu et al., 2011; Liu et al., 2012). Etf-1 is highly upregulated during early exponential growth of *E. chaffeensis* in human monocytes (Liu et al., 2012). In Etf-1–transfected mammalian cells, Etf-1 was found to localize to mitochondria and inhibit apoptosis induced by the treatment with etoposide (Liu et al., 2012) (**Figure 2**). Moreover, in similar experiments with yeast, Etf-1 also localized to mitochondria and inhibited apoptosis induced by heterologous expression of human Bax (Liu et al., 2012). The N-terminal 24 amino-acid residues of Etf-1, especially residue K23, play a critical role in mitochondrial targeting of Etf-1, as deletion mutation of this residue significantly decreased Etf-1 localization to mitochondria (Zhang et al., 2021). The mitochondrial matrix protein manganese superoxide dismutase (MnSOD) maintains a basal level of ROS in cells by scavenging O_2^- and is essential for maintaining aerobic life (Holley et al., 2012). The MnSOD level was found to increase in *E. chaffeensis*–infected cells or Etf-1–transfected cells, and the amount of ROS in infected or Etf-1-transfected cells was significantly lower than that in uninfected or control plasmid–transfected cells (Liu et al., 2012; Yan et al., 2021). These data suggest that, by upregulating mitochondrial MnSOD, Etf-1 serves as an antioxidant to prevent ROS-induced

TABLE 1 | Characteristics of Type IV secretion effectors from *E. chaffeensis*.

Effector	Amino acid residues	C-terminal residues (basic residues underlined)	Protein motifs	Subcellular localization/functions
Etf-1	380	KHFSNPGKVHAR	Near N-terminal mitochondria localization signal	Mitochondria, bacterial inclusions/ Inhibits mitochondria-mediated apoptosis Upregulates MnSOD Binds Beclin 1 and induces autophagy
Etf-2	264	HARQACGRFFRR	An Arg finger and a Gln finger of Tre2-Bub2-Cdc16 domain	Early endosomes and bacterial inclusions/ Binds RAB5-GTP and blocks RABGAP5 engagement with RAB5-GTP
Etf-3	621	RLSEIFSALTRTIAR	*	Ferritinophagolysosomes/ Binds ferritin light chain and induces ferritinophagy

*Research concerning this motif is ongoing.

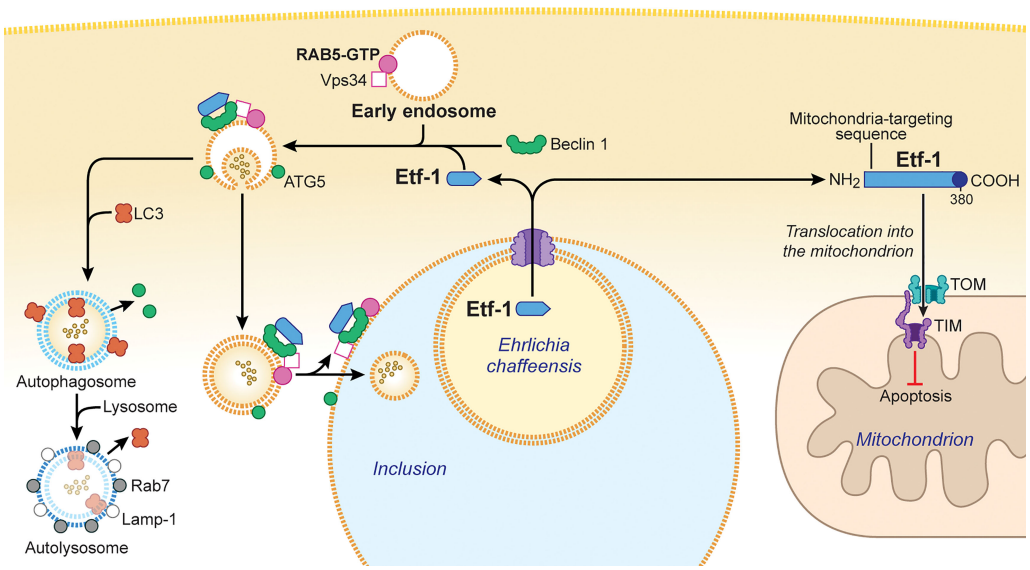

FIGURE 2 | *Ehrlichia chaffeensis* Etf-1 localizes to mitochondria to block apoptosis of host cells. Alternatively, Etf-1 binds to the Belin 1–VPS34–RAB5-GTP complex and induces RAB5-regulated autophagy. (Right) Etf-1 is depicted in blue with the putative T4SS signal depicted in dark blue. Etf-1 has a mitochondria-targeting presequence and localizes to mitochondria. Mitochondria-localized Etf-1 blocks apoptosis of eukaryotic host cells by preventing loss of mitochondrial membrane potential. TOM: transporter outer membrane complex; TIM: transporter inner membrane complex. (Left) Etf-1 binds the Beclin 1–VPS34–RAB5-GTP complex and induces RAB5-regualted autophagy. Etf-1 autophagosomes are recruited to *E. chaffeensis* inclusions and deliver captured host cytoplasmic contents. If not recruited to inclusions, Etf-1 autophagosomes mature to autolysosomes, in which captured substrates are degraded and catabolites are released to the cytoplasmic to promote bacterial proliferation. The drawing was modified from (Rikihisa, 2019), copyright 2017 Taylor & Francis, and from (Rikihisa, 2017), copyright 2017 Springer.

cellular damage and apoptosis to allow intracellular infection (Liu et al., 2012).

To verify the functions of intracellular Etf-1 and investigate the possibility that Etf-1 could be used as a therapeutic target, Etf-1–specific nanobodies were developed by immunizing a llama (Zhang et al., 2021). One particular nanobody could form a stable complex with Etf-1 and thereby block the mitochondrial localization of Etf-1 (Zhang et al., 2021). Intracellular expression of this anti–Etf-1 nanobody inhibited three activities of Etf-1 and *E. chaffeensis*: upregulation of mitochondrial MnSOD, reduction of intracellular ROS, and inhibition of apoptosis (Zhang et al., 2021). Conjugation of this nanobody to cyclized cell-permeable peptide 12 facilitated effective entrance into mammalian cells, where it abrogated the blockade of apoptosis caused by *E. chaffeensis* and inhibited infection by *E. chaffeensis* in cultured cells and in a mouse model of severe combined immunodeficiency (Zhang et al., 2021). Thus, in principle, intracellular nanobodies that interfere with T4SS effector functions could be developed as research tools as well as therapeutic agents.

2.2.2 Etf-1 Induces RAB5-Regulated Autophagy

Autophagy is the process by which eukaryotic cells routinely degrade cellular components to ensure homeostasis and is considered a part of the innate immune response that clears a variety of intracellular pathogens (Levine et al., 2011; Deretic, 2012). However, intracellular replication of *E. chaffeensis* is enhanced by the autophagy inducer rapamycin and inhibited by the autophagy inhibitor 3-methyl adenine (Lin et al., 2016). Use of Spautin-1 (a cell-permeable inhibitor of the autophagy regulator Beclin 1), Beclin 1 small interfering RNA, or mouse bone marrow–derived macrophages from *atg5*$^{flox/flox}$*-Lyz2-Cre* mice (in which *Lyz2* promoter–driven *Cre* expression is used for myeloid cell–specific *Atg5* knockout) demonstrated that autophagy not only enhances ehrlichial infection but also is required for *E. chaffeensis* replication (Lin et al., 2016). In fact, *E. chaffeensis* induces a unique type of cellular autophagy to recycle host-cell catabolites for use during its replication (Lin et al., 2016). *E. chaffeensis*–induced autophagy is independent of the general cellular ubiquitination pathways as well as the canonical autophagy pathway involving MTOR, ULK1, and AMPK (Lin et al., 2016). Etf-1 binds Beclin 1 and VPS34 and activates the class III PtdIns3K (phosphatidylinositol 3-kinase) complex, which is an essential component and master regulator of autophagy initiation (**Figure 2**), but this Etf-1 complex does not recruit the endoplasmic reticulum resident ATG14L, unlike Ats-1 of *Anaplasma phagocytophilum*, that also binds Beclin 1 and VPS34 and induces autophagy (Niu et al., 2010). Rather, the Etf-1-Beclin 1 complex recruits RAB5-GTP (Lin et al., 2016) (**Figure 2**). This type of autophagy is referred to as "RAB5-regulated autophagy" (Ravikumar et al., 2008), as constitutively active RAB5 induces autophagy by binding to the RAB5 effector VPS34, which binds Beclin 1 and hence the class III PtdIns3K

complex. Expansion of a polyglutamine tract within the Huntingtin protein due to the mutation causes its accumulation and aggregation in the cytoplasm, leading to the neurodegenerative genetic disorder Huntington's disease (Raspe et al., 2009). The mutant Huntingtin protein, is poorly degraded in proteasomes but can be degraded *via* RAB5-regulated autophagy (Ravikumar et al., 2008). Etf-1–induced RAB5-regulated autophagy was found to clear an aggregation-prone mutant Huntingtin protein in a class III PtdIns3K–dependent manner (Lin et al., 2016).

During the exponential growth stage of *E. chaffeensis*, the concentrations of free/cytoplasmic L-glutamine and L-glutamate in infected human monocytes increase substantially, making them available for ehrlichial growth (Lin et al., 2016). Indeed, host cell–preincorporated radioactive L-glutamine could be readily taken up by *E. chaffeensis* in an autophagy-dependent manner, and the human cytoplasmic autophagy cargo protein GAPDH could be delivered into *E. chaffeensis* inclusions as well (Lin et al., 2016). In addition to several early-endosome markers, Etf-1 and the early autophagosome marker ATG5 (but not LC3) are present on the membrane of *E. chaffeensis* inclusions (Barnewall et al., 1997; Mott et al., 1999; Lin et al., 2016) (**Figure 2**), and thus the inclusions can be considered as large amphisomes formed by fusion of early endosomes and early autophagosomes. Etf-1–induced autophagy releases host-cell small-molecule catabolites into the host cytoplasm to provide nutrients (e.g., amino acids) to *E. chaffeensis*. Furthermore, Etf-1–induced autophagy creates a host cytoplasmic space for *E. chaffeensis* to grow without lysing host cells.

How are the two competing functions of Etf-1 distributed within *E. chaffeensis*–infected cells? The translocase of the outer membrane of mitochondria (TOM) complex is the main pore for the import of nuclear-encoded proteins into mitochondria, and mitochondrial membrane potential is required for import (Pfanner and Truscott, 2002). The majority of Etf-1 targets mitochondria during the early stage of infection when mitochondrial membrane potential is maximal. As infection progresses, Etf-1 is diverted to autophagosomes as mitochondria begin to lose membrane potential (Wurm et al., 2011). This suggests that host-cell physiologic conditions during infection influence the distribution of Etf-1 between mitochondria and autophagosomes, consequently affecting *E. chaffeensis* growth.

Although Etf-1 interacts with RAB5-GTP *via* Beclin 1 and localizes to *E. chaffeensis* inclusions, inhibition of lysosome fusion with inclusions by keeping RAB5 on inclusions, requires another T4SS effector, Etf-2, because Etf-1-GFP vesicles mature to autolysosomes (Lin et al., 2016).

2.2.3 Etf-2 Prevents Lysosomal Fusion of *E. chaffeensis* Inclusions

Ehrlichia chaffeensis sequesters the regulator of endosomal traffic, RAB5, on its membrane-bound inclusions to avoid being routed to host-cell phagolysosomes (Barnewall et al., 1997; Mott et al., 1999). How is RAB5 sequestered on the ehrlichial inclusion membrane? The answer is *via* its association with Etf-2. Etf-2 directly binds RAB5-GTP on the membrane of early endosomes and of *E. chaffeensis*–containing inclusions (Yan et al., 2018) (**Figure 3**). A yeast two-hybrid assay and a microscale thermophoresis assay revealed that Etf-2 binds tightly to RAB5-GTP but not RAB5-GDP (Yan et al., 2018). This is because Etf-2 contains two conserved motifs of RAB GAP Tre2-Bub2-Cdc16 domain, namely an Arg finger and a Gln finger, although it lacks RAB5-specific GAP activity (Yan et al., 2018). Thus, Etf-2 binding to RAB5-GTP blocks RAB5-GTP engagement with RABGAP5 (**Figure 3**), and consequently RAB5-GTP hydrolysis is delayed on *E. chaffeensis* inclusions (Yan et al., 2018).

2.2.4 Etf-3 Induces Ferritinophagy

Ehrlichia is an obligate aerobe that requires the electron transport chain, thus iron, because its glycolytic pathway is incomplete and it lacks ATP-ADP translocase, unlike *Rickettsia* and *Chlamydia* (Dunning Hotopp et al., 2006). *Ehrlichia chaffeensis* lacks the siderophore biosynthesis pathway and Fe^{3+} uptake regulator (Dunning Hotopp et al., 2006). Instead, *Ehrlichia* acquires iron from the host-cell labile cellular iron pool, and pretreating human monocytes with deferoxamine, a membrane-permeable chelator of this iron pool, blocks *E. chaffeensis* infection (Barnewall and Rikihisa, 1994). *Ehrlichia* enhances host-cell iron uptake *via* upregulating TfR mRNA (Barnewall et al., 1999) and acquires iron from holoTf, as *E. chaffeensis* endosomes intersect with TfR-recycling endosomes and are slightly acidic—enough to release iron from holoTf (Barnewall et al., 1997). In fact, treatment of macrophages with interferon-γ downregulates TfR mRNA and almost completely inhibits *Ehrlichia* infection, and addition of holoTf abrogates this inhibition (Barnewall and Rikihisa, 1994). However, TfR mRNA levels return to basal level after 24 h post-infection, when bacterial exponential growth begins (Barnewall et al., 1999); at that time, treatment with interferon-γ can no longer inhibit infection (Barnewall and Rikihisa, 1994). How, then, does exponentially growing *Ehrlichia* acquire iron from host cells? The answer is Etf-3, which binds directly and tightly to ferritin (the primary eukaryotic cytoplasmic iron storage protein) and thereby induces ferritinophagy, a selective form of autophagy by recruiting NCOA4 (nuclear receptor coactivator 4), a cargo receptor that mediates ferritinophagy, and LC3, an autophagosome biogenesis protein (Yan et al., 2021) (**Figure 4**). Etf-3–induced ferritinophagy causes ferritin degradation and significantly increases the labile cellular iron pool, which can feed *E. chaffeensis* (**Figure 4**). Indeed, an increase in cellular ferritin by adding ferric ammonium citrate to the culture medium, or overexpression of Etf-3 or NCOA4, enhances *E. chaffeensis* proliferation, whereas knockdown of Etf-3 in *Ehrlichia via* transfection with a plasmid encoding an Etf-3 antisense peptide nucleic acid inhibits *Ehrlichia* proliferation (Yan et al., 2021).

Excessive ferritinophagy induces the generation of toxic ROS, which could presumably kill both *Ehrlichia* and host cells. During *Ehrlichia* proliferation, however, there is concomitant upregulation of *Ehrlichia* Fe-superoxide dismutase, the gene that is co-regulated with the *Ehrlichia* T4SS operon, and increase in mitochondrial MnSOD in response to the co-secreted Etf-1 (Yan et al., 2021).

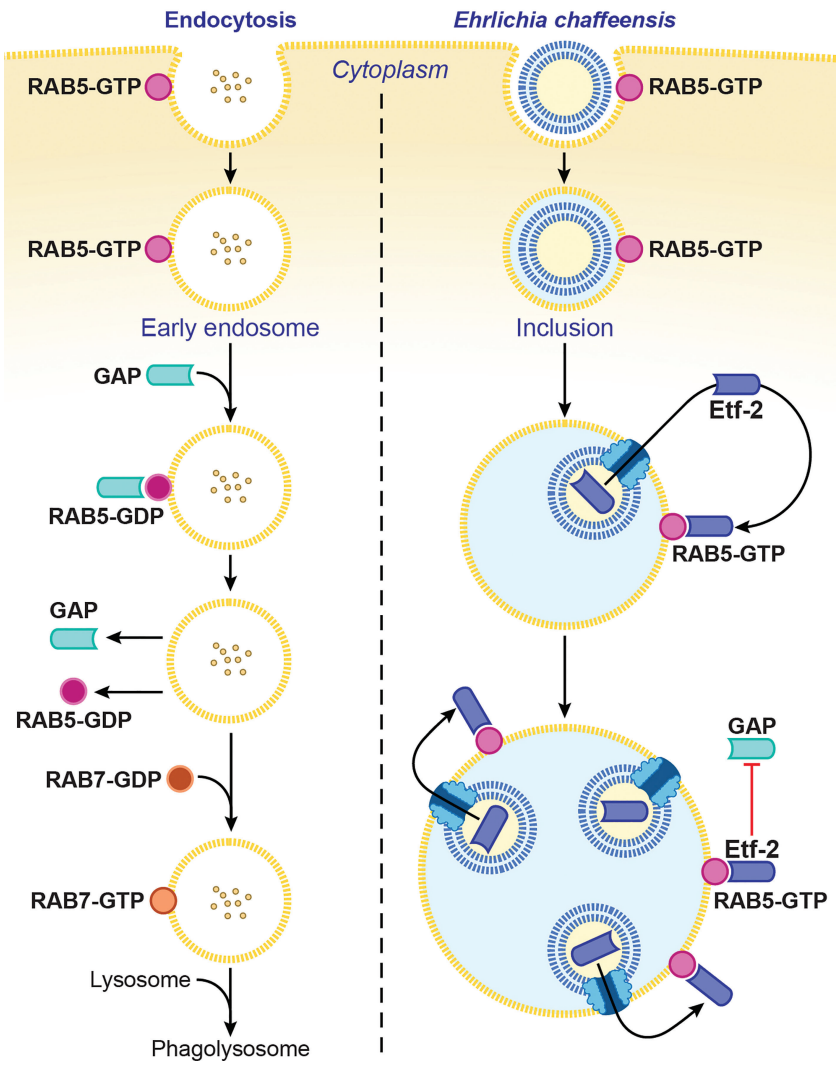

FIGURE 3 | *Ehrlichia chaffeensis* Etf-2 binds RAB5-GTP and blocks RABGAP5 from acting on RAB5. RAB5-GTP hydrolysis by the RAB5-specific GAP is required for endosome maturation and lysosomal fusion (left). Etf-2 is responsible for blocking lysosomal fusion with *E. chaffeensis* inclusions by localizing to *E. chaffeensis* inclusions *via* binding to RAB5-GTP and competitively blocking RABGAP5 from acting on RAB5 on the inclusion surface (right). The drawing is from (Yan et al., 2018), copyright 2018 PNAS.

Consequently, despite enhanced ferritinophagy, cellular ROS levels are reduced in *Ehrlichia*-infected cells compared with uninfected cells (Yan et al., 2021). Thus, *Ehrlichia* robs host-cell iron sequestered in ferritin without killing the host cell.

3 HIJACKING HOST MEMBRANE LIPIDS (CHOLESTEROL AND GLYCEROPHOSPHOLIPID) BY *E. CHAFFEENSIS*

The *E. chaffeensis* cell membrane is cholesterol-rich (Lin and Rikihisa, 2003), but the bacterium cannot synthesize cholesterol and partially lacks genes for glycerophospholipid biosynthesis (Lin et al., 2020). As small Gram-negative bacteria, *Ehrlichia* spp. require abundant membrane lipids for rapid intracellular proliferation. Thus, *E. chaffeensis* must acquire these membrane lipids from host cells. Furthermore, by incorporating eukaryotic lipids such as phosphatidylcholine and cholesterol, *E. chaffeensis* mimics the eukaryotic plasma membrane and, by doing so, adapts to the cellular environment of the host. Indeed, exogenous 7-nitrobenz-2-oxa-1,3-diazol-4-yl (NBD)-phosphatidylcholine, Bodipy-phosphatidylethanolamine, and Bodipy (TopFluor)-cholesterol are rapidly trafficked to ehrlichia inclusions in infected cells (**Figure 5**). DiI (3,3'-dioctadecylindocarbocyanine)-prelabeled host-cell membranes are unidirectionally trafficked to *Ehrlichia* inclusions and the

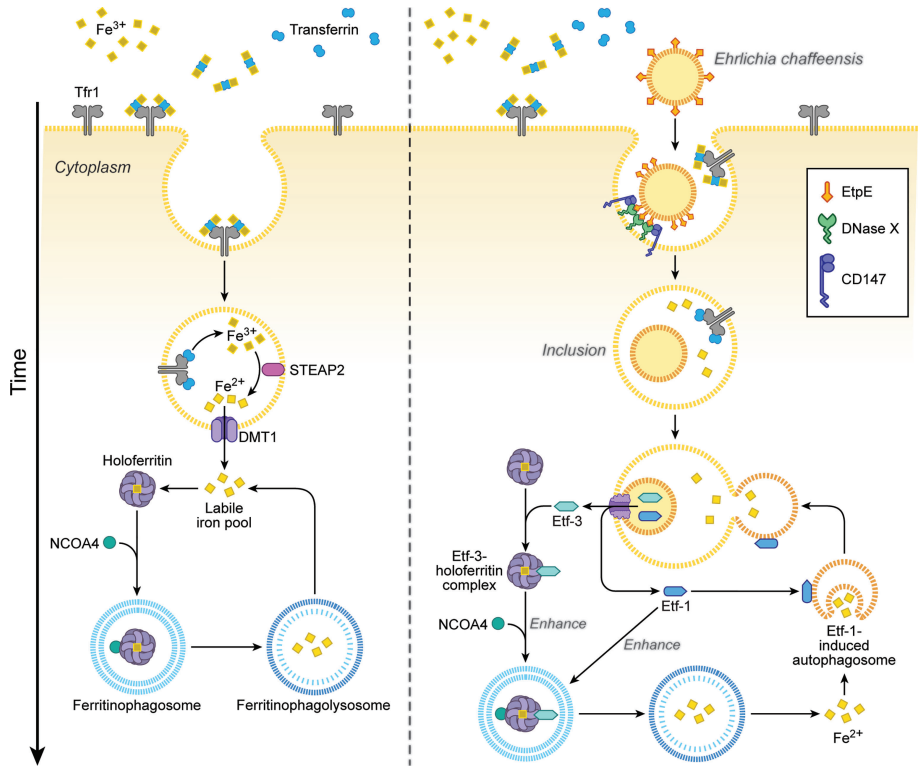

FIGURE 4 | *Ehrlichia chaffeensis* Etf-3 binds ferritin light chain to induce ferritinophagy to increase the labile-iron pool for acquisition of iron by *E. chaffeensis*. Iron homeostasis is tightly regulated in host cells to maintain the labile cellular iron pool (left). Etf-3 directly binds ferritin *via* ferritin light chain and induces ferritinophagy to increase the labile cellular iron pool, thereby providing Fe^{2+} for *E. chaffeensis* proliferation. Etf-1–induced autophagy synergizes with Etf-3 to deliver extra Fe^{2+} to *Ehrlichia* inclusions (right). Tf: transferrin, which binds Fe^{3+} and transports it into cells. TfR: transferrin receptor, which binds and delivers iron-saturated transferrin *via* endocytosis. STEAP2: Six-transmembrane epithelial antigen of prostate-2, a metalloreductase that reduces Fe^{3+} to Fe^{2+}. DMT1: Divalent metal transporter 1 that transports Fe^{2+} from endosomes to the cytoplasm. NCOA4: Nuclear receptor coactivator 4, a cargo receptor that mediates ferritinophagy. The drawing is from (Yan et al., 2021), copyright 2021 PNAS.

bacterial membrane (**Figure 5**), but DiI-prelabeled *Ehrlichia* membranes are not reversibly trafficked to host-cell membranes (Lin et al., 2020). The trafficking of host-cell membranes to *Ehrlichia* inclusions is dependent on both the host endocytic and autophagic pathways as well as bacterial protein synthesis, as the respective inhibitors block the trafficking of DiI-labeled host membranes to *Ehrlichia* as well as infection (Lin et al., 2020). Cryosections of infected cells show numerous membranous vesicles inside *Ehrlichia* inclusions as well as multivesicular bodies docked on the inclusion surface, both of which can be labeled by GFP-tagged 2×FYVE protein that binds to phosphatidylinositol 3-phosphate, a product of PtdIns3K activity (Lin et al., 2020). Focused ion-beam scanning electron microscopy of infected cells has validated the existence of numerous membranous structures inside bacterial inclusions (Lin et al., 2020). These results support the notion that *Ehrlichia* inclusions are amphisomes formed through fusion of early endosomes, multivesicular bodies, and early autophagosomes induced by Etf-1, and they provide the host-cell membrane glycerophospholipids and cholesterol necessary for bacterial proliferation.

4 FUTURE DIRECTIONS

Ehrlichia species propagate *via* perpetual transmission between ticks and mammalian hosts and can proliferate in each of these two distinct environments. Owing to multiple technical limitations, little is known about the bacterial components that enable *Ehrlichia* to thrive throughout this lifecycle. Recently, Himer1 transposon mutagenesis was successfully applied to *E. chaffeensis* as well as other *Ehrlichia* species, and functional knockout mutants have been cloned (Cheng et al., 2013; Bekebrede et al., 2020). Moreover, the application of targeted mutagenesis techniques to *Rickettsia* and *Ehrlichia* species is on the horizon (McClure et al., 2017). Combined with advanced analysis of functional genes in ticks along with molecular and cellular techniques to manipulate ticks, it is expected that *Ehrlichia* Himer1 transposon insertional mutant libraries will facilitate this line of investigation. Further experimental discoveries of bacterial factors and their functions during the natural life cycle of *Ehrlichia*—in which humans are merely accidental hosts—are expected to reveal the remarkable molecular evolution of these

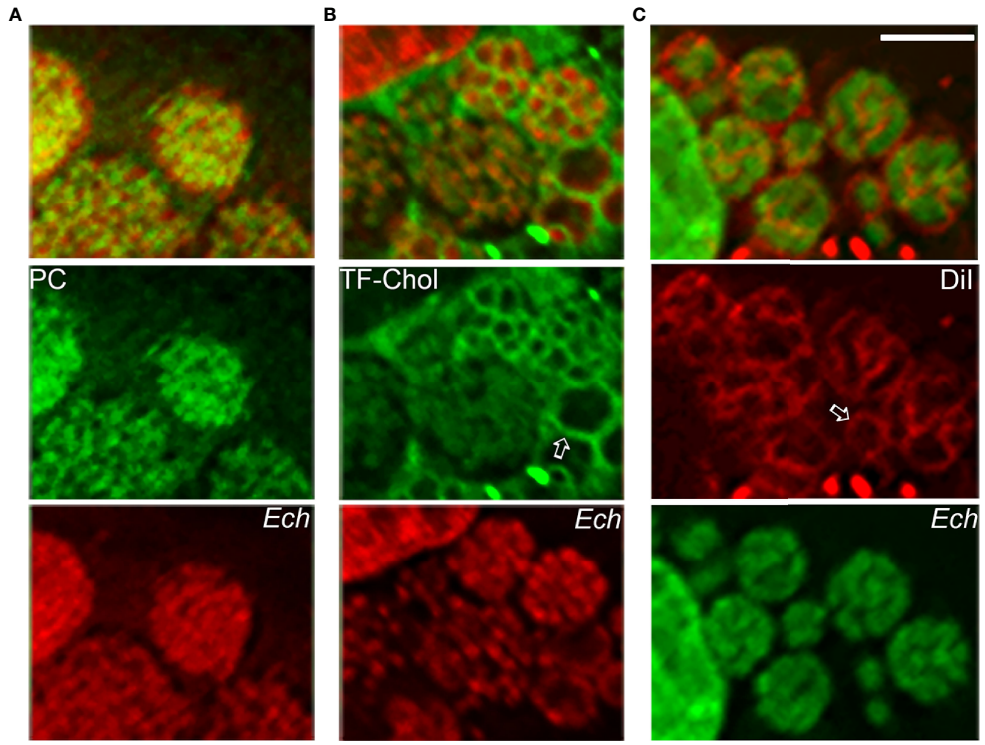

FIGURE 5 | Host-cell membrane lipids (cholesterol and glycerophospholipids) are trafficked to the membrane of *E. chaffeensis* and its inclusions. NBD-phosphatidylcholine **(A)**, TopFluor-cholesterol **(B)**, or DiI **(C)** is added to *E. chaffeensis*–infected RF/6A cells to monitor the intracellular distribution of the fluorescent lipids. DNAs of bacteria and host are stained with Hoechst 33342 (pseudocolored green and red, respectively). Note labeling of densely packed intraluminal *E. chaffeensis* (*Ech*, small cocci stained with Hoechst 33342) with the three fluorescent lipids **(A–C)** and labeling of the bacterial inclusion membrane (open arrows) and intraluminal membranes with TopFluor-cholesterol **(B)** and DiI **(C)**. Bar: 3 μm. The drawing was modified from (Lin et al., 2020), copyright 2020 PNAS.

tick-borne pathogens and inform the development of effective therapeutic strategies and preventative measures for diseases caused by *Ehrlichia* species.

AUTHOR CONTRIBUTIONS

The author confirms being the sole contributor of this review and has approved it for publication.

ACKNOWLEDGMENTS

The author thanks previous and current laboratory members, and T. Vojt for help in preparing the figures. Some of the studies from the author's laboratory reported in this review were supported by grants (R01AI121124, R21AI146736 and R01AI151065) from the National Institutes of Health and CDMRP Award W81XWH-17-1-0519 from the Department of Defense.

REFERENCES

Adams, D. A., Thomas, K. R., Jajosky, R. A., Foster, L., Baroi, G., Sharp, P., et al. (2017). Summary of Notifiable Infectious Diseases and Conditions - United States, 2015. *MMWR Morb Mortal Wkly Rep.* 64, 1–143. doi: 10.15585/mmwr.mm6453a1

Alkishe, A., Raghavan, R. K., and Peterson, A. T. (2021). Likely Geographic Distributional Shifts Among Medically Important Tick Species and Tick-Associated Diseases Under Climate Change in North America: A Review. *Insects* 12, 1–25. doi: 10.3390/insects12030225

Alrutz, M. A., Srivastava, A., Wong, K. W., D'Souza-Schorey, C., Tang, M., Ch'Ng, L. E., et al. (2001). Efficient Uptake of Yersinia Pseudotuberculosis *via* Integrin Receptors Involves a Rac1-Arp 2/3 Pathway That Bypasses N-WASP Function. *Mol. Microbiol.* 42, 689–703. doi: 10.1046/j.1365-2958.2001.02676.x

Alvarez-Martinez, C. E., and Christie, P. J. (2009). Biological Diversity of Prokaryotic Type IV Secretion Systems. *Microbiol. Mol. Biol. Rev.* 73, 775–808. doi: 10.1128/MMBR.00023-09

Barnewall, R. E., Ohashi, N., and Rikihisa, Y. (1999). *Ehrlichia chaffeensis* and *E. sennetsu*, But Not the Human Granulocytic Ehrlichiosis Agent, Colocalize With Transferrin Receptor and Up-Regulate Transferrin Receptor mRNA by Activating Iron-Responsive Protein 1. *Infect. Immun.* 67, 2258–2265. doi: 10.1128/IAI.67.5.2258-2265.1999

Barnewall, R. E., and Rikihisa, Y. (1994). Abrogation of Gamma Interferon-Induced Inhibition of *Ehrlichia Chaffeensis* Infection in Human Monocytes With Iron-Transferrin. *Infect. Immun.* 62, 4804–4810. doi: 10.1128/iai.62.11.4804-4810.1994

Barnewall, R. E., Rikihisa, Y., and Lee, E. H. (1997). *Ehrlichia chaffeensis* Inclusions Are Early Endosomes Which Selectively Accumulate Transferrin Receptor. *Infect. Immun.* 65, 1455–1461. doi: 10.1128/iai.65.4.1455-1461.1997

Bekebrede, H., Lin, M., Teymournejad, O., and Rikihisa, Y. (2020). Discovery of *In Vivo* Virulence Genes of Obligatory Intracellular Bacteria by Random Mutagenesis. *Front. Cell Infect. Microbiol.* 10, 2. doi: 10.3389/fcimb.2020.00002

Biggs, H. M., Behravesh, C. B., Bradley, K. K., Dahlgren, F. S., Drexler, N. A., Dumler, J. S., et al. (2016). Diagnosis and Management of Tickborne Rickettsial Diseases: Rocky Mountain Spotted Fever and Other Spotted Fever Group Rickettsioses, Ehrlichioses, and Anaplasmosis - United States. *MMWR Recomm Rep.* 65, 1–44. doi: 10.15585/mmwr.rr6502a1

Bokoch, G. M., Bohl, B. P., and Chuang, T. H. (1994). Guanine Nucleotide Exchange Regulates Membrane Translocation of Rac/Rho GTP-Binding Proteins. *J. Biol. Chem.* 269, 31674–31679. doi: 10.1016/S0021-9258(18)31748-4

Bokoch, G. M., and Zhao, T. (2006). Regulation of the Phagocyte NADPH Oxidase by Rac GTPase. *Antioxid Redox Signal* 8, 1533–1548. doi: 10.1089/ars.2006.8.1533

Bosse, T., Ehinger, J., Czuchra, A., Benesch, S., Steffen, A., Wu, X., et al. (2007). Cdc42 and Phosphoinositide 3-Kinase Drive Rac-Mediated Actin Polymerization Downstream of C-Met in Distinct and Common Pathways. *Mol. Cell Biol.* 27, 6615–6628. doi: 10.1128/MCB.00367-07

Budachetri, K., Teymournejad, O., Lin, M., Yan, Q., Mestres-Villanueva, M., Brock, G. N., et al. (2020). An Entry-Triggering Protein of Ehrlichia Is a New Vaccine Candidate Against Tick-Borne Human Monocytic Ehrlichiosis. *mBio* 11, 1–13. doi: 10.1128/mBio.00895-20

Byerly, C. D., Patterson, L. L., and McBride, J. W. (2021). Ehrlichia TRP Effectors: Moonlighting, Mimicry and Infection. *Pathog. Dis.* 79, 1–16. doi: 10.1093/femspd/ftab026

Carabeo, R. A., Grieshaber, S. S., Hasenkrug, A., Dooley, C., and Hackstadt, T. (2004). Requirement for the Rac GTPase in Chlamydia Trachomatis Invasion of Non-Phagocytic Cells. *Traffic* 5, 418–425. doi: 10.1111/j.1398-9219.2004.00184.x

Cheng, C., Nair, A. D., Indukuri, V. V., Gong, S., Felsheim, R. F., Jaworski, D., et al. (2013). Targeted and Random Mutagenesis of *Ehrlichia Chaffeensis* for the Identification of Genes Required for *In Vivo* Infection. *PloS Pathog.* 9, e1003171. doi: 10.1371/journal.ppat.1003171

Dawson, J. E., Anderson, B. E., Fishbein, D. B., Sanchez, J. L., Goldsmith, C. S., Wilson, K. H., et al. (1991). Isolation and Characterization of an *Ehrlichia* sp. From a Patient Diagnosed With Human Ehrlichiosis. *J. Clin. Microbiol.* 29, 2741–2745. doi: 10.1128/jcm.29.12.2741-2745.1991

Debeurme, F., Picciocchi, A., Dagher, M. C., Grunwald, D., Beaumel, S., Fieschi, F., et al. (2010). Regulation of NADPH Oxidase Activity in Phagocytes: Relationship Between FAD/NADPH Binding and Oxidase Complex Assembly. *J. Biol. Chem.* 285, 33197–33208. doi: 10.1074/jbc.M110.151555

Deretic, V. (2012). Autophagy: An Emerging Immunological Paradigm. *J. Immunol.* 189, 15–20. doi: 10.4049/jimmunol.1102108

Dunning Hotopp, J. C., Lin, M., Madupu, R., Crabtree, J., Angiuoli, S. V., Eisen, J., et al. (2006). Comparative Genomics of Emerging Human Ehrlichiosis Agents. *PloS Genet.* 2, e21. doi: 10.1371/journal.pgen.0020021

Gabig, T. G., and Babior, B. M. (1981). The Killing of Pathogens by Phagocytes. *Annu. Rev. Med.* 32, 313–326. doi: 10.1146/annurev.me.32.020181.001525

Geiszt, M., Dagher, M. C., Molnar, G., Havasi, A., Faure, J., Paclet, M. H., et al. (2001). Characterization of Membrane-Localized and Cytosolic Rac-GTPase-Activating Proteins in Human Neutrophil Granulocytes: Contribution to the Regulation of NADPH Oxidase. *Biochem. J.* 355, 851–858. doi: 10.1042/bj3550851

Gillespie, J. J., Brayton, K. A., Williams, K. P., Diaz, M. A., Brown, W. C., Azad, A. F., et al. (2010). Phylogenomics Reveals a Diverse Rickettsiales Type IV Secretion System. *Infect. Immun.* 78, 1809–1823. doi: 10.1128/IAI.01384-09

Holley, A. K., Dhar, S. K., Xu, Y., and St Clair, D. K. (2012). Manganese Superoxide Dismutase: Beyond Life and Death. *Amino Acids* 42, 139–158. doi: 10.1007/s00726-010-0600-9

Humphreys, D., Davidson, A. C., Hume, P. J., Makin, L. E., and Koronakis, V. (2013). Arf6 Coordinates Actin Assembly Through the WAVE Complex, a Mechanism Usurped by Salmonella to Invade Host Cells. *Proc. Natl. Acad. Sci. U. S. A.* 110, 16880–16885. doi: 10.1073/pnas.1311680110

Inoue, A., Sawata, S. Y., Taira, K., and Wadhwa, R. (2007). Loss-Of-Function Screening by Randomized Intracellular Antibodies: Identification of hnRNP-K as a Potential Target for Metastasis. *Proc. Natl. Acad. Sci. U. S. A.* 104, 8983–8988. doi: 10.1073/pnas.0607595104

Levine, B., Mizushima, N., and Virgin, H. W. (2011). Autophagy in Immunity and Inflammation. *Nature* 469, 323–335. doi: 10.1038/nature09782

Lin, M., Grandinetti, G., Hartnell, L. M., Bliss, D., Subramaniam, S., and Rikihisa, Y. (2020). Host Membrane Lipids Are Trafficked to Membranes of Intravacuolar Bacterium Ehrlichia Chaffeensis. *Proc. Natl. Acad. Sci. U. S. A.* 117, 8032–8043. doi: 10.1073/pnas.1921619117

Lin, M., Liu, H., Xiong, Q., Niu, H., Cheng, Z., Yamamoto, A., et al. (2016). Ehrlichia Secretes Etf-1 to Induce Autophagy and Capture Nutrients for Its Growth Through RAB5 and Class III Phosphatidylinositol 3-Kinase. *Autophagy* 12, 2145–2166. doi: 10.1080/15548627.2016.1217369

Lin, M., and Rikihisa, Y. (2003). *Ehrlichia chaffeensis* and *Anaplasma phagocytophilum* Lack Genes for Lipid A Biosynthesis and Incorporate Cholesterol for Their Survival. *Infect. Immun.* 71, 5324–5331. doi: 10.1128/IAI.71.9.5324-5331.2003

Lin, M., and Rikihisa, Y. (2007). Degradation of P22phox and Inhibition of Superoxide Generation by *Ehrlichia chaffeensis* in Human Monocytes. *Cell Microbiol.* 9, 861–874. doi: 10.1111/j.1462-5822.2006.00835.x

Liu, H., Bao, W., Lin, M., Niu, H., and Rikihisa, Y. (2012). Ehrlichia Type IV Secretion Effector ECH0825 Is Translocated to Mitochondria and Curbs ROS and Apoptosis by Upregulating Host MnSOD. *Cell Microbiol.* 14, 1037–1050. doi: 10.1111/j.1462-5822.2012.01775.x

Liu, Y., Zhang, Z., Jiang, Y., Zhang, L., Popov, V. L., Zhang, J., et al. (2011). Obligate Intracellular Bacterium *Ehrlichia* Inhibiting Mitochondrial Activity. *Microbes Infect.* 13, 232–238. doi: 10.1016/j.micinf.2010.10.021

Madison-Antenucci, S., Kramer, L. D., Gebhardt, L. L., and Kauffman, E. (2020). Emerging Tick-Borne Diseases. *Clin. Microbiol. Rev.* 33, 1–18. doi: 10.1128/CMR.00083-18

Maeda, K., Markowitz, N., Hawley, R. C., Ristic, M., Cox, D., and McDade, J. E. (1987). Human Infection With *Ehrlichia canis*, A Leukocytic Rickettsia. *N. Engl. J. Med.* 316, 853–856. doi: 10.1056/NEJM198704023161406

McBride, J. W., and Walker, D. H. (2011). Molecular and Cellular Pathobiology of Ehrlichia Infection: Targets for New Therapeutics and Immunomodulation Strategies. *Expert Rev. Mol. Med.* 13, e3. doi: 10.1017/S1462399410001730

McClure, E. E., Chavez, A. S. O., Shaw, D. K., Carlyon, J. A., Ganta, R. R., Noh, S. M., et al. (2017). Engineering of Obligate Intracellular Bacteria: Progress, Challenges and Paradigms. *Nat. Rev. Microbiol.* 15, 544–558. doi: 10.1038/nrmicro.2017.59

Mohan Kumar, D., Lin, M., Xiong, Q., Webber, M. J., Kural, C., and Rikihisa, Y. (2015). EtpE Binding to DNase X Induces Ehrlichial Entry *via* CD147 and hnRNP-K Recruitment, Followed by Mobilization of N-WASP and Actin. *MBio* 6, 1–15. doi: 10.1128/mBio.01541-15

Mohan Kumar, D., Yamaguchi, M., Miura, K., Lin, M., Los, M., Coy, J. F., et al. (2013). *Ehrlichia chaffeensis* Uses Its Surface Protein EtpE to Bind GPI-Anchored Protein DNase X and Trigger Entry Into Mammalian Cells. *PloS Pathog.* 9, e1003666. doi: 10.1371/journal.ppat.1003666

Mott, J., Barnewall, R. E., and Rikihisa, Y. (1999). Human Granulocytic Ehrlichiosis Agent and *Ehrlichia chaffeensis* Reside in Different Cytoplasmic Compartments in HL-60 Cells. *Infect. Immun.* 67, 1368–1378. doi: 10.1128/IAI.67.3.1368-1378.1999

Niu, H., Kozjak-Pavlovic, V., Rudel, T., and Rikihisa, Y. (2010). *Anaplasma phagocytophilum* Ats-1 Is Imported Into Host Cell Mitochondria and Interferes With Apoptosis Induction. *PloS Pathog.* 6, e1000774. doi: 10.1371/journal.ppat.1000774

Paddock, C. D., and Childs, J. E. (2003). *Ehrlichia chaffeensis*: A Prototypical Emerging Pathogen. *Clin. Microbiol. Rev.* 16, 37–64. doi: 10.1128/CMR.16.1.37-64.2003

Panday, A., Sahoo, M. K., Osorio, D., and Batra, S. (2015). NADPH Oxidases: An Overview From Structure to Innate Immunity-Associated Pathologies. *Cell Mol. Immunol.* 12, 5–23. doi: 10.1038/cmi.2014.89

Pfanner, N., and Truscott, K. N. (2002). Powering Mitochondrial Protein Import. *Nat. Struct. Biol.* 9, 234–236. doi: 10.1038/nsb0402-234

Raspe, M., Gillis, J., Krol, H., Krom, S., Bosch, K., van Veen, H., et al. (2009). Mimicking Proteasomal Release of Polyglutamine Peptides Initiates Aggregation and Toxicity. *J. Cell Sci.* 122, 3262–3271. doi: 10.1242/jcs.045567

Ravikumar, B., Imarisio, S., Sarkar, S., O'Kane, C. J., and Rubinsztein, D. C. (2008). Rab5 Modulates Aggregation and Toxicity of Mutant Huntingtin Through Macroautophagy in Cell and Fly Models of Huntington Disease. *J. Cell Sci.* 121, 1649–1660. doi: 10.1242/jcs.025726

Rikihisa, Y. (1991). The Tribe *Ehrlichieae* and Ehrlichial Diseases. *Clin. Microbiol. Rev.* 4, 286–308. doi: 10.1128/CMR.4.3.286

Rikihisa, Y. (2010). *Anaplasma phagocytophilum* and *Ehrlichia chaffeensis*: Subversive Manipulators of Host Cells. *Nat. Rev. Microbiol.* 8, 328–339. doi: 10.1038/nrmicro2318

Rikihisa, Y. (2011). Mechanisms of Obligatory Intracellular Infection With Anaplasma Phagocytophilum. *Clin. Microbiol. Rev.* 24, 469–489. doi: 10.1128/CMR.00064-10

Rikihisa, Y. (2015). Molecular Pathogenesis of *Ehrlichia chaffeensis* Infection. *Annu. Rev. Microbiol.* 69, 283–304. doi: 10.1146/annurev-micro-091014-104411

Rikihisa, Y. (2017). Role and Function of the Type IV Secretion System in *Anaplasma* and *Ehrlichia* Species. *Curr. Top. Microbiol. Immunol.* 413, 297–321. doi: 10.1007/978-3-319-75241-9_12

Rikihisa, Y. (2019). Subversion of RAB5-Regulated Autophagy by the Intracellular Pathogen Ehrlichia chaffeensis. *Small GTPases* 10, 343–349. doi: 10.1080/21541248.2017.1332506

Roberts, A. W., Kim, C., Zhen, L., Lowe, J. B., Kapur, R., Petryniak, B., et al. (1999). Deficiency of the Hematopoietic Cell-Specific Rho Family GTPase Rac2 Is Characterized by Abnormalities in Neutrophil Function and Host Defense. *Immunity* 10, 183–196. doi: 10.1016/S1074-7613(00)80019-9

Seifert, R., Rosenthal, W., and Schultz, G. (1986). Guanine Nucleotides Stimulate NADPH Oxidase in Membranes of Human Neutrophils. *FEBS Lett.* 205, 161–165. doi: 10.1016/0014-5793(86)80886-9

Sharma, P., Teymournejad, O., and Rikihisa, Y. (2017). Peptide Nucleic Acid Knockdown and Intra-Host Cell Complementation of Ehrlichia Type IV Secretion System Effector. *Front. Cell Infect. Microbiol.* 7, 228. doi: 10.3389/fcimb.2017.00228

Teymournejad, O., Lin, M., and Rikihisa, Y. (2017). Ehrlichia Chaffeensis and Its Invasin EtpE Block Reactive Oxygen Species Generation by Macrophages in a DNase X-Dependent Manner. *MBio* 8. doi: 10.1128/mBio.01551-17

Teymournejad, O., and Rikihisa, Y. (2020). Ehrlichia chaffeensis Uses an Invasin To Suppress Reactive Oxygen Species Generation by Macrophages *via* CD147-Dependent Inhibition of Vav1 To Block Rac1 Activation. *mBio* 11, 1–14. doi: 10.1128/mBio.00267-20

Wurm, C. A., Neumann, D., Lauterbach, M. A., Harke, B., Egner, A., Hell, S. W., et al. (2011). Nanoscale Distribution of Mitochondrial Import Receptor Tom20 Is Adjusted to Cellular Conditions and Exhibits an Inner-Cellular Gradient. *Proc. Natl. Acad. Sci. U. S. A.* 108, 13546–13551. doi: 10.1073/pnas.1107553108

Yan, Q., Lin, M., Huang, W., Teymournejad, O., Johnson, J. M., Hays, F. A., et al. (2018). Ehrlichia Type IV Secretion System Effector Etf-2 Binds to Active RAB5 and Delays Endosome Maturation. *Proc. Natl. Acad. Sci. U. S. A.* 115, E8977–E8986. doi: 10.1073/pnas.1806904115

Yan, Q., Zhang, W., Lin, M., Teymournejad, O., Budachetri, K., Lakritz, J., et al. (2021). Iron Robbery by Intracellular Pathogen *via* Bacterial Effector-Induced Ferritinophagy. *Proc. Natl. Acad. Sci. U. S. A.* 118, e2026598118. doi: 10.1073/pnas.2026598118

Yoo, Y., Wu, X., Egile, C., Li, R., and Guan, J. L. (2006). Interaction of N-WASP With hnRNPK and Its Role in Filopodia Formation and Cell Spreading. *J. Biol. Chem.* 281, 15352–15360. doi: 10.1074/jbc.M511825200

Zhang, W., Lin, M., Yan, Q., Budachetri, K., Hou, L., Sahni, A., et al. (2021). An Intracellular Nanobody Targeting T4SS Effector Inhibits Ehrlichia Infection. *Proc. Natl. Acad. Sci. U. S. A.* 118, e2024102118. doi: 10.1073/pnas.2024102118

Zhao, T., Benard, V., Bohl, B. P., and Bokoch, G. M. (2003). The Molecular Basis for Adhesion-Mediated Suppression of Reactive Oxygen Species Generation by Human Neutrophils. *J. Clin. Invest.* 112, 1732–1740. doi: 10.1172/JCI19108

Zhao, X., Carnevale, K. A., and Cathcart, M. K. (2003). Human Monocytes Use Rac1, Not Rac2, in the NADPH Oxidase Complex. *J. Biol. Chem.* 278, 40788–40792. doi: 10.1074/jbc.M302208200

Conflict of Interest: The author declares that the research was conducted in the absence of any commercial or financial relationships that could be construed as a potential conflict of interest.

Publisher's Note: All claims expressed in this article are solely those of the authors and do not necessarily represent those of their affiliated organizations, or those of the publisher, the editors and the reviewers. Any product that may be evaluated in this article, or claim that may be made by its manufacturer, is not guaranteed or endorsed by the publisher.

frontiers in Cellular and Infection Microbiology

MINI REVIEW
published: 27 January 2022
doi: 10.3389/fcimb.2022.784430

Apoptosis and Autophagy: Current Understanding in Tick–Pathogen Interactions

Xin-Ru Wang and Benjamin Cull**

Department of Entomology, University of Minnesota, St. Paul, MN, United States

Tick-borne diseases are a significant threat to human and animal health throughout the world. How tick-borne pathogens successfully infect and disseminate in both their vertebrate and invertebrate hosts is only partially understood. Pathogens have evolved several mechanisms to combat host defense systems, and to avoid and modulate host immunity during infection, therefore benefitting their survival and replication. In the host, pathogens trigger responses from innate and adaptive immune systems that recognize and eliminate invaders. Two important innate defenses against pathogens are the programmed cell death pathways of apoptosis and autophagy. This Mini Review surveys the current knowledge of apoptosis and autophagy pathways in tick-pathogen interactions, as well as the strategies evolved by pathogens for their benefit. We then assess the limitations to studying both pathways and discuss their participation in the network of the tick immune system, before highlighting future perspectives in this field. The knowledge gained would significantly enhance our understanding of the defense responses in vector ticks that regulate pathogen infection and burden, and form the foundation for future research to identify novel approaches to the control of tick-borne diseases.

Keywords: tick, intracellular pathogens, apoptosis, autophagy, cross-talk, *Rickettsia*, *Anaplasma*, *Ehrlichia*

OPEN ACCESS

Edited by:
Daniel E. Voth,
University of Arkansas for Medical Sciences, United States

Reviewed by:
Andréa Cristina Fogaça,
University of São Paulo, Brazil
Isaura Simões,
University of Coimbra, Portugal

***Correspondence:**
Xin-Ru Wang
wang8848@umn.edu
Benjamin Cull
cull0122@umn.edu

Specialty section:
This article was submitted to Bacteria and Host, a section of the journal Frontiers in Cellular and Infection Microbiology

Received: *27 September 2021*
Accepted: *11 January 2022*
Published: *27 January 2022*

Citation:
Wang X-R and Cull B (2022) Apoptosis and Autophagy: Current Understanding in Tick–Pathogen Interactions. Front. Cell. Infect. Microbiol. 12:784430. doi: 10.3389/fcimb.2022.784430

INTRODUCTION

Ticks, as obligate blood-sucking arthropods, can cause substantial public health burdens by direct feeding behaviors and transmitting a broad range of viral, bacterial, and protozoan pathogens to hosts. To date, approximately 80 known tick species are recognized as vectors responsible for spreading emerging infectious diseases throughout the world (**Figure 1**) (Jongejan and Uilenberg, 2004; Ghosh et al., 2007). For example, in the USA, tick-borne diseases (TBDs) accounted for nearly 76.5% of all vector-borne diseases from 2004 to 2016, based on the Centers for Disease Control and Prevention reports (CDC, 2018). Additionally, the effects of human activities and climate change on tick distribution and abundance also increase the risk of emerging and re-emerging diseases (Gray and Banerjee, 1999; Gray et al., 2009). The initial step for the success of intracellular pathogens is survival within their hosts. Tick-borne obligate intracellular pathogens include arboviruses and bacteria, which are responsible for diseases of medical and veterinary importance globally. These pathogens use different strategies to survive within their hosts. For example, after entry into the host cell *Rickettsia* spp. escape the endo-lysosomal pathway and replicate in the cytosol, whilst

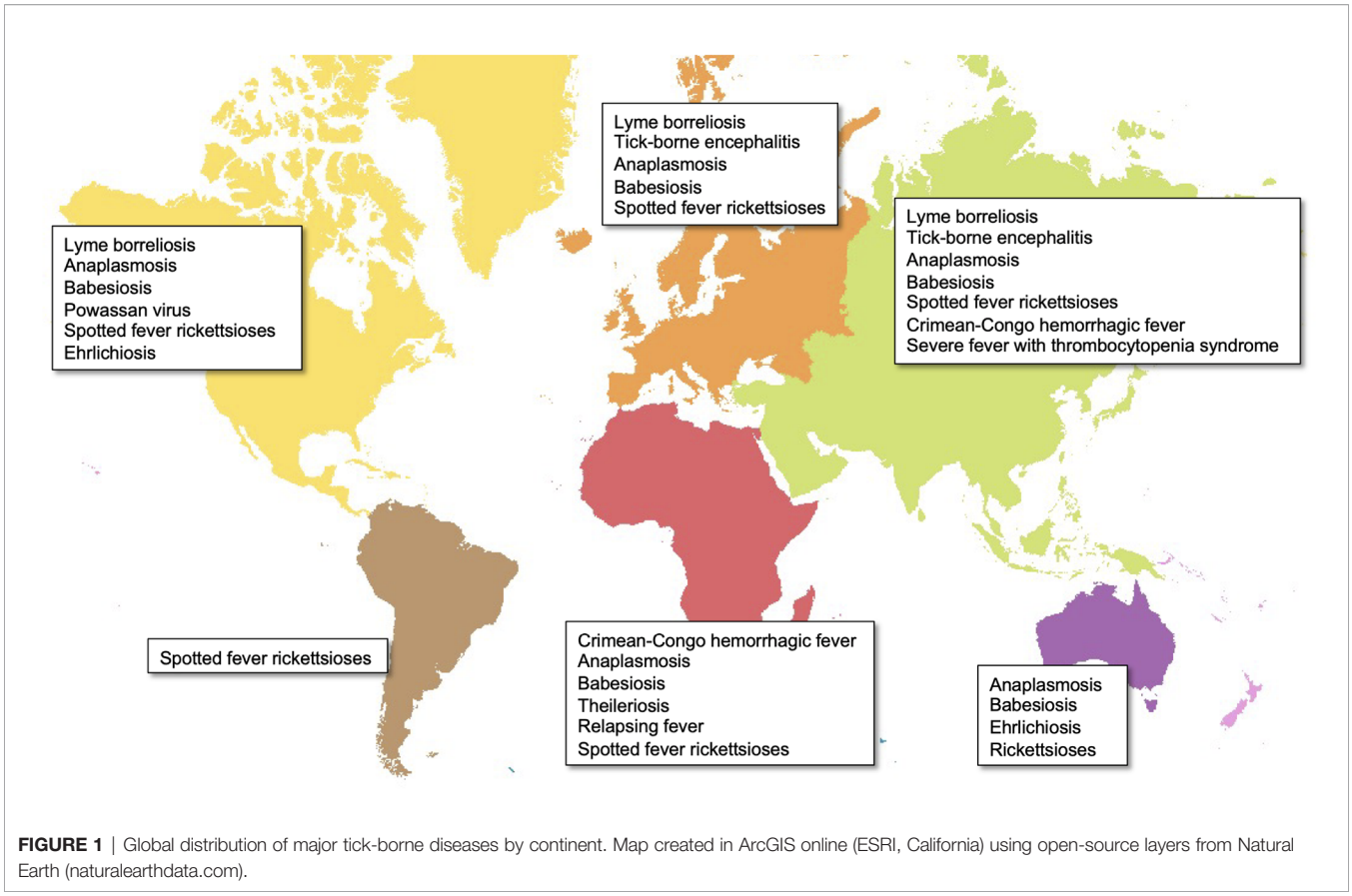

FIGURE 1 | Global distribution of major tick-borne diseases by continent. Map created in ArcGIS online (ESRI, California) using open-source layers from Natural Earth (naturalearthdata.com).

Anaplasma and *Ehrlichia* survive and replicate within specialized vacuoles (Salje, 2021). Considering these diseases are maintained in nature by cycling between ticks and their mammalian hosts, understanding tick-pathogen interactions provides clues for pathogen transmission and establishes a foundation for developing preventative strategies against human infection.

Programmed cell death (PCD) is an essential process in eukaryote homeostasis and development, and includes multiple death programs, such as apoptosis and autophagy (Ameisen, 2002). As a type I PCD mechanism, apoptosis is a genetically regulated process of cellular suicide in multicellular organisms (Taatjes et al., 2008). As a type II PCD mechanism, autophagy is a highly conserved cellular recycling process characterized by lysosomal degradation of cytosol and organelles and recycling of the breakdown products (Levine and Deretic, 2007). Commonly, PCD has been studied in the context of a broad range of human diseases, including neurodegenerative disorders, cancer, and ischemic damage (Elmore, 2007). Recently, different types of PCD have been identified as critical components of innate immunity pathways that act as defense mechanisms against intracellular bacteria, parasites, and viruses, even in insects (Fuchs and Steller, 2011; Romanelli et al., 2014; Koonin and Krupovic, 2019). Like all invertebrates, ticks lack an adaptive immune system but are capable of using the innate immune system to regulate pathogen colonization, persistence, and transmission (Brossard and Wikel, 2004; Hart and Thangamani, 2021). This Mini Review brings together current knowledge on the apoptosis and autophagy pathways from the perspective of tick-pathogen interactions, and our progress in deciphering the mechanisms used by tick-borne pathogens to interact with these pathways. The crosstalk between apoptosis, autophagy and other immune pathways, and how this might be interfered with by intracellular pathogens to benefit their survival are also investigated. Finally, we discuss challenges in studying these pathways in tick-pathogen systems and how these may be overcome in future to improve our understanding of this field and its potential importance to pathogen persistence in ticks and vector competence.

APOPTOSIS

As a genetically regulated process of cellular suicide in multicellular organisms, apoptosis responsible for development and homeostasis has been described in several models, including in some arthropods (Jacobson et al., 1997; Bowman and Sauer, 2004; Taatjes et al., 2008; Menze et al., 2010). In vertebrates, apoptosis is also recognized as an innate immune pathway, and mediates eukaryotic cell response to infection by a wide range of pathogens. However, the roles of apoptosis are still perplexing and complex, with multiple pro- and anti-death factors underlying the diversity of events (Everett and McFadden, 1999; Rudel et al., 2010). In some cases, activation of apoptosis is destructive for the pathogens. Pathogens are internalized and

packed into the apoptosome during infection, resulting in a more efficient fusion of the phagosome/lysosome, followed by digestion and degradation. Upon apoptosis activation, upregulating nucleases and enzymes can also result in cell demise and promote pathogen clearance (Cervantes et al., 2007; Willingham et al., 2007; Taylor et al., 2008). In addition, efferocytosis, as an antimicrobial effect of apoptosis, allows rapid bacterial killing (Martin et al., 2012; Behar and Briken, 2019). On the other hand, apoptosis can also be advantageous for pathogens. For example, infected apoptotic cells may become unable to contain pathogens and cease to function as a barrier, thus promoting their spread to neighboring cells. Also, in some studies it was shown that induction of apoptosis protected the pathogens against phagocytosis and innate host defenses, which was beneficial for pathogen survival (Green and Kroemer, 2004; Riedl and Salvesen, 2007). Another prominent defense strategy of the host is to eliminate the replicative niche of pathogens *via* the destruction of infected tissues, thereby preventing their replication and dissemination (Labbé and Saleh, 2008). Obviously, the relationships between host and pathogens are complex and involve an intricate balance to serve both host and pathogen interests. This balance of pathogen-induced apoptosis depends on the taxa of bacteria, the duration of infection, the host cell type, multiplicity of infection (MOI), and other factors.

Apoptosis is important for tick development as it initiates salivary gland degeneration, which is regulated by a cascade of caspases leading to the degradation of DNA and proteins in acini (Mao et al., 1995; Mao and Kaufman, 1999; L'Amoreaux et al., 2003; Nunes et al., 2005; Scopinho Furquim et al., 2008). Similar to vertebrates, the regulation of apoptosis in some arthropods and the interactions with pathogens they harbor and transmit have been described (Clarke and Clem, 2003; Flegel, 2007; Sokolova, 2009). However, a few mechanistic insights are just beginning to be revealed in this field due to the wide range of pathogens and their various arthropod hosts. Here, we focus on tick-borne obligate intracellular pathogens to illustrate the paradigms of the function of the apoptotic machinery in ticks.

Inhibition of Host Apoptosis by Tick-Borne Intracellular Pathogens

A prime example of intracellular bacteria regulating apoptosis is *Anaplasma phagocytophilum*, a tick-transmitted rickettsial agent that causes human granulocytic anaplasmosis. *In vitro*, *A. phagocytophilum* utilizes several mechanisms to inhibit apoptosis in different species of tick cells. For example, besides interfering with endoplasmic reticulum (ER) and the unfolded protein response in *Ixodes scapularis* ISE6 cells, *A. phagocytophilum* also downregulates expression of a series of kinases, including phosphoenolpyruvate carboxykinase (PEPCK), mitogen-activated protein kinase (MKK), and apoptosis signal-regulating kinase 1 (ASK1) (Ayllón et al., 2013; Villar et al., 2015). In addition, in *I. ricinus* IRE/CTVM20 tick cells, transcriptome analysis and flow cytometry revealed that infection with *A. phagocytophilum* not only regulates JAK and anti-apoptotic factors gene expression but also inhibits the intrinsic apoptosis pathway (Alberdi et al., 2016b; Alberdi et al., 2016a). *In vivo*, *A. phagocytophilum* displays a tissue-specific response to mediate cell apoptosis in tick nymphs (Ayllón et al., 2015). It achieves this by targeting the JAK/STAT pathway and decreasing FAS expression in midguts, while reducing porin (voltage-dependent anion-selective channel) expression to inhibit cytochrome c (one of the mitochondrial proteins associated with apoptosis) release from mitochondria in salivary glands *via* intrinsic apoptosis. Interestingly, tick salivary glands serve as an essential organ for *A. phagocytophilum* colonization, and have a possible role in activating extrinsic apoptosis to limit bacterial infection. Indeed, mitochondria, caspases, and pro/anti-apoptotic molecules are key players associated with apoptosis during pathogen infection. Similar to its manipulation of the arthropod host, *A. phagocytophilum* also modulates activity of the above "players" to inhibit apoptosis for their advantage in vertebrate hosts (Scaife et al., 2003; Borjesson et al., 2005; Choi et al., 2005; Ge and Rikihisa, 2006; Niu et al., 2010).

Another very similar system is exploited by *Rickettsia rickettsii* (agent of Rocky Mountain spotted fever). According to the proteome of *Rhipicephalus microplus* BME26 cells, *R. rickettsii* may hamper apoptosis *via* inhibition of caspase-3 activity, thus favoring bacterial growth and proliferation (Martins et al., 2020). Apart from bacterial pathogens, tick-borne viruses have long received much attention. The *I. ricinus* IRE/CTVM20 tick cell transcriptome exerts different gene expression patterns relative to infection with *A. phagocytophilum* after tick-borne encephalitis virus (TBEV) and louping ill virus (LIV) infection, such as raising cytochrome c expression. Interestingly, some apoptosis-related genes, including caspase and hsp70, are expressed differently in flavivirus and intracellular bacterial infections. Whether flaviviruses could benefit from inhibiting tick apoptosis as does *A. phagocytophilum*, is however unconfirmed (Mansfield et al., 2017).

Activation of Host Apoptosis by Tick-Borne Intracellular Pathogens

Although a critical strategy of intracellular pathogens is induction of vertebrate host-cell apoptosis under certain circumstances, the pro-apoptotic response of ticks to tick-borne pathogens is much less defined. Recently, we have shown that *Rickettsia parkeri*, a tick-transmitted spotted fever group rickettsia, is able to activate mitochondria-dependent apoptosis to promote its infection of and replication in tick cells (Wang X-R. et al., 2021). By employing cell types from different tick species, we demonstrated that *R. parkeri* initiation of apoptosis was a conserved response and required intracellular rickettsial replication. Considering that apoptosis is initiated *via* a series of stressors within a cell, the different growth status (exposure, colonization, invasion, and infection) of pathogens in the host might cause different stimuli, thus playing a diverse role in apoptosis. Indeed, *R. parkeri* exerts pro-and anti-apoptotic activities during different infection phases, which also has been observed in another spotted fever group rickettsia, *R. rickettsii* (Clifton et al., 1998). However, unlike in the arthropod host, *R. parkeri* failed to induce apoptosis in vertebrate host cells at the same infection phase (Wang X-R. et al., 2021). Unsurprisingly, pro-apoptotic activity in one cell type or host species may not be the same as in another cell type or host species. Another example of a pathogen that induces different responses in mammalian and tick hosts is Hazara virus, a tick-borne segmented negative-sense

RNA virus closely related to Crimean-Congo hemorrhagic fever virus (CCHFV), but which causes less severe disease. Cleavage of virus nucleocapsid (N) protein by caspase-3 results in apoptosis in mammalian cells but fails to activate apoptosis in tick cells. The use of two different strategies to modulate apoptosis in the respective hosts by members of the genus Nairovirus could directly affect the infection outcome (Fuller et al., 2019). Obviously, a flexible strategy is important for the successful colonization of vectors and hosts by those pathogens in a broad range of host cell types and host species. However, how intracellular pathogens execute this flexible strategy is largely unexplored in their arthropod hosts.

AUTOPHAGY

Autophagy is an important eukaryotic homeostatic pathway involved in the recycling of intracellular constituents and survival during starvation. Although various subtypes of autophagy exist, the best understood is macroautophagy (often simply called autophagy), characterized by formation of a double membrane-bound vesicle called an autophagosome and subsequent trafficking of the autophagosome to the lysosome for breakdown of its contents (Feng et al., 2014). Compared to our rapidly advancing knowledge of autophagy in vertebrates, that of autophagic processes in ticks is still in its infancy, with the core autophagic machinery only identified in a few species (Umemiya et al., 2007; Kawano et al., 2011; Flores Fernández et al., 2014; Umemiya-Shirafuji et al., 2014; Flores Fernández et al., 2016; Moura-Martiniano et al., 2017; Wang et al., 2020). As well as its important role in starvation (Umemiya-Shirafuji et al., 2010; Umemiya-Shirafuji et al., 2014; Moura-Martiniano et al., 2017; González Castillo et al., 2019; Rosendale et al., 2019; Wang et al., 2020), autophagy in ticks is also involved in embryo development (Umemiya-Shirafuji et al., 2010; Kawano et al., 2011; Umemiya-Shirafuji et al., 2014; Flores Fernández et al., 2014; González Castillo et al., 2019) and degeneration of salivary glands (Yu et al., 2017; Wang et al., 2018; Wang Y. et al., 2021), in which apoptosis also plays a role. Despite autophagy being a key component of host innate immune response to pathogens [known as xenophagy (Wang and Li, 2020)], the function and mechanism of autophagy in the interactions between ticks and tick-borne pathogens is completely unknown. Considering that autophagy is a highly conserved process, the common strategies employed by tick-borne pathogens in vertebrates, such as manipulating the host autophagic machinery to evade engulfment and destruction in the lysosome, and/or to direct autophagic processes, may also apply in ticks. Here, we center on the Rickettsiales (Patterson et al., 2021; Salje, 2021; Voss and Rahman, 2021), to display the autophagy mechanisms exploited by tick-borne intracellular bacteria.

Subversion/Evasion of Host Autophagy by Tick-Borne Intracellular Bacteria

The most well-studied mechanisms used by tick-borne bacteria to manipulate the autophagic pathway come from the Anaplasmataceae in their interactions with mammalian cells. *Anaplasma phagocytophilum* secretes the effector protein Ats-1, which interacts with Beclin1 to recruit autophagosomes to the *A. phagocytophilum* vacuole, supplying nutrients to support pathogen growth (Niu et al., 2012). A similar but distinct process to induce autophagy and trafficking of autophagosomes to the pathogen-containing vacuole is employed by *Ehrlichia chaffeensis* (causative agent of human ehrlichiosis) *via* its effector Etf-1, which interacts with Rab5, Beclin1 and the autophagy-initiating class III phosphatidylinositol 3-kinase complex (Lin et al., 2016). Both *A. phagocytophilum* and *E. chaffeensis* also prevent their vacuoles fusing with the lysosome (Niu et al., 2008; Lin et al., 2016; Lina et al., 2017); this is achieved by *E. chaffeensis* through modulation of the Wnt signaling pathway to inhibit autolysosome formation (Lina et al., 2017).

Infection with a range of spotted fever group rickettsiae (*R. conorii, R. japonica, R. montanensis, R. parkeri* and *R. rickettsii*) results in autophagy induction in mammalian host cells (Uchiyama et al., 2012; Engström et al., 2019; Sahni et al., 2020). Pathogenic rickettsiae appear to be capable of evading this immune response, whilst non-pathogenic species lack this ability (Uchiyama et al., 2012; Engström et al., 2019). Infection of human umbilical vein endothelial cells with *R. rickettsii* or *R. conorii* results in mTOR activation, potentially as a mechanism by which these rickettsiae limit anti-microbial autophagy (Sahni et al., 2020), whilst *Rickettsia parkeri* is able to evade autophagy by employing outer membrane protein B (OmpB) to prevent the ubiquitination of surface proteins and their subsequent recognition by autophagic receptors in both human microvascular endothelial cells and mouse bone-marrow-derived macrophages (Engström et al., 2019). Even in the same cell type, different *Rickettsia* species utilize contrasting strategies to evade autophagy. For example, *R. australis* induces autophagy to aid successful invasion of mouse bone-marrow-derived macrophages (Bechelli et al., 2019), resulting in the inhibition of inflammatory cytokine secretion to favor bacterial survival (Bechelli et al., 2021). Due to the broad range of rickettsial pathogens and different host cell types studied, we are just unveiling the tip of the iceberg regarding the complex interactions between these pathogens and their hosts. Although we can use the situation in vertebrates as a basis for predicting what might occur in ticks, we cannot assume that the strategies employed by pathogens to infect mammals can be generalized to their persistence in arthropods (as shown above with apoptosis), and so further investigation into how pathogens interact with tick autophagy are warranted.

DISCUSSION

Limitations of Apoptosis and Autophagy Study in Tick–Pathogen Interactions

Despite impressive progress being made on how pathogens "tamper with" the tick immune system, including revealing antibacterial and antiviral pathways and identifying molecular effectors and cells (Fogaça et al., 2021), unlike the well-known arthropod-pathogen systems (Buchon et al., 2014), tick-

pathogen interaction is a newly emerging field that is far from completely understood. This is largely due to the tick's own complex development and the diversity of its transmitted pathogens. Firstly, *in vitro* study depends on tick cell lines, which are relatively fragile compared to more common cell types, and have more intensive culture requirements (Munderloh and Kurtti, 1989; Bell-Sakyi, 1991; Mattila et al., 2007; Bell-Sakyi et al., 2009). Additionally, most tick cell lines were derived from embryos, however, their tissue(s) of origin are unconfirmed. Different cell types might possess different characteristics and ontogenies, resulting in unique properties (Mattila et al., 2007; Wang et al., 2020). *In vivo* studies on ticks are more challenging because of their unique life cycle, which is influenced by an array of elements, including species, host feeding preference, different ecological and geographic factors in nature, and strict maintenance requirements in the laboratory (Sonenshine and Roe, 2013; Jia et al., 2020). Besides some medically and veterinary important species, most ticks are a blind-spot due to insufficient data on genomic information, let alone the interactions with potential pathogens that they may harbor. Genomic data is only available for a limited number of tick species including *Ixodes scapularis, Ixodes ricinus, Ixodes persulcatus, Haemaphysalis longicornis, Dermacentor silvarum, Hyalomma asiaticum, Rhipicephalus sanguineus*, and *Rhipicephalus microplus* (Gulia-Nuss et al., 2016; Cramaro et al., 2017; Jia et al., 2020). The most critical difficulty is pathogens themselves, as many different factors such as species/strain pathogenicity, difficulty in laboratory maintenance, etc. may alter the observed results. For example, even different strains of the same pathogen, *R. rickettsii*, exhibits exclusive manners in different cell types or organs (Lehman et al., 2018). Thus, pathogens initiate a critical step for tick immune response, directing more complex communication than simple inhibition or activation. Studies to address these difficulties would pave the way for future research centered on the tick immune system (**Figure 2**).

Future Perspectives of Apoptosis and Autophagy Study in Tick–Pathogens Interaction

It is unquestionable that PCD acts as one piece of the puzzle for tick innate immunity, and more work needs to be done to gain more clues to solve a tick's "Jigsaw puzzles". This would include investigating the network of other immune pathways as well as the cross-talk between apoptosis and autophagy under certain conditions (Fairlie et al., 2020). Paradigms in vertebrate hosts utilize these communications to enhance the recognition and destruction of intracellular pathogens (Hua et al., 2019; Van Opdenbosch and Lamkanfi, 2019), and we expect that immune responses in ticks behave similarly. Interestingly, tick-borne intracellular pathogens also make use of effective communications in their vertebrate hosts to tip the scales in their favor. For example, as well as inducing autophagy, both the *A. phagocytophilum* effector Ats-1 and the *E. chaffeensis* Etf-1 are also translocated into the host mitochondria to inhibit apoptosis initiation (Niu et al., 2010; Liu et al., 2012). Another *A. phagocytophilum* effector AptA induces autophagy and the ubiquitin-proteasome system, whilst reducing the efficiency of apoptosis (Ma et al., 2021). There is also interplay between autophagy and inflammatory pathways during both *Ehrlichia* and *Rickettsia* infection (Tominello et al., 2019; Bechelli et al., 2021), and autophagy induction is balanced by signaling of MyD88 (a downstream adaptor for many pattern recognition receptors) during ehrlichial infection (Kader et al., 2017).

As with other arthropods, crosstalk within the tick innate immune system associated with the response to pathogen infection has also been explored in recent decades (Capelli-Peixoto et al., 2017; Fogaça et al., 2021). Although antibacterial and antiviral pathways, including JAK-STAT (Janus kinase/signal transducer and activator of transcription), Toll, IMD (Immune Deficiency) and RNA interference (RNAi), possess a certain specificity, they are also capable of collaboration under certain conditions. For example, ticks utilize the IMD pathway in response to infection with *B. burgdorferi*, *A. phagocytophilum*, or *A. marginale* (Shaw et al., 2017; McClure Carroll et al., 2019; Kurokawa et al., 2020). The downstream pathways include NF-kB/Relish and Jun N-terminal kinase (JNK) (Ramphul et al., 2015; Chowdhury et al., 2020; Tafesh-Edwards and Eleftherianos, 2020), which are involved in viral-induced apoptosis and have been well characterized in insects. It is possible that bacteria induce a similar response in ticks. However, the components of these pathways in ticks are highly divergent from vertebrate and insect systems, and whether those mechanisms also apply in ticks needs further investigation. Towards this end, identification of the apoptosis and autophagy components of ticks by employing comparative genomics would be a significant step. Utilizing tick and other arthropod genome sequences, the homologues to apoptosis/autophagy-related genes of known function should be confirmed (Wang et al., 2020).

To understand the biological processes involved in apoptosis/autophagy in response to pathogens, multi-omics (including genetics, epigenetics, transcriptomics, proteomics, metabolomics, and cellomics) would be valuable approaches (Hasin et al., 2017; Chu et al., 2021). For example, combining genomic and transcriptome data can reveal apoptosis-related genes and their roles in pathogen infection. Using metabolomics and proteomics, proteins involved in the apoptosis pathway and their connection to molecular changes in metabolic pathways can also be identified. Single-cell/nucleus omics also can determine functional molecules of each cell and specific tick cell subtypes in response to pathogens. Finally, combining properly analyzed approaches and apoptosis assay measurements, the study of apoptosis in tick-pathogen interactions would be significantly enhanced. Genetic tools for editing microorganisms, including mutagenesis and CRISPR as well as RNAi, facilitate the growing body of research in host-pathogen interactions (Durvasula et al., 1997; Billmyre et al., 2013; Wilke and Marrelli, 2015; Vo et al., 2021). As well as using the multi-omics methods outlined above, further work to characterize interactions between pathogens and tick autophagy could employ transgenic reporter bacteria or viruses to visualize responses to autophagy. In addition, with the use of directed mutants or

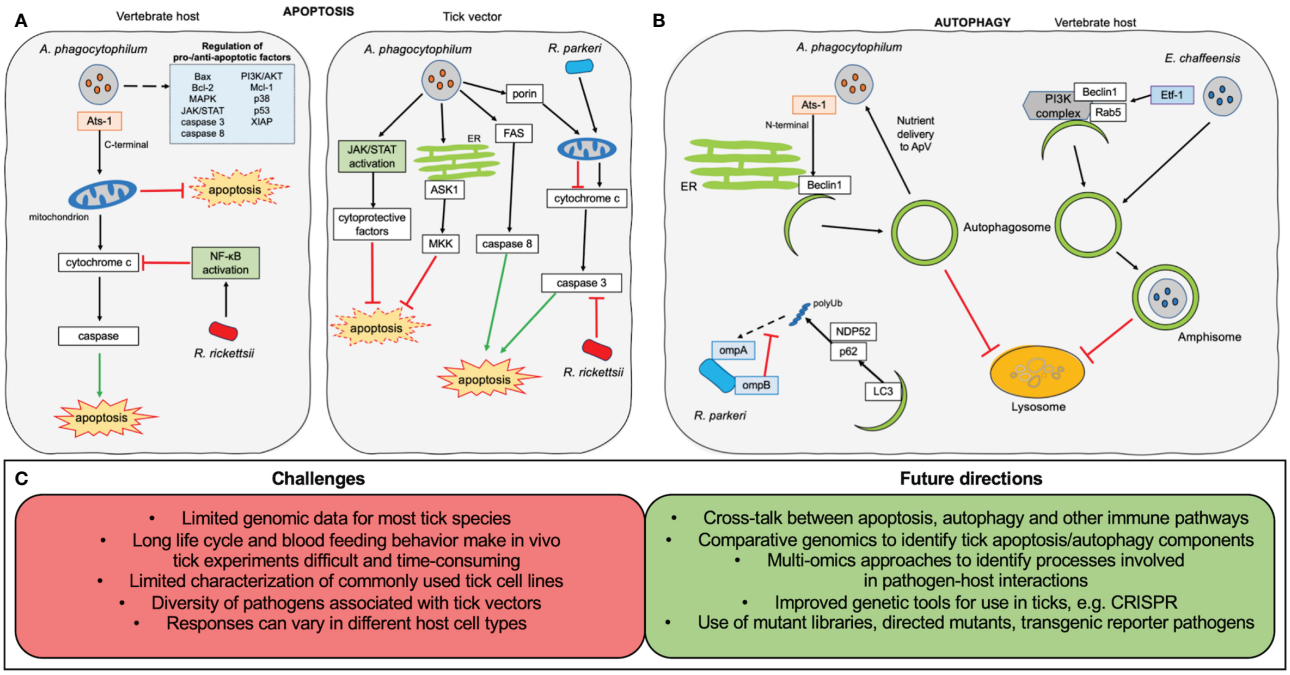

FIGURE 2 | Overview of apoptosis and autophagy research on tick-borne obligate intracellular pathogens. **(A)** Manipulation of apoptosis. In the vertebrate host (left) the C-terminal fragment of the *Anaplasma phagocytophilum* effector Ats-1 localizes to the host mitochondria where it inhibits apoptosis. A large number of kinases and pro-/anti-apoptotic factors (shown in pale blue box) also show changes in expression during *A. phagocytophilum* infection. *Rickettsia rickettsii* infection leads to NF-κB activation, inhibiting cytochrome c release from mitochondria resulting in downstream inhibition of apoptosis. In the tick vector (right), *A. phagocytophilum* uses multiple pathways to inhibit apoptosis, including activation of the JAK/STAT pathway, down-regulation of mitogen-activated protein kinase (MKK) and apoptosis signal-regulating kinase 1 (ASK1), decreasing FAS expression, and reducing porin expression to inhibit cytochrome c release from the mitochondria. *Rickettsia rickettsii* prevents caspase 3 activation in order to inhibit apoptosis. *Rickettsia parkeri* infection is associated with increased mitochondrial cytochrome c release, leading to increased activation of apoptosis, which is essential to its infection of tick cells. **(B)** Manipulation of autophagy. Experimental evidence only exists from mammalian systems. The N-terminal portion of the *A. phagocytophilum* effector Ats-1 localizes to the endoplasmic reticulum (ER) where it interacts with Beclin1 to initiate autophagosome formation. Autophagosomes are prevented from trafficking to the lysosome and instead fuse with the bacterial vacuole to deliver membrane and nutrients to *A. phagocytophilum*. The Etf-1 effector secreted by *Erhlichia chaffeensis* interacts with Beclin1, Rab5 and the PI3K complex to induce autophagosome formation. The autophagosomes fuse with the *Erhlichia*-containing vacuole and are prevented from fusing with the lysosome by bacterial interference with the Wnt signalling pathway. During *R. parkeri* infection of macrophages, ompB shields the rickettsial surface protein ompA from polyubiquitination, preventing its recognition by the autophagy adaptors p62 and NDP52. **(C)** Challenges and future directions in the research of interactions of intracellular tick-borne pathogens with apoptosis and autophagy pathways.

random mutant libraries, the underlying mechanisms used by pathogens to influence autophagy and apoptosis pathways could be revealed, as well as identification of specific factors essential for bacterial invasion and replication in their tick vectors (**Figure 2**).

SUMMARY

Characterization of the involvement of the tick PCD machinery in pathogen acquisition, persistence, and transmission would help explain the natural cycle of tick-borne pathogens, as well as lead to the design of specific targets for new vaccines and drugs to prevent or treat TBDs. Greater knowledge of tick-borne intracellular pathogen and host (both ticks and mammals) interplay could have implications for understanding how the innate immune system contributes to the vector competence of various tick species for different intracellular pathogens and to the ability of vertebrate hosts to act as reservoirs or succumb to disease.

AUTHOR CONTRIBUTIONS

X-RW and BC conceived and wrote the article. All authors contributed to the article and approved the submitted version.

FUNDING

The study was financially supported by a grant to UGM from the NIH (2R01AI049424), and a grant to UGM from the Minnesota Agricultural Experiment Station (MIN-17-078).

ACKNOWLEDGMENTS

We thank Ulrike G. Munderloh for her insightful comments and revisions on this paper.

REFERENCES

Alberdi, P., Espinosa, P. J., Cabezas-Cruz, A., and de la Fuente, J. (2016a). *Anaplasma Phagocytophilum* Manipulates Host Cell Apoptosis by Different Mechanisms to Establish Infection. *Vet. Sci.* 3(3), 15. doi: 10.3390/vetsci3030015

Alberdi, P., Mansfield, K. L., Manzano-Román, R., Cook, C., Ayllón, N., Villar, M., et al. (2016b). Tissue-Specific Signatures in the Transcriptional Response to *Anaplasma Phagocytophilum* Infection of Ixodes Scapularis and Ixodes Ricinus Tick Cell Lines. *Front. Cell. Infect. Microbiol.* 6, 15. doi: 10.3389/fcimb.2016.00020

Ameisen, J. C. (2002). On the Origin, Evolution, and Nature of Programmed Cell Death: A Timeline of Four Billion Years. *Cell Death Differ.* 9, 367–393. doi: 10.1038/sj.cdd.4400950

Ayllón, N., Villar, M., Busby, A. T., Kocan, K. M., Blouin, E. F., Bonzón-Kulichenko, E., et al. (2013). *Anaplasma Phagocytophilum* Inhibits Apoptosis and Promotes Cytoskeleton Rearrangement for Infection of Tick Cells. *Infect. Immun.* 81, 2415–2425. doi: 10.1128/IAI.00194-13

Ayllón, N., Villar, M., Galindo, R. C., Kocan, K. M., Šíma, R., López, J. A., et al. (2015). Systems Biology of Tissue-Specific Response to *Anaplasma Phagocytophilum* Reveals Differentiated Apoptosis in the Tick Vector Ixodes Scapularis. *PloS Genet.* 11, e1005120. doi: 10.1371/journal.pgen.1005120

Bechelli, J., Rumfield, C. S., Walker, D. H., Widen, S., Khanipov, K., and Fang, R. (2021). Subversion of Host Innate Immunity by *Rickettsia Australis via* a Modified Autophagic Response in Macrophages. *Front. Immunol.* 12, 638469. doi: 10.3389/fimmu.2021.638469

Bechelli, J., Vergara, L., Smalley, C., Buzhdygan, T. P., Bender, S., Zhang, W., et al. (2019). Atg5 Supports *Rickettsia Australis* Infection in Macrophages *In Vitro* and *In Vivo*. *Infect. Immun.* 87, e00651–18. doi: 10.1128/IAI.00651-18

Behar, S. M., and Briken, V. (2019). Apoptosis Inhibition by Intracellular Bacteria and its Consequence on Host Immunity. *Curr. Opin. Immunol.* 60, 103–110. doi: 10.1016/j.coi.2019.05.007

Bell-Sakyi, L. (1991). Continuous Cell Lines From the Tick *Hyalomma Anatolicum Anatolicum*. *J. Parasitol.* 77, 1006–1008. doi: 10.2307/3282757

Bell-Sakyi, L., Růžek, D., and Gould, E. A. (2009). Cell Lines From the Soft Tick *Ornithodoros Moubata*. *Exp. Appl. Acarol.* 49, 209–219. doi: 10.1007/s10493-009-9258-y

Billmyre, R. B., Calo, S., Feretzaki, M., Wang, X., and Heitman, J. (2013). RNAi Function, Diversity, and Loss in the Fungal Kingdom. *Chromosome Res.* 21 (6-7), 561–572. doi: 10.1007/S10577-013-9388-2

Borjesson, D. L., Kobayashi, S. D., Whitney, A. R., Voyich, J. M., Argue, C. M., and DeLeo, F. R. (2005). Insights Into Pathogen Immune Evasion Mechanisms: *Anaplasma Phagocytophilum* Fails to Induce an Apoptosis Differentiation Program in Human Neutrophils. *J. Immunol.* 174, 6364–6372. doi: 10.4049/jimmunol.174.10.6364

Bowman, A. S., and Sauer, J. R. (2004). Tick Salivary Glands: Function, Physiology and Future. *Parasitology* 129 (Suppl), S67–S81. doi: 10.1017/s0031182004006468

Brossard, M., and Wikel, S. K. (2004). Tick Immunobiology. *Parasitology* 129, S161–S176. doi: 10.1017/S0031182004004834

Buchon, N., Silverman, N., and Cherry, S. (2014). Immunity in *Drosophila Melanogaster*-From Microbial Recognition to Whole-Organism Physiology. *Nat. Rev. Immunol.* 14, 796–810. doi: 10.1038/nri3763

Capelli-Peixoto, J., Carvalho, D. D., Johnson, W. C., Scoles, G. A., Fogaça, A. C., Daffre, S., et al. (2017). The Transcription Factor Relish Controls *Anaplasma Marginale* Infection in the Bovine Tick *Rhipicephalus Microplus*. *Dev. Comp. Immunol.* 74, 32–39. doi: 10.1016/j.dci.2017.04.005

CDC. (2018). *Tickborne Diseases of the United States. A Reference Manual for Health Care Providers*, *Fifth Edition*. Available at: https://www.cdc.gov/ticks/tickbornediseases/TickborneDiseases-P.pdf.

Cervantes, J., Nagata, T., Uchijima, M., Shibata, K., and Koide, Y. (2007). Intracytosolic *Listeria Monocytogenes* Induces Cell Death Through Caspase-1 Activation in Murine Macrophages. *Cell. Microbiol.* 10, 41–52. doi: 10.1111/j.1462-5822.2007.01012.x

Choi, K. S., Park, J. T., and Dumler, J. S. (2005). *Anaplasma Phagocytophilum* Delay of Neutrophil Apoptosis Through the P38 Mitogen-Activated Protein Kinase Signal Pathway. *Infect. Immun.* 73, 8209–8218. doi: 10.1128/IAI.73.12.8209-8218.2005

Chowdhury, A., Modahl, C. M., Tan, S. T., Wei Xiang, B. W., Missé, D., Vial, T., et al. (2020). JNK Pathway Restricts DENV2, ZIKV and CHIKV Infection by Activating Complement and Apoptosis in Mosquito Salivary Glands. *PloS Pathog.* 16, e1008754. doi: 10.1371/journal.ppat.1008754

Chu, X., Zhang, B., Koeken, V. A. C. M., Gupta, M. K., and Li, Y. (2021). Multi-Omics Approaches in Immunological Research. *Front. Immunol.* 12, 668045. doi: 10.3389/FIMMU.2021.668045

Clarke, T. E., and Clem, R. J. (2003). Insect Defenses Against Virus Infection: The Role of Apoptosis. *Int. Rev. Immunol.* 22, 401–424. doi: 10.1080/08830180305215

Clifton, D. R., Goss, R. A., Sahni, S. K., Van Antwerp, D., Baggs, R. B., Marder, V. J., et al. (1998). NF-κB-Dependent Inhibition of Apoptosis is Essential for Host Cell Survival During *Rickettsia Rickettsii* Infection. *Proc. Natl. Acad. Sci. U. S. A.* 95, 4646–4651. doi: 10.1073/pnas.95.8.4646

Cramaro, W. J., Hunewald, O. E., Bell-Sakyi, L., and Muller, C. P. (2017). Genome Scaffolding and Annotation for the Pathogen Vector *Ixodes Ricinus* by Ultra-Long Single Molecule Sequencing. *Parasit. Vectors* 10, 71. doi: 10.1186/s13071-017-2008-9

Durvasula, R. V., Gumbs, A., Panackal, A., Kruglov, O., Aksoy, S., Merrifield, R. B., et al. (1997). Prevention of Insect-Borne Disease: An Approach Using Transgenic Symbiotic Bacteria. *Proc. Natl. Acad. Sci. U. S. A.* 94, 3274–3278. doi: 10.1073/pnas.94.7.3274

Elmore, S. (2007). Apoptosis: A Review of Programmed Cell Death. *Toxicol. Pathol.* 35, 495–516. doi: 10.1080/01926230701320337

Engström, P., Burke, T. P., Mitchell, G., Ingabire, N., Mark, K. G., Golovkine, G., et al. (2019). Evasion of Autophagy Mediated by Rickettsia Surface Protein OmpB is Critical for Virulence. *Nat. Microbiol.* 4, 2538–2551. doi: 10.1038/s41564-019-0583-6

Everett, H., and McFadden, G. (1999). Apoptosis: An Innate Immune Response to Virus Infection. *Trends Microbiol.* 7, 160–165. doi: 10.1016/S0966-842X(99)01487-0

Fairlie, W. D., Tran, S., and Lee, E. F. (2020). "Crosstalk Between Apoptosis and Autophagy Signaling Pathways," in *International Review of Cell and Molecular Biology* (Amsterdam: Academic Press), 115–158. doi: 10.1016/bs.ircmb.2020.01.003

Feng, Y., He, D., Yao, Z., and Klionsky, D. J. (2014). The Machinery of Macroautophagy. *Cell Res.* 24, 24–41. doi: 10.1038/cr.2013.168

Flegel, T. W. (2007). Update on Viral Accommodation, a Model for Host-Viral Interaction in Shrimp and Other Arthropods. *Dev. Comp. Immunol.* 31, 217–231. doi: 10.1016/j.dci.2006.06.009

Flores Fernández, J. M., Barragán Álvarez, C. P., Sánchez Hernández, C. V., Padilla Camberos, E., González Castillo, C., Ortunõ Sahagún, D., et al. (2016). Molecular Characterization and Expression Analysis of Three Novel Autophagy-Related Genes From the Cattle Tick Rhipicephalus (Boophilus) Microplus (Acari: Ixodidae). *Parasitology* 143, 1802–1809. doi: 10.1017/S0031182016001542

Flores Fernández, J. M., Gutiérrez Ortega, A., Rosario Cruz, R., Padilla Camberos, E., Álvarez, Á. H., and Martínez Velázquez, M. (2014). Molecular Cloning and Characterization of Two Novel Autophagy-Related Genes Belonging to the ATG8 Family From the Cattle Tick *Rhipicephalus (Boophilus) Microplus* (Acari: Ixodidae). *Exp. Appl. Acarol.* 64, 533–542. doi: 10.1007/s10493-014-9838-3

Fogaça, A. C., Sousa, G., Pavanelo, D. B., Esteves, E., Martins, L. A., Urbanová, V., et al. (2021). Tick Immune System: What Is Known, the Interconnections, the Gaps, and the Challenges. *Front. Immunol.* 12, 628054. doi: 10.3389/fimmu.2021.628054

Fuchs, Y., and Steller, H. (2011). Programmed Cell Death in Animal Development and Disease. *Cell* 147, 742–758. doi: 10.1016/j.cell.2011.10.033

Fuller, J., Surtees, R. A., Shaw, A. B., Álvarez-Rodríguez, B., Slack, G. S., Bell-Sakyi, L., et al. (2019). Hazara Nairovirus Elicits Differential Induction of Apoptosis and Nucleocapsid Protein Cleavage in Mammalian and Tick Cells. *J. Gen. Virol.* 100, 392–402. doi: 10.1099/jgv.0.001211

Ge, Y., and Rikihisa, Y. (2006). *Anaplasma Phagocytophilum* Delays Spontaneous Human Neutrophil Apoptosis by Modulation of Multiple Apoptotic Pathways. *Cell. Microbiol.* 8, 1406–1416. doi: 10.1111/j.1462-5822.2006.00720.x

Ghosh, S., Azhahianambi, P., and Yadav, M. P. (2007). Upcoming and Future Strategies of Tick Control: A Review. *J. Vector Borne Dis.* 44, 79–89.

González Castillo, C., Ortuño Sahagún, D., and Martínez Velázquez, M. (2019). Expression Dynamics of Autophagy-Related Genes in the Cattle Tick

Rhipicephalus Microplus During Embryonic Development and Under Increasing Larval Starvation. *Exp. Appl. Acarol.* 79, 255–266. doi: 10.1007/s10493-019-00428-7

Gray, S. M., and Banerjee, N. (1999). Mechanisms of Arthropod Transmission of Plant and Animal Viruses. *Microbiol. Mol. Biol. Rev.* 63, 128–148. doi: 10.1128/MMBR.63.1.128-148.1999

Gray, J. S., Dautel, H., Estrada-Peña, A., Kahl, O., and Lindgren, E. (2009). Effects of Climate Change on Ticks and Tick-Borne Diseases in Europe. *Interdiscip. Perspect. Infect. Dis.* 2009, 593232. doi: 10.1155/2009/593232

Green, D. R., and Kroemer, G. (2004). The Pathophysiology of Mitochondrial Cell Death. *Science* 305, 626–629. doi: 10.1126/science.1099320

Gulia-Nuss, M., Nuss, A. B., Meyer, J. M., Sonenshine, D. E., Roe, M. R., Waterhouse, R. M., et al. (2016). Genomic Insights Into the *Ixodes Scapularis* Tick Vector of Lyme Disease. *Nat. Commun.* 7, 10507. doi: 10.1038/ncomms10507

Hart, C. E., and Thangamani, S. (2021). Tick-Virus Interactions: Current Understanding and Future Perspectives. *Parasite Immunol.* 43, e12815. doi: 10.1111/pim.12815

Hasin, Y., Seldin, M., and Lusis, A. (2017). Multi-Omics Approaches to Disease. *Genome Biol.* 18, 83. doi: 10.1186/s13059-017-1215-1

Hua, F., Li, K., Shang, S., Wang, F., and Hu, Z. (2019). "Immune Signaling and Autophagy Regulation," in *Advances in Experimental Medicine and Biology* (Singapore: Springer), 551–593. doi: 10.1007/978-981-15-0602-4_26

Jacobson, M. D., Weil, M., and Raff, M. C. (1997). Programmed Cell Death in Animal Development. *Cell* 88, 347–354. doi: 10.1016/S0092-8674(00)81873-5

Jia, N., Wang, J., Shi, W., Du, L., Sun, Y., Zhan, W., et al. (2020). Large-Scale Comparative Analyses of Tick Genomes Elucidate Their Genetic Diversity and Vector Capacities. *Cell* 182, 1328–1340.e13. doi: 10.1016/j.cell.2020.07.023

Jongejan, F., and Uilenberg, G. (2004). The Global Importance of Ticks. *Parasitology* 129 (Suppl), S3–14. doi: 10.1017/s0031182004005967

Kader, M., Alaoui-EL-Azher, M., Vorhauer, J., Kode, B. B., Wells, J. Z., Stolz, D., et al. (2017). MyD88-Dependent Inflammasome Activation and Autophagy Inhibition Contributes to Ehrlichia-Induced Liver Injury and Toxic Shock. *PloS Pathog.* 13, e1006644. doi: 10.1371/journal.ppat.1006644

Kawano, S., Umemiya-Shirafuji, R., Boldbaatar, D., Matsuoka, K., Tanaka, T., and Fujisaki, K. (2011). Cloning and Characterization of the Autophagy-Related Gene 6 From the Hard Tick, *Haemaphysalis Longicornis*. *Parasitol. Res.* 109, 1341–1349. doi: 10.1007/s00436-011-2429-x

Koonin, E. V., and Krupovic, M. (2019). Origin of Programmed Cell Death From Antiviral Defense? *Proc. Natl. Acad. Sci.* 116, 16167–16169. doi: 10.1073/pnas.1910303116

Kurokawa, C., Lynn, G. E., Pedra, J. H. F., Pal, U., Narasimhan, S., and Fikrig, E. (2020). Interactions Between *Borrelia Burgdorferi* and Ticks. *Nat. Rev. Microbiol.* 18, 587–600. doi: 10.1038/s41579-020-0400-5

Labbé, K., and Saleh, M. (2008). Cell Death in the Host Response to Infection. *Cell Death Differ.* 15, 1339–1349. doi: 10.1038/cdd.2008.91

L'Amoreaux, W. J., Junaid, L., and Trevidi, S. (2003). Morphological Evidence That Salivary Gland Degeneration in the American Dog Tick, *Dermacentor Variabilis* (Say), Involves Programmed Cell Death. *Tissue Cell* 35, 95–99. doi: 10.1016/S0040-8166(02)00109-X

Lehman, S. S., Noriea, N. F., Aistleitner, K., Clark, T. R., Dooley, C. A., Nair, V., et al. (2018). The Rickettsial Ankyrin Repeat Protein 2 Is a Type IV Secreted Effector That Associates With the Endoplasmic Reticulum. *MBio* 9, e00975–18. doi: 10.1128/mBio.00975-18

Levine, B., and Deretic, V. (2007). Unveiling the Roles of Autophagy in Innate and Adaptive Immunity. *Nat. Rev. Immunol.* 7, 767–777. doi: 10.1038/nri2161

Lina, T. T., Luo, T., Velayutham, T. S., Das, S., and McBride, J. W. (2017). Ehrlichia Activation of Wnt-PI3K-mTOR Signaling Inhibits Autolysosome Generation and Autophagic Destruction by the Mononuclear Phagocyte. *Infect. Immun.* 85, e00690–17. doi: 10.1128/IAI.00690-17

Lin, M., Liu, H., Xiong, Q., Niu, H., Cheng, Z., Yamamoto, A., et al. (2016). Ehrlichia Secretes Etf-1 to Induce Autophagy and Capture Nutrients for Its Growth Through RAB5 and Class III Phosphatidylinositol 3-Kinase. *Autophagy* 12, 2145–2166. doi: 10.1080/15548627.2016.1217369

Liu, H., Bao, W., Lin, M., Niu, H., and Rikihisa, Y. (2012). Ehrlichia Type IV Secretion Effector ECH0825 Is Translocated to Mitochondria and Curbs ROS and Apoptosis by Upregulating Host MnSOD. *Cell. Microbiol.* 14, 1037–1050. doi: 10.1111/j.1462-5822.2012.01775.x

Ma, Z., Li, R., Hu, R., Zheng, W., Yu, S., Cheng, K., et al. (2021). *Anaplasma Phagocytophilum* AptA Enhances the UPS, Autophagy, and Anti-Apoptosis of Host Cells by PSMG3. *Int. J. Biol. Macromol.* 184, 497–508. doi: 10.1016/j.ijbiomac.2021.06.039

Mansfield, K. L., Cook, C., Ellis, R. J., Bell-Sakyi, L., Johnson, N., Alberdi, P., et al. (2017). Tick-Borne Pathogens Induce Differential Expression of Genes Promoting Cell Survival and Host Resistance in Ixodes Ricinus Cells. *Parasit. Vectors* 10, 81. doi: 10.1186/s13071-017-2011-1

Mao, H., and Kaufman, W. R. (1999). Profile of the Ecdysteroid Hormone and its Receptor in the Salivary Gland of the Adult Female Tick, *Amblyomma Hebraeum*. *Insect Biochem. Mol. Biol.* 29, 33–42. doi: 10.1016/S0965-1748(98)00102-7

Mao, H., McBlain, W. A., and Kaufman, W. R. (1995). Some Properties of the Ecdysteroid Receptor in the Salivary Gland of the Ixodid Tick, *Amblyomma Hebraeum*. *Gen. Comp. Endocrinol.* 99, 340–348. doi: 10.1006/gcen.1995.1118

Martin, C. J., Booty, M. G., Rosebrock, T. R., Nunes-Alves, C., Desjardins, D. M., Keren, I., et al. (2012). Efferocytosis Is an Innate Antibacterial Mechanism. *Cell Host Microbe* 12, 289–300. doi: 10.1016/j.chom.2012.06.010

Martins, L. A., Palmisano, G., Cortez, M., Kawahara, R., de Freitas Balanco, J. M., Fujita, A., et al. (2020). The Intracellular Bacterium *Rickettsia Rickettsii* Exerts an Inhibitory Effect on the Apoptosis of Tick Cells. *Parasit. Vectors* 13, 603. doi: 10.1186/s13071-020-04477-5

Mattila, J. T., Burkhardt, N. Y., Hutcheson, H. J., Munderloh, U. G., and Kurtti, T. J. (2007). Isolation of Cell Lines and a Rickettsial Endosymbiont From the Soft Tick *Carios Capensis* (Acari: Argasidae: Ornithodorinae). *J. Med. Entomol.* 44, 1091–1101. doi: 10.1093/jmedent/44.6.1091

McClure Carroll, E. E., Wang, X., Shaw, D. K., O'Neal, A. J., Oliva Chávez, A. S., Brown, L. J., et al. (2019). P47 Licenses Activation of the Immune Deficiency Pathway in the Tick *Ixodes Scapularis*. *Proc. Natl. Acad. Sci.* 116, 205–210. doi: 10.1073/pnas.1808905116

Menze, M. A., Fortner, G., Nag, S., and Hand, S. C. (2010). Mechanisms of Apoptosis in Crustacea: What Conditions Induce Versus Suppress Cell Death? *Apoptosis* 15, 293–312. doi: 10.1007/s10495-009-0443-6

Moura-Martiniano, N. O., Machado-Ferreira, E., Gazêta, G. S., and Soares, C. A. G. (2017). Relative Transcription of Autophagy-Related Genes in *Amblyomma Sculptum* and *Rhipicephalus Microplus* Ticks. *Exp. Appl. Acarol.* 73, 401–428. doi: 10.1007/s10493-017-0193-z

Munderloh, U. G., and Kurtti, T. J. (1989). Formulation of Medium for Tick Cell Culture. *Exp. Appl. Acarol.* 7, 219–229. doi: 10.1007/BF01194061

Niu, H., Kozjak-Pavlovic, V., Rudel, T., and Rikihisa, Y. (2010). *Anaplasma Phagocytophilum* Ats-1 Is Imported Into Host Cell Mitochondria and Interferes With Apoptosis Induction. *PloS Pathog.* 6, e1000774. doi: 10.1371/journal.ppat.1000774

Niu, H., Xiong, Q., Yamamoto, A., Hayashi-Nishino, M., and Rikihisa, Y. (2012). Autophagosomes Induced by a Bacterial Beclin 1 Binding Protein Facilitate Obligatory Intracellular Infection. *Proc. Natl. Acad. Sci. U. S. A.* 109, 20800–20807. doi: 10.1073/pnas.1218674109

Niu, H., Yamaguchi, M., and Rikihisa, Y. (2008). Subversion of Cellular Autophagy by *Anaplasma Phagocytophilum*. *Cell. Microbiol.* 10, 593–605. doi: 10.1111/j.1462-5822.2007.01068.x

Nunes, E. T., Bechara, G. H., Saito, K. C., Denardi, S. E., Oliveira, P. R., and Mathias, M. I. C. (2005). Morphological, Histological, and Ultrastructural Characterization of Degenerating Salivary Glands in Females of the Cattle-Tick *Rhipicephalus (Boophilus) Microplus* (CANESTRINI 1887) (Acari: Ixodidae). *Micron* 36, 437–447. doi: 10.1016/j.micron.2005.03.010

Patterson, L. L., Byerly, C. D., and McBride, J. W. (2021). Anaplasmataceae: Dichotomous Autophagic Interplay for Infection. *Front. Immunol.* 12. doi: 10.3389/fimmu.2021.642771

Ramphul, U. N., Garver, L. S., Molina-Cruz, A., Canepa, G. E., and Barillas-Mury, C. (2015). *Plasmodium Falciparum* Evades Mosquito Immunity by Disrupting JNK-Mediated Apoptosis of Invaded Midgut Cells. *Proc. Natl. Acad. Sci. U. S. A.* 112, 1273–1280. doi: 10.1073/pnas.1423586112

Riedl, S. J., and Salvesen, G. S. (2007). The Apoptosome: Signalling Platform of Cell Death. *Nat. Rev. Mol. Cell Biol.* 8, 405–413. doi: 10.1038/nrm2153

Romanelli, D., Casati, B., Franzetti, E., and Tettamanti, G. (2014). A Molecular View of Autophagy in Lepidoptera. *BioMed. Res. Int.* 2014, 1–11. doi: 10.1155/2014/902315

Rosendale, A. J., Dunlevy, M. E., McCue, M. D., and Benoit, J. B. (2019). Progressive Behavioural, Physiological and Transcriptomic Shifts Over the Course of Prolonged Starvation in Ticks. *Mol. Ecol.* 28, 49–65. doi: 10.1111/mec.14949

Rudel, T., Kepp, O., and Kozjak-Pavlovic, V. (2010). Interactions Between Bacterial Pathogens and Mitochondrial Cell Death Pathways. *Nat. Rev. Microbiol.* 8, 693–705. doi: 10.1038/nrmicro2421

Sahni, A., Narra, H. P., and Sahni, S. K. (2020). Activation of Mechanistic Target of Rapamycin (mTOR) in Human Endothelial Cells Infected With Pathogenic Spotted Fever Group Rickettsiae. *Int. J. Mol. Sci.* 21, 7179. doi: 10.3390/ijms21197179

Salje, J. (2021). Cells Within Cells: Rickettsiales and the Obligate Intracellular Bacterial Lifestyle. *Nat. Rev. Microbiol.* 19, 375–390. doi: 10.1038/s41579-020-00507-2

Scaife, H., Woldehiwet, Z., Hart, C. A., and Edwards, S. W. (2003). *Anaplasma Phagocytophilum* Reduces Neutrophil Apoptosis *In Vivo*. *Infect. Immun.* 71, 1995–2001. doi: 10.1128/IAI.71.4.1995-2001.2003

Scopinho Furquim, K. C., Bechara, G. H., and Camargo Mathias, M. I. (2008). Death by Apoptosis in Salivary Glands of Females of the Tick *Rhipicephalus Sanguineus* (Latreille 1806) (Acari: Ixodidae). *Exp. Parasitol.* 119, 152–163. doi: 10.1016/j.exppara.2008.01.021

Shaw, D. K., Wang, X., Brown, L. J., Chávez, A. S. O., Reif, K. E., Smith, A. A., et al. (2017). Infection-Derived Lipids Elicit an Immune Deficiency Circuit in Arthropods. *Nat. Commun.* 8, 14401. doi: 10.1038/ncomms14401

Sokolova, I. M. (2009). Apoptosis in Molluscan Immune Defense. *Invertebr. Surviv. J.* 6, 49–58.

Sonenshine, D., and Roe, R. M. (2013). *Biology of Ticks*, *2nd ed*, (New York: Oxford University Press).

Taatjes, D. J., Sobel, B. E., and Budd, R. C. (2008). Morphological and Cytochemical Determination of Cell Death by Apoptosis. *Histochem. Cell Biol.* 129, 33–43. doi: 10.1007/s00418-007-0356-9

Tafesh-Edwards, G., and Eleftherianos, I. (2020). JNK Signaling in Drosophila Immunity and Homeostasis. *Immunol. Lett.* 226, 7–11. doi: 10.1016/j.imlet.2020.06.017

Taylor, R. C., Cullen, S. P., and Martin, S. J. (2008). Apoptosis: Controlled Demolition at the Cellular Level. *Nat. Rev. Mol. Cell Biol.* 9, 231–241. doi: 10.1038/nrm2312

Tominello, T. R., Oliveira, E. R. A., Hussain, S. S., Elfert, A., Wells, J., Golden, B., et al. (2019). Emerging Roles of Autophagy and Inflammasome in Ehrlichiosis. *Front. Immunol.* 10. doi: 10.3389/FIMMU.2019.01011

Uchiyama, T., Kishi, M., and Ogawa, M. (2012). Restriction of the Growth of a Nonpathogenic Spotted Fever Group Rickettsia. *FEMS Immunol. Med. Microbiol.* 64, 42–47. doi: 10.1111/j.1574-695X.2011.00879.x

Umemiya, R., Matsuo, T., Hatta, T., Sakakibara, S., Boldbaatar, D., and Fujisaki, K. (2007). Cloning and Characterization of an Autophagy-Related Gene, ATG12, From the Three-Host Tick *Haemaphysalis Longicornis*. *Insect Biochem. Mol. Biol.* 37, 975–984. doi: 10.1016/j.ibmb.2007.05.006

Umemiya-Shirafuji, R., Galay, R. L., Maeda, H., Kawano, S., Tanaka, T., Fukumoto, S., et al. (2014). Expression Analysis of Autophagy-Related Genes in the Hard Tick *Haemaphysalis Longicornis*. *Vet. Parasitol.* 201, 169–175. doi: 10.1016/j.vetpar.2014.01.024

Umemiya-Shirafuji, R., Matsuo, T., Liao, M., Boldbaatar, D., Battur, B., Suzuki, H., et al. (2010). Increased Expression of ATG Genes During Nonfeeding Periods in the Tick *Haemaphysalis Longicornis*. *Autophagy* 6, 473–481. doi: 10.4161/auto.6.4.11668

Van Opdenbosch, N., and Lamkanfi, M. (2019). Caspases in Cell Death, Inflammation, and Disease. *Immunity* 50, 1352–1364. doi: 10.1016/j.immuni.2019.05.020

Villar, M., Ayllón, N., Alberdi, P., Moreno, A., Moreno, M., Tobes, R., et al. (2015). Integrated Metabolomics, Transcriptomics and Proteomics Identifies Metabolic Pathways Affected by *Anaplasma Phagocytophilum* Infection in Tick Cells. *Mol. Cell. Proteomics* 14, 3154–3172. doi: 10.1074/mcp.M115.051938

Vo, P. L. H., Ronda, C., Klompe, S. E., Chen, E. E., Acree, C., Wang, H. H., et al. (2021). CRISPR RNA-Guided Integrases for High-Efficiency, Multiplexed Bacterial Genome Engineering. *Nat. Biotechnol.* 39, 480–489. doi: 10.1038/s41587-020-00745-y

Voss, O. H., and Rahman, M. S. (2021). Rickettsia-Host Interaction: Strategies of Intracytosolic Host Colonization. *Pathog. Dis.* 79, ftab015. doi: 10.1093/femspd/ftab015

Wang, X.-R., Burkhardt, N. Y., Kurtti, T. J., Oliver, J. D., Price, L. D., Cull, B., et al. (2021). Mitochondrion-Dependent Apoptosis Is Essential for *Rickettsia Parkeri* Infection and Replication in Vector Cells. *mSystems* 6, e01209–20. doi: 10.1128/mSystems.01209-20

Wang, X.-R., Kurtti, T. J., Oliver, J. D., and Munderloh, U. G. (2020). The Identification of Tick Autophagy-Related Genes in *Ixodes Scapularis* Responding to Amino Acid Starvation. *Ticks Tick Borne Dis.* 11, 101402. doi: 10.1016/j.ttbdis.2020.101402

Wang, Z., and Li, C. (2020). Xenophagy in Innate Immunity: A Battle Between Host and Pathogen. *Dev. Comp. Immunol.* 109, 103693. doi: 10.1016/j.dci.2020.103693

Wang, Y., Zhang, H., Luo, L., Zhou, Y., Cao, J., Xuan, X., et al. (2021). ATG5 is Instrumental in the Transition From Autophagy to Apoptosis During the Degeneration of Tick Salivary Glands. *PloS Negl. Trop. Dis.* 15, e0009074. doi: 10.1371/journal.pntd.0009074

Wang, H., Zhang, X., Wang, X., Zhang, B., Wang, M., Yang, X., et al. (2018). Comprehensive Analysis of the Global Protein Changes That Occur During Salivary Gland Degeneration in Female Ixodid Ticks *Haemaphysalis Longicornis*. *Front. Physiol.* 9, 1943. doi: 10.3389/fphys.2018.01943

Wilke, A. B. B., and Marrelli, M. T. (2015). Paratransgenesis: A Promising New Strategy for Mosquito Vector Control. *Parasit. Vectors* 8, 342. doi: 10.1186/s13071-015-0959-2

Willingham, S. B., Bergstralh, D. T., O'Connor, W., Morrison, A. C., Taxman, D. J., Duncan, J. A., et al. (2007). Microbial Pathogen-Induced Necrotic Cell Death Mediated by the Inflammasome Components CIAS1/Cryopyrin/NLRP3 and ASC. *Cell Host Microbe* 2, 147–159. doi: 10.1016/j.chom.2007.07.009

Yu, X., Zhou, Y., Cao, J., Zhang, H., Gong, H., and Zhou, J. (2017). Caspase-1 Participates in Apoptosis of Salivary Glands in *Rhipicephalus Haemaphysaloides*. *Parasit. Vectors* 10, 225. doi: 10.1186/s13071-017-2161-1

Conflict of Interest: The authors declare that the research was conducted in the absence of any commercial or financial relationships that could be construed as a potential conflict of interest.

Publisher's Note: All claims expressed in this article are solely those of the authors and do not necessarily represent those of their affiliated organizations, or those of the publisher, the editors and the reviewers. Any product that may be evaluated in this article, or claim that may be made by its manufacturer, is not guaranteed or endorsed by the publisher.

frontiers in Cellular and Infection Microbiology

MINI REVIEW
published: 31 January 2022
doi: 10.3389/fcimb.2022.840802

In Vitro Modelling of *Chlamydia trachomatis* Infection in the Etiopathogenesis of Male Infertility and Reactive Arthritis

Simone Filardo[*†], *Marisa Di Pietro*[†], *Fabiana Diaco* and *Rosa Sessa*

Department of Public Health and Infectious Diseases, Section of Microbiology, University of Rome "Sapienza", Rome, Italy

Chlamydia trachomatis is an obligate, intracellular bacterium responsible for a range of diseases of public health importance, since *C. trachomatis* infection is often asymptomatic and, hence, untreated, leading to chronic complications, including prostatitis, infertility, and reactive arthritis. The ample spectrum of diseases caused by *C. trachomatis* infection is reflected in its ability to infect and multiply within a wide range of different cell types. Cervical epithelial cells, to date, have been the most studied cellular infection model, highlighting the peculiar features of the host-cell inflammatory and immune responses to the infection. Herein, we provide the up-to-date evidence on the interaction between *C. trachomatis* and human prostate epithelial, Sertoli and synovial cells.

Keywords: *Chlamydia trachomatis*, obligate intracellular bacteria, human prostate cells, human Sertoli cells, human synovial cells

OPEN ACCESS

Edited by:
Luís Jaime Mota, NOVA School of Science and Technology, Portugal

Reviewed by:
Daniel Alford Powell, University of Arizona, United States

****Correspondence:***
Simone Filardo
simone.filardo@uniroma1.it

†These authors have contributed equally to this work and share first authorship

Specialty section:
This article was submitted to Molecular Bacterial Pathogenesis, a section of the journal Frontiers in Cellular and Infection Microbiology

Received: *21 December 2021*
Accepted: *11 January 2022*
Published: *31 January 2022*

Citation:
Filardo S, Di Pietro M, Diaco F and Sessa R (2022) In Vitro Modelling of Chlamydia trachomatis Infection in the Etiopathogenesis of Male Infertility and Reactive Arthritis. Front. Cell. Infect. Microbiol. 12:840802. doi: 10.3389/fcimb.2022.840802

INTRODUCTION

Chlamydia trachomatis, obligate, intracellular bacterium responsible for a range of diseases of public health importance, is the leading cause of sexually transmitted bacterial infection worldwide, with estimates of more than 130 million new cases each year (Rowley et al., 2019). In women, the most common clinical manifestations are cervicitis and urethritis, whereas in men these are urethritis and epididymitis, although in the majority of cases *C. trachomatis* genital infection is asymptomatic and, hence, untreated, leading to chronic complications, including prostatitis, infertility, and reactive arthritis (ReA) (O'Connell and Ferone, 2016; Di Pietro et al., 2019).

Prostatitis, one of the most common urologic problems for men younger than 50 years, and risk factor for infertility (Khan et al., 2017), has a prevalence of approximately 8% to 16%, and around 5% to 10% of all cases have a bacterial origin, with *C. trachomatis* involved in up to 27% of all bacterial infections of the prostate (Ostaszewska et al., 1998; Badalyan et al., 2003; Krieger et al., 2008; Ouzounova-Raykova et al., 2010; Trinchieri et al., 2021). Nevertheless, chronic bacterial prostatitis is frequently underestimated because urinary tract infections often remain undocumented and thus neglected (Ouzounova-Raykova et al., 2010). Male infertility also remains a neglected area in sexual and reproductive health although it has a significant impact on public health worldwide, since approximately 15-20% of reproductive age couples are infertile in industrialized countries, and, in 30% of all cases, fertility problems are solely due to the male partner, with around 15% of idiopathic cases attributed to infectious causes (Henkel et al., 2021; Thoma et al., 2021). Similarly,

ReA is a frequently misdiagnosed condition, due to difficulties in relating past infections with compromised joint functions. It is estimated that approximately 4–8% of patients will develop ReA one to six weeks after a urogenital *C. trachomatis* infection, and in 30% of all cases, ReA persists for years, leading, eventually, to joint deformities and ankylosis (Zeidler and Hudson, 2016; Di Pietro et al., 2019; Henkel et al., 2021).

The ample spectrum of diseases caused by *C. trachomatis* infection is reflected in its ability to infect and multiply within a wide range of different cell types, such as cervical epithelial cells, peripheral blood mononuclear cells (Dolat and Valdivia, 2019; Lausen et al., 2019). The typical model of chlamydial intracellular development has been mostly investigated in human cervical epithelial cells (HeLa) and murine fibroblasts (McCoy), for which *C. trachomatis* possesses the highest tropism (Belland et al., 2003; Guseva et al., 2007; Vromman et al., 2014; Petyaev et al., 2017; Sessa et al., 2017a; Filardo et al., 2019a; Liang and Mahony, 2019; Jøraholmen et al., 2020). *C. trachomatis* developmental cycle occurs entirely within a cell-derived membrane bound vesicle termed inclusion, where Chlamydiae alternate between the elementary body (EB), the extracellular and infectious form, and the reticulate body (RB), the metabolically active form, responsible for intracellular replication (AbdelRahman and Belland, 2005). The first stage of chlamydial developmental cycle consists in EBs adhesion to host cell membrane receptors, like glycosaminoglycans (Conant and Stephens, 2007). Then, chlamydial EBs enter the host cell by endocytosis, *via* a two-step process involving a reversible interaction mediated by heparin-sulphate proteoglycans followed by irreversible binding to host receptors (Conant and Stephens, 2007). Soon after attachment to the host cell, EBs are internalized and confined to the inclusion, where they differentiate to RBs; within 24 hours post-infection (h.p.i.), chlamydial RBs replicate by binary fission (Bastidas et al., 2013). As inclusion expands, approximately 24-48 h.p.i., the majority of RBs begin to transition back to EBs in an asynchronous process (AbdelRahman and Belland, 2005). At the end of the developmental cycle, at about 48 h.p.i., the EBs are finally released from the host by cell lysis or extrusion (Yang et al., 2015; Zuck et al., 2016). Thereafter, a multitude of infectious EBs spread and infect neighboring cells, perpetuating the infectious process.

To date, the human cervical epithelial cell has been the most studied cellular infection model, focusing on chlamydial growth and on the peculiar features of the host-cell inflammatory and immune responses to the infection (Lad et al., 2005; Sessa et al., 2017b; Tang et al., 2021). Following chlamydial infection, the host cell response typically begins with the activation of a complex network of immune receptors (TLR2 and TR4) and their respective downstream signaling pathways (myeloid differentiation primary response 88, MyD88, and nuclear factor kappa-light-chain-enhancer of activated B cells, NFkB) (O'Connell et al., 2006; Sellami et al., 2014). This results in the induction of proinflammatory cytokines, involved in either the elimination of *C. trachomatis* or tissue damage related to chronic inflammatory state, including interleukin (IL)-1α, IL-6, IL-8 and interferon (IFN)-γ (O'Connell et al., 2006; Rey-Ladino et al., 2014; Sellami et al., 2014). IFN-γ, in particular, has been identified as a major player in the clearance and protection against *C. trachomatis* infection, by modulating a plethora of host cell signalling pathways, like the activation of NF-kB and the inflammasome network (Rothfuchs et al., 2004; Webster et al., 2017).

Overall, the pathogenic mechanisms underlying *C. trachomatis*-mediated chronic complications have received the most research attention in women, whereas chlamydial survival strategies as well as the host defense pathways, involved in the onset and development of prostatitis, male infertility, and reactive arthritis, are now beginning to emerge. Therefore, herein we provide the up-to-date evidence on the interaction between *C. trachomatis* and human prostate epithelial, Sertoli and synovial cells.

C. TRACHOMATIS INFECTION MODELS IN PROSTATITIS, MALE INFERTILITY AND REACTIVE ARTHRITIS

Human Prostate Epithelial Cells

The first evidence to demonstrate *C. trachomatis* growth within primary human prostate epithelial cells came from Greenberg et al, in 1985 (Greenberg et al., 1985). Since then, few studies on chlamydial interaction with prostate epithelial cells were performed, describing both the ability of *C. trachomatis* to replicate in these cells and the specific host-cell inflammatory and immune pathways in response to the infection. Specifically, a study investigating the inflammatory profile of *C. trachomatis* infection in humane prostate epithelial cells (PNT2) and urethral epithelial cells (THUEC), demonstrated that prostate epithelial cells produced larger quantities of IL-6 and IL-8 than urethral epithelial cells, suggesting the increased levels of these cytokines as possible markers for *C. trachomatis* infection of the prostate (Al-Mously and Eley, 2007).

At a later time, a potential link between the inflammatory damage and *C. trachomatis* infection of the prostate was suggested, since a strong pro-inflammatory response, characterized by NFkB activation and TLR2/TLR4 upregulation, was observed, leading to increased inflammatory cytokine expression, like IL-6, IL-8, IL-1β and tumor necrosis factor (TNF)α (Sellami et al., 2014). Lastly, a recent study has described the efficient propagation of *C. trachomatis* in a malignant prostate epithelial cell line (CWR-R1) (proportion of infected cells 28.1%) accompanied by enhanced transcription of IL-6 and fibroblast growth factor (FGF)-2 genes, encoding two important pro-inflammatory cytokines involved in the progression of prostate cancer (Petyaev et al., 2019).

Human Sertoli Cells

In recent years, a study employing a murine model has postulated the direct infection of the seminiferous tubule epithelium, formed by Sertoli cells, as an interesting

pathophysiological mechanism for *C. trachomatis*-mediated male infertility, leading to compromised spermatogenesis with reduced sperm count, motility and altered morphology of mature spermatozoa (Bryan et al., 2021).

On this basis, we have investigated, for the first time, the interaction between *C. trachomatis* and human primary Sertoli cells *in vitro*, demonstrating a distinct growth profile of *C. trachomatis*, with a very long eclipse period (after 36 h.p.i.), the appearance of infectious EBs beyond 48 h.p.i., the persistence of inclusions up to 96 h.p.i. and a low infection efficiency (Filardo et al., 2019b). This greatly differed from the chlamydial growth cycle as typically seen in cervical epithelial cells, where the transition of RBs to EBs happen after 22 h.p.i. and the release of infectious EBs from host cells is usually observed 36 to 48 h.p.i. (Guseva et al., 2007; Vromman et al., 2014; Skilton et al., 2018). Of great pathological importance, the development of *C. trachomatis* inclusions has also been demonstrated to visibly damage the host cell cytoskeleton, as shown by the reorganization of Vimentin-based intermediate filaments and α-tubulin microtubules in thick fibres surrounding chlamydial inclusions (Filardo et al., 2019b). This, in turn, might alter the integrity of the blood-testis barrier, a structural compartment of the seminiferous tubules essential for germ cell development and maturation, impairing the spermatogenesis and contributing to male infertility (Mruk and Cheng, 2015). On this regard, the evidence that human spermatozoa were unaffected by biomolecules produced by chlamydial infected Sertoli cells, suggests that *C. trachomatis* is more likely to influence the early stages leading to the development of mature spermatozoa.

In addition to structural damage, *C. trachomatis* was also demonstrated to modulate the immune response in human Sertoli cells, characterized by the activation of TLR3 alongside the down-modulation of downstream signaling pathways, namely NFκB and interferon regulatory factor (IRF)3 (Di Pietro et al., 2020a). Consequently, IFNs type-I and type-II, IL-1α and IL-6 were not produced, suggesting that *C. trachomatis* could evade the host immune-mediated killing, surviving in the cells and damaging the testicular tissue.

Human Synovial Cells

The interaction between *C. trachomatis* and human synovial cells was investigated in 1998 by Rödel et al., showing, for the first time, the ability of *C. trachomatis* to infect fibroblast-like cells derived from biopsies of the synovial membrane (Rödel et al., 1998a). Then, *C. trachomatis* infection of synovial cells was also demonstrated to elicit the production of several pro-inflammatory cytokines, such as IL-6 and IFN-β (Rödel et al., 1998b).

Since then, few studies have further researched this interaction, detailing some cellular mechanisms underlying the synovial cell immune response to chlamydial infection. In particular, increased production of IRF1 and interferon-stimulated gene factor (ISGF)-3γ was observed in synovial cells infected with *C. trachomatis*, leading to the production of IFNβ as well as to the upregulation of Human Leukocyte Antigen (HLA)-1 gene expression (Rödel et al., 1999).

In recent years, the unique morphology, and the peculiar growth cycle of chlamydial inclusions in a primary human synovial cell have been described, and differed significantly from those in cervical epithelial cells. In particular, *C. trachomatis* was characterized by heterogeneous shape and size of inclusions and by a delayed developmental cycle, with late appearing infectious EBs (after 36 h.p.i.), as well as by a lower infection efficiency (Filardo et al., 2021).

The investigation of synovial cell immune response toward *C. trachomatis* evidenced a distinct profile characterized by the activation of TLR3 and TLR2 as well as of downstream signaling molecules, like ISG56 and Guanylate Binding Protein (GBP)1, interferon-inducible proteins involved in the cell-autonomous immunity against intracellular bacteria (MacMicking, 2012; Di Pietro et al., 2020b; Honkala et al., 2020). Nevertheless, the synovial cell response to *C. trachomatis* seemed ineffective in controlling the infection, suggesting its potential evasion of synovial cell inflammatory pathways (Filardo et al., 2021). Indeed, the increased expression of caspase-1 gene, in *Chlamydia* infected synovial cells, did not induce a parallel increase in the production of IL-6 as well as IL-1β and IL-18. A further interesting evidence is the observation that caspase activation played an important role in the intracellular growth of *C. trachomatis* in synovial cells, as demonstrated by decreased chlamydial replication after caspase inhibition (Filardo et al., 2021).

Differently, synovial cells were demonstrated to be able to control chlamydial infection when exposed to IFNγ, a well-known pro-inflammatory cytokine involved in the clearance of *C. trachomatis* genital infection. In particular, IFNγ was demonstrated to inhibit chlamydial growth decreasing caspase-1 gene expression while, at the same time, inducing TLR2 and ISG56 gene expression and IL1β, IL-18 and IL-6 production, suggesting the key role of IFNγ for the modulation of inflammatory and immune responses of synovial cells toward *C. trachomatis* (Di Pietro et al., 2020b).

DISCUSSION

Research to elucidate how *C. trachomatis* interact with specific cells of the prostate, male genital tract and joints is fundamental to understand how these interactions influence disease outcomes. To date, the available data provide insights regarding *C. trachomatis* growth within human prostate epithelial, Sertoli and synovial cells, and the related host-cell response pathways (**Figure 1**).

Human prostate epithelial cells showed a similar progression of chlamydial intracellular developmental cycle as that observed in cervical epithelial cells, alongside a comparable infection efficiency (Petyaev et al., 2019). By contrast, in Sertoli and synovial cells, the duration of the different *C. trachomatis* developmental stages, as well as the number of infectious EBs released from host cells, greatly differed as compared to those observed in cervical epithelial cells, routinely used for chlamydial research (Filardo et al., 2019b). The late appearances of infectious

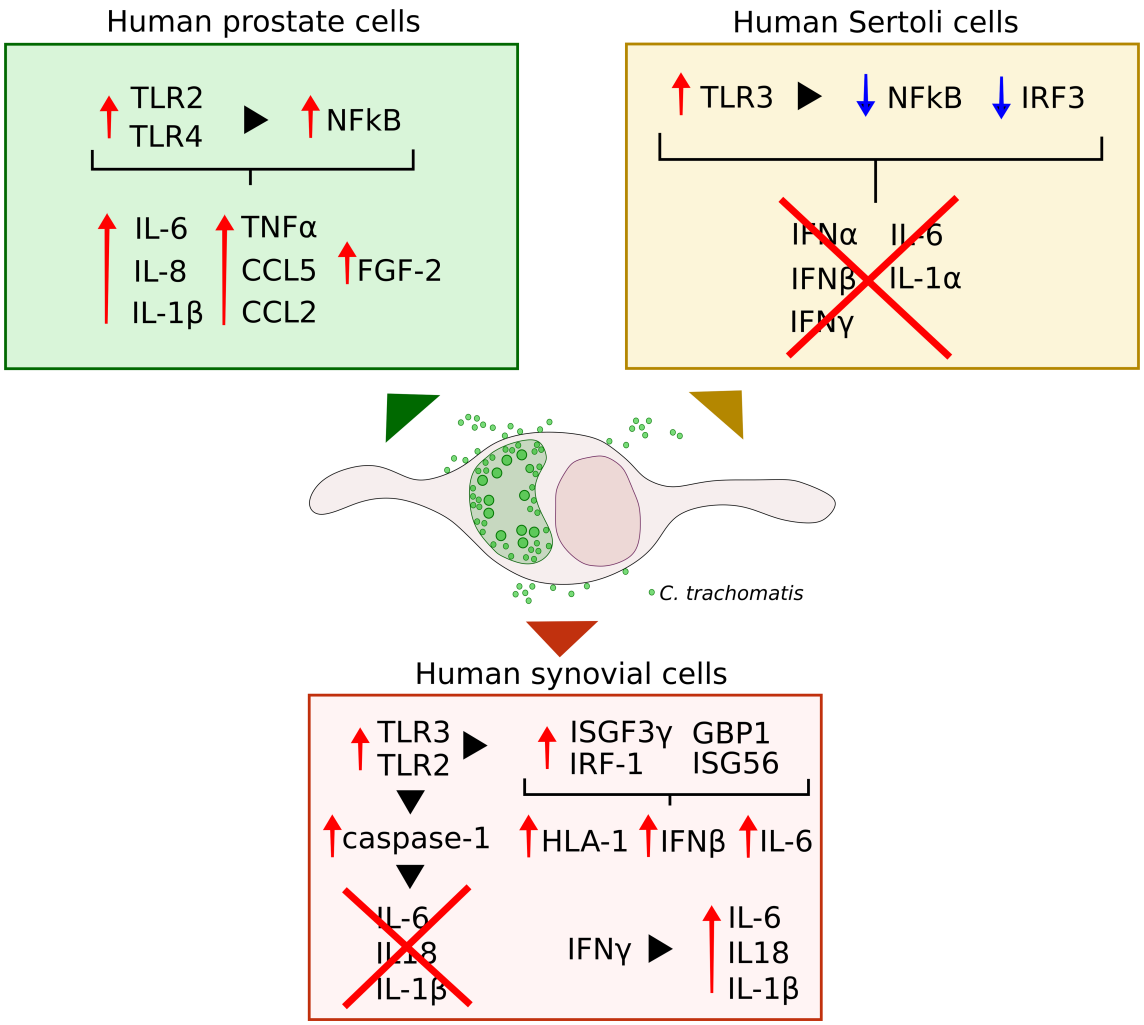

FIGURE 1 | Schematic representation of the immune and inflammatory pathways elicited by *C. trachomatis* infection of human prostate epithelial, Sertoli and synovial cells.

EBs toward the end of the developmental cycle suggests the presence of hostile cellular environment that may partially hinder chlamydial intracellular growth in these cells. In addition, the lower infection efficiency of *C. trachomatis*, previously described, in human Sertoli and synovial cells as compared to prostate epithelial cells, highlights that the prostate is particularly susceptible to *C. trachomatis* infection and, hence, could represent a trojan horse for the subsequent dissemination in the host, including the epididymis/testis or the joint.

Important differences were also observed in the immune and inflammatory host cell responses to *C. trachomatis* infection, with the activation of different molecular sensors, downstream signalling pathways and inflammatory signatures. Indeed, human prostate cells recognition of *C. trachomatis* by TLR2/TLR4 induced a pro-inflammatory state, highlighted by increased levels of IL-1β, IL-6, IL-8 and TNFα (Sellami et al., 2014; Petyaev et al., 2019). By contrast, TLR3-mediated sensing of chlamydial infection in human Sertoli cells did not elicit the activation of the related pathways, namely NFkB and IRF3, as well as the subsequent cytokine production. These results hint that in human prostate epithelial cells inflammation may play a key role in the pathogenesis of *C. trachomatis*-mediated tissue damage and prostate cancer progression. Instead, in Sertoli cells, *C. trachomatis* might induce direct cell-damage, as evidenced by the alteration of host-cell cytoskeleton, and, at the same time, remain within the cell for a long time, leading to a chronic infection. Indeed, in Sertoli cells, *C. trachomatis* appears to modulate the innate immune response, evading, hence, the host immune-mediate killing (Di Pietro et al., 2020a).

A further evasion strategy from host-cell defence pathways was also described in human synovial cells, as shown by *C. trachomatis* hijack of caspase-1 mediated inflammasome network, inhibiting the production of IL-6 as well as Il-1β and IL-18, involved in pyroptosis, a cellular defence mechanism against infectious agents (Man et al., 2017; Filardo et al., 2021).

Surprisingly, earlier reports demonstrated the induction of a pro-inflammatory state in human synovial cells infected by *C. trachomatis*, evidenced by increased IL-6 levels (Rödel et al., 1998b; Rödel et al., 1999), whereas our recent studies evidenced a significant increase in pro-inflammatory cytokine levels following the exposure to IFNγ (Di Pietro et al., 2020b). These discordant results may be dependent on several factors, like, for example, the *C. trachomatis* serovar, since early reports used *C. trachomatis* serovar E, whereas the serovar D was investigated in recent studies (Rödel et al., 1998b; Filardo et al., 2021). The serotype D and E have also been used in studies involving Sertoli and prostate epithelial cells (Greenberg et al., 1985; Al-Mously and Eley, 2007; Filardo et al., 2019b; Di Pietro et al., 2020a); the lymphogranuloma venereum serovar L2 was used in prostate malignant cells (Sellami et al., 2014; Petyaev et al., 2019).

Overall, the path ahead is still long, and, in the future, more complex approaches with 3D cell cultures and organoids will be helpful for shedding light on the etiopathogenesis of *C. trachomatis*-mediated prostatitis, male infertility, and reactive arthritis, since many cell signalling pathways, that might have been elicited in response to chlamydial infection, are still unexplored.

AUTHOR CONTRIBUTIONS

MDP and RS conceived the manuscript. SF and FD performed literature review. SF, MDP, and RS wrote the original manuscript. SF, MDP, and RS revised the manuscript. SF and FD designed the Figure. All authors approved the submitted version.

FUNDING

This research was funded by the University of Rome "Sapienza" to Prof. Rosa Sessa (grant RP11916B6AEB0D37).

REFERENCES

AbdelRahman, Y. M., and Belland, R. J. (2005). The Chlamydial Developmental Cycle: Figure 1. *FEMS Microbiol. Rev.* 29, 949–959. doi: 10.1016/j.femsre.2005.03.002

Al-Mously, N., and Eley, A. (2007). Interaction of Chlamydia Trachomatis Serovar E With Male Genital Tract Epithelium Results in Secretion of Proinflammatory Cytokines. *J. Med. Microbiol.* 56, 1025–1032. doi: 10.1099/jmm.0.47241-0

Badalyan, R. R., Fanarjyan, S. V., and Aghajanyan, I. G. (2003). Chlamydial and Ureaplasmal Infections in Patients With Nonbacterial Chronic Prostatitis. *Andrologia* 35, 263–265. doi: 10.1046/j.1439-0272.2003.00582.x

Bastidas, R. J., Elwell, C. A., Engel, J. N., and Valdivia, R. H. (2013). Chlamydial Intracellular Survival Strategies. *Cold Spring Harbor Perspect. Med.* 3, a010256–a010256. doi: 10.1101/cshperspect.a010256

Belland, R. J., Zhong, G., Crane, D. D., Hogan, D., Sturdevant, D., Sharma, J., et al. (2003). Genomic Transcriptional Profiling of the Developmental Cycle of Chlamydia Trachomatis. *Proc. Natl. Acad. Sci.* 100, 8478–8483. doi: 10.1073/pnas.1331135100

Bryan, E. R., Barrero, R. A., Cheung, E., Tickner, J. A. D., Trim, L. K., Richard, D., et al. (2021). DNA Damage Contributes to Transcriptional and Immunological Dysregulation of Testicular Cells During Chlamydia Infection. *Am. J. Reprod. Immunol.* 86. doi: 10.1111/aji.13400

Conant, C. G., and Stephens, R. S. (2007). Chlamydia Attachment to Mammalian Cells Requires Protein Disulfide Isomerase. *Cell. Microbiol.* 9, 222–232. doi: 10.1111/j.1462-5822.2006.00783.x

Di Pietro, M., Filardo, S., Alfano, V., Pelloni, M., Splendiani, E., Po, A., et al. (2020a). Chlamydia Trachomatis Elicits TLR3 Expression But Disrupts the Inflammatory Signaling Down-Modulating Nfκb and IRF3 Transcription Factors in Human Sertoli Cells. *J. Biol. Regul. Homeost. Agents* 34, 977–986. doi: 10.23812/20-80-A-29

Di Pietro, M., Filardo, S., Frasca, F., Scagnolari, C., Manera, M., Sessa, V., et al. (2020b). Interferon-γ Possesses Anti-Microbial and Immunomodulatory Activity on a Chlamydia Trachomatis Infection Model of Primary Human Synovial Fibroblasts. *Microorganisms* 8. doi: 10.3390/microorganisms8020235

Di Pietro, M., Filardo, S., Romano, S., and Sessa, R. (2019). Chlamydia Trachomatis and Chlamydia Pneumoniae Interaction With the Host: Latest Advances and Future Prospective. *Microorganisms* 7. doi: 10.3390/microorganisms7050140

Dolat, L., and Valdivia, R. H. (2019). A Renewed Tool Kit to Explore Chlamydia Pathogenesis: From Molecular Genetics to New Infection Models. *F1000Research* 8. doi: 10.12688/f1000research.18832.1

Filardo, S., Di Pietro, M., Frasca, F., Diaco, F., Scordio, M., Antonelli, G., et al. (2021). Potential Ifnγ Modulation of Inflammasome Pathway in Chlamydia Trachomatis Infected Synovial Cells. *Life* 11, 1359. doi: 10.3390/life11121359

Filardo, S., Di Pietro, M., Tranquilli, G., and Sessa, R. (2019a). Biofilm in Genital Ecosystem: A Potential Risk Factor for Chlamydia Trachomatis Infection. *Can. J. Infect. Dis. Med. Microbiol.* 2019. doi: 10.1155/2019/1672109

Filardo, S., Skilton, R. J., O'Neill, C. E., Di Pietro, M., Sessa, R., and Clarke, I. N. (2019b). Growth Kinetics of Chlamydia Trachomatis in Primary Human Sertoli Cells. *Sci. Rep.* 9. doi: 10.1038/s41598-019-42396-3

Greenberg, S. B., Harris, D., Giles, P., Martin, R. R., and Wallace, R. J. (1985). Inhibition of Chlamydia Trachomatis Growth in McCoy, HeLa, and Human Prostate Cells by Zinc. *Antimicrob Agents Chemother* 27, 953–957. doi: 10.1128/AAC.27.6.953

Guseva, N. V., Dessus-Babus, S., Moore, C. G., Whittimore, J. D., and Wyrick, P. B. (2007). Differences in *Chlamydia Trachomatis* Serovar E Growth Rate in Polarized Endometrial and Endocervical Epithelial Cells Grown in Three-Dimensional Culture. *Infect Immun.* 75, 553–564. doi: 10.1128/IAI.01517-06

Henkel, R., Offor, U., and Fisher, D. (2021). The Role of Infections and Leukocytes in Male Infertility. *Andrologia* 53. doi: 10.1111/and.13743

Honkala, A. T., Tailor, D., and Malhotra, S. V. (2020). Guanylate-Binding Protein 1: An Emerging Target in Inflammation and Cancer. *Front. Immunol.* 10. doi: 10.3389/fimmu.2019.03139

Jøraholmen, M. W., Johannessen, M., Gravningen, K., Puolakkainen, M., Acharya, G., Basnet, P., et al. (2020). Liposomes-In-Hydrogel Delivery System Enhances the Potential of Resveratrol in Combating Vaginal Chlamydia Infection. *Pharmaceutics* 12. doi: 10.3390/pharmaceutics12121203

Khan, F. U., Ihsan, A. U., Khan, H. U., Jana, R., Wazir, J., Khongorzul, P., et al. (2017). Comprehensive Overview of Prostatitis. *Biomed Pharmacother* 94, 1064–1076. doi: 10.1016/j.biopha.2017.08.016

Krieger, J. N., Lee, S. W. H., Jeon, J., Cheah, P. Y., Liong, M. L., and Riley, D. E. (2008). Epidemiology of Prostatitis. *Int. J. Antimicrob. Agents* 31, 85–90. doi: 10.1016/j.ijantimicag.2007.08.028

Lad, S. P., Fukuda, E. Y., Li, J., de la Maza, L. M., and Li, E. (2005). Up-Regulation of the JAK/STAT1 Signal Pathway During Chlamydia Trachomatis Infection. *J. Immunol.* 174, 7186–7193. doi: 10.4049/jimmunol.174.11.7186

Lausen, M., Christiansen, G., Bouet Guldbæk Poulsen, T., and Birkelund, S. (2019). Immunobiology of Monocytes and Macrophages During Chlamydia Trachomatis Infection. *Microbes Infect* 21, 73–84. doi: 10.1016/j.micinf.2018.10.007

Liang, S., and Mahony, J. B. (2019). Enumeration of Viable Chlamydia From Infected Animals Using Immunofluorescent Microscopy. *Methods Mol. Biol. (Clifton N.J.)* 2042, 237–244. doi: 10.1007/978-1-4939-9694-0_16

MacMicking, J. D. (2012). Interferon-Inducible Effector Mechanisms in Cell-Autonomous Immunity. *Nat. Rev. Immunol.* 12, 367–382. doi: 10.1038/nri3210

Man, S. M., Karki, R., and Kanneganti, T.-D. (2017). Molecular Mechanisms and Functions of Pyroptosis, Inflammatory Caspases and Inflammasomes in Infectious Diseases. *Immunol. Rev.* 277, 61–75. doi: 10.1111/imr.12534

Mruk, D. D., and Cheng, C. Y. (2015). The Mammalian Blood-Testis Barrier: Its Biology and Regulation. *Endocr Rev.* 36, 564–591. doi: 10.1210/er.2014-1101

O'Connell, C. M., and Ferone, M. E. (2016). Chlamydia Trachomatis Genital Infections. *Microb Cell (Graz Austria)* 3. doi: 10.15698/mic2016.09.525

O'Connell, C. M., Ionova, I. A., Quayle, A. J., Visintin, A., and Ingalls, R. R. (2006). Localization of TLR2 and MyD88 to Chlamydia Trachomatis Inclusions. *J. Biol. Chem.* 281, 1652–1659. doi: 10.1074/jbc.M510182200

Ostaszewska, I., Zdrodowska-Stefanow, B., Badyda, J., Pucilo, K., Trybula, J., and Bulhak, V. (1998). Chlamydia Trachomatis : Probable Cause of Prostatitis. *Int. J. STD AIDS* 9, 350–353. doi: 10.1258/0956462981922395

Ouzounova-Raykova, V., Ouzounova, I., and Mitov, I. G. (2010). May Chlamydia Trachomatis be an Aetiological Agent of Chronic Prostatic Infection? *Andrologia* 42, 176–181. doi: 10.1111/j.1439-0272.2009.00973.x

Petyaev, I. M., Zigangirova, N. A., Morgunova, E. Y., Kyle, N. H., Fedina, E. D., and Bashmakov, Y. K. (2017). Resveratrol Inhibits Propagation of *Chlamydia Trachomatis* in McCoy Cells. *BioMed. Res. Int.* 2017, 1–7. doi: 10.1155/2017/4064071

Petyaev, I. M., Zigangirova, N. A., Morgunova, E. Y., Kyle, N. H., Fedina, E. D., and Bashmakov, Y. K. (2019). *Chlamydia Trachomatis* Growth and Cytokine mRNA Response in a Prostate Cancer Cell Line. *Adv. Urol.* 2019, 1–8. doi: 10.1155/2019/6287057

Rey-Ladino, J., Ross, A. G., and Cripps, A. W. (2014). Immunity, Immunopathology, and Human Vaccine Development Against Sexually Transmitted *Chlamydia Trachomatis*. *Hum. Vaccines Immunotherapeutics* 10, 2664–2673. doi: 10.4161/hv.29683

Rödel, J., Groh, A., Vogelsang, H., Lehmann, M., Hartmann, M., and Straube, E. (1998a). Beta Interferon Is Produced by Chlamydia Trachomatis -Infected Fibroblast-Like Synoviocytes and Inhibits Gamma Interferon-Induced HLA-DR Expression. *Infect Immun.* 66, 4491–4495. doi: 10.1128/IAI.66.9.4491-4495.1998

Rödel, J., Groh, A., Hartmann, M., Schmidt, K.-H., Lehmann, M., Lungershausen, W., et al. (1999). Expression of Interferon Regulatory Factors and Indoleamine 2,3-Dioxygenase in Chlamydia Trachomatis- Infected Synovial Fibroblasts. *Med. Microbiol. Immunol.* 187, 205–212. doi: 10.1007/s004300050094

Rödel, J., Straube, E., Lungershausen, W., Hartmann, M., and Groh, A. (1998b). Secretion of Cytokines by Human Synoviocytes During In Vitro Infection With Chlamydia Trachomatis. *J. Rheumatol.* 25, 2161–2168.

Rothfuchs, A. G., Trumstedt, C., Wigzell, H., and Rottenberg, M. E. (2004). Intracellular Bacterial Infection-Induced IFN-γ Is Critically But Not Solely Dependent on Toll-Like Receptor 4-Myeloid Differentiation Factor 88-IFN-αβ-STAT1 Signaling. *J. Immunol.* 172, 6345–6353. doi: 10.4049/jimmunol.172.10.6345

Rowley, J., vander Hoorn, S., Korenromp, E., Low, N., Unemo, M., Abu-Raddad, L. J., et al. (2019). Chlamydia, Gonorrhoea, Trichomoniasis and Syphilis: Global Prevalence and Incidence Estimate. *Bull. World Health Organ.* 97. doi: 10.2471/BLT.18.228486

Sellami, H., Said-Sadier, N., Znazen, A., Gdoura, R., Ojcius, D. M., and Hammami, A. (2014). Chlamydia Trachomatis Infection Increases the Expression of Inflammatory Tumorigenic Cytokines and Chemokines as Well as Components of the Toll-Like Receptor and NF-κb Pathways in Human Prostate Epithelial Cells. *Mol. Cell. Probes* 28, 147–154. doi: 10.1016/j.mcp.2014.01.006

Sessa, R., Di Pietro, M., Filardo, S., Bressan, A., Mastromarino, P., Biasucci, A. V., et al. (2017a). Lactobacilli-Lactoferrin Interplay in Chlamydia Trachomatis Infection. *Pathog. Dis.* 75. doi: 10.1093/femspd/ftx054

Sessa, R., Di Pietro, M., Filardo, S., Bressan, A., Rosa, L., Cutone, A., et al. (2017b). Effect of Bovine Lactoferrin on Chlamydia Trachomatis Infection and Inflammation. *Biochem. Cell Biol.* 95, 34–40. doi: 10.1139/bcb-2016-0049

Skilton, R. J., Wang, Y., O'Neill, C., Filardo, S., Marsh, P., Bénard, A., et al. (2018). The Chlamydia Muridarum Plasmid Revisited: New Insights Into Growth Kinetics [Version 1; Referees: 2 Approved, 1 Approved With Reservations]. *Wellcome Open Res.* 3. doi: 10.12688/wellcomeopenres.13905.1

Tang, C., Liu, C., Maffei, B., Niragire, B., Cohen, H., Kane, A., et al. (2021). Primary Ectocervical Epithelial Cells Display Lower Permissivity to Chlamydia Trachomatis Than HeLa Cells and a Globally Higher Pro-Inflammatory Profile. *Sci. Rep.* 11, 5848. doi: 10.1038/s41598-021-85123-7

Thoma, M., Fledderjohann, J., Cox, C., and Kantum Adageba, R. (2021). "Biological and Social Aspects of Human Infertility: A Global Perspective," in *Oxford Research Encyclopedia of Global Public Health* (Oxford, UK: Oxford University Press). doi: 10.1093/acrefore/9780190632366.013.184

Trinchieri, A., Abdelrahman, K. M., Bhatti, K. H., Bello, J. O., Das, K., Gatsev, O., et al. (2021). Spectrum of Causative Pathogens and Resistance Rates to Antibacterial Agents in Bacterial Prostatitis. *Diagnostics* 11, 1333. doi: 10.3390/diagnostics11081333

Vromman, F., Laverrière, M., Perrinet, S., Dufour, A., and Subtil, A. (2014). Quantitative Monitoring of the Chlamydia Trachomatis Developmental Cycle Using GFP-Expressing Bacteria, Microscopy and Flow Cytometry. *PloS One* 9, e99197. doi: 10.1371/journal.pone.0099197

Webster, S. J., Brode, S., Ellis, L., Fitzmaurice, T. J., Elder, M. J., Gekara, N. O., et al. (2017). Detection of a Microbial Metabolite by STING Regulates Inflammasome Activation in Response to Chlamydia Trachomatis Infection. *PloS Pathog.* 13, e1006383. doi: 10.1371/journal.ppat.1006383

Yang, C., Starr, T., Song, L., Carlson, J. H., Sturdevant, G. L., Beare, P. A., et al. (2015). Chlamydial Lytic Exit From Host Cells Is Plasmid Regulated. *mBio* 6. doi: 10.1128/mBio.01648-15

Zeidler, H., and Hudson, A. (2016). Coinfection of Chlamydiae and Other Bacteria in Reactive Arthritis and Spondyloarthritis: Need for Future Research. *Microorganisms* 4, 30. doi: 10.3390/microorganisms4030030

Zuck, M., Sherrid, A., Suchland, R., Ellis, T., and Hybiske, K. (2016). Conservation of Extrusion as an Exit Mechanism for *Chlamydia*. *Pathog. Dis.* 74, ftw093. doi: 10.1093/femspd/ftw093

Conflict of Interest: The authors declare that the research was conducted in the absence of any commercial or financial relationships that could be construed as a potential conflict of interest.

Publisher's Note: All claims expressed in this article are solely those of the authors and do not necessarily represent those of their affiliated organizations, or those of the publisher, the editors and the reviewers. Any product that may be evaluated in this article, or claim that may be made by its manufacturer, is not guaranteed or endorsed by the publisher.

frontiers in Cellular and Infection Microbiology

MINI REVIEW
published: 10 February 2022
doi: 10.3389/fcimb.2022.828784

Preclinical Animal Models for Q Fever Vaccine Development

Mahelat Tesfamariam[†], *Picabo Binette*[†] *and Carrie Mae Long*[*]

Laboratory of Bacteriology, Division of Intramural Research, National Institute of Allergy and Infectious Diseases, National Institutes of Health, Hamilton, MT, United States

Coxiella burnetii is a zoonotic pathogen responsible for the human disease Q fever. While an inactivated whole cell vaccine exists for this disease, its widespread use is precluded by a post vaccination hypersensitivity response. Efforts for the development of an improved Q fever vaccine are intricately connected to the availability of appropriate animal models of human disease. Accordingly, small mammals and non-human primates have been utilized for vaccine-challenge and post vaccination hypersensitivity modeling. Here, we review the animal models historically utilized in Q fever vaccine development, describe recent advances in this area, discuss the limitations and strengths of these models, and summarize the needs and criteria for future modeling efforts. In summary, while many useful models for Q fever vaccine development exist, there remains room for growth and expansion of these models which will in turn increase our understanding of *C. burnetii* host interactions.

Keywords: *Coxiella burnetii*, Q fever, vaccine, animal modeling, guinea pig, bacterial vaccine

OPEN ACCESS

Edited by:
Daniel E. Voth, University of Arkansas for Medical Sciences, United States

Reviewed by:
Janakiram Seshu, University of Texas at San Antonio, United States
James Samuel, Texas A&M Health Science Center, United States

***Correspondence:**
Carrie Mae Long
carrie.long@nih.gov

[†]*These authors have contributed equally to this work and share first authorship*

Specialty section:
This article was submitted to Bacteria and Host, a section of the journal Frontiers in Cellular and Infection Microbiology

Received: *03 December 2021*
Accepted: *19 January 2022*
Published: *10 February 2022*

Citation:
Tesfamariam M, Binette P and Long CM (2022) Preclinical Animal Models for Q Fever Vaccine Development. Front. Cell. Infect. Microbiol. 12:828784. doi: 10.3389/fcimb.2022.828784

INTRODUCTION

Coxiella burnetii is a zoonotic pathogen responsible for the human disease Q fever. Q-vax®, a whole cell preparation of formalin-inactivated phase I *C. burnetii*, is the only existing vaccine approved for use against Q fever. While this vaccine is highly effective at inducing long-lived immunity against *C. burnetii*, the risk of severe local reactions in individuals with pre-existing immunity (Bell et al., 1964) limits its widespread licensing and use. Intradermal skin testing was implemented in the late 1950s to assess prior exposure to *C. burnetii*, but skin testing is not completely reliable and can be expensive and cumbersome to implement (Schoffelen et al., 2014). An equally efficacious and less reactogenic vaccine is needed to eliminate the need for pre-screening and to broaden vaccination efforts in light of both natural outbreaks and biodefense applications (Long, 2021).

Animal models are invaluable tools used in the preclinical evaluation of all modern vaccine candidates. Animal models are used to evaluate vaccine safety, efficacy, route of delivery, formulation, dose, vaccine-induced immune responses, and correlates of protection (Gerdts et al., 2015). The complexity of vaccine-induced immune responses cannot currently be captured by any strategy other than the use of an intact, living system. A variety of experimental animal models have been utilized for preclinical vaccine development, with no single organism or model providing the parameters required for a streamlined process. Indeed, the most appropriate animal models vary depending on the causative agent of disease targeted by novel vaccines. For Q fever vaccine development, preclinical animal testing is particularly important, given ethical considerations precluding human *C. burnetii* challenge trials. Historically, human Q fever vaccine efficacy has been

evaluated in high risk occupational groups (Marmion et al., 1984). Currently, any novel Q fever vaccine seeking United States Food and Drug Administration (FDA) approval will likely have to satisfy the conditions of the FDA Animal Rule (FDA 21CFR601.90). These conditions include the performance of rigorous animal studies in multiple predictive species resulting in well-understood mechanisms of toxicity and pharmacodynamics for dose selection. The first vaccine to be approved under this rule was the BioThrax Anthrax Vaccine Adsorbed, which received approval for a new indication in 2015 (Beasley et al., 2016). Fortuitously, several preclinical surrogate animal models have been employed for Q fever vaccine development including mice, guinea pigs, and non-human primates (Bewley, 2013). Additional species have served as models for Coxiellosis vaccine development, including livestock (Lisák, 1989) and deer (González-Barrio et al., 2017).

VACCINE-CHALLENGE MODELING

Vaccine-challenge models serve to evaluate the efficacy of vaccine candidates and assist in dose ranging (Golding et al., 2018). Generally, physiologically relevant routes of vaccination and infectious challenge are desired to best recapitulate eventual use of the vaccine candidate in humans. For Q fever vaccine development, ideal test systems would be comprised of physiologically relevant animal species paired with *C. burnetii* challenge *via* the aerosol route. However, models utilizing alternate species and routes of exposure are not without merit and may serve as accessible, informative model systems.

Mice

Mice have been used in many *C. burnetii* infection and vaccination studies likely due to their size, reagent availability, and accessibility. Mice are not generally regarded as optimal models of *C. burnetii* infection due to the absence of a robust febrile response in immunocompetent strains (Theodore and Bengtson, 1942; Franti et al., 1974; Ochoa-Repáraz et al., 2007). Despite this, murine models have been used to evaluate the efficacy of various Q fever vaccine candidates, including the chloroform-methanol residue (CMR) vaccine (Waag et al., 1997) and an lipopolysaccharide peptide mimic vaccine (Peng et al., 2012).

Perhaps one of the most important considerations when using mice to model disease is strain selection. A large-scale evaluation of the susceptibility of inbred mouse strains to *C. burnetii* infection revealed several strains susceptible to clinical disease, including the BALB/c and A/J strains (Scott et al., 1987). Accordingly, the BALB/c, C57Bl/6, and A/J strains have been widely used in *C. burnetii* infection and vaccine challenge models (Bewley, 2013). Indeed, BALB/c strains generally show signs of infection when inoculated with *C. burnetii*; however, they do not display high mortality rates compared to other susceptible inbred strains (Scott et al., 1987). Thus, they have been frequently utilized in infection and vaccine-challenge studies (Scott et al., 1987; Zhang et al., 2007; Schoffelen et al., 2015; Melenotte et al., 2016). Importantly, BALB/c substrain variation may lead to divergent clinical outcomes following infection (Melenotte et al., 2016). C57Bl/6 strains are commonly favored in mechanistic studies because of the widespread ability to access congenic strains (Gregory et al., 2019). While C57Bl/6 strains typically do not exhibit overt signs of clinical illness after intraperitoneal *C. burnetii* inoculation (Scott et al., 1987), this these strains have been used in *C. burnetii* infection modeling (Leone et al., 2007) and Q fever vaccine development studies (Xiong et al., 2016; Kumaresan et al., 2021). Of all inbred strains evaluated, the A/J strain displayed the highest mortality rates when injected intraperitoneally with the virulent Nine Mile I strain of *C. burnetii* (Scott et al., 1987). Recently, Reeves, et al. utilized HLA-DR transgenic mice (B/6 background with expression of a human MHC-II allele) to robustly profile the host immune response in a vaccine-challenge model (Reeves et al., 2020). In addition to strain variation, mouse age has been recognized as a factor related to disease severity in the C57Bl/6 infection model (Leone et al., 2007). Clearly, murine strain selection and individual host factors are important considerations when this organism is used for Q fever vaccine development studies.

Additionally, route of vaccine administration and infectious challenge are both important considerations when evaluating Q fever vaccine candidates. Mice have been vaccinated *via* intraperitoneal, intratracheal, and subcutaneous routes and challenged *via* aerosol, intranasal, and intratracheal routes (Marrie et al., 1996; Waag et al., 1997; Feng et al., 2019; Gregory et al., 2019; Hu et al., 2019; Reeves et al., 2020). Bacterial distribution and tissue pathology appear to be affected by route of infectious challenge; thus, proper interpretation of experimental outcomes based on routes of vaccination and infection are important when using these models.

Guinea Pigs

In contrast to mice, guinea pigs are known to mimic important symptoms of human *C. burnetii* infection, exhibiting a comparable dose-fever response (Benenson and Tigertt, 1956), splenomegaly, and weight loss as indicators of disease (Moos and Hackstadt, 1987; Long et al., 2019). Additionally, guinea pigs exhibit altered airway, pathological, and immunological responses to respiratory pathogens compared to mice that are generally considered to be more physiologically relevant to human disease (Gregory et al., 2019). Guinea pigs are more cumbersome and costly than mice and exhibit unique challenges regarding lack of available reagents and difficulty in performing procedures such as intratracheal instillation (Brewer and Cruise, 1997). Various guinea pig strains have been utilized in *C. burnetii* vaccine-challenge studies, with the outbred Harley strain serving as a popular model (Russell-Lodrigue et al., 2006; Fratzke et al., 2021b; Long et al., 2021).

Non-Human Primates

Non-human primates (NHP) are important preclinical animal models as they exhibit the highest physiological and genetic

similarities with humans. Limitations related to the use of NHPs include cost, ethical considerations, and containment shortcomings (Gerdts et al., 2015). Historically, macaques have served as the NHP species of choice used to model Q fever *via* aerosol inoculation (Gonder et al., 1979; Waag et al., 1999). In these studies, both cynomolgus and rhesus macaques displayed signs of clinical illness similar to that of human disease. The cynomolgus macaque model was utilized to evaluate the efficacy and immunogenicity of a CMR vaccine candidate, serving as a robust model and indicating that this vaccine could confer protection after a variety of vaccine dose and administration regimens (Waag et al., 2002). Recently, direct lower airway bacterial inoculation *via* MicroSprayer aerosolization has been introduced as a viable alternative to traditional NHP aerosol exposure techniques, producing comparable disease outcomes (Gregory et al., 2019). Additionally, the marmoset has proven to be a suitable model for studies of the pathological response to Q fever and will likely be a valuable tool for preclinical Q fever vaccine development (Nelson et al., 2020). NHP models will be particularly useful in late stages of preclinical Q fever vaccine development due to the considerations described above.

POST VACCINATION HYPERSENSITIVITY MODELING

While post vaccination hypersensitivity (PVH) animal modeling has been crucial in the evaluation of emerging Q fever vaccine candidates, both the availability of diverse models and the understanding of immunological mechanisms underlying the PVH response have remained largely elusive. Severe local reactions in pre-immune individuals were first observed in the early 1950s when Q fever vaccination programs were initially implemented (Meiklejohn and Lennette, 1950; Bell et al., 1964). A skin testing regime was adopted to screen individuals with pre-existing immunity to *C. burnetii* and was further refined as new methods for formulating the vaccine became available in the early 1960s (Lackman et al., 1962; Ormsbee, 1962; Luoto et al., 1963).

Early History

Following the development of novel methods of vaccine purification and bacterial fractionation, the human Q fever skin test was adapted to sensitized rabbits (Anacker et al., 1962). Rabbits sensitized *via* intradermal injection of 50 μg phase I *C. burnetii* whole cell vaccine (WCV) were skin tested intradermally with increasing doses of different fractions of *C. burnetii*, ranging from 0.02 to 10 μg, to determine the minimal dose needed to recapitulate the skin reaction observed in sensitized humans. This model was also used to evaluate the reactogenicity of various bacterial fractions. While unsensitized rabbits experienced lesions, these typically did not occur until at least 72 hours post skin testing and at much larger doses (31.1x) than that of the sensitized animals. The responses in the sensitized rabbits were hypothesized to be delayed-type hypersensitivity (DTH) responses, but this was not conclusively evaluated. No major modifications to the rabbit model have been made since these studies.

Guinea Pigs

Ascher et al. introduced the first validated guinea pig PVH model in 1983 (Ascher et al., 1983a). Here, Hartley guinea pigs were sensitized *via* immunization with a 50 μg dose of phase I WCV emulsified in either Freund's complete (QFA) or incomplete adjuvant (IFA) divided into the four footpads and skin tested with a 60 ng dose of the vaccine two six weeks post sensitization in a shaved flank. While skin test depth was not described, the photomicrographs of skin test sites demonstrated reactions in the deep dermis or subcutis, indicating that subcutaneous injections were employed (Wilhelmsen and Waag, 2000). Because data from rabbit models suggested that the PVH reaction could be a DTH response, prior to skin testing, Ascher et al. treated a group of guinea pigs sensitized with WCV with cyclophosphamide, which had previously been shown to enhance DTH responses (Ascher et al., 1977). As hypothesized, the cyclophosphamide-pretreated, sensitized guinea pigs experienced significantly increased reactions, as quantified by increases in skin thickness, further supporting the PVH-DTH hypothesis. Consistent with past human studies, this guinea pig model yielded data suggestive of granulatomous DTH (Ascher et al., 1983b).

Since introduced for PVH, the guinea pig model has remained the gold standard for vaccine reactogenicity studies (Bewley, 2013). Due to undesirable side effects of footpad inoculation, Ruble et al. sensitized hairless Hartley guinea pigs either subcutaneously (SC) or intradermally (ID) with a total of 60 μg WCV or CMR with or without IFA, distributed over numerous injection sites (Ruble et al., 1994). Six weeks later, animals were subcutaneously skin tested with vaccine doses ranging from 60 to 6,000 ng. While human skin tests are performed ID, SC injection was tested as an alternative because the vaccine is administered SC and would therefore more closely mimic the PVH reaction in pre-immune individuals. Hairless Hartley guinea pigs gave comparable results to prior models, with peak induration at 9 days (Ascher et al., 1983a). Using the hairless strain was advantageous as it reduced any additional irritation caused by shaving that could ultimately interfere with interpretation of the skin test response.

Wilhelmsen and Waag evaluated aerosol and intraperitoneal inoculation as alternative sensitization routes to SC vaccination in Hartley guinea pigs (Wilhelmsen and Waag, 2000). A 30 μg sensitization dose was used which was a substantial departure from the maximal 60 ng doses used in prior studies. As in previous studies, induration was greatest at 8-12 days post skin testing.

The latest refinements to the guinea pig model came from a 2018 study performed by Baeten et al. which aimed to standardize the guinea pig PVH model (Baeten et al., 2018). This study further explored intranasal and intraperitoneal sensitization routes and evaluated differences between skin tests performed either intradermally or subcutaneously at different time points post sensitization using Coxevac®, the

ruminant vaccine for Q fever formulated from the NMI strain of *C. burnetii*. Recently, similar guinea pig models have been used to evaluate the reactogenicity of several Q fever vaccine candidates, including a genetically modified WCV (Long et al., 2021), exemplifying the utility of this model. Cumulatively, the data collected from guinea pigs suggest that PVH reactions are likely dominated by a granulatomous DTH reaction in this species, which is mediated by memory T cells producing Th1 cytokines (Kobayashi et al., 2001).

Mice

While the guinea pig reactogenicity model has been useful determining the reactogenicity of vaccine candidates, further characterization of the PVH response has been severely limited due to a lack of experimental reagents available for guinea pigs. Therefore, development of model systems for which there are more reagents readily available should be considered as elucidation of the mechanisms underlying these responses will provide insight for the development of novel Q fever vaccines. The first use of mice in PVH modeling was performed by Kazár et al. in 1987 (Kazár et al., 1987). In this study, mice were sensitized with 100 μg of phase I *C. burnetii* intraperitoneally and mice were skin tested *via* hind footpad injection of WCV and CMR (30-0.003 μg). Mice elicited DTH responses, but at a higher minimum dose (0.3 μg) compared to rabbits and guinea pigs (0.03 μg). Recently, Fratzke et al. tested three different mice strains (SKHI, C57Bl/6 and BALBc) for their ability to recapitulate the DTH response when sensitized, proposing the SKH1 and C57Bl/6 strains as viable options for this purpose (Fratzke et al., 2021a). Currently, guinea pigs are the primary model for assessing Q fever vaccine reactogenicity, but mice are an exciting complementary option. Important considerations regarding PVH modeling are dose selection, skin testing injection depth, sensitization method (e.g. infection vs vaccination), and species selection.

CONCLUSIONS AND OUTLOOK

Ultimately, the quality of a preclinical animal model can be assessed based on its physiologic relevance to human disease. Relevant physiologic characteristics may include redundancy in anatomy and components of the immune system, clinical response to infection, pathogenesis, and duration of biologic responses (Gerdts et al., 2015). Translating preclinical data to human vaccine trials and eventual deployment remains a major challenge but may be addressed by using highly physiologically relevant animal models paired with an understanding of the strengths and limitations of the models chosen. For *C. burnetii* vaccine-challenge and PVH modeling, several species have proven their usefulness in the studies described above and exhibit unique advantages and limitations (**Figure 1**). Guinea pigs appear to be the premier small mammal model of Q fever due to their robust physiologic relevance to human disease. NHPs will likely serve as valuable model systems for Q fever vaccine development but their accessibility precludes widespread use, particularly in early preclinical vaccine development. PVH modeling is dominated by the guinea pig but mice appear to be a promising complementary model for mechanistic evaluation of this response. Recently, a larval *Galleria mellonella* model of *C. burnetii* infection was introduced by Norville, et al. (Norville et al., 2014). This advance introduces the possibility of the use of non-mammalian models in future vaccine development efforts. Perhaps species such as *G. mellonella* or even those with more developed immune systems such as *Danio rerio* (zebrafish) will provide accessible pathways to complement existing mammalian models. Indeed, zebrafish have proven useful for preliminary human vaccine safety screening (Bailone et al., 2020). We feel that expansion of all relevant *C. burnetii* infection, vaccination, and PVH models will increase knowledge of correlates of protection and potential screening biomarkers, serving as valuable tools not only for vaccine development but to increase general knowledge of these important host-pathogen interactions.

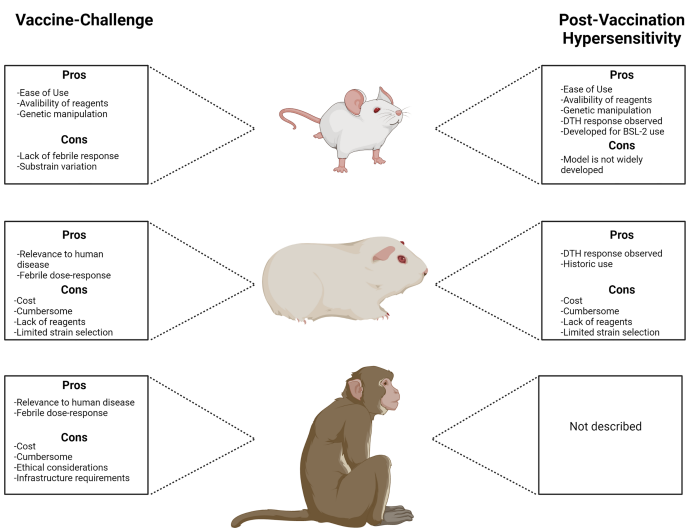

FIGURE 1 | Comparison of animal models used for Q fever vaccine development with principal advantages and disadvantages associated with each model.

Ultimately, we suggest that there is no "perfect model" for Q fever vaccine development. Indeed, the complexity of relevant biologic responses, the challenges of working with *C. burnetii*, and the lack of data regarding human responses to vaccination and infection are a few of the factors contributing to this quandary. Regardless, exciting progress has recently been made in *C. burnetii* host-pathogen animal modeling. The expansion of these models and ensuing comparative analysis will aid in the development of an improved Q fever vaccine by providing the most relevant and useful models possible. For example, it will be crucial to utilize these models to further elucidate the PVH response and relate this to the human condition. Considering that the current QVax® skin test regimen is contained within a 7 day window (Sellens et al., 2018) and prior reports indicate that this test can be read as early as 48 hours post skin testing (Lackman et al., 1962), the possible involvement of a tuberculin-type DTH component in the human PVH response, with clinical symptoms manifesting earlier than that of granulomatous DTH, should be considered during model development. Additional considerations for the field include the influence of biological sex and age on choice of model and Q fever vaccine efficacy. Considerations such as these serve to more wholly represent the human population affected by disease and eventual vaccination. These two factors are known to play a significant role in infectious disease pathogenesis (Bijkerk et al., 2010; Ingersoll, 2017) and vaccine efficacy (Lord, 2013; Fink et al., 2018; Bignucolo et al., 2021). Specifically, they appear to influence similar outcomes related to *C. burnetii* host-pathogen interactions (Franti et al., 1974; Leone et al., 2004; Textoris et al., 2010). With more representative and comprehensive animal models of disease, our vaccine development efforts will thrive for *C. burnetii* and beyond.

AUTHOR CONTRIBUTIONS

MT, PB, and CL conceptualized, wrote, and edited the manuscript. All authors contributed to the article and approved the submitted version.

FUNDING

This work was supported by the Intramural Research Program of the National Institutes of Health, National Institute of Allergy and Infectious Diseases (ZIAAI001331).

ACKNOWLEDGMENTS

Figure 1 was created with Biorender.com.

REFERENCES

Anacker, R. L., Lackman, D. B., Pickens, E. G., and Ribi, E. (1962). Antigenic and Skin-Reactive Properties of Fractions of Coxiella Burnetii. *J. Immunol.* 89, 145.

Ascher, M. S., Berman, M. A., Parker, D., and Turk, J. L. (1983a). Experimental Model for Dermal Granulomatous Hypersensitivity in Q Fever. *Infect. Immun.* 39, 388–393. doi: 10.1128/iai.39.1.388-393.1983

Ascher, M. S., Berman, M. A., and Ruppanner, R. (1983b). Initial Clinical and Immunologic Evaluation of a New Phase I Q Fever Vaccine and Skin Test in Humans. *J. Infect. Dis.* 148, 214–222. doi: 10.1093/infdis/148.2.214

Ascher, M. S., Jahrling, D. Gm., Harrington, D. G., Kishimoto, R. A., and McGann, V. g. (1980). Mechanisms of Protective Immunogenicity of Microbial Vaccines: Effects of Cyclophosphamide Pretreatment in Venezuelan Encephalitis, Q Fever, and Tularemia. *Clin. Exp. Immunol.* 41 (2), 225–236–323.

Baeten, L. A., Podell, B. K., Sluder, A. E., Garritsen, A., Bowen, R. A., and Poznansky, M. C. (2018). Standardized Guinea Pig Model for Q Fever Vaccine Reactogenicity. *PloS One* 13, e0205882. doi: 10.1371/journal.pone.0205882

Bailone, R. L., Fukushima, H. C. S., Ventura Fernandes, B. H., De Aguiar, L. K., Corrêa, T., Janke, H., et al. (2020). Zebrafish as an Alternative Animal Model in Human and Animal Vaccination Research. *Lab. Anim. Res.* 36, 13–13. doi: 10.1186/s42826-020-00042-4

Beasley, D. W. C., Brasel, T. L., and Comer, J. E. (2016). First Vaccine Approval Under the FDA Animal Rule. *NPJ Vaccines* 1, 16013. doi: 10.1038/npjvaccines.2016.13

Bell, J. F., Lackman, D. B., Meis, A., and Hadlow, W. J. (1964). Recurrent Reaction of Site of Q Fever Vaccination in a Sensitized Person. *Mil. Med.* 129, 591–595. doi: 10.1093/milmed/129.7.591

Benenson, A. S., and Tigertt, W. D. (1956). Studies on Q Fever in Man. *Trans. Assoc. Am. Physicians* 69, 98–104.

Bewley, K. R. (2013). Animal Models of Q Fever (*Coxiella Burnetii*). *Comp. Med.* 63, 469–476.

Bignucolo, A., Scarabel, L., Mezzalira, S., Polesel, J., Cecchin, E., and Toffoli, G. (2021). Sex Disparities in Efficacy in COVID-19 Vaccines: A Systematic Review and Meta-Analysis. *Vaccines* 9, 825. doi: 10.3390/vaccines9080825

Bijkerk, P., Van Lier, E. A., Van Vliet, J. A., and Kretzschmar, M. E. (2010). Effects of Ageing on Infectious Disease. *Ned. Tijdschr Geneeskd.* 154, A1613.

Brewer, N. R., and Cruise, L. J. (1997). The Respiratory System of the Guinea Pig: Emphasis on Species Differences. *Contemp. Top. Lab. Anim. Sci.* 36, 100–108.

Feng, J., Hu, X., Fu, M., Dai, L., Yu, Y., Luo, W., et al. (2019). Enhanced Protection Against Q Fever in BALB/C Mice Elicited by Immunization of Chloroform-Methanol Residue of *Coxiella Burnetii via* Intratracheal Inoculation. *Vaccine* 37, 6076–6084. doi: 10.1016/j.vaccine.2019.08.041

Fink, A. L., Engle, K., Ursin, R. L., Tang, W.-Y., and Klein, S. L. (2018). Biological Sex Affects Vaccine Efficacy and Protection Against Influenza in Mice. *Proc. Natl. Acad. Sci.* 115, 12477–12482. doi: 10.1073/pnas.1805268115

Franti, C. E., Behymer, D. E., Goggin, J. E., and Wright, M. E. (1974). Splenomegaly, Sex, and Other Characteristics of Laboratory Animals Used for Primary Isolations of *Coxiella Burnetii*. *Lab. Anim. Sci.* 24, 656–665.

Fratzke, A. P., Jan, S., Felgner, J., Liang, L., Nakajima, R., Jasinskas, A., et al. (2021b). Subunit Vaccines Using TLR Triagonist Combination Adjuvants Provide Protection Against *Coxiella Burnetii* While Minimizing Reactogenic Responses. *Front. Immunol.* 12. doi: 10.3389/fimmu.2021.653092

Fratzke, A. P., Gregory, A. E., Van Schaik, E. J., and Samuel, J. E. (2021a). *Coxiella Burnetii* Whole Cell Vaccine Produces a Th1 Delayed-Type Hypersensitivity Response in a Novel Sensitized Mouse Model. *Front. Immunol.* 12, 754712. doi: 10.3389/fimmu.2021.754712

Gerdts, V., Wilson, H. L., Meurens, F., Van Drunen Littel-Van Den Hurk, S., Wilson, D., Walker, S., et al. (2015). Large Animal Models for Vaccine Development and Testing. *Ilar. J.* 56, 53–62. doi: 10.1093/ilar/ilv009

Golding, H., Khurana, S., and Zaitseva, M. (2018). What is the Predictive Value of Animal Models for Vaccine Efficacy in Humans? The Importance of Bridging Studies and Species-Independent Correlates of Protection. *Cold Spring Harbor Perspect. Biol.* 10, a028902. doi: 10.1101/cshperspect.a028902

Gonder, J. C., Kishimoto, R. A., Kastello, M. D., Pedersen, C. E.Jr., and Larson, E. W. (1979). Cynomolgus Monkey Model for Experimental Q Fever Infection. *J. Infect. Dis.* 139, 191–196. doi: 10.1093/infdis/139.2.191

González-Barrio, D., Ortiz, J. A., and Ruiz-Fons, F. (2017). Estimating the Efficacy of a Commercial Phase I Inactivated Vaccine in Decreasing the Prevalence of

Coxiella Burnetii Infection and Shedding in Red Deer (Cervus Elaphus). *Front. Veterinary Sci.* 4.

Gregory, A. E., Van Schaik, E. J., Russell-Lodrigue, K. E., Fratzke, A. P., and Samuel, J. E. (2019). *Coxiella Burnetii* Intratracheal Aerosol Infection Model in Mice, Guinea Pigs, and Nonhuman Primates. *Infect. Immun.* 87, e00178–19. doi: 10.1128/IAI.00178-19

Hu, X., Yu, Y., Feng, J., Fu, M., Dai, L., Lu, Z., et al. (2019). Pathologic Changes and Immune Responses Against *Coxiella Burnetii* in Mice Following Infection *via* non-Invasive Intratracheal Inoculation. *PloS One* 14, e0225671. doi: 10.1371/journal.pone.0225671

Ingersoll, M. A. (2017). Sex Differences Shape the Response to Infectious Diseases. *PloS Pathog.* 13, e1006688-e1006688. doi: 10.1371/journal.ppat.1006688

Kazár, J., Schramek, S., Lisák, V., and Brezina, R. (1987). Antigenicity of Chloroform-Methanol-Treated *Coxiella Burnetii* Preparations. *Acta Virol.* 31, 158–167.

Kobayashi, K., Kaneda, K., and Kasama, T. (2001). Immunopathogenesis of Delayed-Type Hypersensitivity. *Microsc. Res. Tech* 53, 241–245. doi: 10.1002/jemt.1090

Kumaresan, V., Alam, S., Zhang, Y., and Zhang, G. (2021). The Feasibility of Using *Coxiella Burnetii* Avirulent Nine Mile Phase II Viable Bacteria as a Live Attenuated Vaccine Against Q Fever. *Front. Immunol.* 12. doi: 10.3389/fimmu.2021.754690

Lackman, D. B., Bell, E. J., Bell, J. F., and Pickens, E. G. (1962). Intradermal Sensitivity Testing in Man With a Purified Vaccine for Q Fever. *Am. J. Public Health Nations Health* 52, 87–93. doi: 10.2105/AJPH.52.1.87

Leone, M., Bechah, Y., Meghari, S., Lepidi, H., Capo, C., Raoult, D., et al. (2007). *Coxiella Burnetii* Infection in C57BL/6 Mice Aged 1 or 14 Months. *FEMS Immunol. Med. Microbiol.* 50, 396–400. doi: 10.1111/j.1574-695X.2007.00272.x

Leone, M., Honstettre, A., Lepidi, H., Capo, C., Bayard, F., Raoult, D., et al. (2004). Effect of Sex on *Coxiella Burnetii* Infection: Protective Role of 17beta-Estradiol. *J. Infect. Dis.* 189, 339–345. doi: 10.1086/380798

Lisák, V. (1989). Experience in Vaccinating Farm Animals for Preventing Q Fever in Humans. *Tr Inst. Im Pastera* 66143-153, 174.

Long, C. M. (2021). Q Fever Vaccine Development: Current Strategies and Future Considerations. *Pathogens* 10, 1223. doi: 10.3390/pathogens10101223

Long, C. M., Beare, P. A., Cockrell, D. C., Fintzi, J., Tesfamariam, M., Shaia, C. I., et al. (2021). Contributions of Lipopolysaccharide and the Type IVB Secretion System to *Coxiella Burnetii* Vaccine Efficacy and Reactogenicity. *NPJ Vaccines* 6, 38. doi: 10.1038/s41541-021-00296-6

Long, C. M., Beare, P. A., Cockrell, D. C., Larson, C. L., and Heinzen, R. A. (2019). Comparative Virulence of Diverse *Coxiella Burnetii* Strains. *Virulence* 10, 133–150. doi: 10.1080/21505594.2019.1575715

Lord, J. M. (2013). The Effect of Ageing of the Immune System on Vaccination Responses. *Hum. Vaccines Immunotherapeutics* 9, 1364–1367. doi: 10.4161/hv.24696

Luoto, L., Bell, J. F., Casey, M., and Lackman, D. B. (1963). Q Fever Vaccination of Human Volunteers. I. The Serologic and Skin-Test Response Following Subcutaneous Injections. *Am. J. Hyg.* 78, 1–15. doi: 10.1093/oxfordjournals.aje.a120324

Marmion, B. P., Ormsbee, R. A., Kyrkou, M., Wright, J., Worswick, D., Cameron, S., et al. (1984). Vaccine Prophylaxis of Abattoir-Associated Q Fever. *Lancet* 2, 1411–1414. doi: 10.1016/S0140-6736(84)91617-9

Marrie, T. J., Stein, A., Janigan, D., and Raoult, D. (1996). Route of Infection Determines the Clinical Manifestations of Acute Q Fever. *J. Infect. Dis.* 173, 484–487. doi: 10.1093/infdis/173.2.484

Meiklejohn, G., and Lennette, E. H. (1950). Q Fever in California. I. Observations on Vaccination of Human Beings. *Am. J. Hyg.* 52, 54–64.

Melenotte, C., Lepidi, H., Nappez, C., Bechah, Y., Audoly, G., Terras, J., et al. (2016). Mouse Model of *Coxiella Burnetii* Aerosolization. *Infect. Immun.* 84, 2116–2123. doi: 10.1128/IAI.00108-16

Moos, A., and Hackstadt, T. (1987). Comparative Virulence of Intra- and Interstrain Lipopolysaccharide Variants of *Coxiella Burnetii* in the Guinea Pig Model. *Infect. Immun.* 55, 1144–1150. doi: 10.1128/iai.55.5.1144-1150.1987

Nelson, M., Salguero, F. J., Hunter, L., and Atkins, T. P. (2020). A Novel Marmoset (Callithrix Jacchus) Model of Human Inhalational Q Fever. *Front. Cell Infect. Microbiol.* 10, 621635. doi: 10.3389/fcimb.2020.621635

Norville, I. H., Hartley, M. G., Martinez, E., Cantet, F., Bonazzi, M., and Atkins, T. P. (2014). Galleria Mellonella as an Alternative Model of *Coxiella Burnetii* Infection. *Microbiology* 160, 1175–1181. doi: 10.1099/mic.0.077230-0

Ochoa-Repáraz, J., Sentissi, J., Trunkle, T., Riccardi, C., and Pascual, D. W. (2007). Attenuated *Coxiella Burnetii* Phase II Causes a Febrile Response in Gamma Interferon Knockout and Toll-Like Receptor 2 Knockout Mice and Protects Against Reinfection. *Infect. Immun.* 75, 5845–5858. doi: 10.1128/IAI.00901-07

Ormsbee, R. A. (1962). A Method of Purifying *Coxiella Burnetii* and Other Pathogenic Rickettsiae. *J. Immunol.* 88, 100–108.

Peng, Y., Zhang, Y., Mitchell, W. J., and Zhang, G. (2012). Development of a Lipopolysaccharide-Targeted Peptide Mimic Vaccine Against Q Fever. *J. Immunol.* 189, 4909–4920. doi: 10.4049/jimmunol.1201622

Reeves, P. M., Raju Paul, S., Baeten, L., Korek, S. E., Yi, Y., Hess, J., et al. (2020). Novel Multiparameter Correlates of *Coxiella Burnetii* Infection and Vaccination Identified by Longitudinal Deep Immune Profiling. *Sci. Rep.* 10. doi: 10.1038/s41598-020-69327-x

Ruble, D. L., Elliott, J. J., Waag, D. M., and Jaax, G. P. (1994). A Refined Guinea Pig Model for Evaluating Delayed-Type Hypersensitivity Reactions Caused by Q Fever Vaccines. *Lab. Anim. Sci.* 44, 608–612.

Russell-Lodrigue, K. E., Zhang, G. Q., Mcmurray, D. N., and Samuel, J. E. (2006). Clinical and Pathologic Changes in a Guinea Pig Aerosol Challenge Model of Acute Q Fever. *Infect. Immun.* 74, 6085–91. doi: 10.1128/IAI.00763-06

Schoffelen, T., Herremans, T., Sprong, T., Nabuurs-Franssen, M., van der Meer, J. W., Joosten, L. A., et al. (2014). Immunogenicity of the Q Fever Skin Test. *J. Infect.* 69, 161–164. doi: 10.1016/j.jinf.2014.03.008

Schoffelen, T., Self, J. S., Fitzpatrick, K. A., Netea, M. G., Van Deuren, M., Joosten, L. A., et al. (2015). Early Cytokine and Antibody Responses Against *Coxiella Burnetii* in Aerosol Infection of BALB/C Mice. *Diagn. Microbiol. Infect. Dis.* 81, 234–239. doi: 10.1016/j.diagmicrobio.2014.12.008

Scott, G. H., Williams, J. C., and Stephenson, E. H. (1987). Animal Models in Q Fever: Pathological Responses of Inbred Mice to Phase I *Coxiella Burnetii*. *Microbiology* 133, 691–700. doi: 10.1099/00221287-133-3-691

Sellens, E., Bosward, K. L., Willis, S., Heller, J., Cobbold, R., Comeau, J. L., et al. (2018). Frequency of Adverse Events Following Q Fever Immunisation in Young Adults. *Vaccines (Basel)* 6. doi: 10.3390/vaccines6040083

Textoris, J., Ban, L. H., Capo, C., Raoult, D., Leone, M., and Mege, J.-L. (2010). Sex-Related Differences in Gene Expression Following *Coxiella Burnetii* Infection in Mice: Potential Role of Circadian Rhythm. *PloS One* 5, e12190. doi: 10.1371/journal.pone.0012190

Theodore, L. P., and Bengtson, I. A. (1942). The Histopathology of Experimental "Q" Fever in Mice. *Public Health Rep. (1896-1970)* 57, 790–798. doi: 10.2307/4584109

Waag, D. M., Byrne, W. R., Estep, J., Gibbs, P., Pitt, M. L., and Banfield, C. M. (1999). Evaluation of Cynomolgus (Macaca Fascicularis) and Rhesus (Macaca Mulatta) Monkeys as Experimental Models of Acute Q Fever After Aerosol Exposure to Phase-I *Coxiella Burnetii*. *Lab. Anim. Sci.* 49, 634–638.

Waag, D. M., England, M. J., and Pitt, M. L. (1997). Comparative Efficacy of a *Coxiella Burnetii* Chloroform:Methanol Residue (CMR) Vaccine and a Licensed Cellular Vaccine (Q-Vax) in Rodents Challenged by Aerosol. *Vaccine* 15, 1779–1783. doi: 10.1016/S0264-410X(97)00107-2

Waag, D. M., England, M. J., Tammariello, R. F., Byrne, W. R., Gibbs, P., Banfield, C. M., et al. (2002). Comparative Efficacy and Immunogenicity of Q Fever Chloroform:Methanol Residue (CMR) and Phase I Cellular (Q-Vax) Vaccines in Cynomolgus Monkeys Challenged by Aerosol. *Vaccine* 20, 2623–2634. doi: 10.1016/S0264-410X(02)00176-7

Wilhelmsen, C. L., and Waag, D. M. (2000). Guinea Pig Abscess/Hypersensitivity Model for Study of Adverse Vaccination Reactions Induced by Use of Q Fever Vaccines. *Comp. Med.* 50, 374–378.

Xiong, X., Jiao, J., Gregory, A. E., Wang, P., Bi, Y., Wang, X., et al. (2016). Identification of *Coxiella Burnetii* CD8+ T-Cell Epitopes and Delivery by Attenuated Listeria Monocytogenes as a Vaccine Vector in a C57BL/6 Mouse Model. *J. Infect. Dis.* 215, 1580–1589. doi: 10.1093/infdis/jiw470

Zhang, G., Russell-Lodrigue, K. E., Andoh, M., Zhang, Y., Hendrix, L. R., and Samuel, J. E. (2007). Mechanisms of Vaccine-Induced Protective Immunity Against *Coxiella Burnetii* Infection in BALB/C Mice. *J. Immunol.* 179, 8372–8380. doi: 10.4049/jimmunol.179.12.8372

Conflict of Interest: The authors declare that the research was conducted in the absence of any commercial or financial relationships that could be construed as a potential conflict of interest.

this article, or claim that may be made by its manufacturer, is not guaranteed or endorsed by the publisher.

frontiers in Cellular and Infection Microbiology

ORIGINAL RESEARCH
published: 01 March 2022
doi: 10.3389/fcimb.2022.811407

The *Chlamydia trachomatis* Early Effector Tarp Outcompetes Fascin in Forming F-Actin Bundles *In Vivo*

George F. Aranjuez, Jongeon Kim and Travis J. Jewett*

Division of Immunity and Pathogenesis, Burnett School of Biomedical Sciences, University of Central Florida College of Medicine, Orlando, FL, United States

The intracellular pathogen *Chlamydia trachomatis* secretes multiple early effectors into the host cell to promote invasion. A key early effector during host cell entry, Tarp (translocated actin-recruiting phosphoprotein) is comprised of multiple protein domains known to have roles in cell signaling, G-actin nucleation and F-actin bundle formation. *In vitro*, the actin bundles generated by Tarp are uncharacteristically flexible, however, *in vivo*, the biological significance of Tarp-mediated actin bundles remains unknown. We hypothesize that Tarp's ability to generate unique actin bundles, in part, facilitates chlamydial entry into epithelial cells. To study the *in vivo* interaction between Tarp and F-actin, we transgenically expressed Tarp in *Drosophila melanogaster* tissues. Tarp expressed in *Drosophila* is phosphorylated and forms F-actin-enriched aggregates in tissues. To gain insight into the significance of Tarp actin bundles *in vivo*, we utilized the well-characterized model system of mechanosensory bristle development in *Drosophila melanogaster*. Tarp expression in wild type flies produced curved bristles, indicating a perturbation in F-actin dynamics during bristle development. Two F-actin bundlers, Singed/Fascin and Forked/Espin, are important for normal bristle shape. Surprisingly, Tarp expression in the bristles displaced Singed/Fascin away from F-actin bundles. Tarp's competitive behavior against Fascin during F-actin bundling was confirmed *in vitro*. Loss of either *singed* or *forked* in flies leads to highly deformed bristles. Strikingly, Tarp partially rescued the loss of *singed*, reducing the severity of the bristle morphology defect. This work provides *in vivo* confirmation of Tarp's F-actin bundling activity and further uncovers a competitive behavior against the host bundler Singed/Fascin during bundle assembly. Also, we demonstrate the utility of *Drosophila melanogaster* as an *in vivo* cell biological platform to study bacterial effector function.

Keywords: *Chlamydia*, tarp, *Drosophila*, F-actin, actin bundles, Singed, Fascin

OPEN ACCESS

Edited by:
Daniel E. Voth, University of Arkansas for Medical Sciences, United States

Reviewed by:
Sandra Sousa, Universidade do Porto, Portugal
Mary M. Weber, The University of Iowa, United States

****Correspondence:***
George F. Aranjuez
George.Aranjuez@ucf.edu

Specialty section:
This article was submitted to Bacteria and Host, a section of the journal Frontiers in Cellular and Infection Microbiology

Received: *08 November 2021*
Accepted: *10 February 2022*
Published: *01 March 2022*

Citation:
Aranjuez GF, Kim J and Jewett TJ (2022) The Chlamydia trachomatis Early Effector Tarp Outcompetes Fascin in Forming F-Actin Bundles In Vivo. Front. Cell. Infect. Microbiol. 12:811407. doi: 10.3389/fcimb.2022.811407

INTRODUCTION

Chlamydia is the most commonly reported sexually transmitted bacterial infection in the United States, with an estimated four million cases in the United States in 2018 (Kreisel et al., 2021). Without treatment, Chlamydia infection can lead to pelvic inflammatory disease, which can ultimately lead to permanent damage to the reproductive system. Additionally, infections in

pregnant women can also be passed onto the newborn baby, which can lead to eye or lung infections (Mårdh, 2002).

Chlamydia trachomatis (*C.t.*) is an obligate intracellular pathogen. Host cell entry, therefore, is a key step in its developmental cycle. The infectious stage of *C.t.*, the elementary body (EB), is equipped with a type III secretion system that injects multiple chlamydial proteins, called early effectors, that facilitate host cell invasion and entry (Peters et al., 2007; Betts et al., 2009). Intracellular *C.t.* reside in a parasitophorous vacuole called an inclusion which cloaks the EB as it differentiates into an actively growing and replicating reticulate body (RB) (Moulder, 1991). Finally, RBs differentiate into infectious EBs and are released to the extracellular space to establish new infections, either through lysis or extrusion of the inclusion (Hybiske and Stephens, 2007).

One of the most well-characterized *Chlamydia trachomatis* early effector is **t**ranslocated **a**ctin-**r**ecruiting **p**hosphoprotein, Tarp. The secretion of Tarp into the host cell is closely followed by F-actin accumulation at the nascent site of EB entry (Clifton et al., 2004). Biochemical studies show that Tarp can directly promote polymerization of actin subunits into filaments, mediated by its C-terminal region (Jewett et al., 2006). Also, blocking the actin binding domain of Tarp inhibits *C. trachomatis* invasion in tissue culture (Jewett et al., 2010). These findings indicate that Tarp's ability to reorganize the host actin cytoskeleton is a key molecular function required for efficient chlamydial invasion (Jewett et al., 2006; Ghosh et al., 2020).

F-actin can organize into bundles of parallel filaments *via* the crosslinking action of actin bundling proteins. F-actin bundle formation is one mechanism used by cells to exert force on the cell surface to create structures such as filopodia, microvilli, and other membrane protrusions (Stricker et al., 2010). In addition to promoting actin filament formation, Tarp can also directly assemble actin filaments into bundles *in vitro* (Jiwani et al., 2013). However, the physical stiffness of Tarp-assembled bundles deviates from that of bundles assembled by endogenous actin-bundling proteins such as Fascin and alpha-actinin (Ghosh et al., 2018), suggesting that Tarp-mediated F-actin bundles may harbor unique functions in the cell.

Adult *Drosophila melanogaster* are covered in small and large mechanosensory bristles (microchaetes and macrochaetes, respectively). Bristles are made up of chitin that are deposited along long, cellular protrusions originating from bristle cells. These cellular protrusions are generated, in part, by actin polymerization into filaments which arrange into tight, longitudinal bundles arrayed around the periphery of the protrusion (Tilney et al., 1995; Tilney et al., 1996). Defects in F-actin polymerization and bundling impacts the growth of these cellular protrusions, which then manifests as bristle morphology defects (Cant et al., 1994; Petersen et al., 1994; Verheyen and Cooley, 1994; Wu et al., 2016), easily observable in the adult fly.

Two F-actin bundlers, Singed/Fascin and Forked/Espin, are critical for normal bristle shape (Cant et al., 1994; Petersen et al., 1994; Tilney et al., 1995; Tilney et al., 1998). Both proteins participate in the proper formation of tight, longitudinally arrayed F-actin bundles that support the growth of bristle cell protrusions. The absence of either one produces dramatically short and highly malformed bristles (Tilney et al., 1995).

Though Tarp has been associated with actin polymerization during chlamydial invasion, its F-actin bundling properties are newly described and have not been examined *in vivo*. Understanding Tarp-generated F-actin bundles in a physiological context is highly relevant to the greater understanding of the molecular mechanisms of Tarp-mediated chlamydial entry. To achieve this, we utilized *Drosophila melanogaster* as a cell biology platform to study Tarp's influence on host actin dynamics in an *in vivo* context. Host cell changes due to transgenic expression of Tarp in *Drosophila* tissues can be directly linked to Tarp function without the complex host cell response to active infection. We used the well-characterized development of actin-dependent mechanosensory bristles in *Drosophila* as a platform to understand how Tarp influences actin dynamics in living organisms.

MATERIALS AND METHODS

Generation of Transgenic Flies, Fly Stocks, Crosses, Handling and Rearing

The complete open reading frame of *Chlamydia trachomatis* (serovar L2 strain 434/Bu)(ATCC VR-902B) *Tarp* (Genbank AAT47185.1) and *TmeA* (Genbank AM884176.1, CTL0063), respectively, was cloned into the *Drosophila* transformation and expression vector pUAST (Addgene) (Brand and Perrimon, 1993). The sequence-verified pUAST-Tarp and pUAST-TmeA plasmids were sent for injection into *D. melanogaster* w^{1118} embryos (Model System Injections, North Carolina).

The following *D. melanogaster* stocks were kind gifts from J. McDonald (Kansas State University) or obtained from the Bloomington *Drosophila* Stock Center (stock number in parentheses): yw;ap-GAL4/CyO (J. McDonald), hs-GAL4(II) (2077), hs-GAL4(III) (1799), w;pnr-GAL4/TM3,Ser,UAS-y (3039), w*;ubi-GAL4/CyO (32551), hs-FLP;Act>y+>GAL4, UAS-mCD8:GFP/CyO (J. McDonald), y,w1118;UAS-EGFP5a.2 (5431), y,sc,v;UAS-*forked* RNAi,y+ (41678), y;UAS-s*inged* RNAi, y+ (57805). The following stocks were made to test the ability of Tarp to rescue loss of endogenous bundlers: ap-GAL4, UAS-*singed* RNAi/CyO and pnr-GAL4, UAS-*forked* RNAi, y+. Rescue crosses were kept at 22°C.

The FLPout-GAL4 system (Blair, 2003) was used to generate clonal populations of follicle epithelial cells. Tarp-expressing clones were generated by crossing hs-FLP;Act>y+>GAL4,UAS-mCD8:GFP/CyO (J. McDonald) to UAS-Tarp, and the desired adult progeny subjected to heat shock in a 37°C water bath for 1 hour. The flies were kept at 25°C for 1 day prior to dissection.

Unless otherwise indicated, all fly stocks and crosses were reared at 25°C on Nutri-fly BF media (Genesee Scientific) supplemented with 0.45% v/v propionic acid.

Immunostaining and Confocal Microscopy

Individual ovarioles from *Drosophila* ovaries were dissected as described previously (McDonald and Montell, 2005). Ovarioles were fixed in 4% methanol-free formaldehyde (Thermo) in phosphate-buffered saline with 0.1% v/v Triton-X-100 (PBT) for 10 minutes with rocking. Fixed ovarioles were subsequently blocked with 0.5% w/v bovine serum albumin in PBT for 2 hours. GFP expression marks clonal populations of follicles with active GAL4/UAS expression.

For pupal bristle imaging, pupae were collected at 36-50 hours post-puparium formation—the stage where bristle primordia are actively growing from bristle cells in the dorsal thorax. The dorsal pupal casing was removed, and the dorsal pelt dissected using microscissors and fine dissecting forceps. The dorsal pelt was fixed in 4% methanol-free formaldehyde in PBT at room temperature for 10 minutes and blocked with 0.5% w/v bovine serum albumin in PBT for 2 hours.

The following antibodies were used for immunostaining: mouse anti-Singed, 1:100 (DSHB, sn 7c); rabbit polyclonal anti-Tarp, 1:1000 (Clifton et al., 2004); mouse monoclonal anti-phosphotyrosine (4G10, Millipore-Sigma). F-actin was visualized using Alexa 647-conjugated phalloidin (Molecular Probes, 1:400). The appropriate Alexa-conjugated secondary antibodies (Alexa 350, Alexa 568, Alexa 647, Molecular Probes) were used at 1:400. Immunostained tissue were mounted under a #1.5 cover glass using Aqua-Polymount mounting medium (Polysciences).

A Zeiss LSM 710 confocal microscope was used to acquire fluorescent images of follicle cells using a 40X Plan-Neuofluar oil objective (epithelial follicle cells) or a 100X Plan-Apochromat oil objective (pupal bristle cells). Image acquisition settings and minor adjustments to brightness and contrast post-acquisition were identical between control and Tarp-expressing follicle cells.

Imaging Adult *Drosophila* Bristles

Adult flies, with wings removed, were glued onto wooden picks. The dorsal thorax was imaged using a Zeiss Stemi 508 stereomicroscope equipped with an Axiocam 208 color camera. Minor brightness and contrast adjustments were made in Adobe Photoshop.

Scoring Bristle Morphology Defects

The dorsocentral and scutellar bristles of adult flies were examined under a dissecting stereomicroscope. The following scores were assigned: '0': wild-type bristle—oriented towards the posterior direction, with a gentle, uniform curve, and tapering thickness towards the tip; '1': bristle with an increased curvature, but no sharp bends or kinks; '2': bends or kinks are present but the angle is around 45°; '3': bends or kinks are at approximately 90°; '4': bends or kinks are greater than 90°, multiple bends or kinks are often observed. Pairs of dorsocentral or scutellar bristles were scored and summed up, allowing each fly to get a minimum score of 0 up to a highest possible score of 16.

Actin Bundling Sedimentation Assay

Briefly, actin filaments were generated by adding 1/10 volume of actin polymerization buffer (500mM KCl, 20mM $MgCl_2$, 10mM ATP, in 100mM Tris pH 7.5) to reconstituted monomeric rabbit actin (0.5mg/mL, Cytoskeleton Inc) followed by a 1-hour room temperature incubation. Approximately 5 μg of purified Tarp, Fascin, BSA or a combination of Tarp (1 to 5μg) and Fascin (added simultaneously or sequentially) was added to 40 μg of F-actin and allowed to incubate for 1 hour at room temperature. Actin bundles and bound proteins were separated by differential sedimentation at 10,000 X *g* for 1 hour in a Beckman Optima MAX-TL Ultracentrifuge using a TLA55 or TLA 100.3 rotor (Beckman Coulter, Life Sciences). Proteins associated with the actin bundles in the pellet were compared to unbound proteins that remained in the supernatant by resolving the proteins on 4-12% SDS-polyacrylamide gels followed by Coomassie staining. Densitometric analysis of protein bands were performed in FIJI (Schindelin et al., 2012).

TmeA Antibody Generation and Western Blotting

The complete open reading frame of L2 TmeA (CT694, CTL0063) was cloned into pGEX-6p-1 (Cytiva Life Sciences) and expressed as a GST-fusion. The fusion protein was purified with glutathione sepharose beads and eluted from the column following digestion with PreScission Protease according to the directions of the GST-Bulk kit (Cytiva Life Sciences). The GST-free TmeA was used an immunogen to produce specific guinea pig polyclonal antibodies (Cocalico Biologicals Inc.).

For heat shock induction, fly vials were placed in a 37°C water bath for 1 hour, and immediately homogenized in SDS-PAGE sample buffer. Whole flies were crushed in SDS-PAGE sample buffer (10 flies per 100 μl sample) and heated at 95°C for 10 minutes. Samples were run on 4-12% SDS-polyacrylamide gels. The following antibodies were used: rabbit polyclonal α-Tarp, 1:1000 (Clifton et al., 2004); guinea pig polyclonal α-TmeA (1:50, affinity purified); mouse monoclonal α-GAPDH (Invitrogen, GA1R); mouse monoclonal α-β-actin antibody (BD Biosciences, C4); anti-rabbit and anti-mouse HRP-conjugated antibodies; 1:10,000 (Millipore). Immunoblots were imaged on a Bio-Rad ChemiDoc Imager.

Graphs, Figures, and Statistics

Graphpad Prism was used to generate graphs and perform statistical tests. Figures were generated and assembled using FigureJ (Mutterer and Zinck, 2013), FIJI (Schindelin et al., 2012) and Adobe Illustrator.

RESULTS

Tarp Is Phosphorylated and Forms F-Actin Aggregates in *Drosophila melanogaster*

We generated transgenic *Drosophila melanogaster* engineered to express *Chlamydia trachomatis* L2 Tarp. Expression was temporally and spatially controlled in various tissues of interest using the GAL4-UAS binary expression strategy (Brand and Perrimon, 1993). To drive Tarp expression, UAS-Tarp flies were

mated (a.k.a. crossed) with unique GAL4 flies resulting in progeny capable of tissue-specific Tarp expression (**Figure 1A**).

To verify the expression of Tarp in flies, we ubiquitously expressed Tarp in all tissues using a heat shock-inducible GAL4. Inducible expression allows for temporal control of Tarp expression and bypasses potential toxicity defects that may halt the developmental cycle prior to the adult stage. Western blot analysis shows robust Tarp expression in hs-GAL4/UAS-Tarp flies (Tarp) (**Figure 1B**, left, arrows). We observed bands corresponding to full-length Tarp (>150kDa) as well as possible proteolytic cleavage products. Whole fly lysates from hs-GAL4/UAS-GFP flies served as the negative control.

During chlamydial invasion, Tarp is rapidly phosphorylated in the host cell following translocation *via* type III secretion apparatus (Clifton et al., 2004). We tested whether transgenically expressed Tarp is similarly phosphorylated in *Drosophila*. Western blot analysis revealed a collection of phosphotyrosine-rich proteins whose migration coincided with nearly all Tarp-specific bands (**Figure 1B**, right, black arrows). Control fly lysates revealed a single prominent phosphotyrosine band at ~150 kDa, likely obscuring one of the Tarp-corresponding bands (**Figure 1B**, right, gray arrow). This correlation provides further evidence of Tarp expression in flies and shows that Tarp can be phosphorylated by endogenous *D. melanogaster* kinases.

We also examined the cellular localization of Tarp in *Drosophila* cells by driving expression in epithelial follicle cells of the egg chamber. The egg chamber, the basic subunit of *Drosophila* oogenesis, is completely enveloped by a monolayer of epithelial follicle cells and are highly amenable to dissection and immunofluorescence staining without disrupting tissue organization. Clonal populations of follicle cells that drive ubiquitous transgene expression were randomly generated (see *Materials and Methods*). These clonal follicle cell populations are marked by GFP expression. Tarp expression resulted in the formation of F-actin aggregates and Tarp itself was enriched in said aggregates (**Figure 1C**, bottom). Moreover, these aggregates

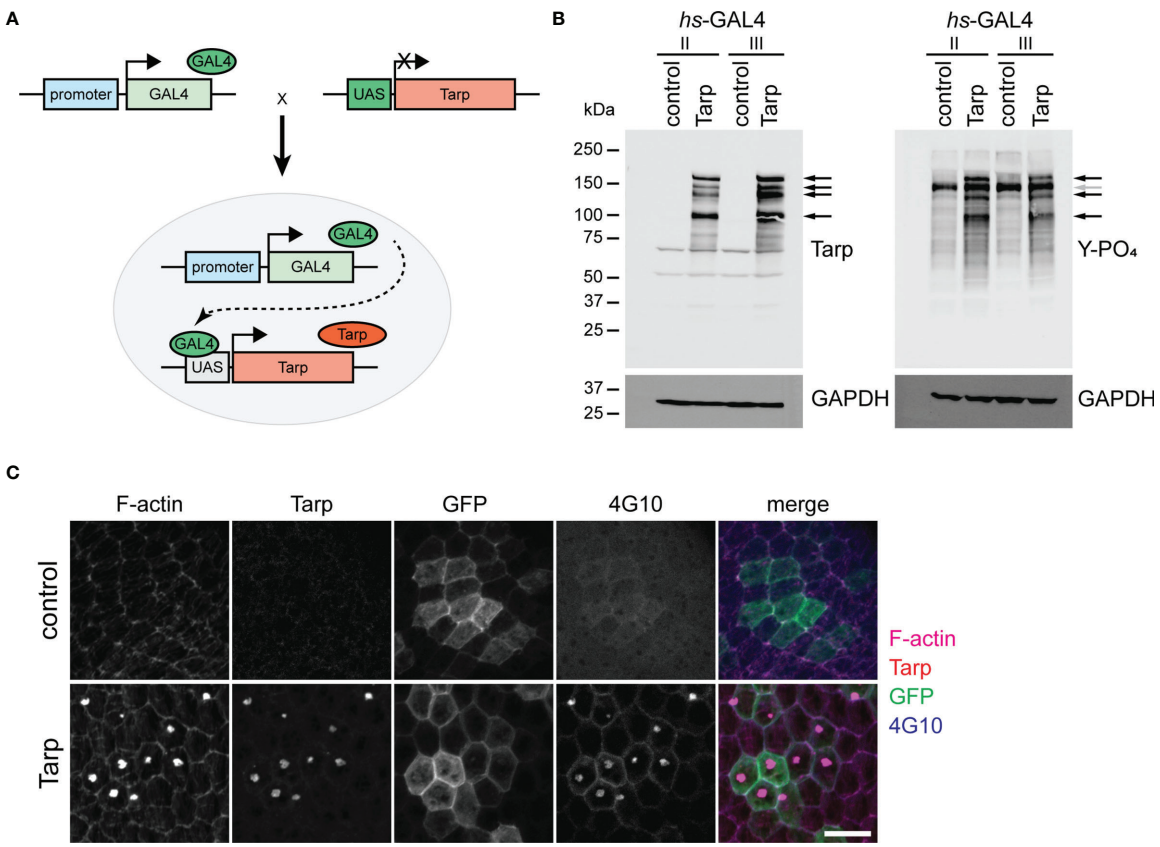

FIGURE 1 | Transgenically expressed Tarp is phosphorylated and forms actin-rich aggregates in flies. **(A)** Schematic diagram of the GAL4/UAS binary expression system. A transgenic fly stock was created, containing the Tarp open reading frame downstream of the UAS promoter. The Tarp transgenic fly is crossed with another fly that encodes for the GAL4 transcription factor with a defined expression pattern. The progeny of the cross combines both components, prompting Tarp expression in cells where GAL4 is expressed. **(B)** Western blots showing Tarp expression and corresponding tyrosine phosphorylation in flies. Black arrows indicate Tarp bands. Gray arrow indicates the location of a Tarp band obscured by endogenous phosphotyrosine signal. hs-GAL4/UAS-Tarp flies were heat-shocked at 37°C for 1 hour. hs-GAL4/+ flies were used as control. Whole fly lysates were analyzed for the expression of Tarp (left) and tyrosine phosphorylation (right). Two unique hs-GAL4 lines were used (II and III). GAPDH was used as loading control. **(C)** Tarp localizes to actin-rich aggregates in epithelial cells. Clonal populations of follicle epithelial cells (see Immunostaining methods) were immunostained for Tarp, F-actin, and tyrosine phosphorylation (4G10). GFP identifies cells in which GAL4/UAS expression is active. Scale bar,10 μm.

were enriched for tyrosine phosphorylation (**Figure 1C**, bottom). Control follicle cells that expressed GFP alone had no detectable F-actin aggregates (**Figure 1C**, top).

Collectively, these results demonstrated that transgenically expressed Tarp was recognized by endogenous kinases in *Drosophila*. Also, the ability of Tarp to modify F-actin was preserved in the cellular environment of *Drosophila* cells. This suggests that Tarp interaction with the cellular environment is conserved between *Drosophila* and humans.

Tarp Induces Abnormal Curvature of the *Drosophila* Mechanosensory Bristles

We sought to prove Tarp functionality in flies by assessing the impact of the effector on *Drosophila* development. We expressed Tarp constitutively in all tissues using ubi-GAL4, which utilizes the ubiquitin gene *Ubi-p5E* promoter. Tarp expression was validated by Western blot (**Figure S1**). The impact of ubiquitous Tarp expression on viability was assessed by comparing the observed proportion of ubi>Tarp flies within the total progeny population to the expected Mendelian ratio (**Figure S2**). Ubiquitous expression of GFP alone (control) did not impact adult viability and did not skew the male-to-female ratio (**Figure 2A**, left). Conversely, ubiquitous expression of Tarp resulted in a marked decrease in adult survival, recovering about half of the expected Tarp-expressing progeny (**Figure 2A**, right). The male-to-female ratio was also skewed with fewer than expected adult males recovered. GAL4-UAS expression in flies is influenced by temperature, with higher fly rearing temperatures associated with stronger expression (Riabinina et al., 2015). Consistent with this, we observed an enhancement of adult lethality upon ubiquitous Tarp expression when flies are reared at slightly higher temperatures (22°C vs. 25°C) (**Figure 2A**).

To test the specificity of the Tarp-induced lethality, we tested transgenic fly lines that can express the *C.t.* early effector TmeA. Similar to Tarp, TmeA is important for host cell invasion by directing cytoskeleton changes *via* altered Arp2/3 dynamics (McKuen et al., 2017; Faris et al., 2020; Keb et al., 2021). Expression of TmeA in flies *via* the ubi-GAL4 driver was validated by Western blot (**Figure S3A**). Importantly, there

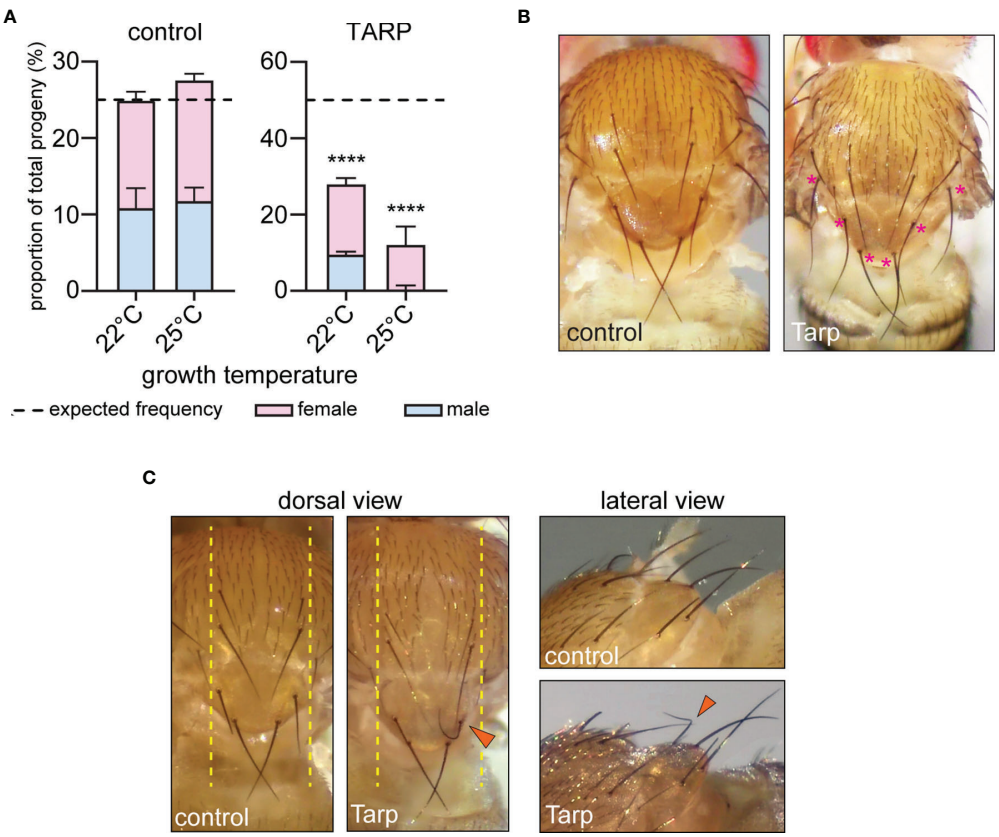

FIGURE 2 | Tarp induces abnormal curvature of large mechanosensory bristles. **(A)** The proportion of ubiquitously expressing GFP (control) or Tarp flies within the progeny population was recorded. The impact of Tarp expression on fly viability was assessed by comparing the observed proportion to expected Mendelian ratio (dashed lines). Fischer's exact test was used to test for significance between observed and expected values (****p<0.0001). The male-to-female ratio is indicated by blue and pink bars, respectively. **(B)** Dorsal thorax of adult flies ubiquitously expressing GFP (control) or Tarp, displaying small and large mechanosensory bristles. In Tarp-expressing flies, asterisks (pink) mark large mechanosensory bristles that display abnormally increased curvature. **(C)** Dorsal thorax of flies that express GFP (control) or Tarp in the central region of the thorax (yellow dashed lines) *via* pnr-GAL4. An abnormally curved bristle (arrowhead) is observed in Tarp-expressing flies. The same flies were imaged in dorsal and lateral view.

was no difference observed in the fly viability upon ubiquitous expression of TmeA compared to GFP (**Figure S3B**).

These findings demonstrate that ubiquitous expression of Tarp in *Drosophila* perturb critical aspects of fly development which manifest as reduced adult survival. From here, we then focused on fly tissues that are sensitive to changes in F-actin dynamics to study Tarp's influence on host actin.

A closer inspection of surviving adult flies that ubiquitously expressed Tarp revealed morphological changes in the large mechanosensory bristles, or macrochaetes, of the dorsal thorax. During pupal development, bristle cells extend a single, cellular protrusion, driven and stabilized by the assembly of large, ordered arrays of F-actin bundles (Tilney and DeRosier, 2005). Macrochaetes of control flies appeared uniformly straight from the dorsal view (**Figure 2B**, left). In contrast, macrochaetes with pronounced curvatures were observed in ubi>Tarp flies examined, particularly the posterior bristles of the thorax (**Figure 2B**, asterisks).

To precisely characterize the observed Tarp-induced bristle curvature, we expressed Tarp in a more defined spatial pattern using a different GAL4 driver, pnr-GAL4, whose expression pattern is restricted to tissues along the dorsal midline (Mummery-Widmer et al., 2009) (**Figure 2C**, dashed lines). Control flies that expressed GFP along the midline had normal macrochaete morphology (**Figure 2C**)(**Table 1**). Consistent with the phenotype of flies ubiquitously expressing Tarp, highly curved macrochaetes were observed for flies expressing Tarp along the midline (**Figure 2C**, arrowhead)(**Table 1**). One third of pnr-GAL4>UAS-Tarp flies (37% of males, 31% of females) (**Table 1**) displayed highly curved macrochaetes and, in most cases, only one macrochaete was visibly affected per fly. Bristle morphology defects were not observed when the *C.t.* effector TmeA is expressed in the thorax (**Figure S3C**), showing Tarp specificity of the phenotypes observed.

Therefore, the presence of Tarp interferes with fly bristle morphology, which manifests as increased bristle curvature. This is likely due to Tarp's specific influence on host actin dynamics since bristle shape depends on actin filament formation and bundling.

Tarp Can Substitute for the Loss of the Endogenous F-Actin Bundler Singed/Fascin During Bristle Development

Tarp can promote actin filament formation from monomeric actin (Jewett et al., 2006). Interestingly, it also induces the formation of F-actin bundles *in vitro* (Jiwani et al., 2013; Ghosh et al., 2018). We tested the physiological relevance of Tarp's F-actin bundling property *in vivo* using *Drosophila* bristles as a cell biological model. There are two F-actin bundlers that are required for normal bristle shape: 1) Forked/Espin; and 2) Singed/Fascin (Tilney et al., 1998). The loss of either *forked* or *singed* leads to short bristles with multiple sharp bends or curls (Cant et al., 1994; Petersen et al., 1994). We tested whether Tarp could alleviate the bristle morphology defect in bristles upon knockdown of endogenous bundlers. Engagement of the RNAi machinery *via* the expression of double-stranded RNA targeting GFP in the thorax does not lead to bristle morphology defects (**Figure S4**). On the other hand, RNAi knockdown of *forked* or *singed* in the thorax led to highly abnormal bristles (**Figure 3A**, top row), similar to the corresponding loss-of-function mutations (Cant et al., 1994; Petersen et al., 1994). Tarp expression in the *forked* RNAi background did not relieve the bristle phenotype (**Figure 3A**, bottom left). In contrast, Tarp expression in the *singed* RNAi background resulted in appreciable reduction of the bristle phenotype (**Figure 3A**, bottom right, asterisks).

To better describe the observed rescue of *singed* knockdown, we devised a scoring rubric to systematically appraise and compare the observed bristle morphology defects across different fly populations (see *Material and Methods*). A bristle defect score of '0' represents normal, wild-type bristles while a maximum score of '16' represents severe malformation of all bristles examined. *singed* knockdown flies show a distribution of scores centered around '10' for both males and females, with the females having a slightly larger spread (**Figure 3B**, blue bars). Expression of Tarp in the *singed* RNAi background results in a leftward shift of the peak of the bristle defect score histogram for both male and female populations (**Figure 3B**). This indicates a partial alleviation of the *singed* knockdown phenotype in the Tarp-expressing fly population.

This demonstrates that Tarp can partially take the place of an endogenous F-actin bundler to promote normal bristle morphology, providing physiological evidence of Tarp's bundling activity.

Tarp Alters the Localization of the Endogenous F-Actin Bundler Singed in Developing Bristles

The final shape and size of mechanosensory bristles is established during pupal development before flies hatch. We dissected the

TABLE 1 | Frequency of bristle phenotypes in control and Tarp-expressing flies using pnr-GAL4.

bristle phenotypes	males								females							
	pnr>GFP				pnr>Tarp				pnr>GFP				pnr>Tarp			
	trial 1	trial 2	trial 3	Ave	trial 1	trial 2	trial 3	Ave	trial 1	trial 2	trial 3	Ave	trial 1	trial 2	trial 3	Ave
scutellar bristle, curved	0%	0%	0%	0%	35%	36%	39%	37%	0%	0%	0%	0%	30%	29%	33%	31%
scutellar bristle, upturned	0%	0%	0%	0%	7%	0%	18%	8%	0%	0%	0%	0%	5%	8%	6%	6%
scutellar bristle, bent	0%	0%	0%	0%	2%	0%	0%	1%	0%	0%	0%	0%	0%	0%	0%	0%
number of flies scored	30	47	26		55	11	28		41	41	29		56	24	36	

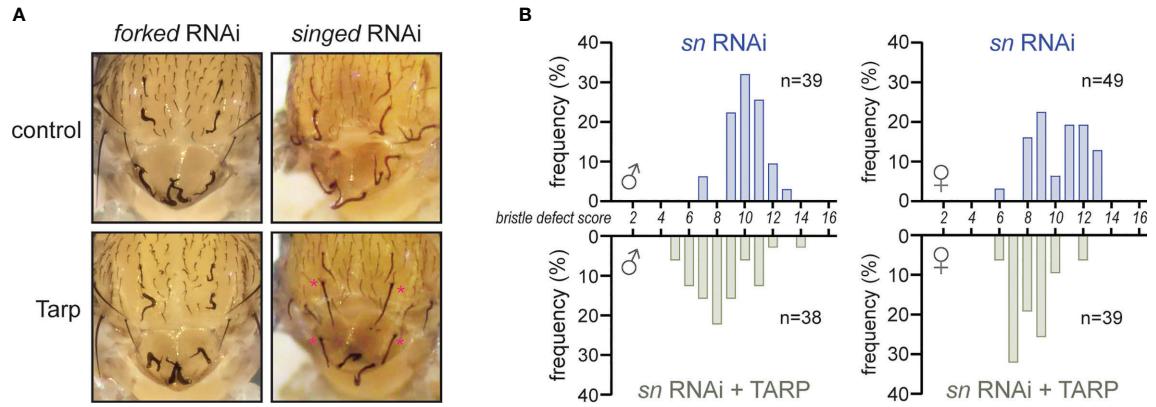

FIGURE 3 | Tarp partially rescues the loss of the host F-actin bundler Singed/Fascin during bristle development. **(A)** RNAi knockdown of host F-actin bundlers *forked* and *singed* result in severe bristle morphology defects. Tarp expression in the *singed* RNAi background restores bristles to near-normal morphology (asterisks). **(B)** Histograms of bristle defect scores of male and female fly populations of *singed* RNAi knockdown alone (blue bars) or with Tarp expression (green bars). Each fly was assigned a bristle defect score: '0' being wildtype; and '16' as complete and severe defect (see *Material and Methods*). There is a leftward shift of bristle defect score distribution in the fly populations that express tarp in the *singed* RNAi background.

dorsal pelt of *Drosophila* pupae to better understand the impact of Tarp expression on bristle cell biology. The elongating bristles of developing macrochaetes are readily visualized using fluorescent phalloidin, highlighting the abundance of F-actin in these structures (**Figure 4A**, left, dashed lines). Singed is also highly enriched in the bristle cells, both in the growing protrusion as well as the bristle cell body (**Figure 4A**, middle, dashed circles). Last, the number and topology of mechanosensory bristles are already established during pupal development. This allows us to identify the specific bristles that exhibit increased curvature in the adult.

Since pnr-GAL4 drives Tarp expression over a broad central region of the thorax made up of different cell types (**Figure S5**), we sought to verify that Tarp is expressed in the developing bristle cells themselves. High-magnification imaging of the cell body of control bristle cells showed F-actin outlining the cell body and enriched at the base of the bristle primordium; Singed is similarly enriched at the bristle primordium base (**Figure 4B**, top row). pnr>Tarp pupal bristle cells appear similarly but with the addition of a striking F-actin-rich Tarp aggregate in the cell body (**Figure 4B**, bottom row). Striped phalloidin staining at the bristle primordium base of both control and Tarp-expressing bristles represent F-actin bundles that extend into the growing bristle primordium.

We further investigated whether Tarp can be found within the growing bristle primordium itself. Control bristles contained longitudinally arranged F-actin bundles (**Figure 4C**, top). Singed was also enriched within growing bristles, in similar longitudinal stripes (**Figure 4C**, top). Bristles from Tarp-expressing cells displayed prominent F-actin bundles as well as longitudinal stripes of Singed enrichment (**Figure 4C**, bottom). In addition, Tarp was detected within the developing bristle itself, enriched in longitudinal stripes but distributed heterogeneously, presenting either as distinct or contiguous clumps (**Figure 4C**, bottom). The large area of Tarp staining outside the bristle comes from surrounding epithelial cells of the pupal pelt. To image distinct F-actin bundles, thin optical sections of the pupal bristle were imaged, which affects the apparent thickness of the bristle. No major difference in pupal bristle thickness was observed between genotypes examined.

We performed line intensity analysis on the immunostained bristles to visualize protein localization within the bristles. Control bristles displayed a strong correlation between the F-actin bundles and the endogenous bundler Singed, consistent with its known function (**Figures 5A, B**, left). Surprisingly, when Tarp was expressed in bristles, the peak Singed fluorescence intensity occurs away from the F-actin bundles (**Figures 5A, B**, right). Pupal bristles from flies that simultaneously knockdown the actin bundler *singed* while expressing Tarp shows a strong correlation between F-actin bundles and Tarp (**Figures 5A, C**), consistent with Tarp's ability to alleviate the *singed* RNAi phenotype.

This observation suggests the possibility of a novel interaction between Tarp and Singed, wherein Tarp may negatively influence the ability of the host F-actin bundler to participate in actin bundle formation.

Tarp Outcompetes Fascin in Forming F-Actin Bundles *In Vitro*

To further investigate the competitive behavior between Tarp and Fascin (Singed), we performed an *in vitro* F-actin bundling assay using purified Tarp and Fascin. Incubation of pre-formed actin filaments with actin bundlers results in the formation of F-actin bundles, which can be isolated *via* low-speed centrifugation. On its own or with bovine serum albumin (BSA) as a negative control, filamentous actin was present primarily in the supernatant, indicating the lack of F-actin bundle formation (**Figure 6A**). Assessed individually, Fascin and Tarp were both potent bundlers of F-actin (**Figure 6A**).

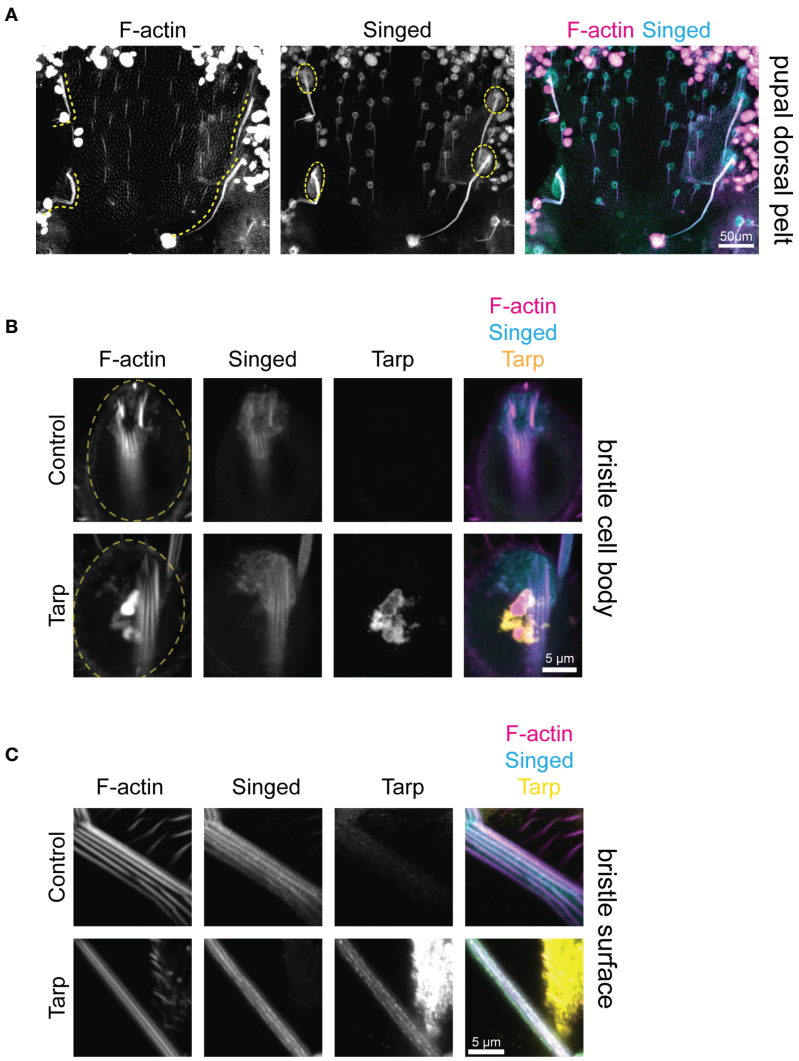

FIGURE 4 | Tarp is found within the growing bristle primordium during pupal development. **(A)** Confocal micrographs of a dissected dorsal pelt of control *Drosophila* pupa immunostained to visualize F-actin and Singed localization. Developing large mechanosensory bristles (yellow dashed lines) emerge from bristle cell bodies (yellow dashed circles). The number and topology of bristles are already determined at the pupal stage. **(B)** High-magnification confocal micrographs of bristle cell bodies (yellow dashed circles) from control or Tarp-expressing pupae. Tarp is enriched in F-actin-abundant aggregates in the bristle cell body. F-actin bundles are found at the base of the bristle primordium. **(C)** Thin optical sections of high-magnification representative confocal micrographs of developing pupal bristles from control (n=9) and Tarp-expressing (n=8) pupae. Longitudinally-arrayed F-actin bundles and Singed localization was observed for both genotypes. Tarp is similarly found within the growing bristle in Tarp-expressing flies. For all panels, Singed and Tarp localization was determined by immunostaining. F-actin was visualized using Alexa-conjugated phalloidin. Tarp expression was driven by pnr-GAL4.

Simultaneous addition of Tarp and Fascin to filamentous actin resulted similarly efficient F-actin bundling, with the vast majority of Tarp found in the pellet fraction (**Figure 6A**). Surprisingly, the converse was true for Fascin, with a majority of Fascin detected in the supernatant fraction (**Figures 6A, B**). Thus, when added simultaneously, Tarp can exclude Fascin from associating with actively assembling F-actin bundles. This suggests that Tarp has a competitive advantage over Fascin in participating in F-actin bundle formation.

As an early effector that is secreted into living cells during infection, beyond driving actin bundle formation *de novo*, Tarp may also interact with existing F-actin bundles. We therefore sought to determine the outcome of Tarp-Fascin dynamics in the presence of pre-assembled actin bundles. To do this, Fascin was added to F-actin and incubated to form bundles (t_0). Subsequently, buffer, BSA (negative control) or Tarp was added to the samples, followed by a second incubation (t_1). Buffer treatment or the addition of BSA did not alter Fascin-assembled F-actin bundles nor the enrichment of Fascin in the pellet fractions (**Figure 6C**). Upon addition of Tarp to Fascin-assembled bundles, a large proportion of Tarp was found in the pellet fraction (**Figure 6C**), indicating an association with F-actin bundles. Interestingly, we did not observe a strong Fascin distribution to the supernate in this condition. Instead, Fascin

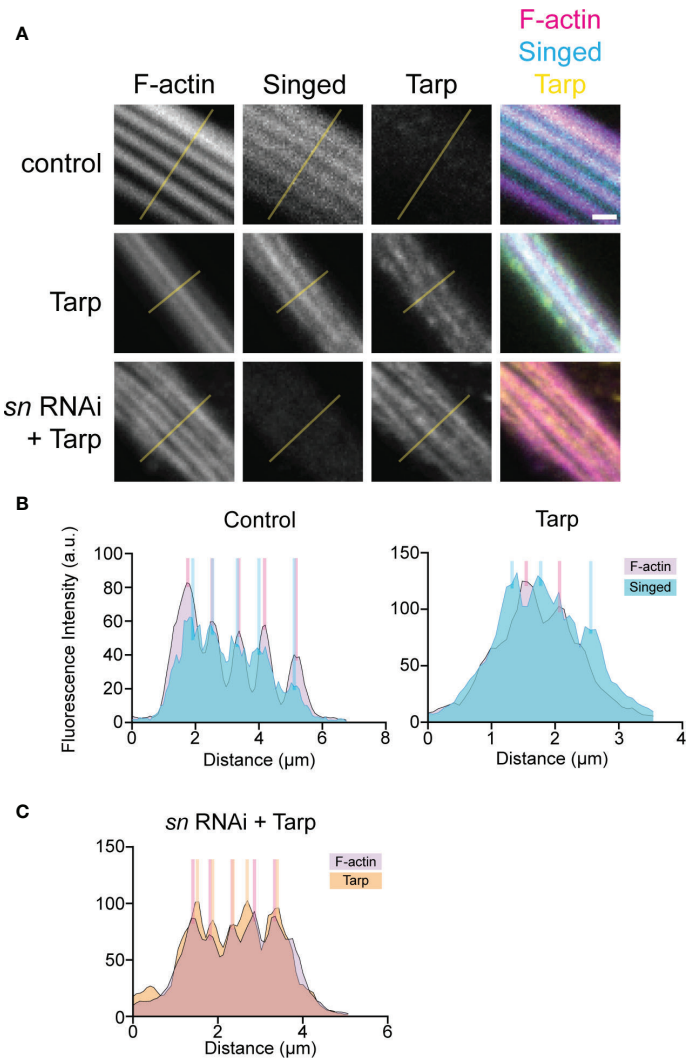

FIGURE 5 | Tarp expression results in mislocalization of host F-actin bundler Singed away from F-actin bundles in developing pupal bristles. **(A)** Line analysis of high-magnification confocal micrographs of control and Tarp-expressing pupal bristles, as well as pupal bristle from flies that express Tarp in the *singed* RNAi background. Fluorescent pixel intensity along the length of the yellow line were plotted for each indicated channel **(B, C)**. Peak fluorescent intensities, corresponding to the localization patterns, were highlighted with colored bars. Scale bar, 1μm. Representative data and images are shown out of three trials.

distribution was comparable to that when Fascin is added to F-actin alone. We further examined this competitive behavior by testing different concentrations of Tarp during simultaneous co-incubation with Fascin. The competitive interaction was preserved even with a reduced amount of Tarp protein ($Tarp_{low}$) (**Figure 6A**, last two lanes). More strikingly, Fascin continues to be outcompeted through sequential reduction of Tarp concentration, remaining strongly enriched in the supernate fraction (**Figure 6D**).

DISCUSSION

Drosophila melanogaster is a highly tractable model organism with a wealth of genetic tools and reagents and is adaptable to numerous experimental modalities. Decades of research led to thorough understanding of its cell and developmental biology. Therefore, perturbations in different aspects of its development can be readily traced back to specific gene/s or pathway/s. These characteristics makes *Drosophila* a valuable tool to discover new or underappreciated functions of bacterial effectors, particularly outside the confounding effects of infection. This approach has been used to study effectors from *Helicobacter* (Reid et al., 2012) and *Chlamydia* (Shehat et al., 2021). *Drosophila*-derived cell lines have also been used to study the *Yersinia* effector YopJ (Paquette et al., 2012).

Tarp promotes F-actin bundling *in vitro* (Jiwani et al., 2013) though, prior to this work, this has not been demonstrated in a physiological context. It is, therefore, significant that Tarp induces a change in shape in wild-type adult mechanosensory

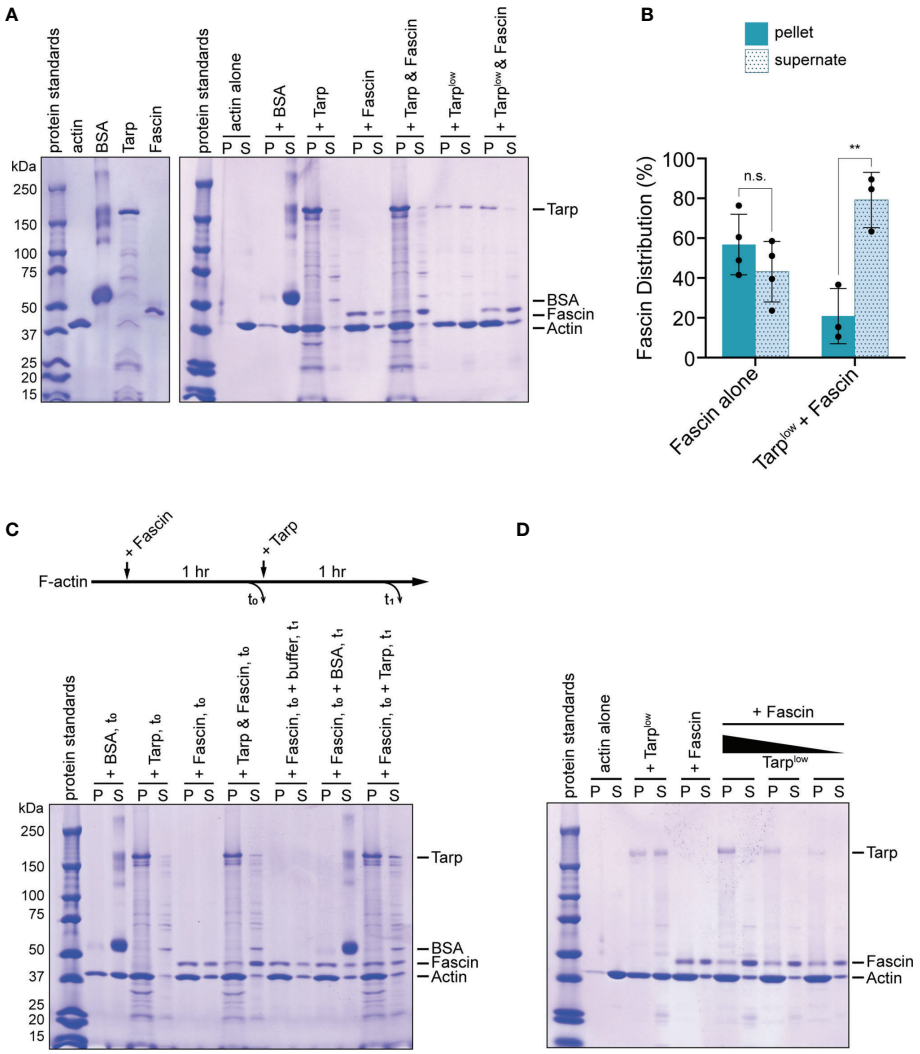

FIGURE 6 | Tarp outcompetes Fascin in F-actin bundling formation *in vitro*. **(A)** An *in vitro* F-actin bundling assay was performed using purified Tarp and Fascin, alone or in combination. Bovine serum albumin (BSA) does not interact with F-actin and serves as negative control. F-actin bundles, together with associated bundling proteins, are enriched in the pellet fraction. In the presence of Tarp or Fascin, actin is enriched in the pellet fraction as well as the corresponding F-actin bundlers. Simultaneous addition of Tarp and Fascin to F-actin results enrichment of actin and Tarp in the pellet fraction, while the majority of Fascin is found in the supernate. Exclusion of Fascin from the pellet fraction still occurs even with a reduced amount of Tarp ($Tarp^{low}$). **(B)** Fascin distribution following F-actin bundling assays when added alone (Fascin alone) or simultaneously with Tarp ($Tarp^{low}$ + Fascin). Multiple trials are represented. Fascin is predominantly found in the supernate fraction when Tarp is present during F-actin bundling (Welch's t test, **p<0.01). n.s. not significant. **(C)** *In vitro* F-actin bundling was further assessed after sequential addition of Tarp and Fascin. Individual proteins, as well as Tarp and Fascin together, added at the beginning of the assay and sampled at t_0, recapitulated the original finding. Fascin, followed by the addition of buffer or BSA, at t_0, resulted in F-actin bundling and enrichment of Fascin in the pellet fraction, upon analysis at t_1. Subsequent addition of Tarp at t_0 to Fascin-assembled bundles resulted in enrichment of Tarp in the pellet fraction when, with minimal impact on Fascin distribution, upon analysis at t_1. **(D)** When added simultaneously, Tarp is able to outcompete Fascin during F-actin bundle formation even with diminishing amounts of Tarp. Individually, Tarp ($Tarp^{low}$) and Fascin efficiently form F-actin bundles and Fascin is highly enriched in the pellet fraction. On the other hand, Fascin is predominantly shifted to the supernate fraction, across all Tarp concentrations tested.

bristles, since bristle shape is intimately linked to F-actin bundling during pupal development. Moreover, we showed that Tarp can partially rescue the morphology defect caused by loss of the endogenous bundler Singed/Fascin. This is a strong demonstration of Tarp's F-actin bundling activity *in vivo*. We also believe that these phenotypic changes are primarily due to Tarp's bundling activity rather than its actin polymerization activity. F-actin polymerization primarily occurs at the growing tip of the pupal bristle (DeRosier and Tilney, 2000), away from the mature F-actin bundles, where Tarp is localized. Last, increased F-actin polymerization in bristles manifest as forking or branching, a phenotype which was not observed upon Tarp expression (Hopmann and Miller, 2003).

We discovered a novel, competitive interaction between Tarp and Fascin during F-actin bundling. When simultaneously added to filamentous actin *in vitro*, Tarp outcompetes Fascin during

bundling, relegating the endogenous bundler away from F-actin bundles. Competitive behavior between different F-actin bundlers has been documented. Two host bundlers, Fascin and alpha-Actinin, exclude each other from bundle formation due to a difference in F-actin packing mediated by the size of the cross-linking molecule (the alpha-Actinin molecule is long; Fascin is compact) (Winkelman et al., 2016). It is possible that the competition observed between Tarp (>150kDa) and Fascin (55kDA) occur *via* a similar mechanism. Alternatively, Tarp might have a higher bundling affinity compared to Fascin, outpacing Fascin's ability to form F-actin bundles. Our *in vitro* finding is consistent with the observed *in vivo* displacement of *Drosophila* Singed from F-actin bundles when Tarp is present and supports a direct influence of Tarp on Singed localization *in vivo* rather than through some other cellular mechanism.

In vivo, Chlamydia infections occur at mucosal linings, whose epithelial cells are covered in microvilli on the apical face. Microvilli are short, hair-like membrane projections that are stabilized by crosslinked F-actin bundles, similar to *Drosophila* pupal bristles. A Chlamydia elementary body will interact and possible enter through this microvilli-rich cell surface, and early effectors such as Tarp may have to interact with this particular actin environment, perhaps through Tarp's ability to compete with endogenous actin bundlers.

The validation of Tarp's bundling activity *in vivo* and its ability to compete with endogenous host bundlers during F-actin bundle formation adds to the repertoire of molecular functions that Tarp can deploy during Chlamydia infection. Promoting F-actin polymerization at the site of entry is a major Chlamydia strategy during host cell invasion (Jewett et al., 2006; McKuen et al., 2017; Ghosh et al., 2020; Keb et al., 2021) but F-actin bundling itself has yet to be mechanistically implicated. Our finding raises the possibility that F-actin bundling and/or competition with host bundlers is a component of Tarp function in promoting Chlamydia infection.

In this study, we demonstrated physiological evidence of Tarp's bundling activity *in vivo*. Furthermore, we discovered that Tarp inhibits Fascin's innate ability to participate in bundle formation. This property is consistent with the *in vivo* observation of Singed/Fascin displacement upon Tarp expression in developing bristles. Lastly, this work establishes the utility of *Drosophila melanogaster* as a platform to discover new effector functions that do not readily manifest in an *in vitro* tissue culture system.

DATA AVAILABILITY STATEMENT

The raw data supporting the conclusions of this article will be made available by the authors, without undue reservation.

AUTHOR CONTRIBUTIONS

GA is responsible for the main concept and design of the study, with advice from TJ. GA and JK performed all Drosophila-related work. TJ performed the *in vitro* bundling assay. GA wrote the drafts of the manuscript. GA and TJ revised and approved the submitted version. All authors contributed to the article and approved the submitted version.

FUNDING

This work is supported by grants from the National Institutes of Health, NIAID, R01AI139242 and R21AI148999 awarded to TJ.

ACKNOWLEDGMENTS

We would like to thank members of TJ and M. Jewett labs for discussion, Dr. Jocelyn McDonald (Kansas State University) for fly stocks, and Dr. Markus Mund (Ries lab, University of Geneva) for key technical advice on pupal bristle dissection and imaging. Stocks obtained from the Bloomington *Drosophila* Stock Center (NIH P40OD018537) were used in this study.

SUPPLEMENTARY MATERIAL

The Supplementary Material for this article can be found online at: https://www.frontiersin.org/articles/10.3389/fcimb.2022.811407/full#supplementary-material

REFERENCES

Betts, H. J., Wolf, K., and Fields, K. A. (2009). Effector Protein Modulation of Host Cells: Examples in the Chlamydia Spp. Arsenal. *Curr. Opin. Microbiol.* 12, 81–87. doi: 10.1016/j.mib.2008.11.009

Blair, S. S. (2003). Genetic Mosaic Techniques for Studying Drosophila development. *Development* 130, 5065–5072. doi: 10.1242/dev.00774

Brand, A., and Perrimon, N. (1993). Targeted Gene Expression as a Means of Altering Cell Fates and Generating Dominant Phenotypes. *Dev. Camb Engl.* 118, 401–415. doi: 10.1242/dev.118.2.401

Cant, K., Knowles, M., and Cooley, L. (1994). Drosophila Singed, a Fascin Homolog, is Required for Actin Bundle Formation During Oogenesis and Bristle Extension. *J. Cell Biol.* 125, 369–380. doi: 10.1083/jcb.125.2.369

Clifton, D., Fields, K., Grieshaber, S., Dooley, C., Fischer, E., Mead, D., et al. (2004). A Chlamydial Type III Translocated Protein is Tyrosine-Phosphorylated at the Site of Entry and Associated With Recruitment of Actin. *P Natl. Acad. Sci. U.S.A.* 101, 10166–10171. doi: 10.1073/pnas.0402829101

DeRosier, D., and Tilney, L. (2000). F-Actin Bundles are Derivatives of Microvilli: What Does This Tell Us About How Bundles Might Form? *J. Cell Biol.* 148, 1–6. doi: 10.1083/jcb.148.1.1

Faris, R., McCullough, A., Andersen, S. E., Moninger, T. O., and Weber, M. M. (2020). The Chlamydia Trachomatis Secreted Effector TmeA Hijacks the N-WASP-ARP2/3 Actin Remodeling Axis to Facilitate Cellular Invasion. *PloS Pathog.* 16, e1008878. doi: 10.1371/journal.ppat.1008878

Ghosh, S., Park, J., Thomas, M., Cruz, E., Cardona, O., Kang, H., et al. (2018). Biophysical Characterization of Actin Bundles Generated by the Chlamydia Trachomatis Tarp Effector. *Biochem. Bioph Res. Co* 500, 423–428. doi: 10.1016/j.bbrc.2018.04.093

Ghosh, S., Ruelke, E. A., Ferrell, J. C., Bodero, M. D., Fields, K. A., and Jewett, T. J. (2020). Fluorescence-Reported Allelic Exchange Mutagenesis-Mediated Gene Deletion Indicates a Requirement for Chlamydia Trachomatis Tarp During *In*

Vivo Infectivity and Reveals a Specific Role for the C Terminus During Cellular Invasion. *Infect. Immun.* 88, e00841–19. doi: 10.1128/IAI.00841-19

Hopmann, R., and Miller, K. G. (2003). A Balance of Capping Protein and Profilin Functions Is Required to Regulate Actin Polymerization in Drosophila Bristle. *Mol. Biol. Cell* 14, 118–128. doi: 10.1091/mbc.e02-05-0300

Hybiske, K., and Stephens, R. S. (2007). Mechanisms of Host Cell Exit by the Intracellular Bacterium Chlamydia. *Proc. Natl. Acad. Sci.* 104, 11430–11435. doi: 10.1073/pnas.0703218104

Jewett, T. J., Fischer, E. R., Mead, D. J., and Hackstadt, T. (2006). Chlamydial TARP is a Bacterial Nucleator of Actin. *Proc. Natl. Acad. Sci.* 103, 15599–15604. doi: 10.1073/pnas.0603044103

Jewett, T. J., Miller, N. J., Dooley, C. A., and Hackstadt, T. (2010). The Conserved Tarp Actin Binding Domain Is Important for Chlamydial Invasion. *PloS Pathog.* 6, e1000997. doi: 10.1371/journal.ppat.1000997

Jiwani, S., Alvarado, S., Ohr, R. J., Romero, A., Nguyen, B., and Jewett, T. J. (2013). Chlamydia Trachomatis Tarp Harbors Distinct G and F Actin Binding Domains That Bundle Actin Filaments. *J. Bacteriol* 195, 708–716. doi: 10.1128/JB.01768-12

Keb, G., Ferrell, J., Scanlon, K. R., Jewett, T. J., and Fields, K. A. (2021). Chlamydia Trachomatis TmeA Directly Activates N-WASP To Promote Actin Polymerization and Functions Synergistically With TarP During Invasion. *Mbio* 12, e02861–20. doi: 10.1128/mBio.02861-20

Kreisel, K. M., Spicknall, I. H., Gargano, J. W., Lewis, F. M. T., Lewis, R. M., Markowitz, L. E., et al. (2021). Sexually Transmitted Infections Among US Women and Men: Prevalence and Incidence Estimate. *Sex Transm Dis.* 48, 208–214. doi: 10.1097/OLQ.0000000000001355

Mårdh, P.-A. (2002). Influence of Infection With Chlamydia Trachomatis on Pregnancy Outcome, Infant Health and Life-Long Sequelae in Infected Offspring. *Best Pract. Res. Cl Ob* 16, 847–864. doi: 10.1053/beog.2002.0329

McDonald, J. A., and Montell, D. J. (2005). *Analysis of Cell Migration Using Drosophila as a Model System* (Totowa, NJ: Humana Press), 175–202.

McKuen, M., Mueller, K., Bae, Y., and Fields, K. (2017). Fluorescence-Reported Allelic Exchange Mutagenesis Reveals a Role for Chlamydia Trachomatis TmeA in Invasion That Is Independent of Host AHNAK. *Infect. Immun.* 85, e00640-17. doi: 10.1128/IAI.00640-17

Moulder, J. W. (1991). Interaction of Chlamydiae and Host Cells *In Vitro*. *Microbiol. Rev.* 55, 143–190. doi: 10.1128/mr.55.1.143-190.1991

Mummery-Widmer, J. L., Yamazaki, M., Stoeger, T., Novatchkova, M., Bhalerao, S., Chen, D., et al. (2009). Genome-Wide Analysis of Notch Signalling in Drosophila by Transgenic RNAi. *Nature* 458, 987. doi: 10.1038/nature07936

Mutterer, J., and Zinck, E. (2013). Quick-And-Clean Article Figures With FigureJ. *J. Microsc-Oxford* 252, 89–91. doi: 10.1111/jmi.12069

Paquette, N., Conlon, J., Sweet, C., Rus, F., Wilson, L., Pereira, A., et al. (2012). Serine/threonine Acetylation of Tgfβ-Activated Kinase (TAK1) by Yersinia Pestis YopJ Inhibits Innate Immune Signaling. *Proc. Natl. Acad. Sci.* 109, 12710–12715. doi: 10.1073/pnas.1008203109

Petersen, N., Lankenau, D., Mitchell, H., Young, P., and Corces, V. (1994). Forked Proteins are Components of Fiber Bundles Present in Developing Bristles of Drosophila Melanogaster. *Genetics* 136, 173–182. doi: 10.1093/genetics/136.1.173

Peters, J., Wilson, D. P., Myers, G., Timms, P., and Bavoil, P. M. (2007). Type III Secretion À La Chlamydia. *Trends Microbiol.* 15, 241–251. doi: 10.1016/j.tim.2007.04.005

Reid, D. W., Muyskens, J. B., Neal, J. T., Gaddini, G. W., Cho, L. Y., Wandler, A. M., et al. (2012). Identification of Genetic Modifiers of CagA-Induced Epithelial Disruption in Drosophila. *Front. Cell Infect. Mi* 2, 24. doi: 10.3389/fcimb.2012.00024

Riabinina, O., Luginbuhl, D., Marr, E., Liu, S., Wu, M. N., Luo, L., et al. (2015). Improved and Expanded Q-System Reagents for Genetic Manipulations. *Nat. Methods* 12, 219–222. doi: 10.1038/nmeth.3250

Schindelin, J., Arganda-Carreras, I., Frise, E., Kaynig, V., Longair, M., Pietzsch, T., et al. (2012). Fiji: An Open-Source Platform for Biological-Image Analysis. *Nat. Methods* 9, 676–682. doi: 10.1038/nmeth.2019

Shehat, M. G., Aranjuez, G. F., Kim, J., and Jewett, T. J. (2021). The Chlamydia Trachomatis Tarp Effector Targets the Hippo Pathway. *Biochem. Bioph Res. Co* 562, 133–138. doi: 10.1016/j.bbrc.2021.05.057

Stricker, J., Falzone, T., and Gardel, M. L. (2010). Mechanics of the F-Actin Cytoskeleton. *J. Biomech* 43, 9–14. doi: 10.1016/j.jbiomech.2009.09.003

Tilney, L., Connelly, P., Smith, S., and Guild, G. (1996). F-Actin Bundles in Drosophila Bristles are Assembled From Modules Composed of Short Filaments. *J. Cell Biol.* 135, 1291–1308. doi: 10.1083/jcb.135.5.1291

Tilney, L. G., Connelly, P. S., Vranich, K. A., Shaw, M. K., and Guild, G. M. (1998). Why Are Two Different Cross-Linkers Necessary for Actin Bundle Formation *In Vivo* and What Does Each Cross-Link Contribute? *J. Cell Biol.* 143, 121–133. doi: 10.1083/jcb.143.1.121

Tilney, L. G., and DeRosier, D. J. (2005). How to Make a Curved Drosophila Bristle Using Straight Actin Bundles. *P Natl. Acad. Sci. U.S.A.* 102, 18785–18792. doi: 10.1073/pnas.0509437102

Tilney, L., Tilney, M., and Guild, G. (1995). F Actin Bundles in Drosophila Bristles. I. Two Filament Cross-Links are Involved in Bundling. *J. Cell Biol.* 130, 629–638. doi: 10.1083/jcb.130.3.629

Verheyen, E., and Cooley, L. (1994). Profilin Mutations Disrupt Multiple Actin-Dependent Processes During Drosophila Development. *Development* 120, 717–728. doi: 10.1242/dev.120.4.717

Winkelman, J. D., Suarez, C., Hocky, G. M., Harker, A. J., Morganthaler, A. N., Christensen, J. R., et al. (2016). Fascin- and α-Actinin-Bundled Networks Contain Intrinsic Structural Features That Drive Protein Sorting. *Curr. Biol.* 26, 2697–2706. doi: 10.1016/j.cub.2016.07.080

Wu, J., Wang, H., Guo, X., and Chen, J. (2016). Cofilin-Mediated Actin Dynamics Promotes Actin Bundle Formation During Drosophila Bristle Development. *Mol. Biol. Cell* 27, 2554–2564. doi: 10.1091/mbc.e16-02-0084

Conflict of Interest: The authors declare that the research was conducted in the absence of any commercial or financial relationships that could be construed as a potential conflict of interest.

frontiers in Cellular and Infection Microbiology

MINI REVIEW
published: 07 March 2022
doi: 10.3389/fcimb.2022.861899

The Impact of Lateral Gene Transfer in *Chlamydia*

Hanna Marti[1]*, *Robert J. Suchland*[2] *and Daniel D. Rockey*[3]

[1] Institute of Veterinary Pathology, Vetsuisse-Faculty, University of Zurich, Zurich, Switzerland, [2] Division of Allergy and Infectious Diseases, Department of Medicine, University of Washington, Seattle, WA, United States, [3] Department of Biomedical Sciences, Carlson College of Veterinary Medicine, Oregon State University, Corvallis, OR, United States

Lateral gene transfer (LGT) facilitates many processes in bacterial ecology and pathogenesis, especially regarding pathogen evolution and the spread of antibiotic resistance across species. The obligate intracellular chlamydiae, which cause a range of diseases in humans and animals, were historically thought to be highly deficient in this process. However, research over the past few decades has demonstrated that this was not the case. The first reports of homologous recombination in the *Chlamydiaceae* family were published in the early 1990s. Later, the advent of whole-genome sequencing uncovered clear evidence for LGT in the evolution of the *Chlamydiaceae*, although the acquisition of tetracycline resistance in *Chlamydia (C.) suis* is the only recent instance of interphylum LGT. In contrast, genome and *in vitro* studies have shown that intraspecies DNA exchange occurs frequently and can even cross species barriers between closely related chlamydiae, such as between *C. trachomatis*, *C. muridarum*, and *C. suis*. Additionally, whole-genome analysis led to the identification of various DNA repair and recombination systems in *C. trachomatis*, but the exact machinery of DNA uptake and homologous recombination in the chlamydiae has yet to be fully elucidated. Here, we reviewed the current state of knowledge concerning LGT in *Chlamydia* by focusing on the effect of homologous recombination on the chlamydial genome, the recombination machinery, and its potential as a genetic tool for *Chlamydia*.

Keywords: horizontal gene transfer, homologous recombination, *Chlamydiaceae*, RecBCD, RecFOR, co-infection, membrane proteins, DNA uptake

OPEN ACCESS

Edited by:
Luís Jaime Mota, NOVA School of Science and Technology, Portugal

Reviewed by:
Sandeep J. Joseph, Centers for Disease Control and Prevention (CDC), United States

***Correspondence:**
Hanna Marti
hanna.marti@uzh.ch

Specialty section:
This article was submitted to Molecular Bacterial Pathogenesis, a section of the journal Frontiers in Cellular and Infection Microbiology

Received: *25 January 2022*
Accepted: *07 February 2022*
Published: *07 March 2022*

Citation:
Marti H, Suchland RJ and Rockey DD (2022) The Impact of Lateral Gene Transfer in Chlamydia. Front. Cell. Infect. Microbiol. 12:861899. doi: 10.3389/fcimb.2022.861899

INTRODUCTION

The gram-negative *Chlamydiaceae* family consists of several pathogenic species that cause diseases ranging from pneumonia to sexually transmitted infections (STI) in humans, livestock, pets, and wildlife. In humans, *Chlamydia (C.) trachomatis* is the cause of chronic eye infections leading to blindness (trachoma), and STI, while *C. pneumoniae* induces community-acquired pneumonia. *C. psittaci* is a zoonotic pathogen primarily detected in birds causing flu-like symptoms to life-threatening pneumonia in humans. *C. abortus* is the cause of ovine enzootic abortion (OEA) in sheep and goats and may also induce miscarriage in women. In contrast, *C. suis*, another chlamydial species with zoonotic potential, is found in the eyes and intestinal tract of pigs, often remaining asymptomatic (Dean et al., 2013; De Puysseleyr et al., 2014; De Puysseleyr et al., 2017; Sachse and Borel, 2020; Jordan et al., 2020). Although the chlamydial obligate intracellular life cycle is reflected

by extensive streamlining and reduction of the genome (Palmer, 2002; Toft and Andersson, 2010), the *Chlamydiaceae* possess a number of genes involved in DNA uptake, recombination, and repair (Stephens et al., 1998; LaBrie et al., 2019) enabling intra- and interspecies lateral gene transfer (Suchland et al., 2009; Somboonna et al., 2011; Joseph and Read, 2012; Joseph et al., 2015; Marti et al., 2017).

Lateral, or horizontal, gene transfer (LGT) involves transfer of genetic material (DNA) from one cell to another and subsequent integration into the genome of the recipient cell. In bacteria, DNA transfer is primarily facilitated by transduction (bacteriophage infection), conjugation/mobilization/conduction (plasmid transfer), and transformation (uptake of naked DNA). DNA integration is then directed by homologous or non-homologous recombination (Redfield, 2001).

Here, we will review the current state of knowledge regarding lateral gene transfer (LGT) in the *Chlamydiaceae* by focusing on i) the impact of recombination on the *Chlamydiaceae* genome, ii) the homologous recombination machinery of the *Chlamydiaceae*, and iii) homologous recombination as a potential genetic tool.

THE IMPACT OF HOMOLOGOUS RECOMBINATION ON THE CHLAMYDIAL GENOME

The first reports providing evidence for intrastrain recombination within *C. trachomatis* were published in the 1990s and were based on gene-specific sequence analysis of *ompA*, which encodes the major outer membrane protein (MOMP) (Lampe et al., 1993; Brunham et al., 1994; Hayes et al., 1994; Hayes et al., 1995). Whole-genome analysis of laboratory and clinical strains later revealed that recombination events occurred across the entire genome during the evolution of *C. trachomatis* (Jeffrey et al., 2010; Joseph et al., 2011; Harris et al., 2012), as well as other chlamydial species such as *C. pneumoniae*, *C. psittaci*, and *C. suis* (Read et al., 2013; Roulis et al., 2015; Joseph et al., 2016; Seth-Smith et al., 2017b). Interestingly, investigation of *C. abortus* revealed no sign of recombination in currently circulating strains (Joseph et al., 2015; Seth-Smith et al., 2017a).

Whole-genome analyses further identified regions of high genomic diversity and, in parallel, regions with apparently higher rates of recombination. In *C. trachomatis* and *C. pneumoniae*; these included *ompA* (Hayes et al., 1994), the polymorphic membrane protein-encoding genes (*pmps*) (Jordan et al., 2001; Rocha et al., 2002; Brunelle and Sensabaugh, 2006), *incA*, and the translocated actin-recruiting phosphoprotein-encoding gene *tarp* (Joseph et al., 2012; Joseph and Read, 2012; Roulis et al., 2015), as well as the plasticity zone (PZ) (Jeffrey et al., 2010). Tarp is an important effector protein involved in the re-structuring of the host cytoskeleton (Tolchard et al., 2018). The PZ encodes for a range of different genes that are hypothesized to have important functions in the pathogenicity of the chlamydiae and may be a site of increased susceptibility for DNA uptake, genetic variation, and functional gene loss (Read et al., 2000; Thomson et al., 2008; Rajaram et al., 2015).

In the evolution and diversification of the *Chlamydiaceae* family, widespread gene rearrangement and translocation were identified between *C. pneumoniae* and *C. trachomatis* (Tillier and Collins, 2000). Furthermore, LGT events were detected both within and among the four major strain clusters of *C. trachomatis*, namely, the lymphogranuloma venereum (LGV), the trachoma, and two urogenital (T1, T2) clusters (Hadfield et al., 2017). Some studies have shown that this could have a clinical impact in terms of virulence and epidemiology (Somboonna et al., 2011; Andersson et al., 2016; Hadfield et al., 2017; Borges et al., 2019). Moreover, the effect of recombination can vary greatly between the four above-mentioned lineages of *C. trachomatis*, with the ocular strains being less affected than the urogenital lineages and the clonal LGV lineage having undergone no significant re-combination (Hadfield et al., 2017; Seth-Smith et al., 2021).

Overall, current data suggest that *C. psittaci*, *C. pneumoniae*, and *C. suis* have undergone higher rates of recombination than the entirety of the four *C. trachomatis* lineages. However, direct comparison between studies remains difficult due to the varying number of available genomes per species and because of the different approaches used to calculate *r/m* and other statistics that aim to quantify the recombination rate of a population (Read et al., 2013; Joseph et al., 2015; Roulis et al., 2015; Joseph et al., 2016; Hadfield et al., 2017; Seth-Smith et al., 2017b).

Additionally, one study proposed that ribosomal binding sites and tRNA may be associated with recombinant breakpoints (Gomes et al., 2006). However, these findings have yet to be confirmed by *in vitro* studies. So far, *in vitro* studies dealing with LGT following co-infection found little evidence for specific patterns, regions, or sites of recombination (Jeffrey et al., 2013; Marti et al., 2021), although there are notable differences between interspecies and intraspecies crosses, with intraspecies crosses generally leading to a higher proportion of donor DNA in the recombinant strains (Suchland et al., 2019). Moreover, the same study found that the replication termination is a target for interspecies recombination.

One very interesting chlamydial species in the context of LGT is *C. suis*. It is the only chlamydial species to have naturally obtained a resistance gene, *tetA*(C), which encodes a tetracycline efflux pump. This resistance allele and its genetic content were integrated as a genomic island (Tet-island) into the *C. suis* chromosome in an invasion-like gene (*inv*), probably during a transposition event directed by the transposase-encoding insertion sequence IScs605, although the exact mode of transmission and integration could not be replicated in an *in vitro* model involving *C. suis* (Dugan et al., 2004; Dugan et al., 2007). This Tet-island is the only evidence for recent acquisition of foreign DNA from other bacteria in *Chlamydia* spp. It shares high nucleotide identity with a pRAS3-type plasmid from the fish pathogen *Aeromonas salmonicida ssp. salmonicida* (Massicotte et al., 2019). It has been hypothesized that the plasmid was transferred *via* feeding of pigs with fish meal (Sandoz and Rockey, 2010) and was selected for with the use of tetracycline as a growth promoter in pig production facilities (Dugan et al., 2004). The use of tetracycline in pigs as prophylactic and

therapeutic treatment has been shown to increase the rate of *C. suis* strains positive for *tetA*(C) (Borel et al., 2012; Borel et al., 2016; Wanninger et al., 2016), and whole-genome analysis and *in vitro* studies have indicated that intraspecies spread of *tetA*(C) is the result of homologous recombination (Joseph et al., 2016; Marti et al., 2017; Marti et al., 2021).

It is concerning that the *tetA*(C) marker can readily and stably integrate into *C. trachomatis* and *C. muridarum* strains *in vitro* (Suchland et al., 2009), leading to the possibility that these strains could acquire tetracycline resistance in clinical settings. This possibility was strengthened when *C. suis* was detected and isolated from the eyes, feces, and pharynges of veterinarians, pig farmers, and abattoir workers, although tetracycline-resistant *C. suis* strains have yet to be isolated from human samples (Dean et al., 2013; De Puysseleyr et al., 2014; De Puysseleyr et al., 2017). Because ocular *C. trachomatis* infection (inclusion conjunctivitis) through autoinoculation with genital *C. trachomatis* strains D-K has been reported (Haller-Schober and El-Shabrawi, 2002), the possibility of Tet-island transmission from *C. suis* to *C. trachomatis* cannot be excluded.

One remarkable finding that has emerged during natural LGT in *Chlamydia* is the difference between cross-species vs. intraspecies genetic transfer occurrence. We envision a model where LGT within the inclusion is very common, to the extent that clonal *C. trachomatis* recombines regularly in inclusions that form following infection with a single EB. The selective driver for such common genetic exchange is currently unclear but would be consistent with the principles of Muller's Ratchet, where it is hypothesized that random mutation in haploid organisms would lead to fully degraded genomes in the absence of LGT (Joseph et al., 2011; Takeuchi et al., 2014). Other selective drivers, such as the Hill–Robertson effect, where the overall responsiveness to selection is reduced in finite populations, may also play a role (Joseph et al., 2011). Therefore, we propose that the reason for such common intraspecies LGT is to regenerate or maintain wild-type genomes in an intracellular environment that otherwise might be considered stressful and mutagenic (MacLean et al., 2013; Maharjan and Ferenci, 2017).

THE CHLAMYDIAL RECOMBINATION MACHINERY

Homologous recombination allows inter- and intragenomic exchange of DNA and therefore plays a crucial role in genetic diversification and DNA repair (Rocha et al., 2005). In bacteria, homologous recombination consists of two major pathways, the RecBCD (**Figure 1A**) and the RecFOR pathway (**Figure 1B**), both of which facilitate DNA exchange between a com-plementary sequence and single-strand DNA (ssDNA) using the RecA protein (Rocha et al., 2005).

In *Chlamydia*, whole-genome sequencing revealed that the genome contains various genes from the recombination and DNA repair machinery (Stephens et al., 1998; Azuma et al., 2006). However, only few studies have investigated the function and exact mechanism of the chlamydial homologous recombination machinery. The first chlamydial recombination-associated protein to be analyzed was RecA in *C. trachomatis*, which was found to have moderate recombinational activity and possessed low efficiency after DNA damage by UV radiation compared to other bacteria (Hintz et al., 1995; Zhang et al., 1995). Chlamydial RecJ has a similar function as that of other gram-negative bacteria, namely, exonuclease activity in RecBCD-independent and conjugational recombination (Hsia and Bavoil, 1996; Rocha et al., 2005). It is expected that the RecBCD and RecFOR pathways of *Chlamydia* work similarly to that of *E. coli*, including formation and resolution of Holliday junctions due to the presence of *ruv* genes (Bastidas and Valdivia, 2016).

Some *Chlamydia*-specific particularities and open questions remain. For example, the histone-like protein Hc1 is involved in the condensation of the chlamydial nucleoid and inhibits RecA activity. Interestingly, however, Hc1 only inhibits its repair and not its recombinational activity (Ennis et al., 2000). For the RecBCD pathway, the exact identity of *Chlamydia*-specific Chi sites is unknown, as indicated in **Figure 1** (Gomes et al., 2006).

Overall, it appears that the recombination machinery of the *Chlamydiaceae* family is complete, which underlines the importance of homologous recombination for a bacterial species that has undergone significant gene reduction (Palmer, 2002). However, more studies are necessary to confirm current assumptions that are only based on genomic data. With increasing options to genetically modify the chlamydiae (Valdivia and Bastidas, 2018), these investigations have become a possibility. First advances have already been made in recent years by the creation of knockout mutants in which genes involved in LGT are inactivated (Kokes et al., 2015; LaBrie et al., 2019; Wang et al., 2019). Currently available knockout mutants concerning LGT involving DNA uptake and ho-mologous recombination are listed in **Table 1**.

HOMOLOGOUS RECOMBINATION AND GENETIC ENGINEERING

Genetic manipulation is an indispensable tool to understanding the biology of eukaryotic and prokaryotic cells. In the *Chlamydia* research field, tools for genetic modification have only recently been developed. The currently available methods have been reviewed in detail (Bastidas and Valdivia, 2016); therefore, we will only discuss genetic engineering in the context of homologous recombination.

The first report of successful, albeit transient, transformation of *Chlamydia* was published in the 1990s (Tam et al., 1994). Fifteen years later, a study could stably introduce kasugamycin and spectinomycin resistance into *C. psittaci* by introducing a pUC derivative, which carried the ribosomal RNA (rrn) region of *C. psittaci* with resistance-inducing point mutations, into the wild type using electroporation (Binet and Maurelli, 2009). Shuttle vectors comprising an *E. coli* vector and the chlamydial plasmid later allowed stable and reproducible transformation of *Chlamydia* (Wang et al., 2011), overhauling the field of *Chlamydia* genetics.

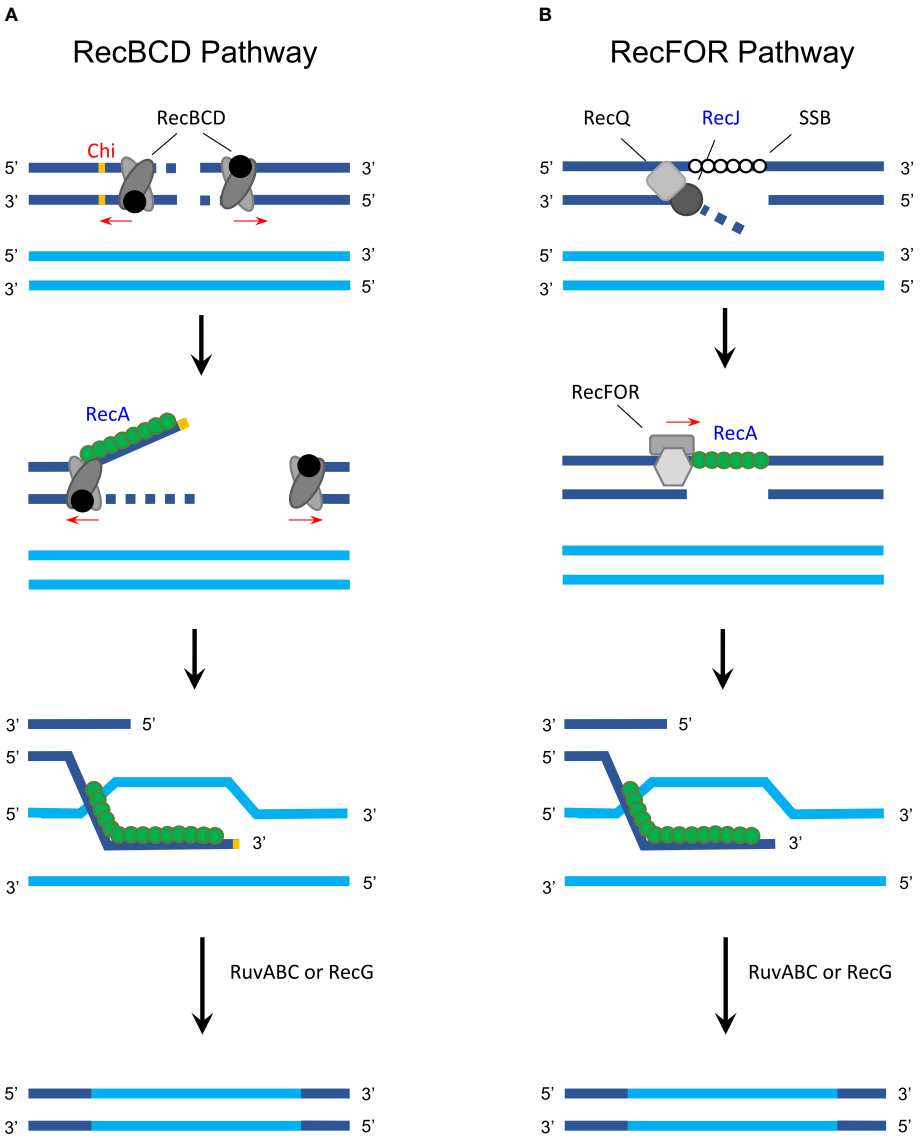

FIGURE 1 | Homologous recombination in gram-negative bacteria. **(A)** The RecBCD pathway is activated following a double-strand break that causes the RecBCD complex to bind on both ends and degrade DNA from the 3′ to 5′ end until one of the complexes encounters a Chi site. RecBCD then degrades the DNA from to 5′ to 3′ end while RecA (green) can bind to the 3′ extension. Next, the RecA-covered single-strand DNA invades a homologous sequence (synapsis formation) and RuvABC (with or without RecG) is used to resolve the Holliday junction, exchanging DNA *via* recombination. **(B)** In the RecFOR pathway, a single-strand break is first unwound with helicase RecQ and degraded with RecJ, while single-stranded binding protein (SSB) attaches to the exposed strand. This is followed by RecFOR promoting the replacement of SSB with RecA followed by the same process as described in the RecBCD pathway. Proteins that were analyzed in detail regarding its function and activity in *Chlamydia* are labeled in blue; protein/sites that are unknown or inexistent in *Chlamydia* are labeled in red. The figure was modified from Rocha et al. (2005), Figure 1, and Snyder et al. (2013), Figures 10.2, 10.3, and 10.4.

One of the remaining challenges of genetic manipulation of *Chlamydia* spp. is the inability of the pathogen to maintain plasmids with replication systems that do not include the native chlamydial plasmid. There has been significant progress in this field when a very recent report used a recombinant construct based on a broad-spectrum plasmid from *Bordetella pertussis* (pBBR1 MCS4) to transform a *C. trachomatis* L2 strain. This plasmid, pBVR1, contained *C. trachomatis* genomic sequences that allowed integration of the element into the *C. trachomatis* chromosome. This construct was maintained as both an episome and an integrated element in transformed strains. It is expected that further work with the pBBR1 vector system will perhaps allow the maintaining of non-chlamydial-plasmid-based genetic elements in transformed strains (Garvin et al., 2021).

Additionally, co-culture models were established as an alternative method to genetically modify the chlamydiae by co-infecting cells with two *C. trachomatis* strains, each carrying resistance-conferring mutations to either ofloxacin, lincomycin,

TABLE 1 | List of knockout mutants concerning genes involved in lateral gene transfer.

Strain name	Species/strain	Mutation	Locus (gene), function	Literature
UWCM026	*Cm*/Nigg	Transposon mutant (knockout)	TC0212 (*rmuC*), DNA recombination protein	Wang et al., 2019
UWCM031	*Cm*/Nigg	Transposon mutant (knockout)	TC0302 (*recD*), RecBCD complex	Wang et al., 2019
ctl10707 (ct447)	*Ct*/L2	Transposon mutant (knockout)	CT447 (*recJ*), RecFOR pathway	LaBrie et al., 2019
ctl10730 (ct470)	*Ct*/L2	Transposon mutant (knockout)	CT470 (*recO*), RecFOR pathway	LaBrie et al., 2019
CTL2M934	*Ct*/L2	Transposon mutant, nonsense SNV[a] (knockout)	CT339 (*com*EC), DNA uptake (transformation)	Kokes et al., 2015; LaBrie et al., 2019
CTL2M_Pool 27	*Ct*/L2	Nonsense SNV[a] (knockout)	CT298 (*radA*), DNA repair protein (recombinase)	Kokes et al., 2015
CTL2M_Pool 23	*Ct*/L2	Nonsense SNV[a] (knockout)	CT040 (*ruvB*), Holliday junction ATP-dependent DNA helicase	Kokes et al., 2015
CTL2M_Pool 30	*Ct*/L2	Nonsense SNV[a] (knockout)	CT825 (*rmuC*), DNA recombination	Kokes et al., 2015
CTL2M924	*Ct*/L2	Nonsense SNV[a] (knockout)	CT660 (*gyrA2*), DNA gyrase subunit 2, DNA replication	Kokes et al., 2015

Cm, C. muridarum; Ct, C. trachomatis.

[a]*Single-nucleotide variant (SNV) created with chemical mutagenesis. Nonsense mutants were listed in Kokes et al. (2015).*

trimethoprim, or rifampicin, and selecting for double-resistant recombinants. These studies detected recombination frequencies of 10^{-4} to 10^{-3} and further proposed that LGT likely played an important part in chlamydial evolution (DeMars et al., 2007; DeMars and Weinfurter, 2008). Similar protocols further demonstrated that interspecies transfer of the Tet-island from *C. suis* to *C. trachomatis* and *C. muridarum*, but not the more distantly related *C. caviae*, is possible. While *C. muridarum* obtained an approximately 100 kb-long sequence (the Tet-island and surrounding genes) as the result of a homologous recombination-mediated crossover event, co-infection of *C. suis* and *C. trachomatis* produced a mosaic strain with three instead of two *rrn* operons (Suchland et al., 2009). Interspecies transfer of the Tet-island *via* homologous recombination has been shown for *C. trachomatis* (Jeffrey et al., 2013) and *C. suis*, both in the presence (Marti et al., 2021) and absence (Marti et al., 2017) of double selection. Interestingly, comparison of *in vitro*-generated recombinant strains with clinical strains demonstrated that there are statistically more breakpoints in *in vitro C. trachomatis* strains compared to clinical strains, especially in the resistance-conferring genes *rpoB* (rifamycin group) and *gyrA* (ofloxacin) (Srinivasan et al., 2012).

The principle of co-infection and selection for recombinants has since become crucial in genetic engineering of the *Chlamydia*. For example, it has been used as a mapping tool in forward genetics, either by chemical mutagenesis and subsequent selection of recombinants using resistance markers (Nguyen and Valdivia, 2013; Nguyen and Valdivia, 2014) or by employing markerless recombination approaches (Brothwell et al., 2016). Moreover, suicide vectors that allow gene deletion following homologous recombination have been successfully constructed and used (Mueller et al., 2016; McKuen et al., 2017; Mueller et al., 2017). Finally, the principle of interspecies LGT has been exploited to create a hybrid strain library of *C. trachomatis*/*C. muridarum* crosses: a *tet*-resistant *C. trachomatis* strain was crossed *in vitro* with *C. muridarum* strains mutated by the plasmid-based Himar transposition system that randomly integrated a chloramphenicol marker into the genome (Suchland et al., 2019; Wang et al., 2019). This method was then used to produce PZ chimeras where the *C. muridarum* PZ replaced that of *C. trachomatis*, which demonstrated that the *C. muridarum*-specific large putative cytotoxins are not responsible for cytopathic and cytotoxic effects. This switch-out method further led to the detection of an inclusion protein, CT147, and CTL0402, which plays a role in the inclusion integrity (Dimond et al., 2021). A back-crossing strategy, which is a technique that can be used to effect functional complementation of mutants, was then used to restore both the wild-type genotype and phenotype.

DISCUSSION AND OUTLOOK

Research over the past two decades has identified a paradox with regard to the genetic exchange and transformation within chlamydiae. First, decades of effort have demonstrated that *Chlamydia* spp. are very challenging to transform genetically, and even now the use of genetic systems remains difficult. This challenge is further exemplified by the near absence of LGT by members of the chlamydiae from bacteria across species. In contrast, some chlamydiae, notably *C. trachomatis*, undergo regular intraspecies LGT between different isolates.

The rarity of interphylum LGT events is contrasted with the presence of abundant LGT machinery retained in the chlamydial genome, even despite the considerable gene reduction following adaptation to its intracellular life cycle (Toft and Andersson, 2010). As described in this review, the recombination machinery of *Chlamydia* is complete, although some questions remain, and of the three major known forms of DNA uptake, two have been described. Specifically, while the *Chlamydiaceae* family does not possess a known conjugation machinery (Greub et al., 2004), transformation and transduction are possible. For example, one recent study showed that CT336 in *C. trachomatis*, a protein with limited sequence similarity to the *Bacillus* ComEC protein, plays an important role in DNA uptake *via* transformation (LaBrie et al., 2019). However, the same study noted that other important genes involved in the uptake of free dsDNA, namely, homologs of PilQ, ComEA, and DprA, are absent, which led to the conclusion that natural transformation in the *Chlamydiaceae* is different from that of other gram-negative bacteria, similar to *Helicobacter pylori* (LaBrie et al., 2019). Furthermore, chlamydiaphages (chlamydial bacteriophages) in the *Chla-mydiamicrovirus* genus have been

described in various chlamydial species such as *C. psittaci*, *C. abortus*, *C. felis*, *C. caviae*, *C. pecorum*, and *C. pneumoniae*, but not in the more distantly related *C. suis*, *C. muridarum*, and *C. trachomatis* (Pawlikowska-Warych et al., 2015; Bastidas and Valdivia, 2016). Effort to use these phages to facilitate genetic in-troduction has not yet been successful, but perhaps future research will identify ways to use transduction as a tool of genetic exchange in *Chlamydia*.

In conclusion, despite significant progress in our understanding of LGT in *Chlamydia*, many open questions remain. For example, most *in vitro* studies concerning LGT and homologous recombination have been conducted with *C. suis*, *C. muridarum*, and *C. trachomatis*. While it is possible to induce competence in *C. psittaci*, *C. felis*, and *C. pneumoniae* (Shima et al., 2018; Shima et al., 2020), we know very little about their DNA uptake system and if it is similar to that of *C. trachomatis*, *C. muridarum*, and *C. suis*. There may be a different mechanism for these species, as there appears to be a barrier of recombination between *C. suis*, *C. trachomatis*, and *C. caviae* (Suchland et al., 2009). Equipped with new genetic tools and a more extensive knowledge of LGT in the *Chlamydiaceae* family, we can tackle these challenging questions and further explore the biology of these complex bacteria.

AUTHOR CONTRIBUTIONS

HM, RS, and DR substantially contributed to the conception and design of the manuscript and reviewed the literature. All authors drafted and/or critically revised the manuscript, finally approved the version to be published, and agreed to be accountable for all aspects of the work.

FUNDING

This work was funded in part by the National MD-Ph.D. scholarship program organized by the Swiss Academy of Medical Sciences (SAMW), sponsored by the Swiss National Science Foundation (SNSF; Grant No. 323530_177579, awarded to HM from September 2017 to August 2020).

ACKNOWLEDGMENTS

We are grateful to Addison DeBoer for a careful reading of the manuscript.

REFERENCES

Andersson, P., Harris, S. R., Smith, H. M. B. S., Hadfield, J., O'Neill, C., Cutcliffe, L. T., et al. (2016). Chlamydia Trachomatis From Australian Aboriginal People With Trachoma Are Polyphyletic Composed of Multiple Distinctive Lineages. *Nat. Commun.* 7, 10688. doi: 10.1038/ncomms10688

Azuma, Y., Hirakawa, H., Yamashita, A., Cai, Y., Rahman, M. A., Suzuki, H., et al. (2006). Genome Sequence of the Cat Pathogen, Chlamydophila Felis. *DNA Res.* 13, 15–23. doi: 10.1093/dnares/dsi027

Bastidas, R. J., and Valdivia, R. H. (2016). Emancipating Chlamydia: Advances in the Genetic Manipulation of a Recalcitrant Intracellular Pathogen. *Microbiol. Mol. Biol. Rev.* 80, 411–427. doi: 10.1128/mmbr.00071-15

Binet, R., and Maurelli, A. T. (2009). Transformation and Isolation of Allelic Exchange Mutants of Chlamydia Psittaci Using Recombinant DNA Introduced by Electroporation. *Proc. Natl. Acad. Sci.* 106, 292–297. doi: 10.1073/pnas.0806768106

Borel, N., Leonard, C., Slade, J., and Schoborg, R. V. (2016). Chlamydial Antibiotic Resistance and Treatment Failure in Veterinary and Human Medicine. *Curr. Clin. Microbiol. Rep.* 3, 10–18. doi: 10.1007/s40588-016-0028-4

Borel, N., Regenscheit, N., Di Francesco, A., Donati, M., Markov, J., Masserey, Y., et al. (2012). Selection for Tetracycline-Resistant Chlamydia Suis in Treated Pigs. *Vet. Microbiol.* 156, 143–146. doi: 10.1016/j.vetmic.2011.10.011

Borges, V., Cordeiro, D., Salas, A. I., Lodhia, Z., Correia, C., Isidro, J., et al. (2019). Chlamydia Trachomatis: When the Virulence-Associated Genome Backbone Imports a Prevalence-Associated Major Antigen Signature. *Microb. Genomics* 5, e000313. doi: 10.1099/mgen.0.000313

Brothwell, J. A., Muramatsu, M. K., Toh, E., Rockey, D. D., Putman, T. E., Barta, M. L., et al. (2016). Interrogating Genes That Mediate Chlamydia Trachomatis Survival in Cell Culture Using Conditional Mutants and Recombination. *J. Bacteriol.* 198, 2131–2139. doi: 10.1128/JB.00161-16

Brunelle, B. W., and Sensabaugh, G. F. (2006). The ompA Gene in Chlamydia Trachomatis Differs in Phylogeny and Rate of Evolution From Other Regions of the Genome. *Infect. Immun.* 74, 578–585. doi: 10.1128/IAI.74.1.578-585.2006

Brunham, R., Yang, C., Maclean, I., Kimani, J., Maitha, G., and Plummer, F. (1994). Chlamydia Trachomatis From Individuals in a Sexually Transmitted Disease Core Group Exhibit Frequent Sequence Variation in the Major Outer Membrane Protein (Omp1) Gene. *J. Clin. Invest* 94, 458–463. doi: 10.1172/JCI117347

Dean, D., Rothschild, J., Ruettger, A., Kandel, R. P., and Sachse, K. (2013). Zoonotic Chlamydiaceae Species Associated With Trachoma, Nepal. *Emerg. Infect. Dis.* 19, 1948–1955. doi: 10.3201/eid1912.130656

DeMars, R., and Weinfurter, J. (2008). Interstrain Gene Transfer in Chlamydia Trachomatis *In Vitro*: Mechanism and Significance. *J. Bacteriol.* 190, 1605–1614. doi: 10.1128/JB.01592-07

DeMars, R., Weinfurter, J., Guex, E., Lin, J., and Potucek, Y. (2007). Lateral Gene Transfer *In Vitro* in the Intracellular Pathogen Chlamydia Trachomatis. *J. Bacteriol.* 189, 991–1003. doi: 10.1128/JB.00845-06

De Puysseleyr, L., De Puysseleyr, K., Braeckman, L., Morré, S. A., Cox, E., and Vanrompay, D. (2017). Assessment of Chlamydia Suis Infection in Pig Farmers. *Transbound Emerg. Dis.* 64, 826–833. doi: 10.1111/tbed.12446

De Puysseleyr, K., De Puysseleyr, L., Dhondt, H., Geens, T., Braeckman, L., Morré, S. A., et al. (2014). Evaluation of the Presence and Zoonotic Transmission of Chlamydia Suis in a Pig Slaughterhouse. *BMC Infect. Dis.* 14, 560. doi: 10.1186/s12879-014-0560-x

Dimond, Z. E., Suchland, R. J., Baid, S., LaBrie, S. D., Soules, K. R., Stanley, J., et al. (2021). Inter-Species Lateral Gene Transfer Focused on the Chlamydia Plasticity Zone Identifies Loci Associated With Immediate Cytotoxicity and Inclusion Stability. *Mol. Microbiol* 116, 1433–48. doi: 10.1111/mmi.14832

Dugan, J., Andersen, A. A., and Rockey, D. D. (2007). Functional Characterization of IScs605, an Insertion Element Carried by Tetracycline-Resistant Chlamydia Suis. *Microbiology* 153, 71–79. doi: 10.1099/mic.0.29253-0

Dugan, J., Rockey, D. D., and Jones, L. (2004). And Andersen, aTetracycline Resistance in Chlamydia Suis Mediated by Genomic Islands Inserted Into the Chlamydial Inv-Like Gene. *A Antimicrob. Agents Chemother.* 48, 3989–3995. doi: 10.1128/AAC.48.10.3989-3995.2004

Ennis, D. G., Woodgate, R., and Shi, M. (2000). Selective Inhibition of RecA Functions by the Hc1 Nucleoid Condensation Protein From *Chlamydia Trachomatis*. *FEMS Microbiol. Lett.* 182, 279–283. doi: 10.1111/j.1574-6968.2000.tb08908.x

Garvin, L., Vande Voorde, R., Dickinson, M., Carrell, S., Hybiske, K., and Rockey, D. (2021). A Broad-Spectrum Cloning Vector That Exists as Both an Integrated Element and a Free Plasmid in Chlamydia Trachomatis. *PloS One* 16, e0261088. doi: 10.1371/journal.pone.0261088

Gomes, J. P., Bruno, W. J., Nunes, A., Santos, N., Florindo, C., Borrego, M. J., et al. (2006). Evolution of Chlamydia Trachomatis Diversity Occurs by Widespread Interstrain Recombination Involving Hotspots. *Genome Res.* 17, 50–60. doi: 10.1101/gr.5674706

Greub, G., Collyn, F., Guy, L., and Roten, C.-A. (2004). A Genomic Island Present Along the Bacterial Chromosome of the Parachlamydiaceae UWE25, an Obligate Amoebal Endosymbiont, Encodes a Potentially Functional F-Like Conjugative DNA Transfer System. *BMC Microbiol.* 4, 48. doi: 10.1186/1471-2180-4-48

Hadfield, J., Harris, S. R., Seth-Smith, H. M. B., Parmar, S., Andersson, P., Giffard, P. M., et al. (2017). Comprehensive Global Genome Dynamics of Chlamydia Trachomatis Show Ancient Diversification Followed by Contemporary Mixing and Recent Lineage Expansion. *Genome Res.* 27, 1220–1229. doi: 10.1101/gr.212647.116

Haller-Schober, E. M., and El-Shabrawi, Y. (2002). Chlamydial Conjunctivitis (in Adults), Uveitis, and Reactive Arthritis, Including SARA. Sexually Acquired Reactive Arthritis. *Best Pract. Res. Clin. Obstet Gynaecol.* 16, 815–828. doi: 10.1053/beog.2002.0320

Harris, S. R., Clarke, I. N., Seth-Smith, H. M. B., Solomon, A. W., Cutcliffe, L. T., Marsh, P., et al. (2012). Whole-Genome Analysis of Diverse Chlamydia Trachomatis Strains Identifies Phylogenetic Relationships Masked by Current Clinical Typing. *Nat. Genet.* 44, 413–419. doi: 10.1038/ng.2214

Hayes, L. J., Pecharatana, S., Bailey, R. L., Hampton, T. J., Pickett, M. A., Mabey, D. C. W., et al. (1995). Extent and Kinetics of Genetic Change in the Omp1 Gene of Chlamydia Trachomatis in Two Villages With Endemic Trachoma. *J. Infect. Dis.* 172, 268–272. doi: 10.1093/infdis/172.1.268

Hayes, L. J., Yearsley, P., Treharne, J. D., Ballard, R. A., Fehler, G. H., and Ward, M. E. (1994). Evidence for Naturally Occurring Recombination in the Gene Encoding the Major Outer Membrane Protein of Lymphogranuloma Venereum Isolates of Chlamydia Trachomatis. *Infect. Immun.* 62, 5659–5663. doi: 10.1128/iai.62.12.5659-5663.1994

Hintz, N. J., Ennis, D. G., Liu, W. F., and Larsen, S. H. (1995). The recA Gene of Chlamydia Trachomatis : Cloning, Sequence, and Characterization in Escherichia Coli. *FEMS Microbiol. Lett.* 127, 175–179. doi: 10.1111/j.1574-6968.1995.tb07470.x

Hsia, R. C., and Bavoil, P. M. (1996). Homologs of Escherichia Coli Recj, gltX and of a Putative "Early" Gene of Avian Chlamydia Psittaci Are Located Upstream of the "Late" Omp2 Locus of Chlamydia Psittaci Strain Guinea Pig Inclusion Conjunctivitis. *Gene* 176, 163–169. doi: 10.1016/0378-1119(96)00240-5

Jeffrey, B. M., Suchland, R. J., Eriksen, S. G., Sandoz, K. M., and Rockey, D. D. (2013). Genomic and Phenotypic Characterization of *In Vitro*-Generated Chlamydia Trachomatis Recombinants. *BMC Microbiol.* 13, 142. doi: 10.1186/1471-2180-13-142

Jeffrey, B. M., Suchland, R. J., Quinn, K. L., Davidson, J. R., Stamm, W. E., and Rockey, D. D. (2010). Genome Sequencing of Recent Clinical Chlamydia Trachomatis Strains Identifies Loci Associated With Tissue Tropism and Regions of Apparent Recombination. *Infect. Immun.* 78, 2544–2553. doi: 10.1128/IAI.01324-09

Jordan, I. K., Makarova, K. S., Wolf, Y. I., and Koonin, E. V. (2001). Gene Conversions in Genes Encoding Outer-Membrane Proteins in H. Pylori and C. Pneumoniae. *Trends Genet.* 17, 7–10. doi: 10.1016/S0168-9525(00)02151-X

Jordan, S., Nelson, D., and Geisler, W. (2020). "Chlamydia Trachomatis Infections," in *Chlamydia Biology: From Genome to Disease*. Eds. M. Tan, J. H. Hegeman and C. Sütterlin (Norfolk: Caister Academic Press), 1–30. doi: 10.21775/9781912530281.01

Joseph, S. J., Didelot, X., Gandhi, K., Dean, D., and Read, T. D. (2011). Interplay of Recombination and Selection in the Genomes of Chlamydia Trachomatis. *Biol. Direct* 6, 28. doi: 10.1186/1745-6150-6-28

Joseph, S. J., Didelot, X., Rothschild, J., de Vries, H. J. C., Morré, S. A., Read, T. D., et al. (2012). Population Genomics of Chlamydia Trachomatis: Insights on Drift, Selection, Recombination, and Population Structure. *Mol. Biol. Evol.* 29, 3933–3946. doi: 10.1093/molbev/mss198

Joseph, S. J., Marti, H., Didelot, X., Castillo-Ramirez, S., Read, T. D., and Dean, D. (2015). Chlamydiaceae Genomics Reveals Interspecies Admixture and the Recent Evolution of Chlamydia Abortus Infecting Lower Mammalian Species and Humans. *Genome Biol. Evol.* 7, 3070–3084. doi: 10.1093/gbe/evv201

Joseph, S. J., Marti, H., Didelot, X., Read, T. D., and Dean, D. (2016). Tetracycline Selective Pressure and Homologous Recombination Shape the Evolution of Chlamydia Suis : A Recently Identified Zoonotic Pathogen. *Genome Biol. Evol.* 8, 2613–2623. doi: 10.1093/gbe/evw182

Joseph, S. J., and Read, T. D. (2012). Genome-Wide Recombination in Chlamydia Trachomatis. *Nat. Genet.* 44, 364–366. doi: 10.1038/ng.2225

Kokes, M., Dunn, J. D., Granek, J. A., Nguyen, B. D., Barker, J. R., Valdivia, R. H., et al. (2015). Integrating Chemical Mutagenesis and Whole-Genome Sequencing as a Platform for Forward and Reverse Genetic Analysis of Chlamydia. *Cell Host Microbe* 17, 716–725. doi: 10.1016/j.chom.2015.03.014

LaBrie, S. D., Dimond, Z. E., Harrison, K. S., Baid, S., Wickstrum, J., Suchland, R. J., et al. (2019). Transposon Mutagenesis in Chlamydia Trachomatis Identifies CT339 as a ComEC Homolog Important for DNA Uptake and Lateral Gene Transfer. *MBio* 10, e01343–19. doi: 10.1128/mBio.01343-19

Lampe, M. F., Suchland, R. J., and Stamm, W. E. (1993). Nucleotide Sequence of the Variable Domains Within the Major Outer Membrane Protein Gene From Serovariants of Chlamydia Trachomatis. *Infect. Immun.* 61, 213–219. doi: 10.1128/iai.61.1.213-219.1993

MacLean, R. C., Torres-Barceló, C., and Moxon, R. (2013). Evaluating Evolutionary Models of Stress-Induced Mutagenesis in Bacteria. *Nat. Rev. Genet.* 14, 221–227. doi: 10.1038/nrg3415

Maharjan, R. P., and Ferenci, T. (2017). A Shifting Mutational Landscape in 6 Nutritional States: Stress-Induced Mutagenesis as a Series of Distinct Stress Input–Mutation Output Relationships. *PloS Biol.* 15, e2001477. doi: 10.1371/journal.pbio.2001477

Marti, H., Bommana, S., Read, T. D., Pesch, T., Prähauser, B., Dean, D., et al. (2021). Generation of Tetracycline and Rifamycin Resistant Chlamydia Suis Recombinants. *Front. Microbiol.* 12, 630293. doi: 10.3389/fmicb.2021.630293

Marti, H., Kim, H., Joseph, S. J., Dojiri, S., Read, T. D., and Dean, D. (2017). Tet(C) Gene Transfer Between Chlamydia Suis Strains Occurs by Homologous Recombination After Co-Infection: Implications for Spread of Tetracycline-Resistance Among Chlamydiaceae. *Front. Microbiol.* 8, 156. doi: 10.3389/fmicb.2017.00156

Massicotte, M.-A., Vincent, A. T., Schneider, A., Paquet, V. E., Frenette, M., and Charette, S. J. (2019). One Aeromonas Salmonicida Subsp. Salmonicida Isolate With a Pasa5 Variant Bearing Antibiotic Resistance and a Pras3 Variant Making a Link With a Swine Pathogen. *Sci. Total Environ.* 690, 313–320. doi: 10.1016/j.scitotenv.2019.06.456

McKuen, M. J., Mueller, K. E., Bae, Y. S., and Fields, K. A. (2017). Fluorescence-Reported Allelic Exchange Mutagenesis Reveals a Role for Chlamydia Trachomatis TmeA in Invasion That Is Independent of Host AHNAK. *Infect. Immun.* 85, e00640–17. doi: 10.1128/IAI.00640-17

Mueller, K. E., Wolf, K., and Fields, K. A. (2016). Gene Deletion by Fluorescence-Reported Allelic Exchange Mutagenesis in Chlamydia Trachomatis. *MBio* 7, e01817–15. doi: 10.1128/mBio.01817-15

Mueller, K. E., Wolf, K., and Fields, K. A. (2017). Chlamydia Trachomatis Transformation and Allelic Exchange Mutagenesis. *Curr. Protoc. Microbiol.* 45, 11A.3.1–11A.3.15. doi: 10.1002/cpmc.31

Nguyen, B. D., and Valdivia, R. H. (2013). Forward Genetic Approaches in Chlamydia Trachomatis. *J. Vis. Exp.* 50636. doi: 10.3791/50636

Nguyen, B., and Valdivia, R. (2014). A Chemical Mutagenesis Approach to Identify Virulence Determinants in the Obligate Intracellular Pathogen Chlamydia Trachomatis. *Methods Mol. Biol.* 1197, 347–358. doi: 10.1007/978-1-4939-1261-2_20

Palmer, G. H. (2002). The Highest Priority: What Microbial Genomes Are Telling Us About Immunity. *Vet. Immunol. Immunopathol.* 85, 1–8. doi: 10.1016/S0165-2427(01)00415-9

Pawlikowska-Warych, M., Śliwa-Dominiak, J., and Deptuła, W. (2015). Chlamydial Plasmids and Bacteriophages. *Acta Biochim. Pol.* 62, 1–6. doi: 10.18388/abp.2014_764

Rajaram, K., Giebel, A. M., Toh, E., Hu, S., Newman, J. H., Morrison, S. G., et al. (2015). Mutational Analysis of the Chlamydia Muridarum Plasticity Zone. *Infect. Immun.* 83, 2870–2881. doi: 10.1128/IAI.00106-15

Read, T. D., Brunham, R. C., Shen, C., Gill, S. R., Heidelberg, J. F., White, O., et al. (2000). Genome Sequences of Chlamydia Trachomatis MoPn and Chlamydia Pneumoniae AR39. *Nucleic Acids Res.* 28, 1397–1406. doi: 10.1093/nar/28.6.1397

Read, T. D., Joseph, S. J., Didelot, X., Liang, B., Patel, L., and Dean, D. (2013). Comparative Analysis of Chlamydia Psittaci Genomes Reveals the Recent Emergence of a Pathogenic Lineage With a Broad Host Range. *MBio* 4, e00604–12-e00604-12. doi: 10.1128/mBio.00604-12

Redfield, R. J. (2001). Do Bacteria Have Sex? *Nat. Rev. Genet.* 2, 634–639. doi: 10.1038/35084593

Rocha, E. P. C., Cornet, E., and Michel, B. (2005). Comparative and Evolutionary Analysis of the Bacterial Homologous Recombination Systems. *PloS Genet.* 1, 0247–0259. doi: 10.1371/journal.pgen.0010015

Rocha, E. P. C., Pradillon, O., Bui, H., Sayada, C., and Denamur, E. (2002). A New Family of Highly Variable Proteins in the Chlamydophila Pneumoniae Genome. *Nucleic Acids Res.* 30, 4351–4360. doi: 10.1093/nar/gkf571

Roulis, E., Bachmann, N. L., Myers, G. S. A., Huston, W., Summersgill, J., Hudson, A., et al. (2015). Comparative Genomic Analysis of Human Chlamydia Pneumoniae Isolates From Respiratory, Brain and Cardiac Tissues. *Genomics* 106, 373–383. doi: 10.1016/j.ygeno.2015.09.008

Sachse, K., and Borel, N. (2020). "Recent Advances in Epidemiology, Pathology and Immunology of Veterinary Chlamydiae," in *Chlamydia Biology: From Genome to Disease*. Eds. M. Tan, J. H. Hegeman and C. Sütterlin (Norfolk: Caister Academic Press), 403–428. doi: 10.21775/9781912530281.17

Sandoz, K. M., and Rockey, D. D. (2010). Antibiotic Resistance in Chlamydiae. *Future Microbiol.* 5, 1427–1442. doi: 10.2217/fmb.10.96

Seth-Smith, B., Bénard, A., Bruisten, S. M., Versteeg, B., Herrmann, B., Kok, J., et al. (2021). Ongoing Evolution of Chlamydia Trachomatis Lymphogranuloma Venereum: Exploring the Genomic Diversity of Circulating Strains. *Microb. Genomics* 7, 599. doi: 10.1099/mgen.0.000599

Seth-Smith, H. M. B., Busó, L. S., Livingstone, M., Sait, M., Harris, S. R., Aitchison, K. D., et al. (2017a). European Chlamydia Abortus Livestock Isolate Genomes Reveal Unusual Stability and Limited Diversity, Reflected in Geographical Signatures. *BMC Genomics* 18, 344. doi: 10.1186/s12864-017-3657-y

Seth-Smith, H. M. B., Wanninger, S., Bachmann, N., Marti, H., Qi, W., Donati, M., et al. (2017b). The Chlamydia Suis Genome Exhibits High Levels of Diversity, Plasticity, and Mobile Antibiotic Resistance: Comparative Genomics of a Recent Livestock Cohort Shows Influence of Treatment Regimes. *Genome Biol. Evol.* 9, 750–760. doi: 10.1093/gbe/evx043

Shima, K., Wanker, M., Skilton, R. J., Cutcliffe, L. T., Schnee, C., Kohl, T. A., et al. (2018). The Genetic Transformation of *Chlamydia pneumoniae*. *mSphere* 3. doi: 10.1128/mSphere.00412-18

Shima, K., Weber, M. M., Schnee, C., Sachse, K., Käding, N., Klinger, M., et al. (2020). Development of a Plasmid Shuttle Vector System for Genetic Manipulation of *Chlamydia Psittaci*. *mSphere* 5, e00787–20. doi: 10.1128/mSphere.00787-20

Snyder, L., Peters, J. E., Henkin, T., Champness, W., and Snyder, L. (2013). *Molecular Genetics of Bacteria. 4th* (Washington DC, USA: American Society for Microbiology (ASM).

Somboonna, N., Wan, R., Ojcius, D. M., Pettengill, M. A., Joseph, S. J., Chang, A., et al. (2011). Hypervirulent Chlamydia Trachomatis Clinical Strain Is a Recombinant Between Lymphogranuloma Venereum (L2) and D Lineages. *MBio* 2, e00045–11. doi: 10.1128/mBio.00045-11

Srinivasan, T., Bruno, W. J., Wan, R., Yen, A., Duong, J., and Dean, D. (2012). *In Vitro* Recombinants of Antibiotic-Resistant Chlamydia Trachomatis Strains Have Statistically More Breakpoints Than Clinical Recombinants for the Same Sequenced Loci and Exhibit Selection at Unexpected Loci. *J. Bacteriol.* 194, 617–626. doi: 10.1128/JB.06268-11

Stephens, R. S., Kalman, S., Lammel, C., Fan, J., Marathe, R., Aravind, L., et al. (1998). Genome Sequence of an Obligate Intracellular Pathogen of Humans: Chlamydia Trachomatis. *Sci. (80-)* 282, 754–759. doi: 10.1126/science.282.5389.754

Suchland, R. J., Carrell, S. J., Wang, Y., Hybiske, K., Kim, D. B., Dimond, Z. E., et al. (2019). Chromosomal Recombination Targets in Chlamydia Interspecies Lateral Gene Transfer. *J. Bacteriol.* 201, e00365–19. doi: 10.1128/JB.00365-19

Suchland, R. J., Sandoz, K. M., Jeffrey, B. M., Stamm, W. E., and Rockey, D. D. (2009). Horizontal Transfer of Tetracycline Resistance Among Chlamydia Spp. *In Vitro*. *Antimicrob. Agents Chemother.* 53, 4604–4611. doi: 10.1128/AAC.00477-09

Takeuchi, N., Kaneko, K., and Koonin, E. V. (2014). Horizontal Gene Transfer can Rescue Prokaryotes From Muller's Ratchet: Benefit of DNA From Dead Cells and Population Subdivision. *G3 Genes Genomes Genet.* 4, 325–339. doi: 10.1534/G3.113.009845/-/DC1

Tam, J. E., Davis, C. H., and Wyrick, P. B. (1994). Expression of Recombinant DNA Introduced Into Chlamydia Trachomatis by Electroporation. *Can. J. Microbiol.* 40, 583–591. doi: 10.1139/m94-093

Thomson, N. R., Holden, M. T. G., Carder, C., Lennard, N., Lockey, S. J., Marsh, P., et al. (2008). Chlamydia Trachomatis: Genome Sequence Analysis of Lymphogranuloma Venereum Isolates. *Genome Res.* 18, 161–171. doi: 10.1101/gr.7020108

Tillier, E. R. M., and Collins, R. A. (2000). Genome Rearrangement by Replication-Directed Translocation. *Nat. Genet.* 26, 195–197. doi: 10.1038/79918

Toft, C., and Andersson, S. G. E. (2010). Evolutionary Microbial Genomics: Insights Into Bacterial Host Adaptation. *Nat. Rev. Genet.* 11, 465–475. doi: 10.1038/nrg2798

Tolchard, J., Walpole, S. J., Miles, A. J., Maytum, R., Eaglen, L. A., Hackstadt, T., et al. (2018). The Intrinsically Disordered Tarp Protein From Chlamydia Binds Actin With a Partially Preformed Helix. *Sci. Rep.* 8, 1960. doi: 10.1038/s41598-018-20290-8

Valdivia, R. H., and Bastidas, R. J. (2018). The Expanding Molecular Genetics Tool Kit in Chlamydia. *J. Bacteriol.* 200, e00590–18. doi: 10.1128/JB.00590-18

Wang, Y., Kahane, S., Cutcliffe, L. T., Skilton, R. J., Lambden, P. R., and Clarke, I. N. (2011). Development of a Transformation System for Chlamydia Trachomatis: Restoration of Glycogen Biosynthesis by Acquisition of a Plasmid Shuttle Vector. *PloS Pathog.* 7, e1002258. doi: 10.1371/journal.ppat.1002258

Wang, Y., LaBrie, S. D., Carrell, S. J., Suchland, R. J., Dimond, Z. E., Kwong, F., et al. (2019). Development of Transposon Mutagenesis for Chlamydia Muridarum. *J. Bacteriol.* 201, e1002258. doi: 10.1128/JB.00366-19

Wanninger, S., Donati, M., Di Francesco, A., Hässig, M., Hoffmann, K., Seth-Smith, H. M. B., et al. (2016). Selective Pressure Promotes Tetracycline Resistance of Chlamydia Suis in Fattening Pigs. *PloS One* 11, e0166917. doi: 10.1371/journal.pone.0166917

Zhang, D. J., Fan, H., McClarty, G., and Brunham, R. C. (1995). Identification of the Chlamydia Trachomatis RecA-Encoding Gene. *Infect. Immun.* 63, 676–680. doi: 10.1128/iai.63.2.676-680.1995

Conflict of Interest: The authors declare that the research was conducted in the absence of any commercial or financial relationships that could be construed as a potential conflict of interest.

Publisher's Note: All claims expressed in this article are solely those of the authors and do not necessarily represent those of their affiliated organizations, or those of the publisher, the editors and the reviewers. Any product that may be evaluated in this article, or claim that may be made by its manufacturer, is not guaranteed or endorsed by the publisher.

frontiers | Frontiers in Cellular and Infection Microbiology

ORIGINAL RESEARCH
published: 03 May 2022
doi: 10.3389/fcimb.2022.880813

Cryptic Genes for Interbacterial Antagonism Distinguish *Rickettsia* Species Infecting Blacklegged Ticks From Other *Rickettsia* Pathogens

Victoria I. Verhoeve[1], *Tyesha D. Fauntleroy*[1], *Riley G. Risteen*[1], *Timothy P. Driscoll*[2] *and Joseph J. Gillespie*[1*]

[1] Department of Microbiology and Immunology, University of Maryland School of Medicine, Baltimore, MD, United States,
[2] Department of Biology, West Virginia University, Morgantown, WV, United States

OPEN ACCESS

Edited by:
Isaura Simões,
University of Coimbra, Portugal

Reviewed by:
Ulrike G. Munderloh,
University of Minnesota Twin Cities, United States
Shahid Karim,
University of Southern Mississippi, United States

***Correspondence:**
Joseph J. Gillespie
Jgillespie@som.umaryland.edu

Specialty section:
This article was submitted to Bacteria and Host, a section of the journal Frontiers in Cellular and Infection Microbiology

Received: 21 February 2022
Accepted: 04 April 2022
Published: 03 May 2022

Citation:
Verhoeve VI, Fauntleroy TD, Risteen RG, Driscoll TP and Gillespie JJ (2022) Cryptic Genes for Interbacterial Antagonism Distinguish Rickettsia Species Infecting Blacklegged Ticks From Other Rickettsia Pathogens. Front. Cell. Infect. Microbiol. 12:880813. doi: 10.3389/fcimb.2022.880813

Background: The genus *Rickettsia* (*Alphaproteobacteria*: Rickettsiales) encompasses numerous obligate intracellular species with predominantly ciliate and arthropod hosts. Notable species are pathogens transmitted to mammals by blood-feeding arthropods. Mammalian pathogenicity evolved from basal, non-pathogenic host-associations; however, some non-pathogens are closely related to pathogens. One such species, *Rickettsia buchneri*, is prevalent in the blacklegged tick, *Ixodes scapularis*. While *I. scapularis* transmits several pathogens to humans, it does not transmit *Rickettsia* pathogens. We hypothesize that *R. buchneri* established a mutualism with *I. scapularis*, blocking tick superinfection with *Rickettsia* pathogens.

Methods: To improve estimates for assessing *R. buchneri* infection frequency in blacklegged tick populations, we used comparative genomics to identify an *R. buchneri* gene (*REIS_1424*) not present in other *Rickettsia* species present throughout the *I. scapularis* geographic range. Bioinformatic and phylogenomics approaches were employed to propose a function for the hypothetical protein (263 aa) encoded by *REIS_1424*.

Results: REIS_1424 has few analogs in other Rickettsiales genomes and greatest similarity to non-Proteobacteria proteins. This cohort of proteins varies greatly in size and domain composition, possessing characteristics of Recombination hotspot (Rhs) and contact dependent growth inhibition (CDI) toxins, with similarity limited to proximal C-termini (~145 aa). This domain was named CDI-like/Rhs-like C-terminal toxin (CRCT). As such proteins are often found as toxin-antidote (TA) modules, we interrogated REIS_1423 (151 aa) as a putative antidote. Indeed, REIS_1423 is similar to proteins encoded upstream of CRCT domain-containing proteins. Accordingly, we named these proteins CDI-like/Rhs-like C-terminal toxin antidotes (CRCA). *R. buchneri* expressed both *REIS_1423* and *REIS_1424* in tick cell culture, and PCR assays showed specificity for *R. buchneri* over other rickettsiae and utility for positive detection in three tick populations. Finally, phylogenomics analyses uncovered divergent CRCT/CRCA modules in varying

states of conservation; however, only *R. buchneri* and related Tamurae/Ixodes Group rickettsiae carry complete TA modules.

Conclusion: We hypothesize that *Rickettsia* CRCT/CRCA modules circulate in the *Rickettsia* mobile gene pool, arming rickettsiae for battle over arthropod colonization. While its functional significance remains to be tested, *R. buchneri* CRCT/CRCA serves as a marker to positively identify infection and begin deciphering the role this endosymbiont plays in the biology of the blacklegged tick.

Keywords: *Rickettsia buchneri*, *Ixodes scapularis*, blacklegged tick, Lyme disease, toxin-antidote, contact-dependent growth inhibition systems, recombination hot spot, lateral gene transfer

INTRODUCTION

The blacklegged tick (*Ixodes scapularis*), more commonly referred to as deer tick, is of vital importance to human health as a vector of several infectious disease agents: e.g., *Borrelia* species (Lyme disease), *Anaplasma phagocytophilum* (anaplasmosis), *Babesia* and *Theileria* parasites (babesiosis, theileriosis), and Powassan Flavivirus (Powassan disease) (Wormser et al., 2006; Madison-Antenucci et al., 2020). Curiously, blacklegged ticks do not transmit rickettsial pathogens to humans, despite overlapping in geographic range with other tick species that do; e.g., American dog tick (*Dermacentor variabilis*), Brown dog tick (*Rhipicephalus* sanguineus), Gulf Coast tick (*Amblyomma maculatum*), and Lone Star tick (*Amblyomma americanum*) (Walker and Ismail, 2008; Lee et al., 2014; Sanchez-Vicente et al., 2019). However, *I. scapularis* is predominantly infected with a species of *Rickettsia*, *R. buchneri*, that is considered a non-pathogen of humans and has not been detected in vertebrates (Kurtti et al., 2015). The presence of *R. buchneri* in tick ovaries (Munderloh et al., 2005), high infection rate in ticks regardless of co-infection with other intracellular bacteria (Magnarelli et al., 1991; Billings et al., 1998; Benson et al., 2004; Swanson and Norris, 2007; Troughton and Levin, 2007; Steiner et al., 2008) or composition of other microbiota (Moreno et al., 2006; Narasimhan et al., 2014; van Treuren et al., 2015; Abraham et al., 2017; Ross et al., 2018; Thapa et al., 2019; Tokarz et al., 2019) hint at an underappreciated host-microbe relationship in need of further investigation.

A decade ago, we reported the first genome sequence of *R. buchneri* by assembling bacterial-like sequencing reads generated by the *I. scapularis* genome project (Gillespie et al., 2012a; Gulia-Nuss et al., 2016). Prior to this, phylogenomics analyses of diverse *Rickettsia* genomes indicated high conservation in synteny, moderate pseudogenization, one or zero plasmids, and relatively few mobile genetic elements (MGEs) (Darby et al., 2007; Fuxelius et al., 2008; Gillespie et al., 2008; Gillespie et al., 2012b). Several attributes emerged from our analyses highlighting the oddity of the *R. buchneri* genome, including 1) pronounced pseudogenization relative to other rickettsiae, especially for genes in other Spotted Fever Group (SFG) rickettsiae with characterized functions in vertebrate pathogenesis, 2) a substantial number of transposases (~30% of total coding sequences (CDS)), 3) four novel plasmids (pREIS1-4), and 4) nine copies (seven chromosomal and two plasmid) of the Rickettsiales Amplified Genetic Element (RAGE), a conjugative transposon found as single-copy in certain other *Rickettsia* genomes (Ogata et al., 2006; Blanc et al., 2007). Estimated phylogenies placed *R. buchneri* basal to all SFG rickettsiae, indicating a substantially different evolutionary track relative to derived SFG rickettsiae lineages, as well as species in the Typhus Group (TG) and Transitional Group (TRG) rickettsiae, yet inordinate lateral gene transfer (LGT) with the ancestral *R. bellii* and other intracellular bacteria. This was exemplified by *R. buchneri's* RAGEs, which encode numerous genes with functions critical for obligate intracellular life, leading to our hypothesis that RAGEs and other MGEs are vehicles for gene acquisitions that offset high rates of pseudogenization (Gillespie et al., 2012a) (**Figure 1A**).

The *R. buchneri* genome was also found to encode many genes lacking homologs in other *Rickettsia* genomes. Noteworthy are those encoding aminoglycoside antibiotic (AGAB) synthesis/resistance genes and polyketide synthase (PKS)-containing nonribosomal protein synthases (NRPS), hinting at a defense arsenal of antibiotics and 2° metabolites. Furthermore, plasmid pREIS2 of *R. buchneri* carries identical duplications of the biotin synthesis operon of obligate microbes (BOOM), (**Figure 1B**), which is only found in a limited range of obligate intracellular species, including certain wolbachiae (Nikoh et al., 2014; Gerth and Bleidorn, 2017; Balvín et al., 2018; Driscoll et al., 2020), *Cardinium* (Penz et al., 2012; Zeng et al., 2018) and *Legionella* (Říhová et al., 2017) species. As some wolbachiae have been shown to provide biotin to their insect hosts (Nikoh et al., 2014; Ju et al., 2019), *R. buchneri* may do so for blacklegged ticks, considering that blood is a poor source of B vitamins (Lehane and Lehane, 2010; Manzano-Marín et al., 2015). This possibility, coupled with potential to provision blacklegged tick with antibiotics and 2° metabolites, indicates *R. buchneri* has characteristics of a mutualistic bacterium unlike any rickettsiae heretofore analyzed from a genomic perspective.

If *R. buchneri* is a mutualist of blacklegged tick, infection frequency should be very high in nature. Reported *R. buchneri* infection rates in *I. scapularis* populations range from under 20% to over 80%; however, this disparity may reflect different sampling strategies not aiming to directly detect *R. buchneri* or distinguish this species from other rickettsiae (i.e., using general *Rickettsia* PCR primers). Differences in tissue sampling across studies could also distort accuracy in detecting *R. buchneri* infection if ovaries are not sampled. Furthermore, infection rates are higher in females and

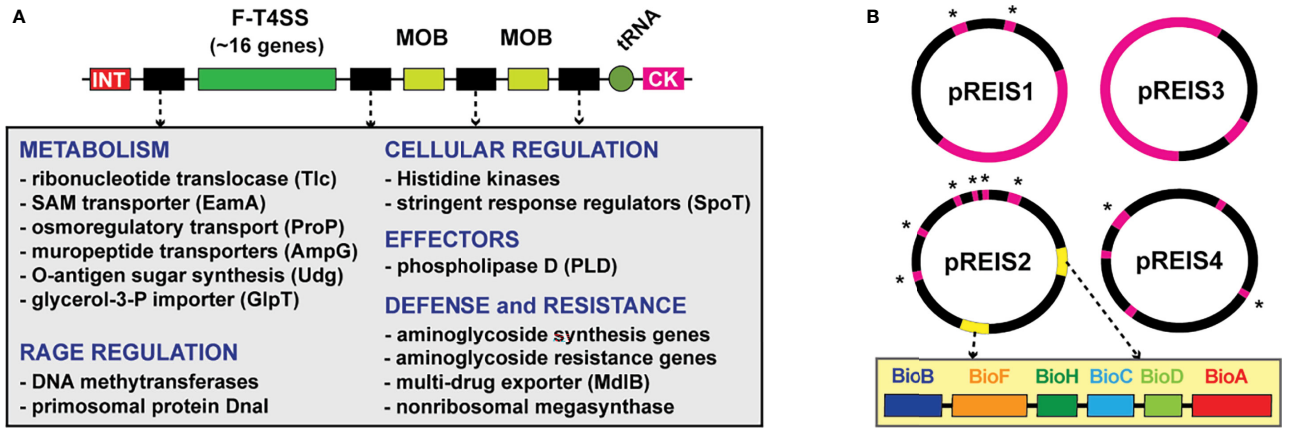

FIGURE 1 | Two extraordinary features of the *R. buchneri* genome include RAGEs and four unique plasmids (pREIS1-4) (Gillespie et al., 2012a). **(A)** General schema of RAGEs: INT, integrase; MOB, mobilization genes (*traT* and *traAI*). RAGEs typically insert in tRNA genes near cytosine kinase (CK)-encoding loci. Cargo genes (black) occur in variable clusters. Grey inset lists recurring cargo genes grouped by class. **(B)** Schema of pREIS plasmids: pink, full-length RAGE; pink w/asterisk, MOB genes; yellow, BOOM (illustrated in yellow inset). BOOM genes are uniquely arrayed relative to other bacteria that carry biotin synthesis genes (Gillespie et al., 2012a).

nymphs (Cross et al., 2018; Hagen et al., 2018; Gil et al., 2020), indicating a reduction in males after molting to adulthood; thus, sexing is important to understand true infection frequency.

In this report, we developed a PCR assay to unambiguously identify *R. buchneri* infection in blacklegged ticks. Our strategy was guided by re-evaluating a set of genes previously determined to be unique to *R. buchneri* (Gillespie et al., 2012a). One gene, *REIS_1424* (encoding a 263 aa hypothetical protein), was shown by *in silico* analysis to be absent in other rickettsiae known throughout the geographic range of *I. scapularis*. Unexpectedly, bioinformatic and phylogenomics analyses indicated that *REIS_1424* and its neighboring gene *REIS_1423* comprise a toxin-antidote (TA) module typical of certain bacterial systems used primarily for interbacterial warfare. As with numerous other *R. buchneri*-specific genes, *REIS_1424* and *REIS_1423* show evidence of LGT from distantly related non-proteobacteria. Similar cryptic TA modules are recurrent in rickettsiae and illuminate a potential mechanism for *Rickettsia* interbacterial antagonism in arthropod hosts.

MATERIALS AND METHODS

Identifying a *R. buchneri*-Specific Gene

A set of genes (739 singletons) from our prior report lacked significant similarity to genes in other *Rickettsia* genomes (Gillespie et al., 2012a); accordingly, these were used as queries in Blastn searches against the NCBI 'Rickettsia' databases (taxid 780). Genes with significant similarity to genes from rickettsiae present within the geographic distribution of *I. scapularis* were removed. Further, we excluded genes encoded on plasmids, those present within chromosomal RAGES, and those encoding transposases or related elements. The remaining genes were then evaluated using bioinformatics analysis to determine the likelihood that they encode functional proteins.

Compiling Toxin and Antidote Datasets

For toxins, proximal (~100 aa) C-terminal sequences of *R. buchneri* protein REIS_1424 (EER22217) and another rickettsial species "*Candidatus* Jidaibacter acanthamoeba" str. UWC36 protein NF27_IC00050 (KIE04387) were used as queries in Blastp searches to compile and analyze diverse proteins harboring significant similarity across complementary proximal C-terminal sequences. For antidotes, entire sequences for *R. buchneri* protein REIS_1423 (EER22217 with an adjusted start site adding 41 aa at the N-terminus) and "*Candidatus* Jidaibacter acanthamoeba" str. UWC36 protein NF27_IC00040 (KIE04386) were used as queries in Blastp searches to compile and analyze diverse proteins harboring significant similarity across the entire lengths of the queries. Analyses utilized our HaloBlast method, which is a combinatorial Blastp-based approach for interrogating proteins for LGT (Driscoll et al., 2013). Individual Blastp searches were conducted against five distinct taxonomic databases: 1) "Rickettsia" (NCBI taxid 780)", 2) "Rickettsiales" (taxid: 766) excluding "Rickettsia", 3) "Alphaproteobacteria" (taxid: 28211) excluding "Rickettsiales", 4) "Proteobacteria" (taxid: 1224) excluding "Alphaproteobacteria", 5) "Bacteria" (taxid: 2) excluding Proteobacteria", and 6) "minus bacteria"). All subjects from each search were ranked by *Sm* score (= $b * I * Q$, where b is the bitscore of the match, I is the percent identity, and Q is the percent length of the query that aligned), a comparative sequence similarity score designed to de-emphasize highly significant matches to short stretches of the query in favor of longer stretches of similarity (Driscoll et al., 2013). The "halos" or separate database searches were then compared to one another to determine the taxon with the strongest similarity to the query sequences.

Toxin Characterization

HaloBlast subjects from the searches with REIS_1424 and NF27_IC00050 as queries were analyzed in two ways. First, only sequences matching the proximal (~100 aa) C-terminal

sequences of the query were compiled and aligned with MUSCLE using default parameters (Edgar, 2004). The entire alignment was then visualized as sequence logos using WebLogo (Crooks et al., 2004). Second, two representative sequences per halo were selected for domain predictions across the entire protein. EMBL's Simple Modular Architecture Research Tool (SMART) (Letunic and Bork, 2017) and/or the Protein Homology/analogY Recognition Engine V 2.0 (Phyre2) (Kelley and Sternberg, 2009) were used to predict and evaluate the following domains: UBA (ubiquitin-associated) (Mueller and Feigon, 2002); haemagglutination activity site (Kajava et al., 2001); hemagglutinin repeats (Pfam ID PF13332); Peptidase M43 domain (Rawlings and Barrett, 1995); endonuclease III (Bruner et al., 2000); RHS repeat (Busby et al., 2013); VENN motif (Aoki et al., 2010; Zhang et al., 2011); DUF637: hemagglutinin-/hemolysin-associated domain (PF04830); alanine-rich-conserved phenylalanine (ALF) motif (Yeats et al., 2003); Laminin_G_3 (PF13385); LamG-like jellyroll fold domain (Liu et al., 2007; Weyer et al., 2007); HintN domain (Perler, 1998). Individual protein schemas were generated using Illustrator of Biological Sequences (Liu et al., 2015) with manual adjustment.

Antidote Characterization

HaloBlast subjects from the searches with REIS_1423 and NF27_IC00040 as queries were compiled and aligned with MUSCLE (default parameters), with the entire alignment visualized as sequence logos using WebLogo. Additionally, CDS flanking certain HaloBlast subjects (i.e. those with NCBI reference protein accession numbers) from the searches with REIS_1424 and NF27_IC00050 were evaluated for their size and potential for encoding an N-terminal sequence motif (LS/ADXE/DXQXXXW) determined to be highly conserved in subjects retrieved in Blastp searches with REIS_1423 and NF27_IC00040 as queries. Finally, HMMER (Finn et al., 2011) searches using NF27_IC00040 or NF27_IC00050 were utilized to evaluate our Blastp-based identification and compilation of both toxin and antidote datasets.

Phylogeny Estimation

Antidote Phylogeny

Selected antidotes were aligned using MUSCLE (default parameters). A phylogeny was estimated with the WAG substitution model (gamma model of rate heterogeneity) using RAxML v8.2.4 (50). Branch support was assessed with 1,000 pseudo-replications.

Rickettsia Phylogeny

Protein sequences (n = 121,310) from 92 sequenced genomes were used to estimate a genus-level *Rickettsia* phylogeny. *Rickettsia* genomes were retrieved from the NCBI Assembly database (n = 92). The Rapid Annotation using Subsystem Technology (RAST) v 2.0 server (Aziz et al., 2008) was used to annotate three *Rickettsia* assemblies that were not previously annotated. A total of 3,707 orthologous gene families were constructed from this data set using *fastortho*, a modified version of OrthoMCL (Feris et al., 2003), at an inflation of 1.5 and a percent identity threshold of 40%. A subset of 263 single-copy families conserved across all 92 taxa was independently aligned with MUSCLE (Edgar, 2004) using default parameters, and regions of poor alignment were masked using Gblocks (Talavera and Castresana, 2007). All modified alignments were concatenated into a single data set (74,799 positions) for phylogeny estimation using RAxML v8.2.4 (Stamatakis et al., 2005), using a gamma model of rate heterogeneity and estimation of the proportion of invariable sites. Branch support was assessed with 1,000 pseudo-replications.

DNA and RNA Extraction, PCR

For *R. buchneri* analysis, ticks from New York, New Hampshire, and Pennsylvania (see **Figure 6** for locality information) were stored in 100% ethanol at -20°C until isolation. DNA was extracted from *I. scapularis* adults and nymphs, as well as rickettsiae infecting ISE6 cells (both kindly provided by Drs. Munderloh and Kurtii, University of Minnesota) and using the DNeasy kit (Qiagen) as per manufacturer's protocols for cell culture and tissue extraction, respectively. Briefly, ticks were surface sterilized with 5 min washes (1% bleach, 70% ethanol, and 1xPBS), cut into quarters with a sterile scalpel blade, incubated with kit-provided digestion buffer with proteinase K at 56°C overnight, and extracted using the tissue protocol with a final elution of 50µl of molecular grade water. Rickettsiae grown in culture were collected in their host cells, and DNA extracted using the cell culture protocol with a 50µl elution with molecular grade water. For analysis of non-target rickettsiae, all bacteria were grown in cell culture prior to DNA extraction and PCR analysis. DNA was qPCR amplified using PowerUp Sybr Mastermix (Thermo) in 20µl reactions containing 400nm of each primer and 50-100ng of DNA. Primers pairs are as follows for *R. buchneri*-specific targets: Rb-1424-120-F-5'-acaggcgtaaaac tagacaatct-3' with Rb-1424-120-R-5'-aggaaatccaagcttttcaggta-3' for the amplification of *rCRCT* and Rb-1423-116-F-5'-gcatagggtttat agcggtgc-3' with Rb-1423-116-R-5'-ccataagtttcttcctattgtgctt-3' for the amplification of *rCRCA*. *Rickettsia gltA* was amplified for all rickettsiae using the following primers: CSRT-F-5'-tcgcaaat gttcacggtacttt-3' and CSRT-R-5'-tcgtgcaattctttccattgt-3' (Stenos et al., 2005). Reactions were amplified under the following conditions: 1 cycle for 2 min at 95°C, 45 cycles at 95°C for 15 sec and 60°C for 30 sec, followed by a melt curve analysis. All primer sets were considered positive if the cycle threshold was 37 cycles or less. All primer sets were validated for range and efficiency of amplification using pCR4-TOPO plasmid standard curves with ligated amplicons. Primer sets described in this manuscript only amplify their intended products as verified by sanger sequencing and melt curve analyses of each reaction. For visualization of qPCR products (**Figure 6**) gel electrophoresis was performed using a 2% agarose gel with ethidium bromide straining and visualization using a gel imaging station. For transcriptional analysis, *R. buchneri* growing during log growth in ISE6 cells were collected in 600µl TRIzol (Invitrogen) and RNA extracted using the DirectZol (Zymo) kit using manufacturer's instructions and on-column DNase treatment. RNA was further DNase treated using the RQ1 DNase (Promega) prior to enzyme removal and concentration with the Zymo Clean and Concentrator-5 kit. The iScript Select cDNA synthesis kit (Bio-Rad) was used for cDNA synthesis using random hexamers in 20µl reactions with 200ng of DNase-free RNA. RNA was determined to be free of DNA with no reverse

transcriptase reactions with 200ng of RNA which resulted in no detectable DNA by qPCR. cDNA was analyzed for transcription of *rCRCT*, *rCRCA* and *I. scapularis* β-actin (primers IsActin-95-F-5'-aatcggcaacgagaggttcc-3' and IsActin-95-R-5'-agttgtacgtggtctcgtgg-3') using the same qPCR parameters as above.

RESULTS AND DISCUSSION

Characterizing a *R. buchneri*-Specific Gene

Our prior analysis of the first sequenced *R. buchneri* genome (Wikel *I. scapularis* colony) indicated 32% of CDS were absent from other *Rickettsia* genomes (Gillespie et al., 2012a). Given that dozens of new *Rickettsia* genomes have been sequenced and assembled since 2012, we revisited this list and allowed for candidate genes to also be present in the *R. buchneri* str. ISO7 assembly (Kurtti et al., 2015). Further, to increase the likelihood of a stable gene present in all *R. buchneri* populations, we excluded genes 1) encoded on plasmids, 2) flanked by transposases, 3) containing annotations reflecting an association with MGEs, and 4) containing Blastp profiles indicating pseudogenization (e.g., gene fragments, split genes, etc.). These collective constraints yielded a small list of candidate genes, one of which (*REIS_1424*, NCBI accession no. EER22217) was selected for further analysis.

REIS_1424 encodes a hypothetical protein of 263 aa; the homolog in the *R. buchneri* str. ISO7 assembly (KDO03356) is identical yet has a different predicted start site that adds 35 aa to the N-terminus. The only remaining significant Blastp matches are from *R. tamurae* str. AT-1, with two CDS spanning the entirety REIS_1424 indicating a split gene (WP_215426163 and WP_032138795). This is consistent with the close phylogenetic position of *R. tamurae* and *R. buchneri* (Hagen et al., 2018); however, since *R. tamurae* has not been reported from the Western hemisphere, these CDS are not a concern for utilization of *REIS_1424* as a diagnostic for *R. buchneri* infection.

REIS_1424 Carries a Cryptic Toxin Domain

REIS_1424-based Blastp searches outside of the *Rickettsia* taxon database yielded only two significant matches: a 2192 aa protein (hypothetical protein NF27_IC00050, KIE04387) from a rickettsial amoeba-associated endosymbiont, "*Candidatus* Jidaibacter acanthamoeba" str. UWC36 (Rickettsiales: Midichloriaceae) (Schulz et al., 2016), and a 97 aa protein (hypothetical protein E1266_17330, TDB94289) from the actinobacterium *Actinomadura* sp. 7K534 (Streptosporangiales; Thermomonosporaceae). Both alignments indicated that **1)** REIS_1424, NF27_IC00050, and E1266_17330 share over a dozen conserved residues, 2) the REIS_1424 and NF27_IC00050 match aligns the proximal C-terminal sequences of both proteins, and 3) E1266_17330 is truncated and lacks N-terminal sequence outside of the matches. Unlike REIS_1424, NF27_IC00050- or E1266_17330-based Blastp searches yielded many significant matches to diverse bacteria (discussed further below). However, no functional domains for the region shared across these proteins could be predicted with searches against the NCBI Conserved Domains Database or using SMART.

Given that the REIS_1424-NF27_IC00050 match spanned greater sequence in each protein (~137 aa) and "*Cand.* J. acanthamoeba" is another rickettsial taxon, NF27_IC00050 (aa residues 2068-2192) was used as a proxy for further Blastp searches and *in silico* characterization. NF27_IC00050-based HaloBlast analysis revealed strongest similarity to certain non-proteobacterial proteins (**Figure 2A**). All obtained sequences matched $NF27\_IC00050_{2068\text{-}2192}$ at their proximal C-termini (**Figure 2B**). Intriguingly, this cohort of proteins (n = 155) varied greatly in size across regions outside of the conserved C-terminal sequence (**Figure 2C**). A wide assortment of domains was predicted for these proteins, with many having modular architectures and other characteristics of contact dependent growth inhibition (CDI) and/or Recombination hotspot (Rhs) toxins (**Figure 2D**). While no functional domain could be predicted for any of the analogous C-terminal regions, sufficient conservation was found to strongly indicate a unifying functional role (**Figures 2E**, **S1A**). We hereafter refer to these analogous regions as CDI-like/Rhs-like C-terminal toxin (CRCT) domains, and to larger proteins possessing them as CRCT domain-containing proteins (CRCT-DCP).

The fusion of small, toxin-antidote (TA) pairs to the C-termini of CDI and Rhs toxins has previously been described and is thought to expand the diversity of toxic activities deployed by both CDI and Rhs systems (Aoki et al., 2010; Poole et al., 2011; Zhang et al., 2011; Ruhe et al., 2018). The extreme polymorphic nature of these TA modules indicates bacterial arms races, with selection operating on species- and strain-level recognition that shapes communities (Willett et al., 2015). For instance, many of the CRCT domain-containing proteins we identified in diverse bacteria lack the CRCT domain in closely related strains (data not shown). Furthermore, we found many small proteins containing only the CRCT domain (**Figure 2C** and **Table S1**), as well as larger proteins carrying truncated CRCT domains (data not shown), suggesting the mobile nature of these toxins and a rapid "birth and death" process. These observations, combined with small size and limited sequence conservation, collectively challenge computational approaches for identifying these polymorphic toxins. This is evinced by HaloBlast profiles for REIS_1424 that mirror those for $NF27\_IC00050_{2068\text{-}2192}$ once a *Rickettsia*-specific insertion is removed from the query in Blastp and HMMR searches (**Figures 2E**, **S1B**).

REIS_1423 Is a Cryptic Immunity Antidote to REIS_1424

As CRCTs are often found as TA modules, we interrogated genes up- and downstream of *REIS_1424*, *NF27_IC00050*, and the genes encoding the 153 other identified CRCT-DCPs. This revealed probable antidotes, hereafter named CDI-like/Rhs-like C-terminal toxin antidotes (CRCA), adjacent to 37% of the 155 CRCT-DCPs (**Figure 3A**). NF27_IC00040-based HaloBlast analysis mirrored that for $NF27\_IC00050_{2068\text{-}2192}$, revealing strongest similarity to non-proteobacterial proteins (**Figure 3B**). Taxonomic breakdown of these non-proteobacterial proteins for both CRCT-DCPs and CRCAs revealed a majority from Actinomycetia and Cyanobacteria genomes (**Figure 3C**). While all CRCAs are strongly constrained in length (~140 aa), with only a few proteins fused to partial genes with unrelated functions (**Figure 3D**), Blastp profiles for the best scoring

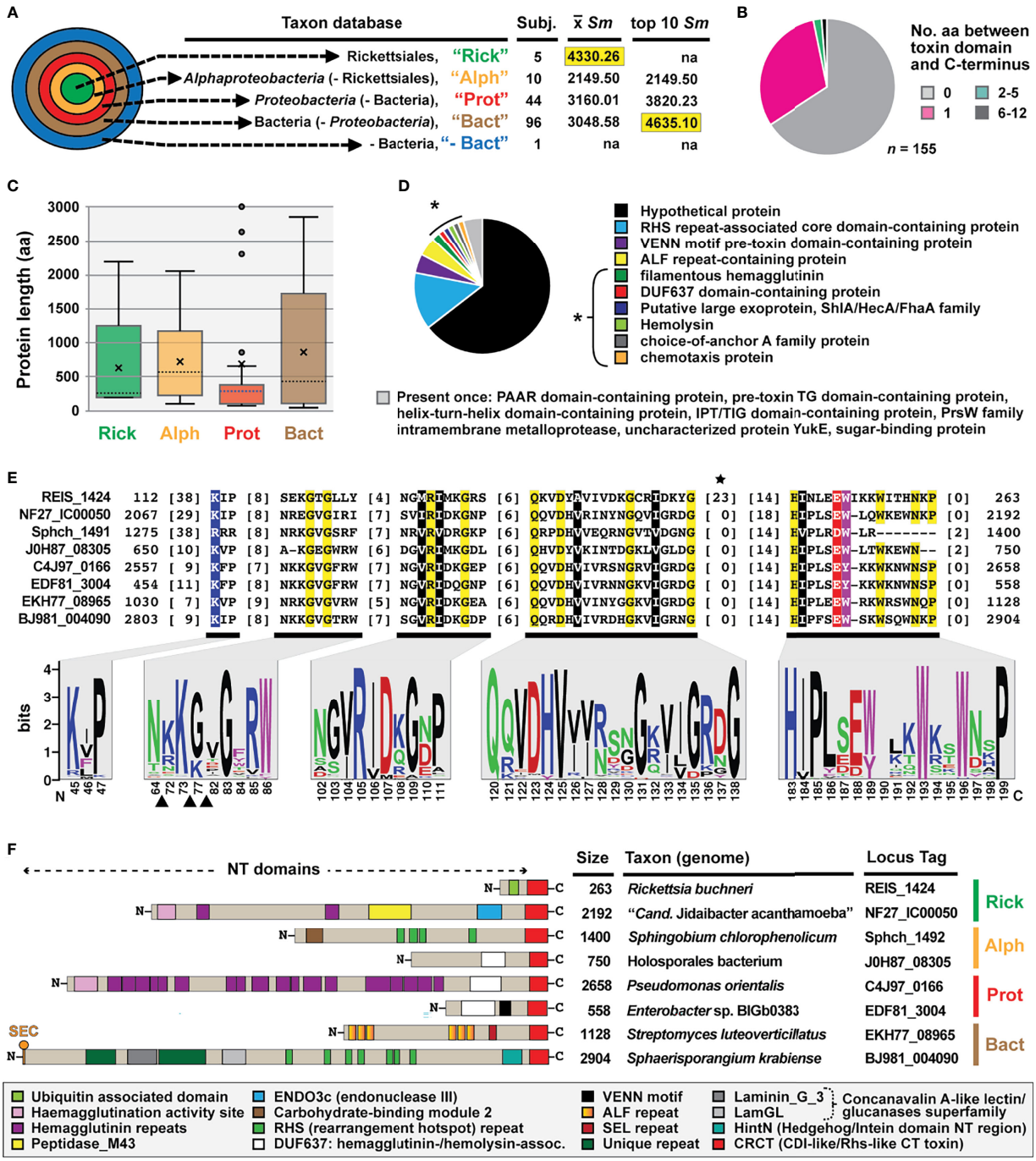

FIGURE 2 | REIS_1424 of *Rickettsia buchneri* contains a C-terminal toxin domain characteristic of some bacterial contact-dependent growth inhibition (CDI) and rearrangement hotspot (Rhs) toxins. This domain was named CDI-like/Rhs-like C-terminal toxin (CRCT). **(A)** HaloBlast analysis for "*Candidatus* Jidaibacter acanthamoeba" CRCT of NF27_IC00050 (NCBI acc. no. KIE04387; aa residues 2068-2192). Concentric halos depict hierarchical taxonomic databases increasing in divergence from the center. Average *Sm* score (see text for details) for all subjects and top ten subjects are provided, with highest score per database highlighted. 'na', not applicable. All corresponding information for proteins from HaloBLAST analyses are provided in **Table S1**. **(B–E)** For compiled bacterial CRCT-containing proteins (n = 155): **(B)** number of aa residues between CRCT and C-terminus, **(C)** lengths for associated N-terminal regions parsed by taxonomic group (the two largest proteins for *Proteobacteria* (AZE30872, *Pseudomonas chlororaphis* subsp. Aureofaciens and TVR95235, Wenzhouxiangellaceae bacterium are not shown), **(D)** NCBI protein annotations, and **(E)** conservation within the CRCT with sequence logo illustrating alignment of 155 CRCTs (see full alignment in **Figure S1**) and amino acid coloring as follows: black, hydrophobic; red, negatively charged; green, hydrophilic; purple, aromatic; blue, positively charged; star depicts unique *Rickettsia* insertion and triangles other insertions). **(F)** Diverse CRCT-containing proteins from select genomes.

matches parsed by taxonomy strongly indicate *Rickettsia* CRCT/CRCA (rCRCT/CRCA) modules were acquired from distant non-proteobacteria *via* LGT (**Figure 3E**).

Like analyzed CRCTs, predicted CRCAs possess enough conservation to indicate a common function (**Figures 3F**, **S2**). Still, efforts to thread either CRCTs or CRCAs to solved structures of CdiA-CT/CdiI toxin/immunity complexes (Morse et al., 2012; Beck et al., 2014; Johnson et al., 2016; Michalska et al., 2018) were futile. Many of the characterized CdiA-CT toxins are from proteobacterial species and function as Rnases, specifically targeting tRNAs or rRNAs (Willett et al., 2015). Using SMART or searching against the NCBI CDD did not indicate CRCTs harbor nuclease activities, and no similarity of CRCAs to CdiI domains (e.g., cd20694: CdiI_Ct-like) or members of the SUKH superfamily of immunity proteins (Zhang et al., 2011) could be made. CdiI antidotes have been hypothesized to drive CdiA-CT/CdiI module diversification since they evolve faster than CdiA-CT toxins (Nikolakakis et al., 2012). While we observed greater conservation in CRCTs (**Figure 2E**) versus CRCAs (**Figure 3F**), HaloBlast and HMMER (data not shown) searches recovered more CRCA (**Figure 3B**) versus CRCT-DCPs (**Figure 2A**). Still, the presence of CRCT/CRCA modules across diverse bacterial phyla, with some drastic differences in lifestyle (i.e. obligate intracellular versus extracellular, eukaryote-dependent versus environmental, etc.) indicates a common universal cellular target of CRCTs such as membrane, DNA, or RNA previously characterized for all other studied CdiA-CT/CdiI modules (Aoki et al., 2009; Aoki et al., 2010).

A Rickettsial CRCT/CRCA Module Mobilized to a Eukaryote?

We identified a eukaryotic genome harboring a possible LGT of a rickettsial CRCT-DCP/CRCA system. The genome of the smooth cauliflower coral (*Stylophora pistillata*) contains a gene encoding a large Rhs-like toxin (YbeQ) that was assembled on an unincorporated scaffold with other bacterial-like genes (**Figure 4**). YebQ has highest similarity to a few smaller rickettsial proteins that are remnants of degraded Rhs-like toxins (see next section), yet consistent similarity to larger toxins from non-proteobacterial genomes (**Table S3**). While YebQ does not contain a CRCT domain, smaller *S. pistillata* genes were found encoding the CRCT and CRCA domains with higher similarity to rickettsial equivalents than other bacteria (**Table S3**). This attests to the mobile nature of CRCT/CRCA modules and their tendency to incorporate into larger bacterial toxins. It also resonates on our prior work showing another aquatic animal, the placozoan *Trichoplax adhaerens*, contains LGTs from bacteria (particularly rickettsiae) (Driscoll et al., 2013). While the presence of introns in many of these bacterial-like *S. pistillata* gene models supports integration, mis-assembly of reads from a rickettsial endosymbiont is also possible.

Diverse CRCA/CRCT Modules Are Recurrent in *Rickettsia* Genomes

Inspection of the genomic region where rCRCT/CRCA modules have inserted revealed two interesting findings, both of which further attest to the mobile nature of these polymorphic TA modules and their rapid birth and death process. First, the rCRCT/CRCA loci of *R. buchneri* and *R. tamurae* occur in a recombination hotspot adjacent to the SecA gene (**Figure 5A**). This region is highly variable across *Rickettsia* genomes (**Figure S3A**) and contains small CDS with matches to the *S. pistillata* YebQ Rhs toxin described above (**Figure S4A**). Despite extraordinary variability in the number and size of CDS in this region across *Rickettsia* genomes, a conserved tRNA-Ala^{TGC} locus is always present, corroborating prior observations for CidA-CT/CdiAI modules often inserting near tRNA genes in bacterial genomes.

Second, Blastp searches with a concatenated query (REIS_1427-REIS_1423) revealed matches to additional rCRCA proteins, indicating other rCRCT/CRCA modules elsewhere in *Rickettsia* genomes (**Figure 5A**, dashed box). We designated these divergent rCRCA proteins as components of "rCRCT/CRCA-2" modules, with the above-described system named "rCRCT/CRCA-1" modules. Like the rCRCA-1 protein of *R. tamurae*, most rCRCA-2 genes are truncated or fragmented, yet a complete protein was found for the *Rickettsia* endosymbiont of *Ixodes pacificus* (hereafter REIP) (**Figure S4B**). Despite limited similarity (~30%ID), an estimated phylogeny grouped rCRCA-1 and rCRCA-2 proteins together to the exclusion of other CRCA proteins (**Figures 5B**; **S4B**). *rCRCA-2* loci all mapped to a second recombination hotspot in *Rickettsia* genomes adjacent to the conserved BamA and tRNA-Thr^{CGT} genes (**Figures 5C**, **S3B**). As with rCRCA-1, we could not identify similarity between rCRCA-2 proteins and domains of CdiI proteins or SUKH immunity proteins.

Searching upstream of *rCRCA-2* for potential cognate toxins instead yielded additional genes encoding CRCA antidotes that are duplicated and highly divergent from rCRCA-1 and rCRCA-2 proteins (**Figure 5C**). This arrangement of arrayed immunity antidotes is more characteristic of *cdiA-CT/cdiI* loci in many proteobacterial genomes (Aoki et al., 2010). Indeed, we were able to identify CdiI-like domains in these proteins using the NCBI Conserved Domains Database (cd20694). Accordingly, we named these antidotes rCRCA-3 proteins. Further inspection of rCRCA-3 genes identified eight genomes with additional copies found in a third recombination hotspot between the genes encoding the cytochrome oxidase subunits 2 (CyoA) and 1 (CyoB) (**Figures 5C**, **S3C**). Seven *Rickettsia* genomes have rCRCA-3 genes in both the BamA and CyoA/B recombination hotspots, indicating recent recombination between these loci (**Figure S4C**). We designated rCRCA-3a and rCRCA-3b proteins to distinguish between those located at the BamA or CyoA/B recombination hotspots, respectively.

At the BamA recombination hotspot, we identified cognate rCRCT-3a toxins with CdiA-CT-like domains (cd20695) in the *R. tamurae* and REIP genomes (**Figure 5C**). These two toxins have strongest similarity to counterparts in proteobacterial genomes, particularly *Pseudomonas* and *Moraxella* species (**Figures S4D, E**). We modeled the *R. tamurae* rCRCT-3a toxin to the CdiA-CT structure of *Cupriavidus taiwanensis* (Kryshtafovych et al., 2018) with high confidence, indicating rCRCT-3 toxins are unrelated to rCRCT-1 toxins (**Figures S4F, G**). The rCRCA-3 antidotes could not be modeled to the CdiI structure of *C. taiwanensis* or any other CdiI structures, making the association of rCRCT-3 with rCRCA-3 supported by genome proximity alone. Collectively, this analysis of rCRCT/CRCA genes in *Rickettsia* genomes illuminates recurrent

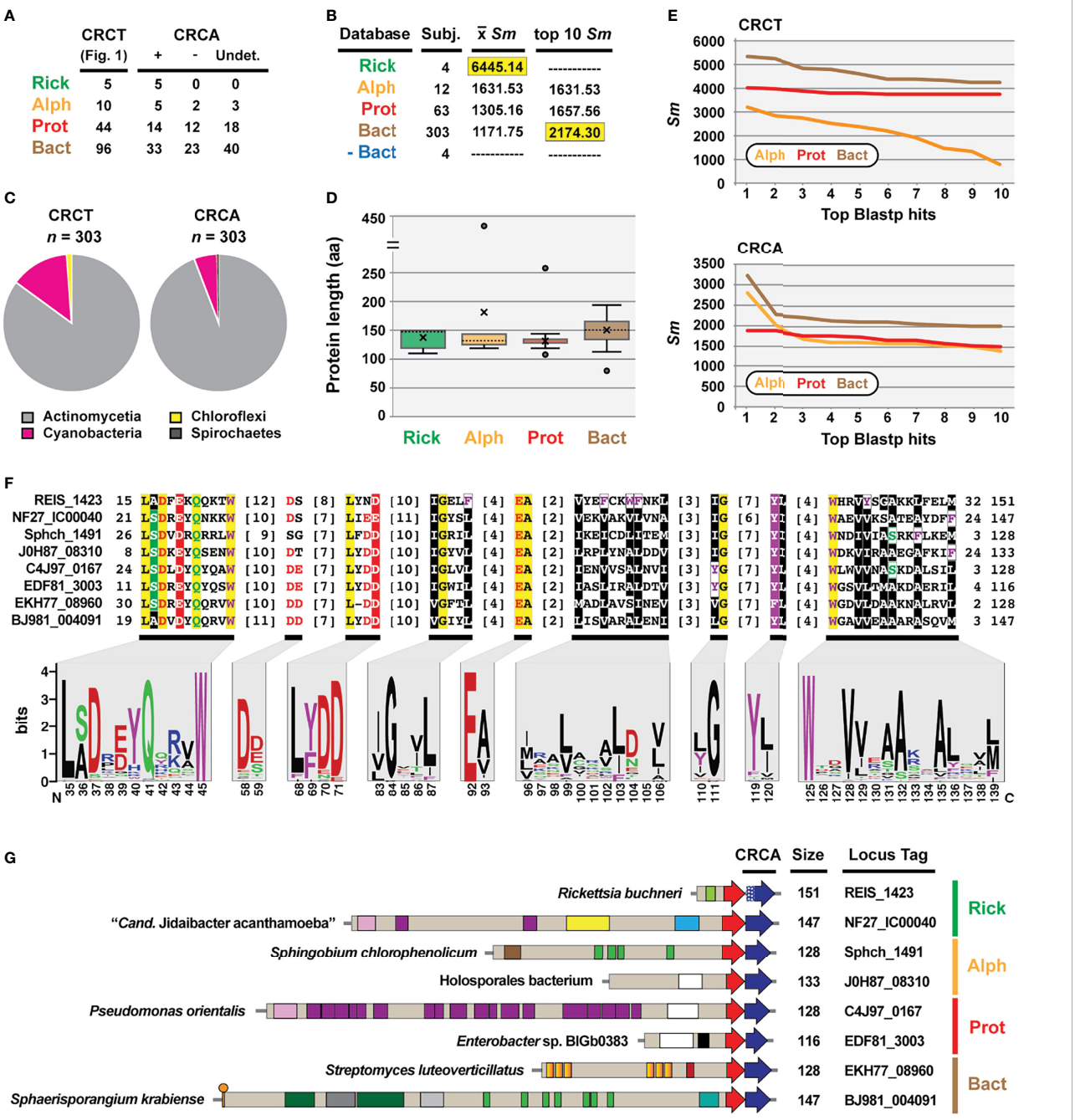

FIGURE 3 | REIS_1423 of *Rickettsia buchneri* is a predicted antidote to REIS_1424. REIS_1423 and related proteins were named CDI-like/Rhs-like immunity antidotes (CRCA). **(A)** Blastp searches with REIS_1423 and NF27_IC00040 unearthed putative CRCAs adjacent to 37% of the 155 CRCT domain-containing toxins. In 61 cases, assignment of CRCAs to adjacent CRCT domain-containing toxins could not be made due to the lack of strain-specific NCBI reference protein accession numbers (non-redundant protein record (WP_) only). **(B)** HaloBlast analysis for "*Candidatus* Jidaibacter acanthamoeba" CRCT of NF27_IC00040 (NCBI acc. no. KIE04386). Concentric halos depict hierarchical taxonomic databases increasing in divergence from the center. Average *Sm* score (see text for details) for all subjects and top ten subjects are provided, with highest score per database highlighted. 'na', not applicable. All corresponding information for proteins from HaloBLAST analyses are provided in **Table S2**. **(C)** Taxonomic breakdown of non-proteobacterial hits retrieved in HaloBlast analysis of CRCT domain-containing toxins and CRCAs. **(D)** Lengths for CRCAs. **(E)** Top ten blastp subjects by *Sm* score (see text for details) from 'Alph', 'Prot', and 'Bact' searches for CRCT domain-containing toxins and CRCAs. **(F)** CRCA conservation; sequence logos illustrate alignment of 380 CRCAs (see full alignment in **Figure S2**), with amino acid coloring as follows: black, hydrophobic; red, negatively charged; green, hydrophilic; purple, aromatic; blue, positively charged; star depicts unique *Rickettsia* insertion and triangles other insertions). **(G)** Diverse CRCT/CRCA modules from select genomes. White stipples on REIS_1423 indicate an adjusted start site.

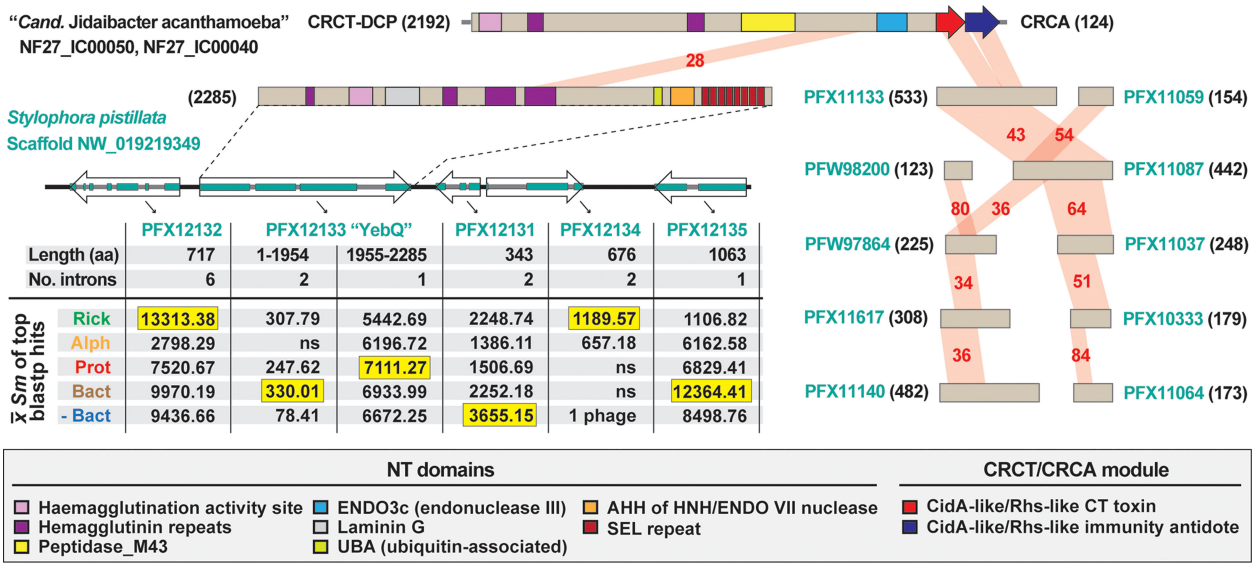

FIGURE 4 | The mobile nature of CRCT/CRCA modules captured in a eukaryotic genome assembly. In blastp searches against the NCBI "non-bacteria" database, the CRCT/CRCA module of "*Candidatus* Jidaibacter acanthamoeba" str. UWC36 consistently hit only predicted proteins from the smooth cauliflower coral (*Stylophora pistillata*) genome. *Left*, the large N-terminal region of NF27_IC00050 is similar to a large protein (PFX12133, 2285 aa) encoded on a five-gene *S. pistillata* scaffold (NW_019219349). PFX12133 domain architecture (descriptions in gray inset at bottom) is reminiscent of large, multi-domain hemagglutinin-like RHS toxins that may or may not carry CRCT domains (see **Figures 2**, **3**). The HaloBlast profile of PFX12133 and adjacent proteins indicates either rampant bacterial gene incorporation into the *S. pistillata* genome or mis-assembly of bacterial sequencing reads from *S. pistillata*-associated microbes. See text and **Figure 2** legend for description of HaloBlast. PFX12132: stomatin-like protein 2, mitochondrial; PFX12133: uncharacterized protein YbeQ; PFX12133: uncharacterized protein YqaJ; PFX12133: hypothetical protein AWC38_SpisGene23959; PFX12135: DNA polymerase I. *Right*, the complete or partial CRCT/CRCA module was detected in ten smaller predicted *S. pistillata* proteins encoded by genes on scaffolds not incorporated into the *S. pistillata* assembly.

genome integration, possibly in larger Rhs toxins that have degraded over time. The presence of complete, yet divergent rCRCT/CRCA modules in different species of the Tamurae/Ixodes Group (TIG) rickettsiae (**Figures 5D, E**) indicates weaponry for interbacterial antagonism may be functional for these species and implicates a previously unrealized mechanism for rickettsial competition in the same arthropod host

Probing rCRCT/CRCA-1 for a Role in *R. buchneri* Biology

Consideration for Another Factor Behind a Putative Mutualism

Factors that that distinguish parasitic rickettsiae from species exhibiting other host associations are sorely needed for Rickettsiology. Previously, we searched for genes underlying potential mutualism within the intriguing *R. felis* system, wherein typical strains infect blood-feeding arthropods (mostly the cat flea, *Ctenocephalides felis*) yet another has developed a tight host association with a non-blood-feeding insect (the booklouse *Liposcelis bostrychophila*) (Gillespie et al., 2015a). Only the *L. bostrychophila*-infecting strain harbored the unique plasmid, pLbAR, which we postulated encoded factors inducing parthenogenesis in booklice since sexually reproducing populations are only observed in the absence of *R. felis* (Yang et al., 2015). A TA module on pLbAR was found to have similarity to gene pairs in *Wolbachia* reproductive parasites that were later characterized as the factors underpinning cytoplasmic incompatibility (or male sterilization) (Beckmann et al., 2017; LePage et al., 2017). We later reported on the widespread occurrence in intracellular species of highly diverse TA modules with rudimentary similarity to the *Wolbachia* and *R. felis* TA modules (Gillespie et al., 2018). Despite its high frequency of infection in *I. scapularis* populations, we found no evidence for these TA modules in *R. buchneri*, although other different factors inducing reproductive parasitism could still be present.

The presence of genes in *R. buchneri* that encode AGAB synthesis/resistance proteins and PKS-containing NRPS modules hint at arsenals of antibiotics and 2° metabolites possibly used for defense against certain microbes also infecting blacklegged tick. Furthermore, two copies of BOOM suggest this species supplements the blacklegged tick diet with biotin. Absence (AGAB synthesis/resistance and PKS-containing NRPS) (Hagen et al., 2018) or scarce (BOOM) (Driscoll et al., 2020) distribution of these genes in other *Rickettsia* genomes suggests they are at least utilized for functions generally not employed by other rickettsiae. For instance, a similar type I PKS of a honey bee endosymbiont has recently been shown to suppress growth of fungal pathogens and protect bee brood from infection (Miller et al., 2020). We previously showed that, unlike the conserved AGAB synthesis/resistance genes, the PKS NRPS module is variable in gene content across *R. buchneri* strains from different populations (Hagen et al., 2018). More recently, the PKS NRPS

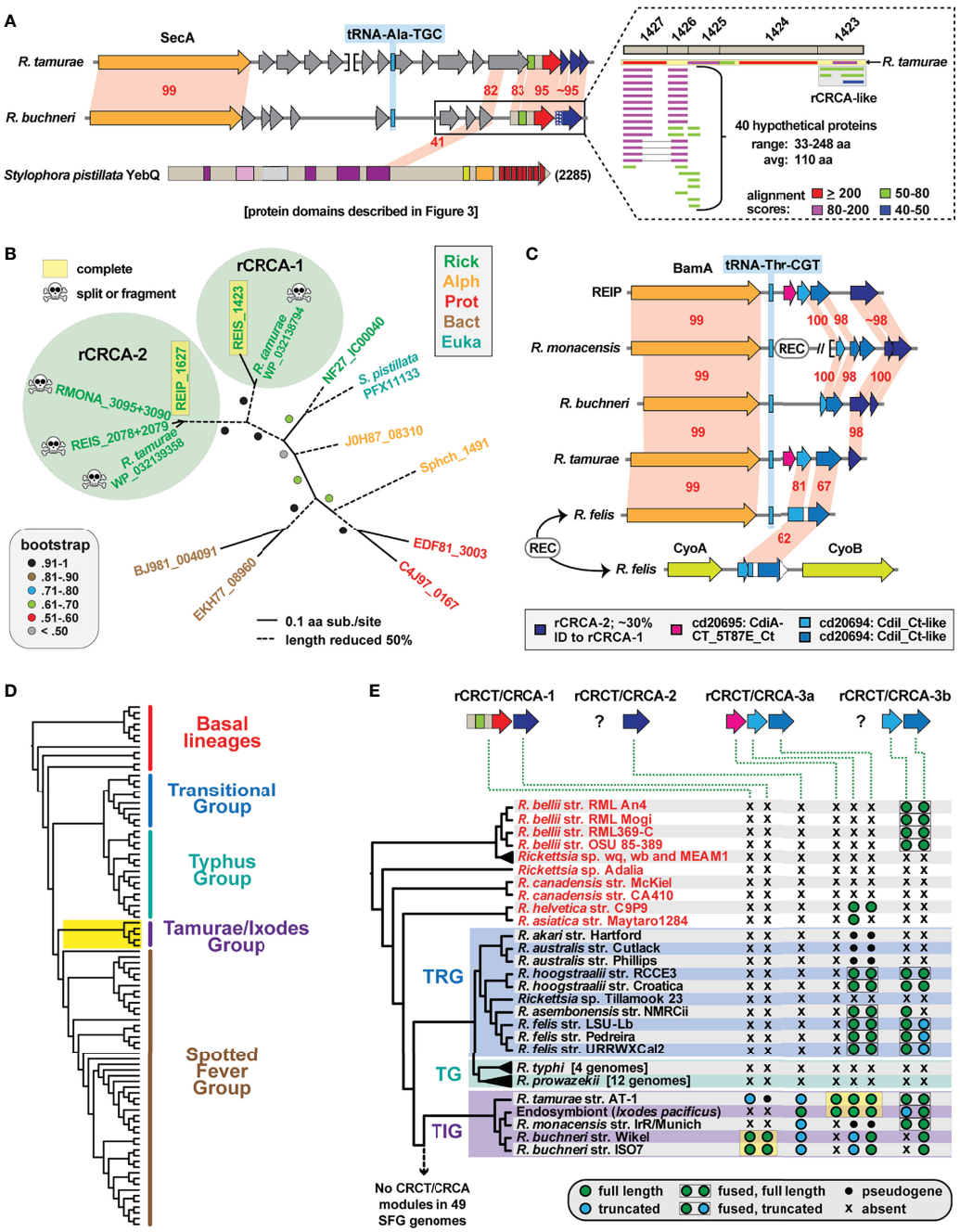

FIGURE 5 | Evolution of *Rickettsia* CRCT/CRCA modules. **(A)** Comparison of *R. tamurae* and *R. buchneri* genomic regions containing *Rickettsia* CRCT/CRCA module 1 (rCRCT/CRCA-1). Gray genes encode hypothetical proteins. Limited similarity between *R. buchneri* REIS_1425 and *Stylophora pistillata* YebQ is shown. Dashed inset: subjects retrieved from a Blastp search against the NCBI nr database using five concatenated *R. buchneri* proteins (REIS_1427-REIS_1423) as the query (further information provided in **Figure S4A**). Gray box illustrates additional rCRCA-like sequences identified by this search. **(B)** rCRCA-2 genes are divergent from rCRCA-1 and pseudogenized in all Tamurae/Ixodes Group (TIG) rickettsiae except *Rickettsia* endosymbiont of *Ixodes pacificus*. Phylogeny of rCRCA-1, rCRCA-2 and other CRCA proteins was estimated with the WAG substitution model (gamma model of rate heterogeneity) using RAxML v8.2.4 (Stamatakis, 2014). Branch support was assessed with 1,000 pseudo-replications. Final ML optimization likelihood was -3490.9. **(C)** rCRCT/CRCA modules 2 and 3a are mostly clustered near the BamA gene in some *Rickettsia* genomes, while rCRCA-3b genes occur between genes encoding the cytochrome oxidase subunits 2 (CyoA) and 1 (CyoB) in certain *Rickettsia* genomes (see **Figure S3** for illustration of genomic regions near *secA*, *bamA* and *cyoA/B* loci). **(D)** *Rickettsia* phylogeny estimated from 92 genomes (see **Figure S5** for more information). Yellow highlighting depicts TIG rickettsiae as the only species harboring complete CRCT/CRCA modules. **(E)** Phylogenomics analysis of rCRCT/CRCA modules. Yellow highlighting indicates complete rCRCT/CRCA modules. Further information is provided for rCRCT-1 (**Table S1**), rCRCA-1 (**Table S2**), rCRCA-2 (**Figure S4B**), rCRCA-3a and rCRCA-3b (**Figure S4C**), and rCRCT-3a (**Figures S4D-G**).

module and the AGAB synthesis/resistance gene array were investigated for their possible roles in limiting superinfection of pathogenic rickettsia in tick cells infected with *R. buchneri* str. ISO7 (Cull et al., 2022). Despite demonstrating that *R. buchneri* substantially reduced superinfection by pathogenic *R. parkeri* in cell culture, no anti-bacterial activity against either *R. parkeri* or extracellular bacteria (*Escherichia coli* and *Staphylococcus aureus*) was shown by the unknown product(s) of these loci, leaving their function in *R. buchneri* unclear.

rCRCT/CRCA Modules Are Tailored for Interspecific Antagonism

The sequence profiles that strongly indicate rCRCT/CRCA modules were acquired from distant non-proteobacteria (**Figures 2A**; **3A–C, E**) are similar to those we previously reported for AGAB synthesis/resistance proteins (Gillespie et al., 2012a) and PKS-containing NRPS modules (Hagen et al., 2018). This implicates LGT in shaping these factors that likely underpin interbacterial antagonism. While the target of the product of the PKS-containing NRPS module is hard to predict, it is possible that the aminoglycosides synthesized by proteins encoded on the AGAB gene array do not target rickettsiae, as this class of antibiotics is ineffective against *Rickettsia* species (Rolain et al., 1998) and overall generally poor for destroying intracellular bacteria due to limited transport into eukaryotic cells (Maurin and Raoult, 2001). However, aminoglycosides produced by *R. buchneri* could affect other rickettsiae that superinfect cells already occupied by *R. buchneri*. Similarly, the rCRCT/CRCA-1 module may function in intrageneric antagonism given most described CdiA-CT/CdiI and Rhs TA modules arm bacteria for battle with self or closely related species (Aoki et al., 2010; Poole et al., 2011; Zhang et al., 2011).

While often tethered to larger N-terminal sequences with toxic activity, CdiA-CT domains themselves are toxins (Nikolakakis et al., 2012). Curiously, the N-terminal sequence of REIS_1424 contains a putative ubiquitin-associated (UBA) domain that is separated from the C-terminal CRCT domain by two "VENN" motifs, which typically demarcate the CdiA-CT domain from the remaining protein in most other CDI systems (Aoki et al., 2010; Zhang et al., 2011) (**Figure S6**). If functional, this UBA domain may recruit host ubiquitin to the target cell and render it vulnerable to proteasomal destruction, which would be highly effective for killing conspecific bacteria in the intracellular environment.

rCRCT/CRCA-1 Expression and Possible Routes for Secretion

During infection of ISE6 cells, which were originally derived from *I. scapularis* embryos (Munderloh et al., 1999), both genes of the rCRCT/CRCA module are expressed by R. buchneri (data not shown). The same primers did not amplify product in PCR reactions using DNA template from 10 diverse rickettsiae, illustrating their specificity and efficacy for future surveys of blacklegged tick populations (**Figure 6A**). This is demonstrated by testing the primers on a small sampling of blacklegged ticks from three different populations throughout the *I. scapularis* range (**Figure 6B**). Future sequencing of these loci will provide resolution on the conservation rCRCT/CRCA-1 and whether there is evidence for an arms race between *R. buchneri* that have diverged throughout the *I. scapularis* geographic range.

As *R. buchneri* REIS_1424 lacks a predicted signal sequence, it is likely secreted *via* one of two Sec-independent pathways: type I secretion system (T1SS) or type IV secretion system (T4SS), which are both conserved in rickettsiae (Gillespie et al., 2015b). Inspection of the neighborhood loci around select CRCT/CRCA modules indicates several diverse secretion pathways for some CRCT-DCPs, including T4SS (*Sphingobium chlorophenolicum*) and type VI secretion system (T6SS) (*Sphaerisporangium krabiense*), as well as typical CDI systems (*Pseudomonas orientalis* and *Enterobacter* sp. BIGb0383) with nearby *cdiB* loci, which encode the outer membrane CdiB that translocates the large CdiA protein as a type Vb secretion system (T5bSS) (**Figures S7A-G**). Using CdiB as a query in Blastp searches against the major taxa harboring CRCT/CRCA modules revealed their scarcity in Rickettsiales (none detected in rickettsiae), Actinobacteria, Chloroflexi, and Spirochaetes genomes, but widespread distribution in other proteobacterial and Cyanobacteria genomes (**Figures S7H, I**). This indicates that bacteria employing the CRCT/CRCA modules we describe here for warfare utilize a variety of secretions systems (e.g., T1SS, T4SS, T5bSS, T6SS, and likely others) consistent with the plethora of secretory pathways now characterized for diverse TA modules involved in interbacterial antagonism (Ruhe et al., 2018; Lin et al., 2020). The lack of *cdiB* genes and evidence that rCRCT toxins were originally appended to larger proteins indicates these modular Rhs toxins were once widespread in *Rickettsia* genomes. This is reminiscent of the large modular toxins we identified across numerous intracellular bacteria that encode a myriad of eukaryotic-like domains, some of which function in commandeering host reproduction (Gillespie et al., 2018). Like rCRCT/CRCA modules, many of these variable toxins are found adjacent to genes encoding probable antidotes, indicating a recapitulating theme for toxin architecture that persists evolutionarily and drives innovative strategies for colonizing eukaryotic hosts.

CONCLUSION

Since our initial report on its genome (Gillespie et al., 2012a) and its subsequent formal species description (Kurtti et al., 2015), the appreciation for the oddity of *R. buchneri* relative to other rickettsiae has grown. Numerous reports on the *I. scapularis* microbiome now attest to the high infection rate of this microbe, particularly in females, throughout the blacklegged tick geographic range. While few reports indicate tick salivary gland infection (Steiner et al., 2008; Zolnik et al., 2016; Al-Khafaji et al., 2020), ovaries are the predominant tissue infected, consistent with the lack of reports on vertebrate infection or presence in other arthropods that co-feed on blacklegged tick hosts. This indicates a unique endosymbiosis, the intricacies of which stand to be illuminated in light of the powerful tools created by Kurtti, Munderloh and colleagues for studying this system (Munderloh et al., 1999; Simser et al., 2002; Kurtti et al., 2016; Oliver et al., 2021). Ultimately, the fitness of blacklegged ticks uninfected with *R. buchneri* (Oliver et al., 2021) needs to be evaluated, as does the

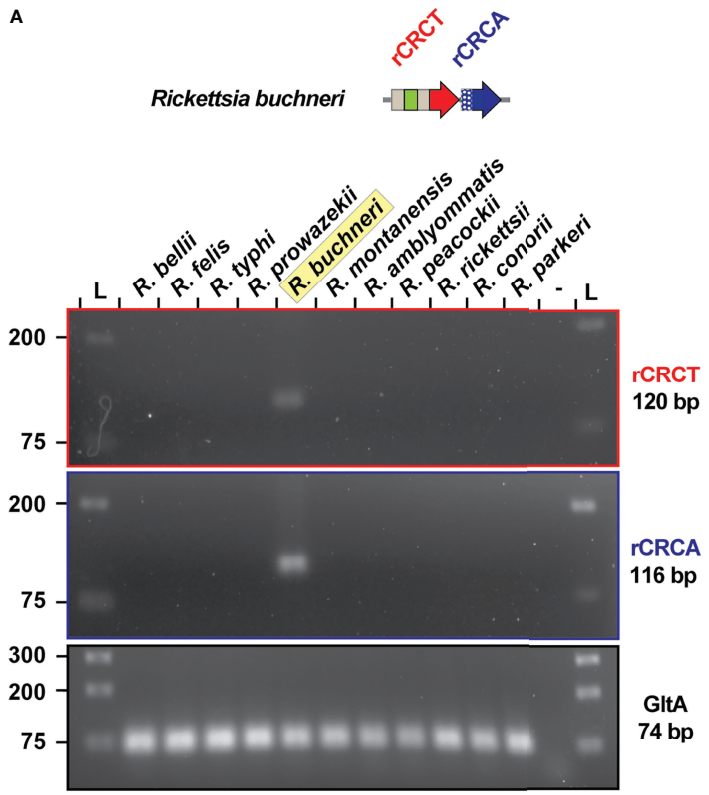

B

Locality	rCRCT F	rCRCT M	rCRCT N	rCRCA F	rCRCA M	rCRCA N
NY	4/5	5/5	---	5/5	5/5	---
NH	5/5	3/5	---	5/5	5/5	---
PA	---	---	9/10	---	---	7/10

FIGURE 6 | REIS_1424/REIS_1423 is a species-specific marker. **(A)** PCR assay for *rCRCT* and *rCRCA* in 11 different rickettsiae. Citrate synthase (*gltA*) was used as a positive control. **(B)** The same PCR assay was conducted on *I. scapularis* from three populations.

possibility that other endosymbionts may replace *R. buchneri* in a mutualistic capacity.

While previously observed in ticks (Burgdorfer et al., 1981; Macaluso et al., 2002; Wright et al., 2015; Levin et al., 2018) and cell culture (Cull et al., 2022), the ability of *Rickettsia* infection to block *Rickettsia* superinfection remains a sorely understudied aspect of vector biology. Our identification and characterization of rCRCT/CRCA modules adds to a short list of factors, namely BOOM, AGAB and PKS-NRPS, that have been hypothesized to underpin a mutualism between *R. buchneri* and blacklegged tick. Future characterization of these factors will determine their contribution to blocking superinfection of *I. scapularis* by *Rickettsia* pathogens (Cull et al., 2022). When mutagenesis is someday an efficacious tool for bioengineering Rickettsiae, this line of research will offer a gene drive tool (*R. buchneri*) ready to disseminate into blacklegged tick populations to combat the spread of human disease agents.

DATA AVAILABILITY STATEMENT

The original contributions presented in the study are included in the article/**Supplementary Material**. Further inquiries can be directed to the corresponding author.

AUTHOR CONTRIBUTIONS

VV, TD, and JG conceived the project and designed the experiments. All authors performed the experiments. VV, TD, and JG analyzed the results. All authors wrote the manuscript. All authors contributed to the article and approved the submitted version.

FUNDING

This work was supported with funds from the National Institute of Health/National Institute of Allergy and Infectious Diseases grant R21AI156762 (JJG and TPD). TDF was supported by the Biotechnical Institute of Maryland. The funders had no role in study design, data collection and analysis, decision to publish, or preparation of the manuscript.

ACKNOWLEDGMENTS

We thank Alison Luce-Fedrow (Shippensburg University), Richard Ostfeld (Cary Institute of Ecosystem Studies), and Kathryn Cottingham (Dartmouth College) for providing tick specimens, and Kevin Macaluso (University of South Alabama) and Sean Riley (University of Maryland College Park) for providing rickettsial genomic DNA. We are grateful to Uli Munderloh and Tim Kurtti (University of Minnesota) for sharing the ISE6 cell line and *R. buchneri* strain IS07.

SUPPLEMENTARY MATERIAL

The Supplementary Material for this article can be found online at: https://www.frontiersin.org/articles/10.3389/fcimb.2022.880813/full#supplementary-material

Supplementary Figure 1 | Sequence analysis of 155 predicted CRCTs integrated into diverse bacterial toxins. **(A)** Sequence logos (Crooks et al., 2004) depict complete protein alignment generated using MUSCLE, default parameters (Edgar, 2004). Information for all proteins is provided in **Table S1**. Regions shown in **Figures 2** are denoted with a bar above the logos. Amino acid coloring as follows: black, hydrophobic; red, negatively charged; green, hydrophilic; purple, aromatic; blue, positively charged. Unique *Rickettsia* insertion is shown in orange. Other insertions noted by triangles in **Figure 2** are highlighted yellow). **(B)** HaloBlast profiles for REIS_1424 with and without a 23 aa insertion (see **Figure 2E** and text for more details).

Supplementary Figure 2 | Sequence analysis of 380 predicted CRCAs. Sequence logos (Crooks et al., 2004) depict complete protein alignment generated using MUSCLE, default parameters (Edgar, 2004). Information for all proteins is provided in **Table S2**. Regions shown in **Figures 3** are denoted with a bar above the logos. Amino acid coloring as follows: black, hydrophobic; red, negatively charged; green, hydrophilic; purple, aromatic; blue, positively charged. Sequence spanning the adjusted start site of REIS_1423 (*Rickettsia buchneri*) insertion is shown in blue.

Supplementary Figure 3 | *Rickettsia* CRCT/CRCA modules occur in three recombination hotspots. **(A)** rCRCT/CRCA-1 occurs in a recombination hotspot near the SecA and tRNA-Ala^{TGC} genes. **(B)** rCRCT/CRCA-2 occurs in a recombination hotspot near the BamA and tRNA-Thr^{CGT} genes. A second TA module, rCRCT/CRCA-3a, also occurs in this region and is distinct from rCRCT/CRCA-1 and rCRCT/CRCA-2 (cd20695: CdiA-CT_5T87E_Ct, cd20694: CdiI_Ct-like). **(C)** rCRCT/CRCA-3b proteins are analogous to rCRCT/CRCA-3a and occur in a subset of *Rickettsia* genomes between *cyoB* and *cyoA*, which encode the cytochrome *c* oxidase subunits I and II, respectively.

Supplementary Figure 4 | Evidence for recurrent integration of diverse CRCT/CRCA modules in *Rickettsia* genomes at recombination hotspots. **(A)** Subjects (n = 40) retrieved from a Blastp search against the NCBI nr database using five concatenated *R. buchneri* proteins (REIS_1427-REIS_1423) as the query. *Bottom*, a portion of the large protein (PFX12133, 2285 aa) from the coral *Stylophora pistillata* shares similarity with these smaller *Rickettsia* proteins. **(B)** rCRCT-2 proteins are analogous to rCRCT-1 proteins. Alignment performed using MUSCLE with default settings (Edgar, 2004). **(C)** rCRCA-3 proteins recovered from Blastp searches using *R. bellii* rCRCA-3b as a query (the largest rCRCA-3 protein). na, sequences not recovered in Blastp searches against the NCBI 'Rickettsia' database but retrieved from PATRIC (asterisks denote PATRIC Local Family IDs). Subjects are listed accordingly to their placement in the phylogeny presented in **Figures 5E**. Colored boxes unite rCRCA-3 proteins recombined within the same genome. **(D)** rCRCT-3a HaloBalst analysis. *R. tamurae* rCRCT-3a (WP_051965318) was used as the query. Concentric halos depict hierarchical taxonomic databases increasing in divergence from the center. Average *Sm* score (see text for details) for all subjects and top ten subjects are provided, with highest score per database highlighted. 'na', not applicable. **(E)** Top 25 subjects from the Blastp search against 'Proteobacteria' using *R. tamurae* rCRCT-3a as the query. **(F)** Comparison of the *Cupriavidus taiwanensis* str. DSM 17343 CdiA toxin (Uniprot acc. B3R1C1) to rCRCT-3a of *R. tamurae*. Domains were predicted with SMART (Letunic and Bork, 2017). Amino acid similarity (%ID, red shading) was assessed using Blastp. **(G)** Structural analysis of a rCRCT/CRCA-3a module. (top) Alignment of residues 3391-3469 of *C. taiwanensis* CdiA, *R. tamurae* rCRCT-3a, and REIP rCRCT-3a. Structural information from *C. taiwanensis* CdiA (PDB:5T87) (Kryshtafovych et al., 2018) is provided at top. Alignment performed using MUSCLE with default settings (Edgar, 2004). (bottom left) Modeling with Phyre2 of *R. tamurae* rCRCT-3a to the CdiA-CT toxin structure of *C. taiwanensis* CdiA (PDB:5T87). The threading was done with 100% confidence. (bottom right) While the *C. taiwanensis* module was solved as a co-complex (Kryshtafovych et al., 2018), Phyre2 modeling could not thread *R. tamurae* rCRCA-3a to the antidote CdiI within the TA co-complex. The best model (46.3% confidence, 12% ID) for *R. tamurae* rCRCA-3a was to the structure of *Drosophila melanogaster* MAST/Orbit N-terminal domain PDB:4G3A (De La Mora-Rey et al., 2013)

Supplementary Figure 5 | *Rickettsia* genome-based phylogeny estimation. *Rickettsia* groups follow previous classification (Gillespie et al., 2007), except that we recognize Tamurae/Ixodes Group (TIG) rickettsiae as a distinct clade from SFG rickettsiae. *R. buchneri* is highlighted. Phylogeny was estimated for 92 *Rickettsia* genomes; gray inset described details (see "Materials and Methods" for more details). Branch support was assessed with 1,000 pseudoreplications.

Supplementary Figure 6 | REIS_1424 contains a ubiquitin-associated domain demarcated from the C-terminal toxin by two predicted VENN motifs. (Mueller and Feigon, 2002); (E) Schemas for a few. Accession nos. Described domains here or in the M&M and get refs from SMART (Letunic and Bork, 2017). Wolbachia supergroups are within colored ellipses. Ctenocephalides felis-

Supplementary Figure 7 | Gene neighborhoods for CRCT/CRCA modules in diverse bacteria. **(A-G)** Genome neighborhoods for the CRCT/CRCA modules shown in and for **(A)** "*Candidatus* Jidaibacter acanthamoeba", **(B)** *Sphingobium chlorophenolicum*, **(C)** Holosporales bacterium, **(D)** *Pseudomonas orientalis*, **(E)** *Enterobacter* sp. BIGb0383, **(F)** *Streptomyces luteoverticillatus*, **(G)** *Sphaerisporangium krabiense*. **(H)** Results of Blastp searches against these seven genomes (specific taxon databases at NCBI) using the CdiB protein of *Escherichia coli* (UniProtKB-Q3YL97). **(I)** Occurrence of CdiB and CdiB-like proteins in the major taxa in which CRCT/CRCA modules were identified.

Supplementary Table 1 | Information pertaining to 155 predicted CRCTs integrated into diverse bacterial toxins.

Supplementary Table 2 | Information pertaining to 380 predicted CRCAs.

Supplementary Table 3 | Evidence for CRCT/CRCA modules in the *Stylophora pistillata* genome assembly.

REFERENCES

Abraham, N. M., Liu, L., Jutras, B. L., Yadav, A. K., Narasimhan, S., Gopalakrishnan, V., et al. (2017). Pathogen-Mediated Manipulation of Arthropod Microbiota to Promote Infection. *Proc. Natl. Acad. Sci.* 114, E781–E790. doi: 10.1073/pnas.1613422114

Al-Khafaji, A. M., Armstrong, S. D., Varotto Boccazzi, I., Gaiarsa, S., Sinha, A., Li, Z., et al. (2020). Rickettsia Buchneri, Symbiont of the Deer Tick Ixodes Scapularis, Can

Colonise the Salivary Glands of Its Host. *Ticks Tick Borne Dis.* 11, 101299. doi: 10.1016/J.TTBDIS.2019.101299

Aoki, S. K., Diner, E. J., De Roodenbeke, C. T. K., Burgess, B. R., Poole, S. J., Braaten, B. A., et al. (2010). A Widespread Family of Polymorphic Contact-Dependent Toxin Delivery Systems in Bacteria. *Nature* 468, 439–442. doi: 10.1038/nature09490

Aoki, S. K., Webb, J. S., Braaten, B. A., and Low, D. A. (2009). Contact-Dependent Growth Inhibition Causes Reversible Metabolic Downregulation in Escherichia Coli. *J. Bacteriol.* 191, 1777–1786. doi: 10.1128/JB.01437-08/ASSET/94ABFA58-D59C-4950-AC3A-44EED9C05FEE/ASSETS/GRAPHIC/ZJB0060985500007.JPEG

Aziz, R. K., Bartels, D., Best, A. A., DeJongh, M., Disz, T., Edwards, R. A., et al. (2008). The RAST Server: Rapid Annotations Using Subsystems Technology. *BMC Genomics* 9, 75. doi: 10.1186/1471-2164-9-75

Balvín, O., Roth, S., Talbot, B., and Reinhardt, K. (2018). Co-Speciation in Bedbug Wolbachia Parallel the Pattern in Nematode Hosts. *Sci. Rep.* 8, 8797. doi: 10.1038/s41598-018-25545-y

Beckmann, J. F., Ronau, J. A., and Hochstrasser, M. (2017). A Wolbachia Deubiquitylating Enzyme Induces Cytoplasmic Incompatibility. *Nat. Microbiol.* 2, 17007. doi: 10.1038/nmicrobiol.2017.7

Beck, C. M., Morse, R. P., Cunningham, D. A., Iniguez, A., Low, D. A., Goulding, C. W., et al. (2014). CdiA From Enterobacter Cloacae Delivers a Toxic Ribosomal RNase Into Target Bacteria. *Structure* 22, 707–718. doi: 10.1016/J.STR.2014.02.012/ATTACHMENT/638214C1-C3F9-493D-BF50-00C4042D7460/MMC1.PDF

Benson, M. J., Gawronski, J. D., Eveleigh, D. E., and Benson, D. R. (2004). Intracellular Symbionts and Other Bacteria Associated With Deer Ticks (Ixodes Scapularis) From Nantucket and Wellfleet, Cape Cod, Massachusetts. *Appl. Environ. Microbiol.* 70, 616–620. doi: 10.1128/AEM.70.1.616-620.2004

Billings, A. N., Teltow, G. J., Weaver, S. C., and Walker, D. H. (1998). Molecular Characterization of a Novel Rickettsia Species From Ixodes Scapularis in Texas. *Emerg. Infect. Dis.* 4, 305–309. doi: 10.3201/eid0402.980221

Blanc, G., Ogata, H., Robert, C., Audic, S., Claverie, J. M., and Raoult, D. (2007). Lateral Gene Transfer Between Obligate Intracellular Bacteria: Evidence From the Rickettsia Massiliae Genome. *Genome Res.* 17, 1657–1664. doi: 10.1101/gr.6742107

Bruner, S. D., Norman, D. P. G., and Verdine, G. L. (2000). Structural Basis for Recognition and Repair of the Endogenous Mutagen 8-Oxoguanine in DNA. *Nat. 2000 4036772* 403, 859–866. doi: 10.1038/35002510

Burgdorfer, W., Hayes, S. F., and Mavros, A. J. (1981). *"Rickettsiae and Rickettsial Diseases,"*. Eds. W. Burgdorfer and R. L. Anacker (New York, NY: Academic Press), 585–594. doi: 10.3/JQUERY-UI.JS

Busby, J. N., Panjikar, S., Landsberg, M. J., Hurst, M. R. H., and Lott, J. S. (2013). The BC Component of ABC Toxins Is an RHS-Repeat-Containing Protein Encapsulation Device. *Nature* 501, 547–550. doi: 10.1038/nature12465

Crooks, G. E., Hon, G., Chandonia, J.-M., and Brenner, S. E. (2004). WebLogo: A Sequence Logo Generator. *Genome Res.* 14, 1188–1190. doi: 10.1101/gr.849004

Cross, S. T., Kapuscinski, M. L., Perino, J., Maertens, B. L., Weger-Lucarelli, J., Ebel, G. D., et al. (2018). Co-Infection Patterns in Individual Ixodes Scapularis Ticks Reveal Associations Between Viral, Eukaryotic and Bacterial Microorganisms. *Viruses* 10, 1–19. doi: 10.3390/v10070388

Cull, B., Burkhardt, N. Y., Wang, X. R., Thorpe, C. J., Oliver, J. D., Kurtti, T. J., et al. (2022). The Ixodes Scapularis Symbiont Rickettsia Buchneri Inhibits Growth of Pathogenic Rickettsiaceae in Tick Cells: Implications for Vector Competence. *Front. Vet. Sci.* 8. doi: 10.3389/FVETS.2021.748427/BIBTEX

Darby, A. C., Cho, N.-H., Fuxelius, H.-H., Westberg, J., and Andersson, S. G. E. (2007). Intracellular Pathogens Go Extreme: Genome Evolution in the Rickettsiales. *Trends Genet.* 23, 511–520. doi: 10.1016/j.tig.2007.08.002

De La Mora-Rey, T., Guenther, B. D., and Finzel, B. C. (2013). The Structure of the TOG-Like Domain of Drosophila Melanogaster Mast/Orbit. *urn:issn:1744-3091* 69, 723–729. doi: 10.1107/S1744309113015182

Driscoll, T. P., Gillespie, J. J., Nordberg, E. K., Azad, A. F., and Sobral, B. W. (2013). Bacterial DNA Sifted From the Trichoplax Adhaerens (Animalia: Placozoa) Genome Project Reveals a Putative Rickettsial Endosymbiont. *Genome Biol. Evol.* 5, 621–645. doi: 10.1093/gbe/evt036

Driscoll, T. P., Verhoeve, V. I., Brockway, C., Shrewsberry, D. L., Plumer, M., Sevdalis, S. E., et al. (2020). Evolution of *Wolbachia* Mutualism and Reproductive Parasitism: Insight From Two Novel Strains That Co-Infect Cat Fleas. *PeerJ* 8, e10646. doi: 10.7717/peerj.10646

Edgar, R. C. (2004). MUSCLE: Multiple Sequence Alignment With High Accuracy and High Throughput. *Nucleic Acids Res.* 32, 1792–1797. doi: 10.1093/nar/gkh340

Feris, K. P., Ramsey, P. W., Frazar, C., Rillig, M. C., and Gannon, J. E. (2003). Structure and Seasonal Dynamics of Hyporheic Zone Microbial Communities in Free-Stone Rivers of the Western United States. *Microb. Ecol.* 46, 200–215. doi: 10.1007/BF03036883

Finn, R. D., Clements, J., and Eddy, S. R. (2011). HMMER Web Server: Interactive Sequence Similarity Searching. *Nucleic Acids Res.* 39, W29–W37. doi: 10.1093/NAR/GKR367

Fuxelius, H.-H., Darby, A. C., Cho, N.-H., and Andersson, S. G. (2008). Visualization of Pseudogenes in Intracellular Bacteria Reveals the Different Tracks to Gene Destruction. *Genome Biol.* 92 (9), 1–15. doi: 10.1186/GB-2008-9-2-R42

Gerth, M., and Bleidorn, C. (2017). Comparative Genomics Provides a Timeframe for Wolbachia Evolution and Exposes a Recent Biotin Synthesis Operon Transfer. *Nat. Microbiol.* 2, 16241. doi: 10.1038/nmicrobiol.2016.241

Gil, J. C., Helal, Z. H., Risatti, G., and Hird, S. M. (2020). Ixodes Scapularis Microbiome Correlates With Life Stage, Not the Presence of Human Pathogens, in Ticks Submitted for Diagnostic Testing. *PeerJ* 8, e10424. doi: 10.7717/PEERJ.10424/SUPP-10

Gillespie, J. J., Beier, M. S., Rahman, M. S., Ammerman, N. C., Shallom, J. M., Purkayastha, A., et al. (2007). Plasmids and Rickettsial Evolution: Insight From Rickettsia Felis. *PloS One* 2, e266. doi: 10.1371/journal.pone.0000266

Gillespie, J. J., Driscoll, T. P., Verhoeve, V. I., Rahman, M. S., Macaluso, K. R., and Azad, A. F. (2018). A Tangled Web: Origins of Reproductive Parasitism. *Genome Biol. Evol.* 10, 2292–2309. doi: 10.1093/gbe/evy159

Gillespie, J. J., Driscoll, T. P., Verhoeve, V. I., Utsuki, T., Husseneder, C., Chouljenko, V. N., et al. (2015a). Genomic Diversification in Strains of Rickettsia Felis Isolated From Different Arthropods. *Genome Biol. Evol.* 7, 35–56. doi: 10.1093/gbe/evu262

Gillespie, J. J., Joardar, V., Williams, K. P., Driscoll, T. P., Hostetler, J. B., Nordberg, E., et al. (2012a). A Rickettsia Genome Overrun by Mobile Genetic Elements Provides Insight Into the Acquisition of Genes Characteristic of an Obligate Intracellular Lifestyle. *J. Bacteriol.* 194, 376–394, 47–80. doi: 10.1128/JB.06244-11

Gillespie, J. J., Kaur, S. J., Sayeedur Rahman, M., Rennoll-Bankert, K., Sears, K. T., Beier-Sexton, M., et al. (2015b). Secretome of Obligate Intracellular Rickettsia. *FEMS Microbiol. Rev.* 39, 47-80. doi: 10.1111/1574-6976.12084

Gillespie, J. J., Nordberg, E. K., Azad, A. A., and Sobral, B. W. (2012b). "Phylogeny And Comparative Genomics: The Shifting Landscape In The Genomics Era", in *Intracellular Pathogens II: Rickettsiales*. Eds. A. F. Azad and G. H. Palmer (Boston: American Society of Microbiology), 84–141.

Gillespie, J. J., Williams, K., Shukla, M., Snyder, E. E., Nordberg, E. K., Ceraul, S. M., et al. (2008). Rickettsia Phylogenomics: Unwinding the Intricacies of Obligate Intracellular Life. *PloS One* 3, 1–34. doi: 10.1371/journal.pone.0002018

Gulia-Nuss, M., Nuss, A. B. A. B., Meyer, J. M. J. M., Sonenshine, D. E. D. E., Roe, R. M. M., Waterhouse, R. M. R. M., et al. (2016). Genomic Insights Into the Ixodes Scapularis Tick Vector of Lyme Disease. *Nat. Commun.* 7, 10507. doi: 10.1038/ncomms10507

Hagen, R., Verhoeve, V. I., Gillespie, J. J., and Driscoll, T. P. (2018). Conjugative Transposons and Their Cargo Genes Vary Across Natural Populations of Rickettsia Buchneri Infecting the Tick Ixodes Scapularis. *Genome Biol. Evol.* 10, 3218–3229. doi: 10.1093/gbe/evy247

Johnson, P. M., Gucinski, G. C., Garza-Sánchez, F., Wong, T., Hung, L. W., Hayes, C. S., et al. (2016). Functional Diversity of Cytotoxic Trnase/Immunity Protein Complexes From Burkholderia Pseudomallei*. *J. Biol. Chem.* 291, 19387–19400. doi: 10.1074/JBC.M116.736074

Ju, J.-F., Bing, X.-L., Zhao, D.-S., Guo, Y., Xi, Z., Hoffmann, A. A., et al. (2019). Wolbachia Supplement Biotin and Riboflavin to Enhance Reproduction in Planthoppers. *ISME J.* 14, 1–12. doi: 10.1038/s41396-019-0559-9

Kajava, A. V., Cheng, N., Cleaver, R., Kessel, M., Simon, M. N., Willery, E., et al. (2001). Beta-Helix Model for the Filamentous Haemagglutinin Adhesin of Bordetella Pertussis and Related Bacterial Secretory Proteins. *Mol. Microbiol.* 42, 279–292. doi: 10.1046/J.1365-2958.2001.02598.X

Kelley, L. A., and Sternberg, M. J. E. (2009). Protein Structure Prediction on the Web: A Case Study Using the Phyre Server. *Nat. Protoc.* 4, 363–371. doi: 10.1038/nprot.2009.2

Kryshtafovych, A., Albrecht, R., Baslé, A., Bule, P., Caputo, A. T., Carvalho, A. L., et al. (2018). Target Highlights From the First Post-PSI CASP Experiment (CASP12, May–August 2016). *Proteins Struct. Funct. Bioinform.* 86, 27–50. doi: 10.1002/PROT.25392

Kurtti, T. J., Burkhardt, N. Y., Heu, C. C., and Munderloh, U. G. (2016). Fluorescent Protein Expressing Rickettsia Buchneri and Rickettsia Peacockii for Tracking Symbiont-Tick Cell Interactions. *Vet. Sci.* 3, 34. doi: 10.3390/VETSCI3040034

Kurtti, T. J., Felsheim, R. F., Burkhardt, N. Y., Oliver, J. D., Heu, C. C., and Munderloh, U. G. (2015). Rickettsia Buchneri Sp. Nov., a Rickettsial Endosymbiont of the Blacklegged Tick Ixodes Scapularis. *Int. J. Syst. Evol. Microbiol.* 65, 965–970. doi: 10.1099/ijs.0.000047

Lee, S., Kakumanu, M. L., Ponnusamy, L., Vaughn, M., Funkhouser, S., Thornton, H., et al. (2014). The Skin of Outdoor Workers in North Carolina. *Parasites Vectors* 7, 1–14. doi: 10.1186/s13071-014-0607-2

Lehane, M. J., and Lehane, M. J. (2010). ""Managing the Blood Meal,"," in *The Biology of Blood-Sucking in Insects* (Cambridge, England: Cambridge University Press), 84–115. doi: 10.1017/cbo9780511610493.007

LePage, D. P., Metcalf, J. A., Bordenstein, S. R., On, J., Perlmutter, J. I., Shropshire, J. D., et al. (2017). Prophage WO Genes Recapitulate and Enhance Wolbachia-Induced Cytoplasmic Incompatibility. *Nature* 543, 243–247. doi: 10.1038/nature21391

Letunic, I., and Bork, P. (2017). 20 Years of the SMART Protein Domain Annotation Resource. *Nucleic Acids Res*46, D493-D496. doi: 10.1093/nar/gkx922

Levin, M. L., Schumacher, L. B. M., and Snellgrove, A. (2018). Effects of Rickettsia Amblyommatis Infection on the Vector Competence of Amblyomma Americanum Ticks for Rickettsia Rickettsii. *Vector Borne Zoonotic Dis.* 18, 579–587. doi: 10.1089/VBZ.2018.2284

Lin, H. H., Filloux, A., and Lai, E. M. (2020). Role of Recipient Susceptibility Factors During Contact-Dependent Interbacterial Competition. *Front. Microbiol.* 11. doi: 10.3389/FMICB.2020.603652/BIBTEX

Liu, X., Bulgakov, O. V., Darrow, K. N., Pawlyk, B., Adamian, M., Liberman, M. C., et al. (2007). Usherin Is Required for Maintenance of Retinal Photoreceptors and Normal Development of Cochlear Hair Cells. *Proc. Natl. Acad. Sci.* 104, 4413–4418. doi: 10.1073/PNAS.0610950104

Liu, W., Xie, Y., Ma, J., Luo, X., Nie, P., Zuo, Z., et al. (2015). IBS: An Illustrator for the Presentation and Visualization of Biological Sequences. *Bioinformatics* 31, 3359–3361. doi: 10.1093/bioinformatics/btv362

Macaluso, K. R., Sonenshine, D. E., Ceraul, S. M., and Azad, A. F. (2002). Rickettsial Infection in Dermacentor Variabilis (Acari: Ixodidae) Inhibits Transovarial Transmission of a Second Rickettsia. *J. Med. Entomol.* 39, 809–813. doi: 10.1603/0022-2585-39.6.809

Madison-Antenucci, S., Kramer, L. D., Gebhardt, L. L., and Kauffman, E. (2020). Emerging Tick-Borne Diseases. *Clin. Microbiol. Rev.* 33, 1–34. doi: 10.1128/CMR.00083-18

Magnarelli, L. A., Andreadis, T. G., Stafford, K. C., and Holland, C. J. (1991). Rickettsiae and Borrelia Burgdorferi in Ixodid Ticks. *J. Clin. Microbiol.* 29, 2798–2804. doi: 10.1128/jcm.29.12.2798-2804.1991

Manzano-Marín, A., Oceguera-Figueroa, A., Latorre, A., Jiménez-García, L. F., and Moya, A. (2015). Solving a Bloody Mess: B-Vitamin Independentmetabolic Convergence Among Gammaproteobacterial Obligate Endosymbionts From Blood-Feeding Arthropods and the Leech Haementeria Officinalis. *Genome Biol. Evol.* 7, 2871–2884. doi: 10.1093/gbe/evv188

Maurin, M., and Raoult, D. (2001). Use of Aminoglycosides in Treatment of Infections Due to Intracellular Bacteria. *Antimicrob. Agents Chemother.* 45, 2977–2986. doi: 10.1128/AAC.45.11.2977-2986.2001

Michalska, K., Quan Nhan, D., Willett, J. L. E., Stols, L. M., Eschenfeldt, W. H., Jones, A. M., et al. (2018). Functional Plasticity of Antibacterial EndoU Toxins. *Mol. Microbiol.* 109, 509–527. doi: 10.1111/MMI.14007

Miller, D. L., Smith, E. A., and Newton, I. L. G. (2020). A Bacterial Symbiont Protects Honey Bees From Fungal Disease. *bioRxiv* 12, 2020.01.21.914325. doi: 10.1101/2020.01.21.914325

Moreno, C. X., Moy, F., Daniels, T. J., Godfrey, H. P., and Cabello, F. C. (2006). Molecular Analysis of Microbial Communities Identified in Different Developmental Stages of Ixodes Scapularis Ticks From Westchester and Dutchess Counties, New York. *Environ. Microbiol.* 8, 761–772. doi: 10.1111/j.1462-2920.2005.00955.x

Morse, R. P., Nikolakakis, K. C., Willett, J. L. E., Gerrick, E., Low, D. A., Hayes, C. S., et al. (2012). Structural Basis of Toxicity and Immunity in Contact-Dependent Growth Inhibition (CDI) Systems. *Proc. Natl. Acad. Sci. U. S. A.* 109, 21480–21485. doi: 10.1073/PNAS.1216238110/-/DCSUPPLEMENTAL

Mueller, T. D., and Feigon, J. (2002). Solution Structures of UBA Domains Reveal a Conserved Hydrophobic Surface for Protein–Protein Interactions. *J. Mol. Biol.* 319, 1243–1255. doi: 10.1016/S0022-2836(02)00302-9

Munderloh, U. G., Jauron, S. D., Fingerle, V., Leitritz, L., Hayes, S. F., Hautman, J. M., et al. (1999). Invasion and Intracellular Development of the Human Granulocytic Ehrlichiosis Agent in Tick Cell Culture. *J. Clin. Microbiol.* 37, 2518–2524. doi: 10.1128/JCM.37.8.2518-2524.1999/ASSET/225E7731-33D8-4A77-AB6E-0910DAE543E2/ASSETS/GRAPHIC/JM0890090005.JPEG

Munderloh, U. G., Jauron, S. D., and Kurtti, T. J. (2005). ""Chapter 3 : The Tick: A Different Kind of Host for Human Pathogens,"," in *Tick-Borne Diseases of Humans*. Eds. J. L. Goodman, D. T. Dennis and D. E. Sonenshine (Boston: American Society for Microbiology).

Narasimhan, S., Rajeevan, N., Liu, L., Zhao, Y. O., Heisig, J., Pan, J., et al. (2014). Gut Microbiota of the Tick Vector Ixodes Scapularis Modulate Colonization of the Lyme Disease Spirochete. *Cell Host Microbe* 15, 58–71. doi: 10.1016/j.chom.2013.12.001

Nikoh, N., Hosokawa, T., Moriyama, M., Oshima, K., Hattori, M., and Fukatsu, T. (2014). Evolutionary Origin of Insect-Wolbachia Nutritional Mutualism. *Proc. Natl. Acad. Sci. U. S. A.* 111, 10257–10262. doi: 10.1073/pnas.1409284111

Nikolakakis, K., Amber, S., Wilbur, J. S., Diner, E. J., Aoki, S. K., Poole, S. J., et al. (2012). The Toxin/Immunity Network of Burkholderia Pseudomallei Contact-Dependent Growth Inhibition (CDI) Systems. *Mol. Microbiol.* 84, 516. doi: 10.1111/J.1365-2958.2012.08039.X

Ogata, H., La Scola, B., Audic, S., Renesto, P., Blanc, G., Robert, C., et al. (2006). Genome Sequence of Rickettsia Bellii Illuminates the Role of Amoebae in Gene Exchanges Between Intracellular Pathogens. *PloS Genet.* 2, 733–744. doi: 10.1371/JOURNAL.PGEN.0020076

Oliver, J. D., Price, L. D., Burkhardt, N. Y., Heu, C. C., Khoo, B. S., Thorpe, C. J., et al. (2021). Growth Dynamics and Antibiotic Elimination of Symbiotic Rickettsia Buchneri in the Tick Ixodes Scapularis (Acari: Ixodidae). *Appl. Environ. Microbiol.* 87, 1–9. doi: 10.1128/AEM.01672-20

Penz, T., Schmitz-Esser, S., Kelly, S. E., Cass, B. N., Müller, A., Woyke, T., et al. (2012). Comparative Genomics Suggests an Independent Origin of Cytoplasmic Incompatibility in Cardinium Hertigii. *PloS Genet.* 8, e1003012. doi: 10.1371/journal.pgen.1003012

Perler, F. B. (1998). Protein Splicing of Inteins and Hedgehog Autoproteolysis: Structure, Function, and Evolution. *Cell* 92, 1–4. doi: 10.1016/S0092-8674(00)80892-2

Poole, S., Diner, E., Aoki, S., Braaten, B., t'Kint de Roodenbeke, C., Low, D., et al. (2011). Identification of Functional Toxin/Immunity Genes Linked to Contact-Dependent Growth Inhibition (CDI) and Rearrangement Hotspot (Rhs) Systems. *PloS Genet.* 7, 1–14. doi: 10.1371/JOURNAL.PGEN.1002217

Rawlings, N. D., and Barrett, A. J. (1995). Evolutionary Families of Metallopeptidases. *Methods Enzymol.* 248, 183–228. doi: 10.1016/0076-6879(95)48015-3

Říhová, J., Nováková, E., Husník, F., and Hypša, V. (2017). Legionella Becoming a Mutualist: Adaptive Processes Shaping the Genome of Symbiont in the Louse Polyplax Serrata. *Genome Biol. Evol.* 9, 2946–2957. doi: 10.1093/gbe/evx217

Rolain, J. M., Maurin, M., Vestris, G., and Raoult, D. (1998). *In Vitro* Susceptibilities of 27 Rickettsiae to 13 Antimicrobials. *Antimicrob. Agents Chemother.* 42, 1537–1541. doi: 10.1128/AAC.42.7.1537

Ross, B. D., Hayes, B., Radey, M. C., Lee, X., Josek, T., Bjork, J., et al. (2018). Ixodes Scapularis Does Not Harbor a Stable Midgut Microbiome. *ISME J.* 12, 2596–2607. doi: 10.1038/s41396-018-0161-6

Ruhe, Z. C., Subramanian, P., Song, K., Nguyen, J. Y., Stevens, T. A., Low, D. A., et al. (2018). Programmed Secretion Arrest and Receptor-Triggered Toxin Export During Antibacterial Contact-Dependent Growth Inhibition. *Cell* 175, 921–933.e14. doi: 10.1016/J.CELL.2018.10.033/ATTACHMENT/98B0A2F7-BB29-42E7-8C39-7312137CD8F5/MMC1.PDF

Sanchez-Vicente, S., Tagliafierro, T., Coleman, J. L., Benach, J. L., and Tokarz, R. (2019). Polymicrobial Nature of Tick-Borne Diseases. *MBio* 10, 1–17. doi: 10.1128/mBio.02055-19

Schulz, F., Martijn, J., Wascher, F., Lagkouvardos, I., Kostanjšek, R., Ettema, T. J. G., et al. (2016). A Rickettsiales Symbiont of Amoebae With Ancient Features. *Environ. Microbiol.* 18, 2326–2342. doi: 10.1111/1462-2920.12881

Simser, J. A., Palmer, A. T., Fingerle, V., Wilske, B., Kurtti, T. J., and Munderloh, U. G. (2002). Rickettsia Monacensis Sp. Nov., a Spotted Fever Group Rickettsia, From Ticks (Ixodes Ricinus) Collected in a European City Park. *Appl. Environ. Microbiol.* 68, 4559–4566. doi: 10.1128/AEM.68.9.4559-4566.2002

Stamatakis, A. (2014). RAxML Version 8: A Tool for Phylogenetic Analysis and Post-Analysis of Large Phylogenies. *Bioinformatics* 30, 1312–1313. doi: 10.1093/bioinformatics/btu033

Stamatakis, A., Ludwig, T., and Meier, H. (2005). RAxML-III: A Fast Program for Maximum Likelihood-Based Inference of Large Phylogenetic Trees. *Bioinformatics* 21, 456–463. doi: 10.1093/bioinformatics/bti191

Steiner, F. E., Pinger, R. R., Vann, C. N., Grindle, N., Civitello, D., Clay, K., et al. (2008). Infection and Co-Infection Rates of <I>Anaplasma Phagocytophilum</I> Variants, <I>Babesia</I> Spp., <I>Borrelia Burgdorferi</I>, and the Rickettsial Endosymbiont in <I>Ixodes Scapularis</I> (Acari: Ixodidae) From Sites in Indiana, Maine, Pennsylvania, and. *J. Med. Entomol.* 45, 289–297. doi: 10.1603/0022-2585(2008)45[289:iacroa]2.0.co;2

Stenos, J., Graves, S. R., and Unsworth, N. B. (2005). A Highly Sensitive and Specific Real-Time PCR Assay for the Detection of Spotted Fever and Typhus Group Rickettsiae. *Am. J. Trop. Med. Hyg.* 73, 1083–1085. doi: 10.4269/ajtmh.2005.73.1083

Swanson, K. I., and Norris, D. E. (2007). Co-Circulating Microorganisms in Questing Ixodes Scapularis Nymphs in Maryland. *J. Vector Ecol.* 32, 243. doi: 10.3376/1081-1710(2007)32[243:cmiqis]2.0.co;2

Talavera, G., and Castresana, J. (2007). Improvement of Phylogenies After Removing Divergent and Ambiguously Aligned Blocks From Protein Sequence Alignments. *Syst. Biol.* 56, 564–577. doi: 10.1080/10635150701472164

Thapa, S., Zhang, Y., and Allen, M. S. (2019). Bacterial Microbiomes of Ixodes Scapularis Ticks Collected From Massachusetts and Texas, USA. *BMC Microbiol.* 19, 1–12. doi: 10.1186/s12866-019-1514-7

Tokarz, R., Tagliafierro, T., Sameroff, S., Cucura, D. M., Oleynik, A., Che, X., et al. (2019). Microbiome Analysis of Ixodes Scapularis Ticks From New York and Connecticut. *Ticks Tick Borne Dis.* 10, 894–900. doi: 10.1016/j.ttbdis.2019.04.011

Troughton, D. R., and Levin, M. L. (2007). Life Cycles of Seven Ixodid Tick Species (Acari: Ixodidae) Under Standardized Laboratory Conditions. *J. Med. Entomol.* 44, 732–740. doi: 10.1093/jmedent/44.5.732

van Treuren, W., Ponnusamy, L., Brinkerhoff, R. J., Gonzalez, A., Parobek, C. M., Juliano, J. J., et al. (2015). Variation in the Microbiota of Ixodes Ticks With Regard to Geography, Species, and Sex. *Appl. Environ. Microbiol.* 81, 6200–6209. doi: 10.1128/AEM.01562-15

Walker, D. H., and Ismail, N. (2008). Emerging and Re-Emerging Rickettsioses: Endothelial Cell Infection and Early Disease Events. *Nat. Rev. Microbiol.* 6, 375–386. doi: 10.1038/nrmicro1866

Weyer, K., Boldt, H. B., Poulsen, C. B., Kjaer-Sorensen, K., Gyrup, C., and Oxvig, C. (2007). A Substrate Specificity-Determining Unit of Three Lin12-Notch Repeat Modules Is Formed in Trans Within the Pappalysin-1 Dimer and Requires a Sequence Stretch C-Terminal to the Third Module *. *J. Biol. Chem.* 282, 10988–10999. doi: 10.1074/JBC.M607903200

Willett, J. L. E., Ruhe, Z. C., Goulding, C. W., Low, D. A., and Hayes, C. S. (2015). Contact-Dependent Growth Inhibition (CDI) and CdiB/CdiA Two-Partner Secretion Proteins. *J. Mol. Biol.* 427, 3754–3765. doi: 10.1016/J.JMB.2015.09.010

Wormser, G. P., Dattwyler, R. J., Shapiro, E. D., Halperin, J. J., Steere, A. C., Klempner, M. S., et al. (2006). The Clinical Assessment, Treatment, and Prevention of Lyme Disease, Human Granulocytic Anaplasmosis, and Babesiosis: Clinical Practice Guidelines by the Infectious Diseases Society of America. *Clin. Infect. Dis.* 43, 1089–1134. doi: 10.1086/508667

Wright, C. L., Sonenshine, D. E., Gaff, H. D., and Hynes, W. L. (2015). Rickettsia Parkeri Transmission to Amblyomma Americanum by Cofeeding With Amblyomma Maculatum (Acari: Ixodidae) and Potential for Spillover. *J. Med. Entomol.* 52, 1090–1095. doi: 10.1093/JME/TJV086

Yang, Q., Kučerová, Z., Perlman, S. J., Opit, G. P., Mockford, E. L., Behar, A., et al. (2015). Morphological and Molecular Characterization of a Sexually Reproducing Colony of the Booklouse Liposcelis Bostrychophila (Psocodea: Liposcelididae) Found in Arizona. *Sci. Rep.* 5, 10429. doi: 10.1038/srep10429

Yeats, C., Bentley, S., and Bateman, A. (2003). New Knowledge From Old: In Silico Discovery of Novel Protein Domains in Streptomyces Coelicolor. *BMC Microbiol.* 3, 1–20. doi: 10.1186/1471-2180-3-3/FIGURES/13

Zeng, Z., Fu, Y., Guo, D., Wu, Y., Ajayi, O. E., and Wu, Q. (2018). Bacterial Endosymbiont Cardinium Csfur Genome Sequence Provides Insights for Understanding the Symbiotic Relationship in Sogatella Furcifera Host. *BMC Genomics* 19, 688. doi: 10.1186/s12864-018-5078-y

Zhang, D., Iyer, L. M., and Aravind, L. (2011). A Novel Immunity System for Bacterial Nucleic Acid Degrading Toxins and Its Recruitment in Various Eukaryotic and DNA Viral Systems. *Nucleic Acids Res.* 39, 4532–4552. doi: 10.1093/NAR/GKR036

Zolnik, C. P., Prill, R. J., Falco, R. C., Daniels, T. J., and Kolokotronis, S. O. (2016). Microbiome Changes Through Ontogeny of a Tick Pathogen Vector. *Mol. Ecol.* 25, 4963–4977. doi: 10.1111/MEC.13832

Author Disclaimer: The content is solely the responsibility of the authors and does not necessarily represent the official views of the funding agencies.

Conflict of Interest: The authors declare that the research was conducted in the absence of any commercial or financial relationships that could be construed as a potential conflict of interest.

Publisher's Note: All claims expressed in this article are solely those of the authors and do not necessarily represent those of their affiliated organizations, or those of the publisher, the editors and the reviewers. Any product that may be evaluated in this article, or claim that may be made by its manufacturer, is not guaranteed or endorsed by the publisher.

frontiers | Frontiers in Cellular and Infection Microbiology

ORIGINAL RESEARCH
published: 26 May 2022
doi: 10.3389/fcimb.2022.902492

Chlamydia trachomatis Requires Functional Host-Cell Mitochondria and NADPH Oxidase 4/p38MAPK Signaling for Growth in Normoxia

*Jeewan Thapa[1], Gen Yoshiiri[2], Koki Ito[2], Torahiko Okubo[2], Shinji Nakamura[3], Yoshikazu Furuta[4], Hideaki Higashi[4] and Hiroyuki Yamaguchi[2]**

[1] Division of Bioresources, International Institute for Zoonosis Control, Hokkaido University, Sapporo, Japan, [2] Department of Medical Laboratory Science, Faculty of Health Sciences, Hokkaido University, Sapporo, Japan, [3] Laboratory of Morphology and Image Analysis, Research Support Center, Juntendo University Graduate School of Medicine, Tokyo, Japan, [4] Division of Infection and Immunity, International Institute for Zoonosis Control, Hokkaido University, Sapporo, Japan

OPEN ACCESS

Edited by:
Luís Jaime Mota, NOVA School of Science and Technology, Portugal

Reviewed by:
Yimou Wu, University of South China, China
Nadja Käding, University Medical Center Schleswig-Holstein, Germany

***Correspondence:**
Hiroyuki Yamaguchi
hiroyuki@med.hokudai.ac.jp

Specialty section:
This article was submitted to Bacteria and Host, a section of the journal Frontiers in Cellular and Infection Microbiology

Received: *23 March 2022*
Accepted: *22 April 2022*
Published: *26 May 2022*

Citation:
Thapa J, Yoshiiri G, Ito K, Okubo T, Nakamura S, Furuta Y, Higashi H and Yamaguchi H (2022) Chlamydia trachomatis Requires Functional Host-Cell Mitochondria and NADPH Oxidase 4/p38MAPK Signaling for Growth in Normoxia. Front. Cell. Infect. Microbiol. 12:902492. doi: 10.3389/fcimb.2022.902492

Chlamydia trachomatis (Ct) is an intracellular energy-parasitic bacterium that requires ATP derived from infected cells for its growth. Meanwhile, depending on the O_2 concentration, the host cells change their mode of ATP production between oxidative phosphorylation in mitochondria (Mt) and glycolysis; this change depends on signaling *via* reactive oxygen species (ROS) produced by NADPH oxidases (NOXs) as well as Mt. It has been proposed that Ct correspondingly switches its source of acquisition of ATP between host-cell Mt and glycolysis, but this has not been verified experimentally. In the present study, we assessed the roles of host-cell NOXs and Mt in the intracellular growth of CtL2 (L2 434/Bu) under normoxia (21% O_2) and hypoxia (2% O_2) by using several inhibitors of NOXs (or the downstream molecule) and Mt-dysfunctional (Mt^d) HEp-2 cells. Under normoxia, diphenyleneiodonium, an inhibitor of ROS diffusion, abolished the growth of CtL2 and other Chlamydiae (CtD and *C. pneumoniae*). Both ML171 (a pan-NOX inhibitor) and GLX351322 (a NOX4-specific inhibitor) impaired the growth of CtL2 under normoxia, but not hypoxia. NOX4-knockdown cells diminished the bacterial growth. SB203580, an inhibitor of the NOX4-downstream molecule p38MAPK, also inhibited the growth of CtL2 under normoxia but not hypoxia. Furthermore, CtL2 failed to grow in Mt^d cells under normoxia, but no effect was observed under hypoxia. We conclude that under normoxia, Ct requires functional Mt in its host cells as an ATP source, and that this process requires NOX4/p38MAPK signaling in the host cells. In contrast to hypoxia, crosstalk between NOX4 and Mt *via* p38MAPK may be crucial for the growth of Ct under normoxia.

Keywords: *Chlamydia trachomatis*, mitochondria, normoxia, hypoxia, NADPH oxidase, NOX4, p38MAPK

INTRODUCTION

The obligate intracellular bacterium *Chlamydia trachomatis* (Ct), which is an energy parasite, is the leading cause of bacterial sexually transmitted infections, with an estimated 131 million new cases of infection annually worldwide (O'Connell and Ferone, 2016). The normal O_2 concentration at the infection site is around 5% (Juul et al., 2007), and Ct also provokes an inflammatory response that consumes O_2, resulting in hypoxia (Eltzschig and Carmeliet, 2011). Ct clearly favors hypoxia, and activates phosphatidylinositol-3 kinase (PI3K)/protein kinase B (AKT) in its host, which prompts glycolysis (Rupp et al., 2007; Thapa et al., 2020). However, Ct can grow well in host cells regardless of O_2 conditions (Shima et al., 2011; Jerchel et al., 2014; Thapa et al., 2020).

Ct matures in infected host cells *via* a unique developmental cycle consisting of an infectious form (the elementary body, EB) and a replicating form (the reticular body) (Cossé et al., 2018). The successful maturation of Ct occurs in a customized plasma membrane, referred to as an inclusion body (Elwell et al., 2016); sufficient ATP is critical for the maturation. Because Ct possesses an incomplete tricarboxylic acid cycle (Tipples and McClarty, 1993; Harris et al., 2012), the maturation of Ct in the host cells absolutely relies on a stable supply of ATP derived from the host regardless of O_2 conditions. However, the mechanism by which Ct acquires ATP from infected cells regardless of the O_2 concentration is not well understood.

Mitochondria (Mt) are the main power plant in eukaryotic cells, responsible for generating ATP in an O_2-dependent manner (Sousa et al., 2018). However, when O_2 levels become low, the cells shift ATP production from Mt to glycolysis (Lunt and Vander Heiden, 2011). The molecular mechanism responsible for the switch is gradually becoming clear from research into cancer cells, and reactive oxygen species (ROS) generated by NADPH oxidases (NOXs) as well as Mt are a key factor (Kang et al., 2015; Phadwal et al., 2021). Specifically, studies have demonstrated that changes in the amount of ROS in the cells play a crucial role in switching cellular signals between p38MAPK signaling, which is responsible for the stabilization of Mt (Corbi et al., 2013), and AKT signaling, which is responsible for the activation of glycolysis (Xie et al., 2019; Kim et al., 2020; Vaupel and Multhoff, 2021). Furthermore, crosstalk between NOXs and Mt *via* p38MAPK has been proposed to be a crucial mechanism for prompting survival processes such as angiogenesis and tissue repair demanded more energy ATP (Fukai and Ushio-Fukai, 2020), which presumably also supports the intracellular growth of Ct under normoxia. However, the roles of Mt and NOXs in the intracellular growth of Ct and its response to O_2 concentration and the associated signals have not yet been verified. Moreover, it has not yet been determined whether Ct in infected cells requires Mt as the site of ATP acquisition depending on O_2 condition.

In the present study, we thus compared the roles of NOXs and Mt in the intracellular growth of Ct under normoxia (21% O_2) and hypoxia (2% O_2) by using Mt-dysfunctional (Mt^d) human epithelial (HEp-2) cells and several inhibitors of NOXs and p38MAPK, which is a NOX4-related molecule.

Abbreviations: Ct, *Chlamydia trachomatis*; Cp, *Chlamydia pneumoniae*; Mt, mitochondria; NOX, NADPH oxidase; DPI, diphenyleneiodonium; AKT, protein kinase B; EB, elementary body; ROS, reactive oxygen species; q, quantitative; RT, reverse transcription; PCR, polymerase chain reaction; EtBr, ethidium bromide; TEM, transmission electron microscopy; GFP, green fluorescent protein; TBS-T, Tris-buffered saline and 0.1% Tween 20.

RESULTS AND DISCUSSION

Cytotoxicity of the Inhibitors Used, Expression Levels of NOXs, and the Effect of Diphenyleneiodonium on the Growth of Chlamydiae

Four inhibitors were used in this study—they block the diffusion of ROS (DPI) (Iacovino et al., 2020), or the activation of NOXs or related molecules (ML171, pan-NOXs; GLX351322, a NOX4 specific inhibitor; and SB203580, a p38MAPK-specific inhibitor) (Zhou et al., 2010; Cifuentes-Pagano et al., 2012; Anvari et al., 2015). No cytotoxicity of DPI, ML171, GLX351322, and SB203580 on HEp-2 cells was seen at ≤5 nM, ≤20 μM, ≤20 μM, and ≤20 μM, respectively (**Figure 1**). On the basis of these results, the inhibitors were used in our experiments at a concentration where no cytotoxicity was observed. Next, the expression levels of NOXs in the immortal human epithelial (HEp-2) cells used were examined by quantitative (q) reverse transcription (RT)-polymerase chain reaction (PCR). The expression level of NOX4 was the highest among the NOXs, at least 10 times that of the other NOXs (**Figure S1A**), indicating that, among NOXs, NOX4 could play the most important role in the growth of Ct. Furthermore, the effect of DPI on the growth of other chlamydiae [CtL2 (267, see *Methods*) and CtD (D/UW3/CX)] was assessed by using qPCR targeting the Ct *16S rDNA* gene. DPI significantly suppressed the growth of the Ct in a similar way (**Figure S1B**), indicating that Ct relies on ROS derived form NOXs for growth *via* a mechanism that might be conserved.

Although DPI at low concentrations suppressed the growth of various Chlamydiae, at ≥10 nM it showed strong cytotoxicity toward HEp-2 cells. DPI not only suppresses the activity of various NOXs (Iacovino et al., 2020) but also strongly inhibits the activities of cytochrome P-450 reductase (Chakraborty and Massey, 2002), xanthine oxidase (Sanders et al., 1997), nitric oxide synthase (Stuehr et al., 1991), and NADH-ubiquinone oxidoreductase (Majander et al., 1994). Overall, such pleiotropic effects are considered to be the cause of the strong cytotoxicity. Therefore, experiments with more selective inhibitors are needed to validate the role of NOXs in chlamydial intracellular growth.

As noted above, we found high expression of NOX4 in HEp-2 cells compared with that of other NOXs (**Figure S1B**). This result was consistent with the previous finding that, in contrast to other NOXs, NOX4 is highly expressed in cellular membrane in vascular cells or endothelial cells (Ago et al., 2004; Griendling, 2004). NOX4 is constitutively active, involving the control of cytoskeletal integrity (Lyle et al., 2009; Nisimoto, 2010), required for the growth of Ct. Furthermore, NOX4-dependent ROS is involved in many physiological functions, including immune

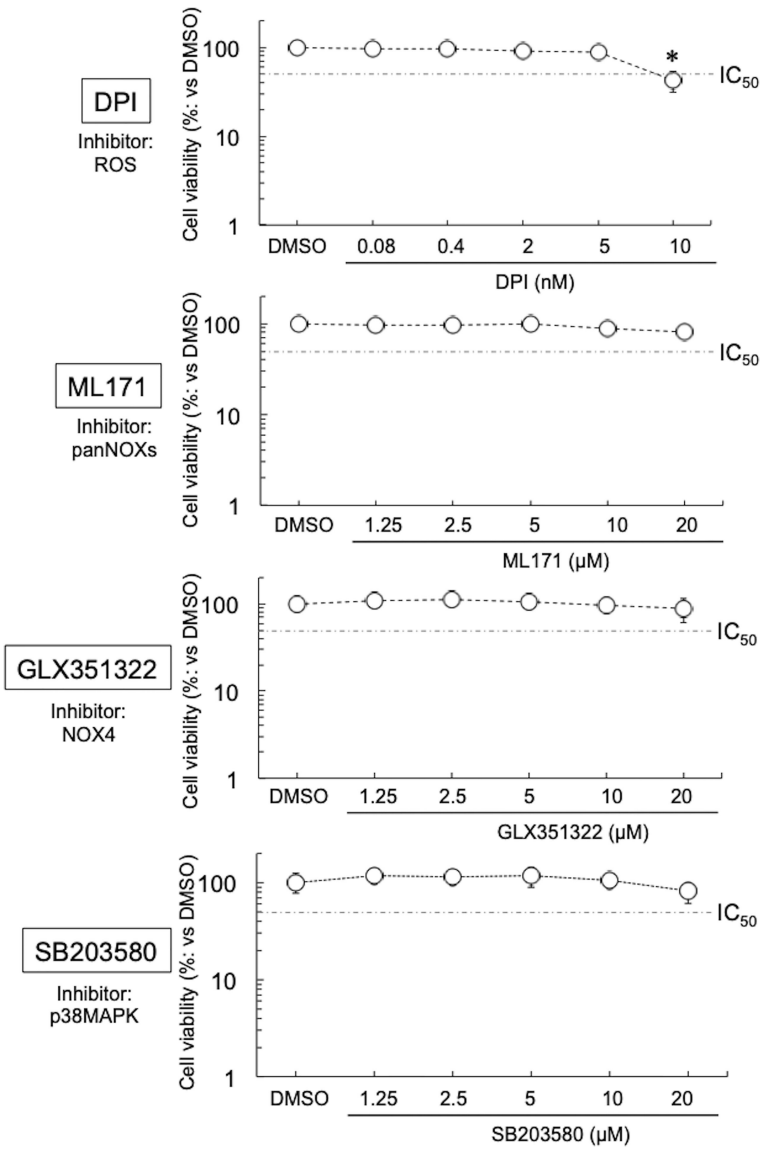

FIGURE 1 | Viability of HEp-2 cells in the presence of inhibitors (DPI, ML171, GLX351322, and SB203580). The cells were cultured with or without inhibitor for 24 h, and then the cell viabilities were assessed using Cell Counting Kit-8 (see *Methods*). Data show means ± SD (n = 6) as a relative value of the cell-only (dimethylsulfoxide-treated) viability (which is defined as 100%). *$p < 0.05$ *vs*. dimethylsulfoxide-treated. Dotted lines show IC_{50} values.

host defense and the activation of multiple cellular signaling pathways such as SAPK/JNK, ERK1/2, and p38MAPK, which are responsible for ATP energy production *via* Mt) (Irani, 2000). Some of these pathways have already been reported to be targets of Ct (Shima et al, 2011; Jerchel et al., 2014; Thapa et al., 2020). Thus, we hypothesized that NOX4 is one of the targets of Ct for its successful intracellular growth under normoxia; if so, that would impact the production of ROS from NOXs as well as Mt.

CtL2 Uses NOX4/p38MAPK Signaling for Its Growth Under Normoxia

To test this hypothesis, the effect of more specific NOX inhibitors (ML171 and GLX351322) on the growth of CtL2 under normoxia (21% O_2) and hypoxia (2% O_2) was compared. In contrast to hypoxia, both inhibitors significantly inhibited the growth of CtL2 under normoxia in a concentration-dependent manner (**Figure S2** and **Figure 2**). The growth of CtL2 was also significantly suppressed in NOX4-knockdown cells treated with small interfering RNA (siRNA) against NOX4 under normoxia (**Figure S3**). Thus, NOX4 clearly plays a crucial role in the growth of Ct under normoxia, but not under hypoxia. Next, the role of p38MAPK, which is a NOX4-related molecule (Corbi et al., 2013), on the growth of CtL2 was assessed using a p38MAPK-specific inhibitor, SB203580. Similar to the effects of ML171 and GLX351322, the presence of SB203580 significantly diminished the intracellular growth of CtL2 under

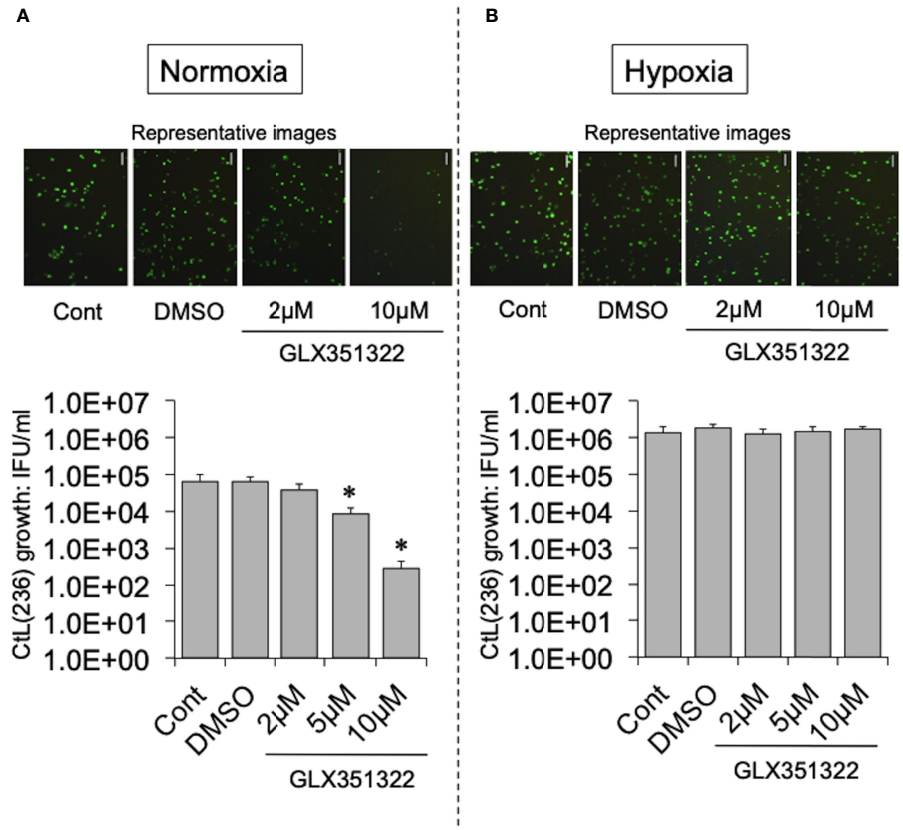

FIGURE 2 | Effect of NOX4-specific inhibitor GLX351322 on the intracellular growth of green fluorescent protein (GFP)-expressing CtL2 (236) under normoxia **(A)** and hypoxia **(B)**. HEp-2 cells were infected at a multiplicity of infection (MOI) = 5 with GFP-expressing CtL2 (236) in the presence or absence of the drug, and cultured for 48 h. Representative images show inclusion bodies (green) formed in infected HEp-2 cells. Bars = 100 μm. The number of bacteria was calculated by inclusion-forming unit (IFU) assay of infected cells cultured for 48 h. Data show means ± SD obtained from at least three experiments. *$p < 0.05$ vs. the value for each control (Cont).

normoxia, but not under hypoxia (**Figure 3**). Thus, as expected, our findings indicated that CtL2 relies on NOX4/p38MAPK signaling for its growth under normoxia, but not under hypoxia.

As supported by several studies (Irani, 2000; Basuroy et al., 2011; Lee et al., 2014; Ribeiro-Pereira et al., 2014; Beretta et al., 2020), NOX4-dependent ROS has an important role as second messengers associated with cellular survival under normoxia. The mechanism involves the stabilization of mitochondrial function, which is responsible for the stable supply of ATP, *via* cross-talk between NOX4 and Mt (Dan Dunn et al., 2015). The exposure of cells to ROS can activate p38MAPK, which is a NOX4-related molecule (Bedard and Krause, 2007). Thus, ROS may play an important role in the requirement of NOX/p38MAPK for the intracellular growth of CtL2 under normoxia.

The inhibitors ML171, GLX351322, and SB203580, however, had no effect on the growth of Ct under hypoxia. Unlike under normoxia, the energy source of Ct in low O_2 conditions is ATP produced by glycolysis in the infected host cells following the activation of PI3K/AKT (Jerchel et al., 2014; Lavu et al., 2020; Thapa et al., 2020) In fact, several studies have reported that Ct activates PI3K, which regulates glycolysis, by phosphorylating AKT (Zou et al., 2019; Thapa et al., 2020; Huang et al., 2021).

CtL2 Relies on Host-Cell Mt for its Growth Under Normoxia, but Not Under Hypoxia

According to a previous report (Yu et al., 2007), Mt^d-HEp-2 cells were successfully established by the passage of HEp-2 cells for 6 months in the presence of ethidium bromide (EtBr) at low concentration (50 ng/ml) with subsequent cloning (**Figure S4A**); five strains (P52-B3, P52-B10, P52-C7, P52-E2, P52-H8) were established. The mitochondrial genome consists of 37 genes, including tRNAs (Nicholls and Minczuk, 2014). The Mt^d-HEp-2 cells that we generated had lost the *D-loop*, which is associated with replication of the mitochondrial genome, and *COXII*, which encodes a component of respiratory chain Complex IV (**Figure S4B**). Compared with HEp-2 cells without EtBr exposure, the amounts of NADH and NADPH significantly increased in the Mt^d-HEp-2 cells under normoxia, indicating an activation of aerobic glycolysis, referred to as the Warburg effect (**Figure S4C**) (Vaupel and Multhoff, 2021). Confocal laser fluorescence imaging and transmission electron microscopy (TEM) observations

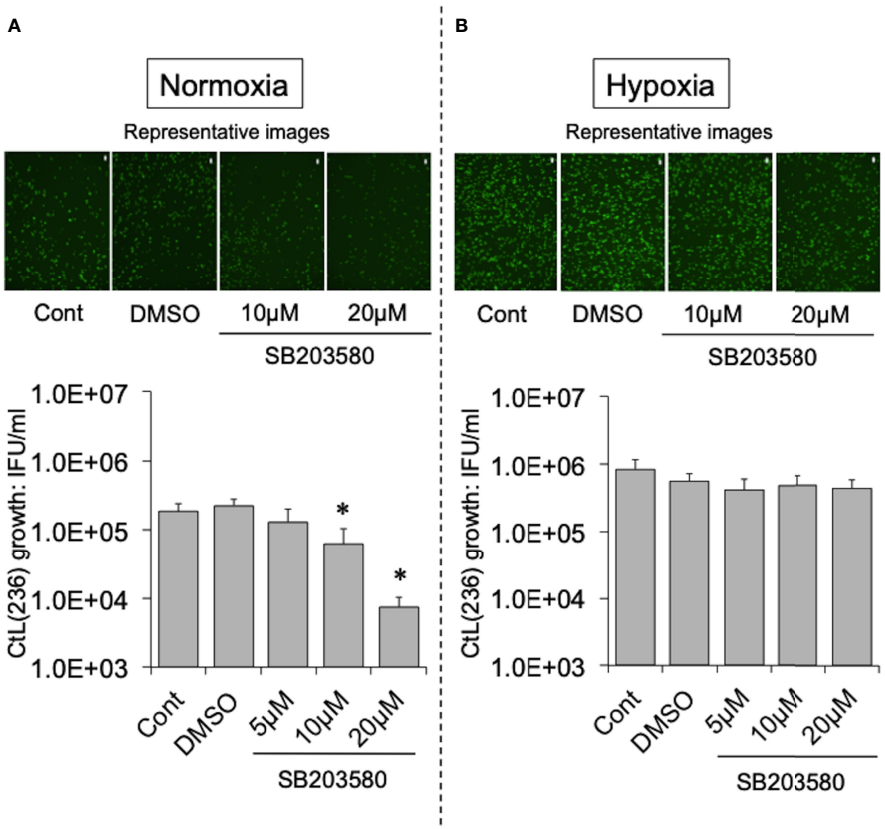

FIGURE 3 | Effect of NOX4-downstream molecule p38MAPK-specific inhibitor SB203580 on the intracellular growth of GFP-expressing CtL2 (236) under normoxia **(A)** and hypoxia **(B)**. The HEp-2 cells were infected at MOI = 5 with GFP-expressing CtL2 (236) in the presence or absence of the drug, and cultured for 48 h. Representative images show inclusion bodies (green) formed in infected HEp-2 cells. Bars = 200 μm. The number of bacteria was calculated by IFU assay of infected cells cultured for 48 h. Data show means ± SD obtained from at least three experiments. *$p < 0.05$ vs. the value of each control (Cont).

revealed that in Mt^d-HEp-2 cells, the Mt swelled (**Figure 4A**), corresponding to the observations in the previous report (Yu et al., 2007) (**Figure 4B**). Together, these findings showed that in Mt^d-HEp-2 cells, the Mt became dysfunctional, indicating that this cell line was a useful tool for verifying the effects of Mt on the intracellular growth of Ct. Under normoxia, Ct growth was significantly inhibited in Mt^d-HEp-2 cells; under hypoxia, there was no growth inhibition (**Figure 5**). Thus, under normoxia, Ct relies on functional Mt as a source of ATP, consisting with the previous studies showing the presence of crosstalk between Ct metabolism and mitochondria (Szaszák et al., 2011; Chowdhury and Rudel, 2017).

EtBr selectively binds to DNA and its accumulation causes mutations and deletions in DNA (Hayashi et al., 1994). The damage to DNA is more pronounced in mitochondrial DNA, whose repair mechanism is fragile, compared with genomic (nuclear) DNA. Thus, the application of EtBr can selectively induce cells with dysfunctional Mt (Yu et al., 2007; Luo et al., 2013). As expected, the Hep-2 cells serially passaged with EtBr exposure here showed morphological changes of the Mt and the Warburg effect. We therefore concluded that Mt^d-HEp-2 cells were successfully established (Yu et al., 2007). Meanwhile, subculture of the cells in the absence of EtBr for >1 week decreased the amount of NADH and NADPH (data not shown), which showed restoration of normal mitochondrial function, indicating that not all of the Mt in the cells were completely dysfunctional. However, because the culture period of the infected cells without EtBr in our experiments was only 2 days, the effect of mitochondrial restoration was minimal.

Although no difference was observed under hypoxia, under normoxia, the growth of Ct in Mt^d-HEp-2 cells was significantly decreased compared with that in the parental HEp-2 cells. This finding indicates that under normoxia, Ct relies on Mt as its source of ATP. We also found that NOX4/p38MAPK signaling, which is involved in the control of mitochondrial function (Bedard and Krause, 2007; Dan Dunn et al., 2015), plays a critical role in the intracellular growth of Ct under normoxia. Furthermore, it is evident that the amounts of ROS generated from NOXs is increased under normoxia compared with hypoxia (Basuroy et al., 2011; Lee et al., 2014; Ribeiro-Pereira et al., 2014; Beretta et al., 2020), and crosstalk between NOXs and Mt has been proposed to be a crucial mechanism for cellular survival (Fukai and Ushio-Fukai, 2020), as well as being responsible for maintaining a stable supply of ATP to Ct. Thus, under normoxia,

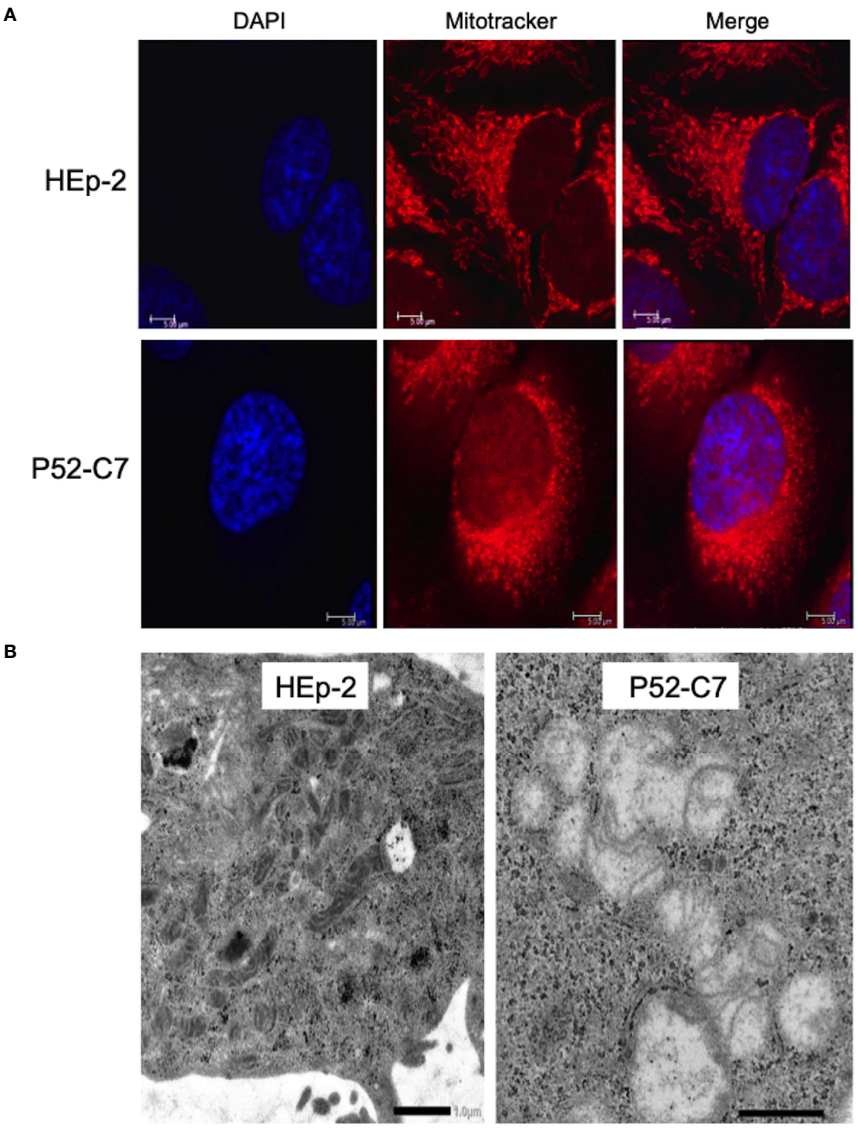

FIGURE 4 | Morphological features of mitochondria (Mt) in HEp-2 cells with or without ethidium bromide exposure. **(A)** Representative confocal laser microscopy images showing the localization and morphology of Mt in Mt^{d}-HEp-2 (P52-C7) cells and parental HEp-2 cells stained using MitoTracker (see *Methods*). Bars = 5 μm. **(B)** Representative transmission electron microscopy images showing the detailed morphology of Mt in Mt^{d}-HEp-2 (P52-C7) cells and parental HEp-2 cells. Scale bars = 1 μm.

Ct require functional Mt with the activation of NOX4/p38MAPK signaling, presumably *via* ROS as a second messenger. Crosstalk between NOX4 and Mt *via* p38MPAK may be crucial for supporting the intracellular growth of Ct in the presence of O_2.

Under hypoxia, Ct obtains ATP from glycolysis by the activation of PI3K/AKT signaling (Zou et al., 2019; Thapa et al., 2020; Huang et al., 2021). We therefore speculate that Ct switches its energy source between Mt and glycolysis in response to change in the ATP-production site in the infected cells, which in turn depends on the cellular O_2 concentration. We also expect that Ct modifies host cell signaling using effector molecules that are injected into the cytoplasm *via* the type III secretion system (Dai and Li, 2014). Meanwhile, further study is needed to verify this in detail and to establish the switching mechanism and effectors. Also, there was a limitation of the used cell line producing ATP mainly *via* glycolysis that should be addressed by additional experiments.

CONCLUSIONS

In contrast to hypoxia, CtL2 requires functional Mt with NOX4/p38MAPK-mediated signaling for its growth under normoxia. Crosstalk between NOX4 and Mt *via* p38MAPK may be crucial for the growth of Ct under normoxia. These findings provide novel insight into the complicated biology and pathogenesis of *Chlamydia*.

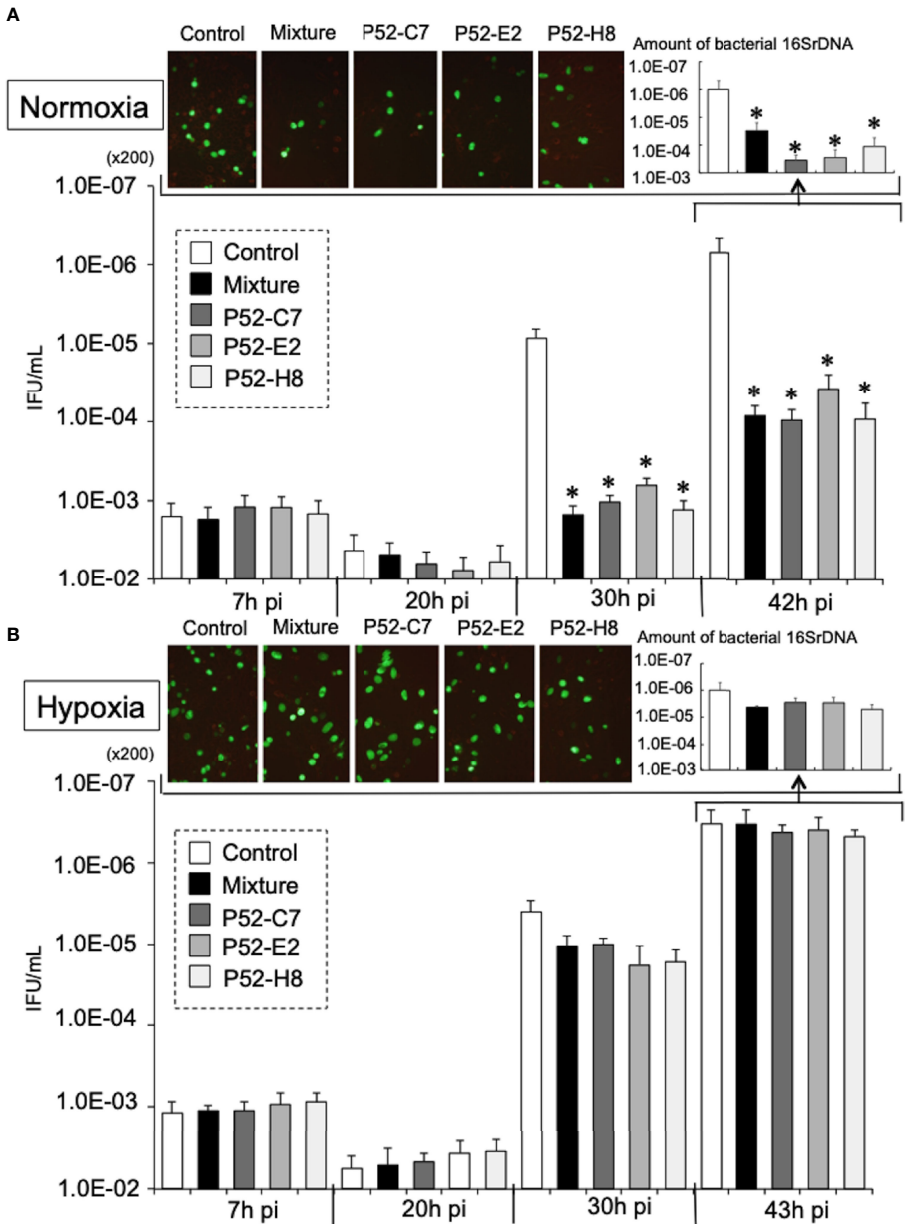

FIGURE 5 | Growth kinetics of GFP-expressing CtL2 (236) in Mt^{d}-HEp-2 (P52-C7, P52-E2, P52-H8) cells and parental HEp-2 cells under normoxia **(A)** and hypoxia **(B)**. The cells were infected with GFP-expressing CtL2 (236) at MOI = 5 and then cultured for 48 h under normoxia or hypoxia. Bacterial numbers were determined at 7, 20, 30, and 43 h by IFU assay and qPCR. Magnification for images, ×200. The quantities of chlamydial *16S rDNA* were normalized to that of *β-actin*. Data show the means ± SD obtained from at least three experiments. *$p < 0.05$ vs. the value of each control (white bar).

METHODS

Bacteria and Human Cells

Chlamydiae [CtL2 (L2 434/Bu) and CtD (D/UW3/CX)] and immortal human epithelial HEp-2 cells were used for this study. The bacteria were propagated into HEp-2 cells in Dulbecco's Modified Eagle's Medium (Sigma, Burlington, MA) containing 10% fetal calf serum and antibiotics (10 μg/ml gentamicin, 10 μg/ml vancomycin, and 1 μg/ml amphotericin B) at 37°C under normoxia, and then stored at −80°C, according to a previously described protocol (Thapa et al., 2020). CtL2 were transformed using green fluorescent protein (pGFP)::SW2 with a promoter (p) derived from *Neisseria meningitidis* replaced with p-CT236 (hypothetical gene) or p-CT267 (hypothetical gene), both of which can bind more efficiently to the ribosome (as determined using a ribosome binding site calculator) than the original promoter (Howard, 2011), according to the protocol for chlamydial transformation (Bauler and Hackstadt, 2014).

Establishment of Mt^d-HEp-2 Cells

As shown in **Figure S4A**, Mt^d-HEp-2 cells (P52-B3, P52-B10, P52-C7, P52-E2, and P52-H8) were established by the passage of HEp-2 cells for 6 months in the presence of EtBr (50 ng/ml) with supplements [sodium pyruvate (100 μg/ml) and uridin (50 ng/ml)] and subsequent cloning with a limited dilution method, according to previous report (Yu et al., 2007). The dysfunctional state of Mt was confirmed by the loss of two genes (*D-loop* and *COXII*) from the mitochondrial genome by qPCR, increased amounts of NADH/NADPH (aerobic glycolysis, Warburg effect), and changed mitochondrial morphology (see below).

Establishment of NOX4-Knockdown Cells

Transient NOX4-knockdown HEp-2 cells were established by 24-h transfection of cells with NOX4 siRNA (sc-41586; Santa Cruz Bio). Non-targeting scramble RNA (sc-37007; Santa Cruz Bio) was used as a control. Transfection of siRNA (or scramble RNA) into cells was performed with Lipofectamine™ RNAiMAX Transfection Reagent (Thermo Fisher), according to the manufacturer's protocol. The amount of the complex brought into the culture system was 250 μl [Cont-siRNA (250) and NOX4-siRNA (250)] or 50 μl [Cont-siRNA (50) and NOX4-siRNA (50)] (see **Figure S3**).

Assessing Inclusion-Forming Units

The number of infectious progeny (EB) was determined as IFU by counting chlamydial inclusion bodies formed in epithelial cells using a fluorescein isothiocyanate-conjugated anti-chlamydial monoclonal antibody specific to *Chlamydia* lipopolysaccharide (Denka Seiken, Tokyo, Japan), as described previously (Thapa et al., 2020). Cells were observed using an Olympus culture microscope, model CKX41.

Infection and Culture

Cells were infected at an appropriate multiplicity of infection (MOI) with Ct (some expressing GFP as described above) or Cp, and then cultured in 10% FCS-RPMI medium with or without inhibitors of NOXs [DPI (anti-ROS: 0.4-10 nM), ML171 (anti-NOXs: 2-10 μM), GLX351322 (anti-NOX4: 2-10 μM), or SB203580 (anti-p38MAPK: 2.5-10 μM)] for 48 h under normoxia (21% O_2) or hypoxia (2% O_2). Hypoxia was established using a dedicated MIC-101 chamber (Billups-Rothenberg) to which mixed gas containing 2% O_2, 5% CO_2, and 93% N_2 was supplied, as previously described (Thapa et al., 2020). O_2 conditions were continuously monitored using an oxygen meter.

Assessing Amounts of NADH and NADPH

The total amounts of NADH/NADPH in cultures were quantified by using the Cell Counting Kit-8 (Dojindo), according to the manufacturer's protocol. The values were calculated from measurements of $OD_{450\ nm}$.

Imaging of Mt

Cells were stained with MitoTracker® Red CMXRos, and then fixed with 4% paraformaldehyde in phosphate-buffered saline (PBS), following the manufacturer's protocol (Cell Signaling). The stained cells were observed using a confocal laser fluorescence microscope (TCSSP5, Leica) or a conventional fluorescence microscope (BZX800, Keyence). Furthermore, infected cells were fixed using 3% glutaraldehyde in PBS. The cells were immersed in alcohol for dehydration after washing with PBS and then embedded in Epon 813. Ultrathin sections were obtained and stained with lead citrate and uranium acetate, followed by TEM observation (JEM-1400Flash, JEOL Ltd.), as described previously (Matsuo et al., 2008).

DNA and RNA Extraction

Total DNAs and RNAs were extracted from cells using an Instagene kit (Bio-Rad, Hercules) and High Pure RNA Isolation Kit (Roche), respectively, following the manufacturers' protocols. The reverse transcription of total RNA to cDNA was performed with ReverTraAce qPCR RT Master Mix (Toyobo).

Quantitative PCR

Amplifications of DNA or cDNA were quantified by CFX Connect (Bio-Rad) with SYBR Green (KOD SYBR qPCR Mix, TOYOBO) targeting *D-loop* (forward: 5′- CCT GTC CTT GTA GTA TAA AC -3′; reverse: 5′- TTG AGG AGG TAA GCT ACA T -3′) (Yu et al., 2007), *COXII* (forward: 5′- TTC ATG ATC ACG CCC TCA TA -3′; reverse: 5'- CGG GAA TTG CAT CTG TTT TTA -3') (Yu et al., 2007), chlamydial *16S rDNA* (forward: 5′-CGG CGT GGA TGA GGC AT-3′; reverse: 5′-TCA GTC CCA GTG TTG GC-3′), or *β-actin* (forward: 5′- GAC CAC ACC TAC AAT GAG -3′; reverse: 5′- GCA TAC CCC TCG TAG GG -3′) (Ishida et al., 2014). The quantities of *D-loop*, *COXII*, and chlamydial *16SrDNA* were normalized to that of *β-actin*.

Western Blotting

Cells were lysed in RIPA buffer containing 0.1% sodium dodecyl sulfate (SDS; Nacalai Tesque). The proteins in each sample were separated by 8% SDS-polyacrylamide gel electrophoresis. The separated proteins were transferred to a polyvinylidene difluoride membrane by semi-dry electroblotting using the Trans-Blot® Turbo™ blotting system (Bio-Rad). After blocking with 3% skim milk in Tris-buffered saline and 0.1% Tween 20 (TBS-T), membranes were incubated with primary antibody [anti-NOX4 (Abcam): ×2000; anti-tubulin (Santa Cruz Bio): ×2000] overnight at 4°C. After washing with TBS-T, membranes were incubated with secondary antibody for 4–6 h at 4°C. After washing, membranes were developed with Clarity™ Western ECL substrate (Bio-Rad) and visualized using a Chemi Doc™ XRS (Bio-Rad).

Statistical Analyses

Comparisons among group values were performed by using the Bonferroni/Dunn test. A p-value of < 0.05 was considered statistically significant.

DATA AVAILABILITY STATEMENT

The original contributions presented in the study are included in the article/**Supplementary Material**. Further inquiries can be directed to the corresponding author.

AUTHOR CONTRIBUTIONS

HY conceived and designed the study. JT, GY, KI, and TO performed the laboratory work. JT and HY analyzed the data. SN performed imaging. YF, HH, and HY established the GFP-expressing Ct. HY wrote the manuscript with revision by JT. All authors contributed to the article and approved the submitted version.

FUNDING

This study was supported by grants-in-aid from the Japan Society for Scientific Research KAKENHI (Grant numbers: 16H05225 and 21H02726). The funder had no role in the study design, data collection and analysis, decision to publish, or preparation of the manuscript.

ACKNOWLEDGMENTS

We thank Edanz Group (https://jp.edanz.com/ac) for editing a draft of this manuscript.

SUPPLEMENTARY MATERIAL

The Supplementary Material for this article can be found online at: https://www.frontiersin.org/articles/10.3389/fcimb.2022.902492/full#supplementary-material

Supplementary Figure 1 | Gene expression levels of NADPH oxidases (NOXs 1–4) **(A)** and effect of diphenyleneiodonium (DPI; 0.08–5 nM) on the growth of Chlamydiae **(B)**. Gene expression was assessed by quantitative (q) reverse transcription (RT) polymerase chain reaction (PCR), and expressed as a value of $2^{\Delta;\Delta;-Ct}$. The quantities of NOXs were normalized to that of *β-actin*. Data show averages from duplicate experiments. HEp-2 cells were infected at an appropriate multiplicity of infection [MOI; GFP-expressing CtL2 (267) MOI 5; CtD: MOI 5] and cultured for 72 h. The number of bacteria in cultures was then determined by qPCR assay. The quantities of chlamydial *16S rDNA* were normalized to that of *β-actin*. Data show means ± SD from at least three experiments. *$p < 0.05$ *vs*. the value of each positive control (PC).

Supplementary Figure 2 | Effect of ML171 (2 and 10 μM) on the intracellular growth of green fluorescent protein (GFP)-expressing CtL2 (236) in HEp-2 cells under normoxia **(A)** and hypoxia **(B)**. The HEp-2 cells were infected at MOI 5 with CtL2 (236), and then cultured for 48 h. Representative images show inclusion bodies (green) formed in infected HEp-2 cells. Bars = 100 μm. The number of bacteria was calculated by inclusion-forming unit (IFU) assay of infected cells cultured for 48 h. Data show means ± SD from at least three experiments. *$p < 0.05$ *vs*. the value of each PC.

Supplementary Figure 3 | The growth of GFP-expressing CtL2 (236) in NOX4-knockdown HEp-2 cells and confirmation of the NOX4 knockdown by western blotting. Transfected cells were infected with CtL2 (236) for 48 h, and the numbers of IFU were verified. The upper images show inclusion bodies in the knockdown cells [NOX4-siRNA (250)] with Cont-siRNA (250) used as the control (see *Methods*). The graph shows the number of IFU 48 h after infection. Data show means ± SD from five fields per well from a single experiment. *$p < 0.05$ *vs*. each control [Cont-siRNA (250) or Cont-siRNA (50)]. The lower images show the amount of NOX4 protein in the knockdown cells (with α-tubulin used as a loading control).

Supplementary Figure 4 | The establishment of Mt^{d}-HEp-2 cells using ethidium bromide (EtBr). **(A)** Culture schedule of HREp-2 cells in the presence of EtBr. **(B)** The image (left) shows expression levels of the *D-loop* and *COXII* genes in the cells and the graph (right) shows the quantified amount of *COXII* gene expression. **(C)** The image (left) shows color changes indicating the amount of NADH and NADPH in the cells, and the graph (right) shows the amounts of NADH/NADPH in the culture of Mt^{d}-HEp-2 cells. The controls were medium and parental (non-EtBr-treated) HEp-2 cells. *$p < 0.05$ *vs*. parental HEp-2 cells.

REFERENCES

Ago, T., Kitazono, T., Ooboshi, H., Iyama, T., Han, Y. H., Takada, J., et al. (2004). Nox4 as the Major Catalytic Component of an Endothelial NAD(P)H Oxidase. *Circ.* 109, 227–233. doi: 10.1161/01.CIR.0000105680.92873.70

Anvari, E., Wikström, P., Walum, E., and Welsh, N. (2015). The Novel NADPH Oxidase 4 Inhibitor GLX351322 Counteracts Glucose Intolerance in High-Fat Diet-Treated C57BL/6 Mice. *Free Radic. Res.* 49, 1308–1318. doi: 10.3109/10715762.2015.1067697

Basuroy, S., Tcheranova, D., Bhattacharya, S., Leffler, C. W., and Parfenova, H. (2011). Nox4 NADPH Oxidase-Derived Reactive Oxygen Species, via Endogenous Carbon Monoxide, Promote Survival of Brain Endothelial Cells During TNF-Alpha-Induced Apoptosis. *Am. J. Physiol. Cell Physiol.* 300, C256–C265. doi: 10.1152/ajpcell.00272.2010

Bauler, L. D., and Hackstadt, T. (2014). Expression and Targeting of Secreted Proteins From Chlamydia Trachomatis. *J. Bacteriol.* 196, 1325–1334. doi: 10.1128/JB.01290-13

Bedard, K., and Krause, K.-H. (2007). The NOX Family of ROS-Generating NADPH Oxidases: Physiology and Pathophysiology. *Physiol. Rev.* 87, 245–313. doi: 10.1152/physrev.00044.2005

Beretta, M., Santos, C. X., Molenaar, C., Hafstad, A. D., Miller, C. C., Revazian, A., et al. (2020). Nox4 Regulates InsP(3) Receptor-Dependent Ca(2+) Release Into Mitochondria to Promote Cell Survival. *EMBO J.* 39, e103530. doi: 10.15252/embj.2019103530

Chakraborty, S., and Massey, V. (2002). Reaction of Reduced Flavins and Flavoproteins With Diphenyliodonium Chloride. *J. Biol. Chem.* 277, 41507–41516. doi: 10.1074/jbc.M205432200

Chowdhury, S. R., and Rudel, T. (2017). *Chlamydia* and Mitochondria - an Unfragmented Relationship. *Microb. Cell.* 4, 233–235. doi: 10.15698/mic2017.07.582

Cifuentes-Pagano, E., Csanyi, G., and Pagano, P. J. (2012). NADPH Oxidase Inhibitors: A Decade of Discovery From Nox2ds to HTS. *Cell Mol. Life Sci.* 69, 2315–2325. doi: 10.1007/s00018-012-1009-2

Corbi, G., Conti, V., Russomanno, G., Longobardi, G., Furgi, G., Filippelli, A., et al. (2013). Adrenergic Signaling and Oxidative Stress: A Role for Sirtuins? *Front. Physiol.* 4. doi: 10.3389/fphys.2013.00324

Cossé, M. M., Hayward, R. D., and Subtil, A. (2018). One Face of *Chlamydia Trachomatis*: The Infectious Elementary Body. *Curr. Top. Microbiol. Immunol.* 412, 35–58. doi: 10.1007/82_2016_12

Dai, W., and Li, Z. (2014). Conserved Type III Secretion System Exerts Important Roles in Chlamydia Trachomatis. *Int. J. Clin. Exp. Pathol.* 7, 5404–5414.

Dan Dunn, J., Alvarez, L. A., Zhang, X., and Soldati, T. (2015). Reactive Oxygen Species and Mitochondria: A Nexus of Cellular Homeostasis. *Redox. Biol.* 6, 472–485. doi: 10.1016/j.redox.2015.09.005

Eltzschig, H. K., and Carmeliet, P. (20112011). Hypoxia and Inflammation. *N. Engl. J. Med.* 364, 656–665. doi: 10.1056/NEJMra0910283

Elwell, C., Mirrashidi, K., and Engel, J. (2016). Chlamydia Cell Biology and Pathogenesis. *Nat. Rev. Microbiol.* 14, 385–400. doi: 10.1038/nrmicro.2016.30

Fukai, T., and Ushio-Fukai, M. (2020). Cross-Talk Between NADPH Oxidase and Mitochondria: Role in ROS Signaling and Angiogenesis. *Cells.* 9, 1849. doi: 10.3390/cells9081849

Griendling, K. K. (2004). Novel NAD(P)H Oxidases in the Cardiovascular System. *Heart.* 90, 491–493. doi: 10.1136/hrt.2003.029397

Harris, S. R., Clarke, I. N., Seth-Smith, H. M., Solomon, A. W., Cutcliffe, L. T., Marsh, P., et al. (2012). Whole-Genome Analysis of Diverse Chlamydia

Trachomatis Strains Identifies Phylogenetic Relationships Masked by Current Clinical Typing. *Nat. Genet.* 244 (4), 413–419, S1. doi: 10.1038/ng.2214

Hayashi, J., Takemitsu, M., Goto, Y., and Nonaka, I. (1994). Human Mitochondria and Mitochondrial Genome Function as a Single Dynamic Cellular Unit. *J. Cell Biol.* 125, 43–50. doi: 10.1083/jcb.125.1.43

Howard, M. S. (2011). Chapter Two-The Ribosome Binding Site Calculator. *Methods Enzymol.* 498, 19–42. doi: 10.1016/B978-0-12-385120-8.00002-4

Huang, X., Tan, J., Chen, X., Liu, M., Zhu, H., Li, W., et al. (2021). Akt Phosphorylation Influences Persistent Chlamydial Infection and Chlamydia-Induced Golgi Fragmentation Without Involving Rab14. *Front. Cell Infect. Microbiol.* 11. doi: 10.3389/fcimb.2021.675890

Iacovino, L. G., Reis, J., Mai, A., Binda, C., and Mattevi, A. (2020). Diphenylene Iodonium Is a Noncovalent MAO Inhibitor: A Biochemical and Structural Analysis. *ChemMedChem.* 15, 1394–1397. doi: 10.1002/cmdc.202000264

Irani, K. (2000). Oxidant Signaling in Vascular Cell Growth, Death, and Survival : A Review of the Roles of Reactive Oxygen Species in Smooth Muscle and Endothelial Cell Mitogenic and Apoptotic Signaling. *Circ. Res.* 87, 179–183. doi: 10.1161/01.res.87.3.179

Ishida, K., Matsuo, J., Yamamoto, Y., and Yamaguchi, H. (2014). *Chlamydia Pneumoniae* Effector Chlamydial Outer Protein N Sequesters Fructose Bisphosphate Aldolase A, Providing a Benefit to Bacterial Growth. *BMC Microbiol.* 14, 330. doi: 10.1186/s12866-014-0330-3

Jerchel, S., Kaufhold, I., Schuchardt, L., Shima, K., and Rupp, J. (2014). Host Immune Responses After Hypoxic Reactivation of IFN-Gamma Induced Persistent *Chlamydia Trachomatis* Infection. *Front. Cell Infect. Microbiol.* 4. doi: 10.3389/fcimb.2014.00043

Juul, N., Jensen, H., Hvid, M., Christiansen, G., and Birkelund, S. (2007). Characterization of *In Vitro* Chlamydial Cultures in Low-Oxygen Atmospheres. *J. Bacteriol.* 189, 6723–6726. doi: 10.1128/JB.00279-07

Kang, S. W., Lee, S., and Lee, E. K. (2015). ROS and Energy Metabolism in Cancer Cells: Alliance for Fast Growth. *Arch. Pharm. Res.* 38 (3), 338–345. doi: 10.1007/s12272-015-0550-6

Kim, N. H., Sung, N. J., Youn, H. S., and Park, S. A. (2020). Gremlin-1 Activates Akt/STAT3 Signaling, Which Increases the Glycolysis Rate in Breast Cancer Cells. *Biochem. Biophys. Res. Commun.* 533, 1378–1384. doi: 10.1016/j.bbrc.2020.10.025

Lavu, N., Richardson, L., Bonney, E., and Menon, R. (2020). Glycogen Synthase Kinase (GSK) 3 in Pregnancy and Parturition: A Systematic Review of Literature. *J. Matern Fetal Neonatal Med.* 33, 1946–1957. doi: 10.1080/14767058.2018.1531843

Lee, J. E., Cho, K. E., Lee, K. E., Kim, J., and Bae, Y. S. (2014). Nox4-Mediated Cell Signaling Regulates Differentiation and Survival of Neural Crest Stem Cells. *Mol. Cells* 37, 907–911. doi: 10.14348/molcells.2014.0244

Lunt, S. Y., and Vander Heiden, M. G. (2011). Aerobic Glycolysis: Meeting the Metabolic Requirements of Cell Proliferation. *Annu. Rev. Cell Dev. Biol.* 27, 441–464. doi: 10.1146/annurev-cellbio-092910-154237

Luo, Y., Hu, Y., Zhang, M., Xiao, Y., Song, Z., and Xu, Y. (2013). EtBr-Induced Selective Degradation of Mitochondria Occurs *via* Autophagy. *Oncol. Rep.* 30, 1201–1208. doi: 10.3892/or.2013.2590

Lyle, A. N., Deshpande, N. N., Taniyama, Y., and Seidel-Rogol, B. (2009). Poldip2, a Novel Regulator of Nox4 and Cytoskeletal Integrity in Vascular Smooth Muscle Cells. *Circ. Res.* 105, 249–259. doi: 10.1161/CIRCRESAHA.109.193722

Majander, A., Finel, M., and Wikström, M. (1994). Diphenyleneiodonium Inhibits Reduction of Iron-Sulfur Clusters in the Mitochondrial NADH-Ubiquinone Oxidoreductase (Complex I). *J. Biol. Chem.* 269, 21037–21042. doi: 10.1016/S0021-9258(17)31926-9

Matsuo, J., Hayashi, Y., Nakamura, S., Sato, M., Mizutani, Y., Asaka, M., et al. (2008). Novel *Parachlamydia Acanthamoebae* Quantification Method Based on Coculture With Amoebae. *Appl. Environ. Microbiol.* 74, 6397–6404. doi: 10.1128/AEM.00841-08

Nicholls, T. J., and Minczuk, M. (2014). In D-Loop: 40 Years of Mitochondrial 7S DNA. *Exp. Gerontol* 56, 175–181. doi: 10.1016/j.exger.2014.03.027

Nisimoto, Y., Jackson, H. M., Ogawa, H., Kawahara, T., and Lambeth, J. D. (2010). Constitutive NADPH-Dependent Electron Transferase Activity of the Nox4 Dehydrogenase Domain. *Biochem.* 49, 2433–2442. doi: 10.1021/bi9022285

O'Connell, C. M., and Ferone, M. E. (2016). *Chlamydia Trachomatis* Genital Infections. *Microb. Cell.* 3, 390–403. doi: 10.15698/mic2016.09.525

Phadwal, K., Vrahnas, C., Ganley, I. G., and MacRae, V. E. (2021). Mitochondrial Dysfunction: Cause or Consequence of Vascular Calcification? *Front. Cell Dev. Biol.* 9. doi: 10.3389/fcell.2021.611922

Ribeiro-Pereira, C., Moraes, J. A., Souza Mde, J., Laurindo, F. R., Arruda, M. A., and Barja-Fidalgo, C. (2014). Redox Modulation of FAK Controls Melanoma Survival–Role of NOX4. *PLos One* 9, e99481. doi: 10.1371/journal.pone.0099481

Rupp, J., Gieffers, J., Klinger, M., van Zandbergen, G., Wrase, R., Maass, M., et al. (2007). *Chlamydia Pneumoniae* Directly Interferes With HIF-1alpha Stabilization in Human Host Cells. *Cell Microbiol.* 9, 2181–2191. doi: 10.1111/j.1462-5822.2007.00948.x

Sanders, S. A., Eisenthal, R., and Harrison, R. (1997). NADH Oxidase Activity of Human Xanthine Oxidoreductase–Generation of Superoxide Anion. *Eur. J. Biochem.* 245, 541–548. doi: 10.1111/j.1432-1033.1997.00541.x

Shima, K., Szaszák, M., Solbach, W., Gieffers, J., and Rupp, J. (2011). Impact of a Low-Oxygen Environment on the Efficacy of Antimicrobials Against Intracellular Chlamydia Trachomatis. *Antimicrob. Agents Chemother.* 55, 2319–2324. doi: 10.1128/AAC.01655-10

Sousa, J. S., D'Imprima, E., and Vonck, J. (2018). Mitochondrial Respiratory Chain Complexes. *Subcell Biochem.* 87, 167–227. doi: 10.1007/978-981-10-7757-9_7

Stuehr, D. J., Fasehun, O. A., Kwon, N. S., Gross, S. S., Gonzalez, J. A., Levi, R., et al. (1991). Inhibition of Macrophage and Endothelial Cell Nitric Oxide Synthase by Diphenyleneiodonium and its Analogs. *FASEB J.* 5, 98–103. doi: 10.1096/fasebj.5.1.1703974

Szaszák, M., Steven, P., Shima, K., Orzekowsky-Schröder, R., Hüttmann, G., König, I. R., et al. (2011). Fluorescence Lifetime Imaging Unravels C. Trachomatis Metabolism and its Crosstalk With the Host Cell. *PLos Pathog.* 7, e1002108. doi: 10.1371/journal.ppat.1002108

Thapa, J., Hashimoto, K., Sugawara, S., Tsujikawa, R., Okubo, T., Nakamura, S., et al. (2020). Hypoxia Promotes *Chlamydia Trachomatis* L2/434/Bu Growth in Immortal Human Epithelial Cells *via* Activation of the PI3K-AKT Pathway and Maintenance of a Balanced NAD(+)/NADH Ratio. *Microbes Infect.* 22, 441–450. doi: 10.1016/j.micinf.2020.04.010

Tipples, G., and McClarty, G. (1993). The Obligate Intracellular Bacterium *Chlamydia Trachomatis* is Auxotrophic for Three of the Four Ribonucleoside Triphosphates. *Mol. Microbiol.* 8, 1105–1114. doi: 10.1111/j.1365-2958.1993.tb01655.x

Vaupel, P., and Multhoff, G. (2021). Revisiting the Warburg Effect: Historical Dogma Versus Current Understanding. *J. Physiol.* 599, 1745–1757. doi: 10.1113/JP278810

Xie, Y., Shi, X., Sheng, K., Han, G., Li, W., Zhao, Q., et al. (2019). PI3K/Akt Signaling Transduction Pathway, Erythropoiesis and Glycolysis in Hypoxia (Review). *Mol. Med. Rep.* 19, 783–791. doi: 10.3892/mmr.2018.9713

Yu, M., Shi, Y., Wei, X., Yang, Y., Zhou, Y., Hao, X., et al. (2007). Depletion of Mitochondrial DNA by Ethidium Bromide Treatment Inhibits the Proliferation and Tumorigenesis of T47D Human Breast Cancer Cells. *Toxicol. Lett.* 170, 83–93. doi: 10.1016/j.toxlet.2007.02.013

Zhou, W. D., Yang, H. M., Wang, Q., Su, D. Y., Liu, F. A., Zhao, M., et al. (2010). SB203580, a P38 Mitogen-Activated Protein Kinase Inhibitor, Suppresses the Development of Endometriosis by Down-Regulating Proinflammatory Cytokines and Proteolytic Factors in a Mouse Model. *Hum. Reprod.* 25, 3110–3116. doi: 10.1093/humrep/deq287

Zou, Y., Lei, W., Su, S., Bu, J., Zhu, S., Huang, Q., et al. (2019). *Chlamydia Trachomatis* Plasmid-Encoded Protein Pgp3 Inhibits Apoptosis *via* the PI3K-AKT-Mediated MDM2-P53 Axis. *Mol. Cell Biochem.* 452, 167–176. doi: 10.1007/s11010-018-3422-9

Conflict of Interest: The authors declare that the research was conducted in the absence of any commercial or financial relationships that could be construed as a potential conflict of interest.

Publisher's Note: All claims expressed in this article are solely those of the authors and do not necessarily represent those of their affiliated organizations, or those of the publisher, the editors and the reviewers. Any product that may be evaluated in this article, or claim that may be made by its manufacturer, is not guaranteed or endorsed by the publisher.

frontiers | Frontiers in Cellular and Infection Microbiology

ORIGINAL RESEARCH
published: 26 May 2022
doi: 10.3389/fcimb.2022.828605

Anaplasma phagocytophilum Ankyrin A Protein (AnkA) Enters the Nucleus Using an Importin-β-, RanGTP-Dependent Mechanism

Yuri Kim[1,2], *Jianyang Wang*[1,2], *Emily G. Clemens*[1], *Dennis J. Grab*[1] *and J. Stephen Dumler*[1]*

[1] Department of Pathology, Uniformed Services University of the Health Sciences, Bethesda, MD, United States, [2] Henry M. Jackson Foundation for the Advancement of Military Medicine, Bethesda, MD, United States

OPEN ACCESS

Edited by:
Isaura Simões, University of Coimbra, Portugal

Reviewed by:
Jason A. Carlyon, Virginia Commonwealth University, United States
Sean Phillip Riley, University of Maryland, College Park, United States

***Correspondence:**
J. Stephen Dumler
john.dumler@usuhs.edu

Specialty section:
This article was submitted to Bacteria and Host, a section of the journal Frontiers in Cellular and Infection Microbiology

Received: *03 December 2021*
Accepted: *20 April 2022*
Published: *26 May 2022*

Citation:
Kim Y, Wang J, Clemens EG, Grab DJ and Dumler JS (2022) Anaplasma phagocytophilum Ankyrin A Protein (AnkA) Enters the Nucleus Using an Importin-β-, RanGTP-Dependent Mechanism. Front. Cell. Infect. Microbiol. 12:828605. doi: 10.3389/fcimb.2022.828605

Anaplasma phagocytophilum, a tick-borne obligately intracellular bacterium of neutrophils, causes human granulocytic anaplasmosis. Ankyrin A (AnkA), an effector protein with multiple ankyrin repeats (AR) is injected via type IV-secretion into the host neutrophil to gain access to the nucleus where it modifies the epigenome to promote microbial fitness and propagation. AR proteins transported into the host cell nucleus must use at least one of two known eukaryotic pathways, the classical importin β-dependent pathway, and/or the RanGDP- and AR (ankyrin-repeat)-dependent importin β-independent (RaDAR) pathway. Truncation of the first four AnkA N-terminal ARs (AR1-4), but not other regions, prevents AnkA nuclear accumulation. To investigate the mechanism of nuclear import, we created point mutations of AnkA N-terminal ARs, predicted to interfere with RaDAR protein import, and used importazole, a specific inhibitor of the importin α/β, RanGTP-dependent pathway. Nuclear colocalization analysis shows that nuclear localization of AnkA is unaffected by single AR1-4 mutations but is significantly reduced by single mutations in consecutive ARs suggesting RaDAR protein nuclear import. However, AnkA nuclear localization was also decreased with importazole, and with GTPγS. Furthermore, *A. phagocytophilum* growth in HL-60 cells was completely suppressed with importazole, indicating that *A. phagocytophilum* propagation requires a β-importin-dependent pathway. A typical classical NLS overlapping AR4 was subsequently identified suggesting the primacy of the importin-α/β system in AnkA nuclear localization. Whether the mutational studies of putative key residues support RaDAR NLS function or simply reflect structural changes that diminish engagement of an AR-NLS-importin pathway needs to be resolved through careful structure-function studies.

Keywords: *Anaplasma phagocytophilum*, AnkA, ankyrin repeat proteins, nuclear localization signal, RaDAR

INTRODUCTION

Anaplasma phagocytophilum is an obligately intracellular bacterium that colonizes human neutrophil vacuoles and is the causative agent of human granulocytic anaplasmosis, an emerging immunomodulatory tick-borne disease among humans (Bakken and Dumler, 2015). *A. phagocytophilum* utilizes type IV-secretion system effector protein ankyrin A (AnkA), which gains access to the infected neutrophil nucleus where it binds DNA, to epigenetically modify chromatin structure and transcriptional programs (Park et al., 2004; Lin et al., 2007; Garcia-Garcia et al., 2009a; Garcia-Garcia et al., 2009b; Rennoll-Bankert et al., 2015; Rikihisa, 2017; Bierne and Pourpre, 2020). This protein contains approximately 1230 amino acids, for which sequences and length vary by strain. AnkA also accumulates in the nucleus of infected cells (Garcia-Garcia et al., 2009b). As the protein's name implies, the characteristic feature of AnkA is the presence of 8-15 ankyrin repeats (ARs), depending on the strain, a structural motif found in several hundred proteins across broad classes of eukaryotes and prokaryotes, that mediate diverse functions, such as protein-protein, protein-DNA, and protein-lipid interactions (Caturegli et al., 2000; Pan et al., 2008; Jernigan and Bordenstein, 2014; Islam et al., 2018). The AR is a conserved amino acid sequence containing approximately 33 residues which is characterized by two α-helices with 8-10 residues each connected with a β-loop. AnkA interacts with host DNA at multiple genomic sites where chromatin alterations occur leading to changes in transcriptional programs (Dumler et al., 2016); however, the mechanism of how AnkA accesses the nucleus is yet to be revealed.

We previously showed that truncation of the first four N-terminal ARs prevents nuclear accumulation of AnkA, suggesting their importance in nuclear transport (Rennoll-Bankert et al., 2015). A common mechanism of large protein-facilitated nuclear transport involves binding of importin-β and RanGDP to cargo protein in the cytoplasm, allowing the protein to cross the nuclear pore complex and to be released after RanGTP/RanGDP exchange inside the nucleus (Cavazza and Vernos, 2016). The concentration gradients of RanGDP and RanGTP across the nuclear membrane are critical for nuclear shuttling of the RanGDP/RanGTP, importin-β and cargo bound to importin-α *via* classical nuclear localization sequences, and are supported by the cytoplasmic RanGTPase-activating protein (RanGAP) and nuclear Ran guanine nucleotide exchange factor (RanGEF) (Lu et al., 2021).

For a group of human ankyrin repeat proteins (ARPs), importation into nucleus occurs due to hydrophobic residues, in particular leucine, isoleucine, phenylalanine, or cysteine at the 13th position of two consecutive ARs at positions that interact with and bind RanGDP by an importin-independent mechanism (RaDAR) (Lu et al., 2014). While the precise 3D structure of AnkA ARs is not yet resolved, the four N-terminal ARs within the N-terminal region that is important for nuclear accumulation of AnkA have motifs similar to those in humans that utilize importin-independent, RanGDP-dependent (RaDAR) nuclear import (Rennoll-Bankert et al., 2015). Here, we tested whether ARs of *A. phagocytophilum* AnkA have similar requirements in nuclear accumulation as for human ARPs or whether nuclear localization is importin-dependent. While mutations of the 13th residues of two consecutive ARs indeed disrupts nuclear import of AnkA and requires RanGTP, nuclear localization and *A. phagocytophilum* propagation were dependent on β-importin, confirming the essential nature of the importin α/β pathway for AnkA nuclear entry and *A. phagocytophilum* propagation.

RESULTS

Single AnkA Mutations of N-Terminal ARs Do Not Prevent Nuclear Accumulation

To test that *A. phagocytophilum* AnkA is transported into the nucleus *via* the RaDAR mechanism (Lu et al., 2014), and noting that the 13th positions in AR1 and AR2 do not comply with the hydrophobic residue hypothesis, we used recombinant eGFP-tagged AnkA proteins with single mutations to alter hydrophobicity at the 13th position of N-terminal ARs 1, 2, 3 and 4 (**Figure 1** and **Supplementary Figure 1**).

Compared to wild type AnkA, none of single mutations at the 13th position of ARs 1-4 reduced AnkA nuclear localization, while nuclear localization for the AR4 AnkA.M228R mutant was significantly lower than AnkA.R56A (p=0.049), and either AnkA.G157A (p=<0.001) or G157R (p<0.031), as well as

```
AR1(44-74)    EGRTLLHYAASSRNFYGILVGRGCVTNIK
AR2(145-176)  KGHGVLHLACIEGSDPSFTSSLMLKGCSLNIKD
AR3(178-214)  DGNTPLHTAASSVGKNALGNLDVLCDKALIADVNAKG
AR4(216-247)  GGNTPLHIATERMDHQKVKHLLSRLSDISVAN
```

FIGURE 1 | Amino acid sequences of N-terminal ankyrin repeats (AR) of *A. phagocytophilum* AnkA (WP_020849331.1). Point mutation of the amino acid at 13th position tested for each AR in the study is marked in red. In AR1 the hydrophilic Arg was replaced with hydrophobic Ala (AnkA.R56A) or neutral/aliphatic Gly (AnkA.R56G). In AR2 the neutral/aliphatic Gly was replaced with hydrophobic Ala (AnkA.G157A) or hydrophilic Arg (AnkA.G157R). In AR3 the hydrophobic Val was replaced with hydrophilic Asn (AnkA.V190N) and in AR4 the hydrophobic Met was replaced with hydrophilic Arg (AnkA.M228R). Numbers in brackets show location of the corresponding ARs in full-length AnkA protein of *A. phagocytophilum* Webster^{T} strain. For proper alignment, the lysine-histidine pair conserved in all ARs is marked in green.

AnkA.V190N (p=0.031) (**Figure 2**). Interestingly, when the non-polar, achiral hydrophobic amino acid glycine at position 13 in AR2 was replaced with alanine, a more hydrophobic residue (AnkA.G157A), a significant increase in nuclear localization of AnkA was observed. None of the single mutants was predicted to create any structural change sufficient to damage protein function (**Supplementary Figure 2**). The unpredictable behavior on nuclear localization with these unintentional residue changes at seemingly non-critical AR positions suggests the importance of preserving the structural integrity of the N-terminal ARs. This unintentional discovery resulted when several mutants created in preliminary studies were examined for impact on nuclear localization, but after sequencing were discovered to have incorrect residue changes, substitutions or inadvertent additional mutations (**Supplementary Table 1**). Although nuclear localization studies were conducted using these mutants prior to sequence analyses, sequencing did not identify any of the proposed single mutations in this group. However, double mutations were identified to include AnkA.[R56A]; [T162A] (positions 13 in AR1 and 18 in AR2, respectively), which resulted in reduced nuclear localization, and in AnkA.[N57S]; [T162A] (position 14 in AR1 and position 18 in AR2, respectively), which did not localize to the nucleus. Similarly, mutations in non-sequential ARs 1 and 3, AnkA.[R56A (position 13 in AR1)]; AnkA.[R56A]; [L183I] (positions 13 in AR1 and 6 in AR3) did not alter nuclear localization, but the non-sequential mutant that included positions 14 in AR1 and 13 in AR4 (AnkA.[N57S];[M228A] and N57S) did localize to the nucleus. Two other sequential mutants AnkA.[N57S]; [T162A]; [V190A] (positions AR1 14, AR2 18, and AR3 13, respectively), and AnkA.[T162A]; [V190A] reduced nuclear localization (**Supplementary Table 1**). Because of the inaccurate placement of these mutations for assessment of RaDAR function, none were used for primary analyses.

To investigate the potential structural impact of the individual mutations on the putative binding regions in ARs 1-4, the N-terminal 300 residues of wild type AnkA were modeled using Phyre 2 (Kelley et al., 2015). The top hit was 4RLV (RCSG Protein Data Bank) encoded as Ank1 (*Mus musculus*) and ANK2 (*Homo sapiens*). The crystal structure of 4RLV was determined to comprise 24 ANK repeats when complexed with its AnkR-specific auto-inhibitory segment (Wang et al., 2014). The alignment of 4RLV to the N-terminal 300 residues of AnkA identified with 287 residues (96% of AnkA N-terminal sequence) created a model with 100.0% confidence and 31% identity at a 3.49 Å resolution. The AnkA model aligned the first AnkA AR with AR2 of 4RVL, the second AnkA AR with AR5 of 4RVL, followed by a 499-residue gap and alignment of the third and fourth AnkA ARs with AR21 and AR22 of 4RVL, respectively (**Supplementary Figures 2–4**). The modeled AnkA structure demonstrated the specific locations of the 13th residue mutations at the loops between α helices in predicted AnkA ARs. Impacts of mutations at these sites were also estimated to be negligible or absent using Missense3D and Phyre2 Run Investigator (**Supplementary Figure 4**). However, individual residue changes outside of the AR hydrophobic fold that centers on residue 13 are predicted to have potentially significant structural impacts (**Supplementary Table 2**).

Single-Mutations of Two Consecutive N-Terminal ARs Reduces Nuclear Localization of AnkA

In contrast to the inability of AnkA mutations in single ARs to inhibit nuclear localization, mutations in two consecutive ARs significantly decreased nuclear localization of mutant eGFP-AnkAs as demonstrated for AR mutation combinations AR1/AR2, AR2/AR3 and AR3/AR4 (**Figure 3**). While residue changes in AR1 and AR2 would not provide a dramatic reduction in

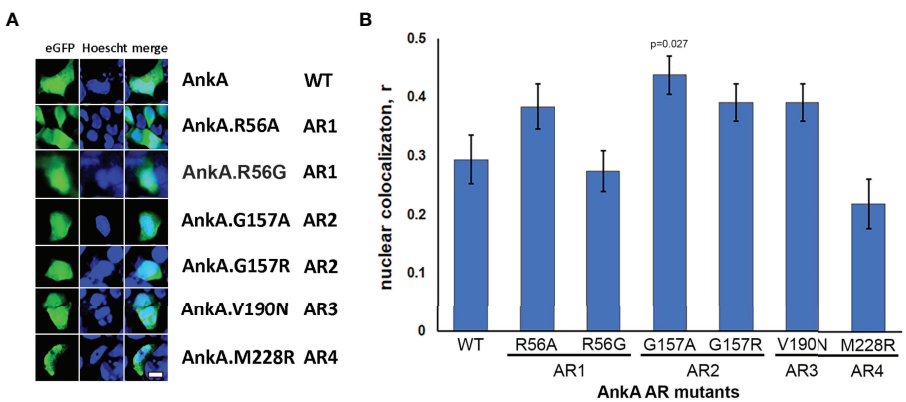

FIGURE 2 | Single mutations of N-terminal ankyrin repeats did not reduce nuclear localization of AnkA. HEK293 cells were transfected with eGFP plasmid constructs of wild-type AnkA or AnkA N-terminal ankyrin repeats 1, 2, 3 and 4 with point mutations, as described in Experimental Procedures. After 48 hours, the cells were fixed, washed, stained with cell-permeable nuclear label Hoescht33342 (Hoescht) and visualized with fluorescent microscopy. **(A)** Representative images of cells transfected with eGFP-AnkA and ankyrin repeat mutants of eGFP-AnkA. **(B)** Statistical analysis of nuclear colocalization of AnkA mutants with nuclear staining relative to wild type AnkA. Data are mean ± SEM, n=20-40 of randomly selected ROIs (region of interest) containing 120-200 transfected cells. ANOVA *post hoc* Bonferroni corrected p values <0.05 relative to wild type AnkA are shown. Bar – 20 μm.

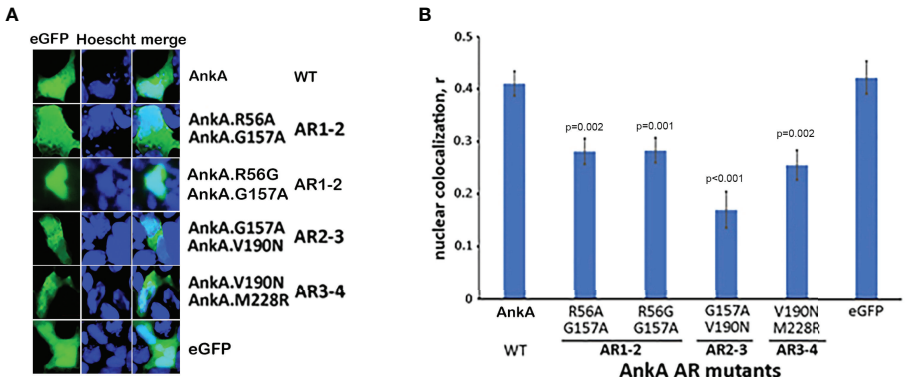

FIGURE 3 | Single mutations in two adjacent N-terminal ARs significantly reduce nuclear localization of AnkA. HEK293T cells were transfected with eGFP plasmid constructs of AnkA or AnkA AR mutants in which two neighboring ankyrin repeats 1 & 2, 2 & 3 or 3 & 4 (AR1-2, AR2-3, AR3-4) had a single amino acid replacement. After fixing and washing, the cell nuclei were stained with Hoescht33342 and visualized with fluorescent microscopy. **(A)** Representative images of cells with eGFP-AnkA and dual-mutated ankyrin repeats are shown. **(B)** Nuclear colocalization of AnkA and mutants were determined by using the colocalization module of Olympus CellSense software. Data shown are mean ± SEM of Pearson correlation coefficient, r, from 20-40 ROIs containing 100-200 transfected cells of two independent experiments in duplicate. ANOVA *post hoc* Bonferroni corrected p values <0.05 relative to wild type AnkA are shown. Bar-20 μm.

hydrophobicity at the 13 position, and the changes in AR3 (AnkA.V190N) and AR4 (AnkA.M228R) would, these data demonstrate that pairs of adjacent N-terminal ARs could play a role in nuclear translocation of AnkA, similar to that seen in the eukaryotic RaDAR system (Lu et al., 2014).

AnkA Is Transported by an Importin-β, RanGTP-Dependent Mechanism

To investigate whether nuclear import of AnkA is mediated by the importin α/β pathway, we utilized importazole, a specific inhibitor of importin-β/RanGTP interaction (Soderholm et al., 2011), and GTPγS (guanosine 5'-O-[gamma-thio]triphosphate), a non-or slowly-hydrolysable GTP analog. We expected that the small molecule, cell-permeable importazole would interfere with importin-β/RanGDP transport across nuclear membrane, and its use should not alter nuclear localization if the RaDAR system was important. Additionally, we anticipated that loading cells with GTPγS would result in a rise of RanGTP concentration in the cytoplasm by suppressing activity of RanGTPase-activating protein (RanGAP). This would in turn block RanGTP/RanGDP shuttling across the nuclear membrane and thus import of AnkA - important in both importin α/β and RaDAR nuclear transport. We found that transfection of recombinant eGFP-AnkA into HEK293T cells that were separately loaded with importazole-β or GTPγS, resulted in significant reductions of AnkA nuclear localization (**Figure 4**). Moreover, when used with

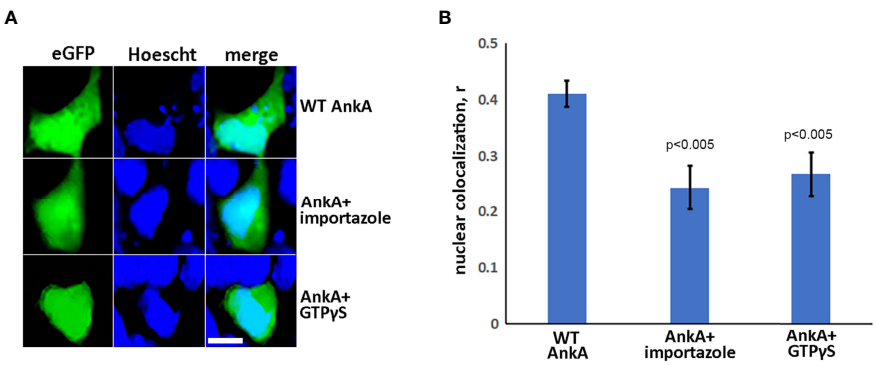

FIGURE 4 | AnkA is transported into nucleus through importin-β, RanGTP-dependent nuclear-transporting system. HEK293T cells were transfected with eGFP-AnkA plasmid constructs and treated or sham-treated with 30 μM importazole or simultaneously loaded during transfection protocol with GTPγS, a non-hydrolysable analog of GTP. After 48 hours, cells were fixed, washed, stained with nuclear label Hoescht33342 and visualized by fluorescence microscopy. **(A)** Representative images of AnkA-transfected cells in the absence or presence of importazole or GTPγS. **(B)** Nuclear colocalization of AnkA proteins in the presence of importazole or GTPγS relative to untreated cells. Control cells transfected with pure eGFP plasmid construct are shown. The Pearson correlation coefficient, r, was used for the analysis. Data are mean ± SEM of 30-40 randomly selected ROIs containing 100-200 transfected cells of two independent experiments in duplicate. Student t-test p values compared to wild type AnkA are shown. Bar- 20μm.

A. phagocytophilum-infected HL-60 cells, importazole inhibited bacterial propagation by >99% ($p<0.005$) without reducing cell viability (**Figure 5**). While GTPγS was partly toxic to HL-60 cells, the viability of GTPγS-treated HL-60 cells was not further diminished by *A. phagocytophilum* infection, whereas GTPγS inhibited *A. phagocytophilum* propagation by 71% ($p<0.05$) in treated HL-60 cells (**Figure 6**). The impact of the AnkA AR mutants on *A. phagocytophilum* growth could not be assessed since it is largely refractory to genetic manipulation.

A Predicted Bipartite NLS in AR4

We previously used a range of publicly available NLS prediction algorithms to screen AnkA, and identified a putative bipartite NLS in the carboxy-terminus, that was disproven by creating truncation mutants (Rennoll-Bankert et al., 2015). Since dependency on the importin α/β system for AnkA nuclear localization and microbial propagation was shown, we applied additional alternative algorithms to discern the existence of previously unidentified NLSs. SeqNLS did not identify any putative NLSs, while NLStradamus identified putative NLSs only within the carboxy terminus that was already excluded as mechanistically important for AnkA nuclear import by experimental truncation of that region (Rennoll-Bankert et al., 2015). However, using cNLS Mapper (Kosugi et al., 2009b), three putative bipartite importin-β NLSs were identified, including two in the AnkA carboxy terminus (positions 1075-1106 and 1143-1177), and a single putative NLS at position 227-261 that overlaps AR4, including the AR4 mutation AnkA.M228R (**Figure 7**). cNLS Mapper predicted that the AnkA.M228R mutant sequence would not alter recognition of the NLS.

DISCUSSION

AnkA, a type IV secretion system effector protein of the tick-borne bacterium *A. phagocytophilum*, is essential for bacterial growth and has several roles in cellular infection and fitness (Lin et al., 2007; Sinclair et al., 2014; Rennoll-Bankert et al., 2015; O'Conor et al., 2021). The characteristic feature of AnkA is the presence of multiple ankyrin repeat motifs that span nearly 2/3 of the length of the protein (Scharf et al., 2011; Rennoll-Bankert et al., 2015). Depending on the strain, the number of ARs can vary from 8 to 15 (Scharf et al., 2011), but the N-terminal 4 ARs are highly conserved (Rennoll-Bankert et al., 2015). In general, ARs have multifunctional roles in protein-protein, protein-lipid and protein-DNA interactions. AnkA belongs to an increasingly

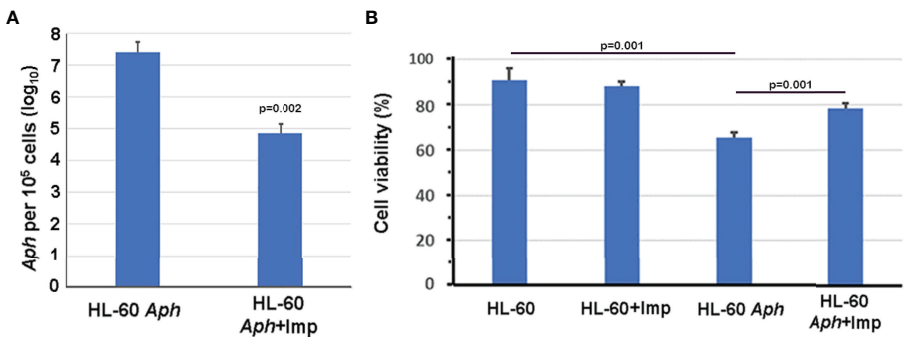

FIGURE 5 | Importazole, an inhibitor of cargo binding to importin-β, inhibits *A. phagocytophilum* propagation in HL-60 cells **(A)** without inducing detrimental HL-60 cell viability **(B)**. *Aph*, *A. phagocytophilum*; Imp, importazole; ANOVA with Tukey *post hoc* p values <0.05 are shown. Error bars represent s.e.m.

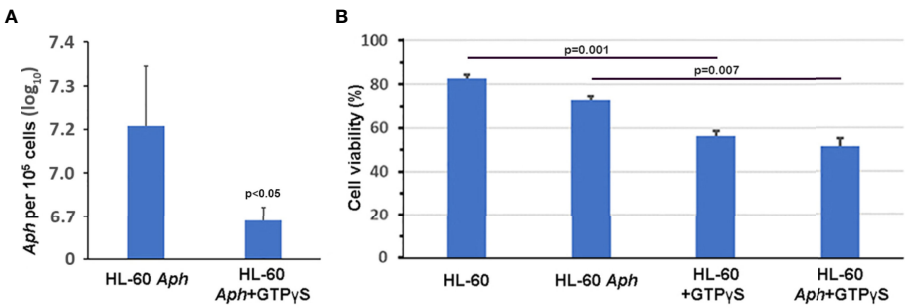

FIGURE 6 | GTPγS, a non-hydrolysable GTP analog that inhibits RanGTP/RanGDP-dependent nuclear translocation by importin-α/β and RaDAR mechanisms and likely many other cellular processes, significantly impairs *A. phagocytophilum* growth *in vitro* **(A)** without further compromising viability of infected HL-60 cells **(B)**. *Aph*, *A. phagocytophilum*; Error bars represent s.e.m.

FIGURE 7 | Prediction of importin-α/β pathway NLSs in full length *A. phagocytophilum* Webster^{T} strain AnkA. Three predictive algorithms were applied to identify putative NLSs. Shown is the full-length AnkA protein sequence with yellow highlights for the ankyrin repeats, ankyrin repeat mutations in enlarged font, NLS predicted by the cNLS Mapper algorithm (see text) in red text, and NLS predicted by NLStradamus (see text) in blue highlights. Note the predicted NLS overlapping the 4th ankyrin repeat including the site of mutation that led to diminished nuclear translocation.

large group of ARPs of prokaryotic origin with a very diverse functions (Al-Khodor et al., 2010; Islam et al., 2018). Understanding how the various protein domains, motifs, and structures influence functional properties informs approaches toward a better comprehension of pathogenesis. AnkA plays a critical role in modifying epigenetics of its host cell in mammals, the neutrophil (Garcia-Garcia et al., 2009b; Rennoll-Bankert et al., 2015; Sinclair et al., 2015; Dumler et al., 2016; Dumler et al., 2018). While AnkA appears to act as a nuclear chromatin organizer in the host cell *via* binding intergenic DNA locations to the nuclear lamina, its best known function is to bind DNA at host defense gene promoters (Garcia-Garcia et al., 2007; Garcia-Garcia et al., 2009b; Rennoll-Bankert et al., 2015; Dumler et al., 2016). It is at gene promoters that histone deacetylase-1 (HDAC1) is recruited after AnkA-DNA binding to deacetylate adjacent histone H3 and close chromatin accessibility to transcriptional activators and RNA polymerase. Additional nuclear functions for this prokaryotic protein are under study, including how it may affect the coordination of neutrophil transcriptional programs that enhance proinflammatory activities, delay apoptosis, and yet deactivate antimicrobial functions that enhance their fitness by promoting propagaton and transmission (Sinclair et al., 2014; Dumler et al., 2016; Dumler et al., 2018). Thus, understanding how AnkA enters the nucleus is a key to understanding disease pathogenesis.

ARs located in the middle or carboxy-end of AnkA play a role in binding to host DNA and in promoter silencing, presumably through recruitment of HDAC1 (Rennoll-Bankert et al., 2015).

At the same time, truncation of the N-terminus of AnkA that includes the first four ARs results in a significant decrease of nuclear localization of the protein, implying the presence of a previously undetected nuclear localization sequence in this region. Classical importin-dependent nuclear localization requires bipartite or monopartite cargo NLS interactions with ARM motifs in importin-α before binding importin-β and transiting the nuclear pore complex, where RanGTP binding releases the cargo protein (Lu et al., 2021). A critical component of this process relies on cytoplasmic RanGDP complexed with nuclear transport factor 2 (NTF2) to enter the nucleus before conversion to RanGTP (Ribbeck et al., 1998).

In contrast, structural analysis of some of human ARPs suggest that alternate NLS interactions take place in a hydrophobic pocket formed by at-least two ARs of the same ARP or with a tandem of ARs of two ARPs (Lu et al., 2014). For a group of ARPs that are imported into the nucleus, this transport requires the RaDAR pathway that requires two adjacent ARs, importin-β-independence, and involvement of RanGDP binding to translocate into the nucleus. The distinguishing feature of these ARPs is that their nuclear transport is defined by ARs with a hydrophobic residue at the 13th position that mediates binding to similar hydrophobic residues in RanGDP; replacement of these with hydrophilic residues (e.g. K, R, E, Q) in two consecutive ARs abrogates nuclear import of the ARPs by the RaDAR system (Lu et al., 2014). While the tertiary structure of AnkA is not yet fully resolved, truncation of the N-terminal ARs leads to loss of nuclear importation that is restored when the SV40 NLS is added to the C-terminus. This also restores typical DNA binding of AnkA, thus focusing attention on the unique NLS properties of the N-terminal ARs and implying that AnkA might also be transported by the RaDAR system (Lu et al., 2014; Rennoll-Bankert et al., 2015).

Here, we interrogated the potential involvement of the RaDAR nuclear localization mechanism and found that point mutations of two consecutive ARs, such as AR1/AR2, AR2/AR3 or AR3/AR4 significantly reduced nuclear importation of AnkA. Although consistent with the RaDAR mechanism, single mutations at ARs 1-4 did not reduce AnkA nuclear localization. There is controversy regarding the requirement for the two consecutive AR principle of RaDAR function; for example, Ank13 of *O. tsutsugamushi* uses the RaDAR mechanism, but mutation of a single AR 13th residue is sufficient to reduce nuclear entry (Adcox et al., 2021). While replacement of hydrophobic with hydrophilic 13th residues of the consecutive AR3/AR4 resulted in a reduction of nuclear localization, mutations that increase hydrophobicity at AR1/AR2 and AR2/AR3 also reduce nuclear localization, a finding inconsistent with a stringent interpretation of the RaDAR mechanism. Mutations at the 13th residues of ARs do not lead to structural changes in the RanGDP binding site (Lu et al., 2014), and such changes are not predicted to disrupt key structural features of the protein (**Supplementary Figure 2**), yet these and our supplemental findings (**Supplementary Table 1**) suggest otherwise. While individual deletions of AR1, 2, 3 and 4 could be informative, the likely disruption to protein structure could confound interpretation of their nuclear localization (Lu et al., 2014). Moreover, our data with mutations not relevant to RaDAR nuclear importation that affect the same ARs also suggests the importance of AR structural integrity for AnkA nuclear transport.

In contrast, the use of importazole, a specific inhibitor of importin-β-dependent cargo protein nuclear delivery, showed that AnkA transport was importin-α/β-dependent. The identification of importin-dependence and the inhibition of *A. phagocytophilum* growth in its presence prompted a further search for an alternate NLS not previously identified. While prediction algorithms for NLSs vary, each possesses weaknesses; for greatest validity the approach would be confirmed by several methods and experimentally (Lin and Hu, 2013). The predicted colocalization of a putative bipartite importin-α NLS that overlaps AR4 perhaps offers support for the former hypothesis, although the M228R mutation is not predicted to significantly modify structure or classical bipartite NLS function; definitive evidence will require additional mutational studies. These data suggest that the RaDAR mechanism is either a supplemental, redundant or minor contributor for nuclear localization activity of AnkA. This is reasoned because if the RaDAR system, that by definition does not require importin, was critical for the essential protein AnkA nuclear localization, inhibition of importin-dependent nuclear translocation would not have the profound effect on *A. phagocytophilum* propagation noted here. While it appears that AnkA utilizes traditional nuclear import to enter the nucleus, the supplemental use of the RaDAR mechanism might provide an evolutionary advantage in pathogen fitness, although propagation dependence on importin contradicts that hypothesis. What is less clear is the impact of amino acid residue substitutions in proximity to position 13, where Lu et al. found AR structural stability at positions 3, 5, 13 and 14 (Lu et al., 2014). These findings suggest instability at other residues in ARs or to non-AR amino acid sequence could impact protein structure and have profound effects on protein function, further supporting the primacy of the importin-α/β nuclear import for AnkA.

Similar to *A. phagocytophilum* AnkA, *Orientia tsutsugamushi* ARPs Ank1 and Ank6 require importin-β, but Ank13 utilizes the RaDAR pathway (Evans et al., 2018; Adcox et al., 2021), suggesting the coexistence of both processes utilized by a single bacterium, albeit for distinct proteins, and that perhaps two consecutive ARs with 13th position hydrophobic residues are not required for prokaryotic proteins. Interestingly, a related tick-borne pathogen, *Ehrlichia chaffeensis*, uses an AR-rich protein, p200, to modify transcriptional activity of its host monocyte (Zhu et al., 2009). The p200 protein contains about 20 ARs among its 1422 residues tightly clustered in 3 locations. However, as in the case with *O. tsutsugamushi* Ank1 and Ank6, an analysis of amino acid sequences of p200 ARs reported in Protein databases and GenBank do not meet stringent criteria that define the RaDAR nuclear import pathway. Given the increasing ubiquity of ARPs discovered in prokaryotes through genome analyses, future studies should address whether they use the RaDAR transporting system as do many human ARPs,

whether they use classical importin-α/β-dependent nuclear transport pathway, serve supplemental or redundant roles, or do not contribute to nuclear importation. Since different dual combinations of N-terminal AR mutations affect AnkA nuclear localization, future studies of AnkA tertiary structure will be of critical importance to understand a role for the four N-terminal ARs in nuclear import or other AnkA functions.

Given the essential nature and importance noted for AnkA in the fitness of *A. phagocytophilum*, understanding the function of all protein motifs and domains is essential to understanding pathogenicity and to ultimately develop improved strategies for disease control. Additionally, the application of ankyrin repeats for use as biological tools and pharmaceuticals (Boersma, 2018; Mittl et al., 2020) suggests that improved properties and ranges of function could be discerned by studying those features already selected for specific properties by microbes, like *A. phagocytophilum*.

EXPERIMENTAL PROCEDURES

Cell Culture

HEK293T, human embryonic kidney cells (CRL3216, ATCC), were grown in RPMI 1640 (GIBCO) medium supplemented with 10% FBS (GemCell, Gemini), 2 mM L-glutamine and 1 mM sodium pyruvate at 37°C and 5% CO_2. *A. phagocytophilum* (*Aph*) Webster^T strain was maintained in HL-60 cells, a human promyelocytic cell line, that were cultured in RPMI 1640 with 10% FBS supplemented with 2 mM glutamine and 1 mM pyruvate.

Construction of Point Mutation AnkA Plasmids

To preclude major structural variations of AnkA with AR deletions that would potentially impact its binding, we avoided deletion of individual N-terminal ARs in favor of specific point mutations that would better elucidate potential RaDAR nuclear transport involvement. Plasmids pEGFPC1-AnkA and N-terminal ankyrin repeat mutants of AnkA were generated (GenScript; Piscataway, NJ) according to the full AnkA sequence of *A. phagocytophilum* Webster^T strain (WP_020849331.1). We modified the 13th amino acid residues in each of the first four N-terminal ARs to hydrophilic or neutral residues anticipating a change in hydrophobic interactions with RanGDP that would impact nuclear localization (**Figure 1**). In total, 11 single or double AR mutations of AnkA were created. AR1 and AR2 of AnkA differ from human ARs involved in RaDAR nuclear transport in that they have a hydrophilic and aliphatic neutral residue at the 13th position, arginine and glycine, respectively. Thus, recombinant mutants of the protein were created in which the 13th residues were replaced with more hydrophobic or neutral/hydrophilic residues, alanine (AnkA.R56A) or glycine (AnkA.R56G) for AR1, and alanine (AnkA.G157A) or arginine (AnkA.G157R) for AR2. In contrast, AR3 and AR4 of AnkA have amino acid sequences identical to ARs of many human proteins involved in RaDAR nuclear transport, such as the presence of a highly conserved LH pair at the 5th and 6th positions and of hydrophobic residues at the 13th position, valine and methionine, respectively. We replaced these with hydrophilic asparagine (AnkA.V190N) because of its similar molecular size, and arginine (AnkA.M228R) because of its similar size and structure, respectively. Wild type eGFP-AnkA and mutated plasmids were transfected into HEK293T cells and their nuclear localizations were compared.

Cell Transfection

For cell transfection and subsequent visualization, HEK293 cells were seeded into collagen-coated 8-chamber optical glass slides (LabTek) at 4-5x10^4 cells/per well in 400 μL of growth medium. After 24h, the attached cells were transfected with the AnkA or AnkA N-terminal ankyrin repeat mutant plasmids. Transfection (FuGENE HD Promega) was achieved using 2 μg of plasmid DNA and 3:1 ratio of the reagent (6 μL) per well, in accordance with manufacturer recommendations. After 48h incubation, cells were washed in PBS, fixed for 10 min in 4% paraformaldehyde, washed in PBS and then stained with Hoescht 33342, a cell-permeable nuclear label, at 1:1000 dilution for 3 minutes. After final washing in PBS, the chamber walls were removed and the dried optical slides were fixed, and labeled cells were mounted (ProLong Diamond Antifade mounting solution, Invitrogen) and visualized using fluorescence microscopy.

Image Analysis

Slides were visualized using an Olympus BX-40 fluorescent microscope equipped with DP74 camera, 40x-objective and precision stage (ProScanIII from Prior). For image analysis, the Olympus CellSense Dimension software with the colocalization software module was used (Casavan et al., 2021). In this program, Pearson's correlation coefficient accounts only for the similarity of shapes between two colocalized images highlighted by distinct fluorescence in the nucleus, and does not depend upon image pixel intensity values. 20-40 regions of interest (ROIs) containing 100-200 transfected nuclei stained with Hoescht (blue) were randomly selected and examined for colocalization with eGFP fluorescence (**Supplementary Figure 1** shows an example of this analysis). The images used include eGFP fluorescent signal within, above and below the nucleus, such that the minimal colocalization signal will never be zero, but that with increased nuclear eGFP presence, will increase. To optimize visual differences in colocalized signal, for each image displayed, we utilized the image/adjustment/levels feature in Photoshop 22 to remove red (output level 0), and adjusted both green and blue channels. Based on this colocalization analysis and comparing wild type to mutants, Pearson coefficients, R(r), from two independent experiments done in duplicate, were statistically analyzed using either Student's t-test for comparing two conditions or one-way ANOVA with *post-hoc* Tukey test for multiple conditions, or for comparisons related to control only, Bonferroni corrections were performed.

Bacterial Growth and Infectivity

To evaluate the infectivity of *A. phagocytophilum* in HL-60 cells we used a cytological Romanowsky staining method; trypan blue exclusion was used with the Countess II (Invitrogen) automatic

cell counter to determine cell viability. To study the role of importin-dependent nuclear transport in *A. phagocytophilum* growth, $3x10^5$ HL-60 cells were seeded in 12-well plates (Costar) containing 1 mL of growth medium in the presence or absence of 10 μM importazole, a specific nuclear transport inhibitor (Soderholm et al., 2011). To investigate the role of RanGTP/RanGDP-dependent nuclear transport system in *A. phagocytophilum* growth, $3x10^5$ HL-60 cells were loaded with non-hydrolysable GTP analog, GTPγS using the transfection protocol described for cell transfection with AnkA plasmids. Here, nanoparticles were incubated with 100 μM GTPγS and then added to *A. phagocytophilum*-infected or non-infected HL-60 cells. To ascertain the effects of importazole and GTPγS on *A. phagocytophilum* propagation, 10^5 infected HL-60 cells were added to 9 x 10^5 uninfected HL-60 cells to achieve 10% infected cells, for an average of 1 bacterium per cell. These and 10^6 control uninfected HL-60 cells, both in 5 mL, were supplemented to achieve final concentrations of 10 μM importazole or 100 μM GTPγS. After 3 days of incubation, control treated and untreated cells and *A. phagocytophilum*-infected, importazole/GTPyS-treated and sham-treated HL-60 cells were collected for cell count, viability evaluation, and for quantitation of *A. phagocytophilum* by qPCR targeting *A. phagocytophilum msp2* (Reller and Dumler, 2020). This qPCR assay is based on a 5-prime nuclease assay targeting a highly conserved region of the multicopy *msp2*, for which at least 100 copies exist in the *A. phagocytophilum* genome. The assay has been demonstrated to detect up to 86 distinct copies in the *A. phagocytophilum* Webster^T strain genome. Thus, using *msp2* plasmid standards ranging from 10^1 to 10^6 copies was used to determine the *msp2* copies per μL in technical duplicates or triplicates for each condition with 3 biological replicates. DNA was prepared from 10^5 infected or uninfected, treated or untreated cells suspended in 200 μL, and wells of a 384 well PCR plate received 1-3 μL of DNA in addition to master mix, in a final 10 μL well volume. To establish the number of bacteria, the number of *msp2* copies/μL in each condition was divided by the volume tested and by 86 copies/*A. phagocytophilum* genome to obtain *A. phagocytophilum*/μL, then multiplied by 200 to obtain the total number of bacteria in 10^5 cells.

Bioinformatic Screening of β-Importin Nuclear Localization Signals in AnkA

While AnkA had initially been screened for the presence of putative NLSs (Rennoll-Bankert et al., 2015), the dependence on importazole and GTP hydrolysis for translocation prompted an additional search using recently developed publically-available software programs that utilize distinct search algorithms, including SeqNLS (http://mleg.cse.sc.edu/seqNLS/, using Final-score cutoffs of 0.3, 0.5 and default 0.86) (Lin and Hu, 2013); NLStradamus (https://predictprotein.org/, using 2 state HMM static and dynamic, and 4 state HMM static models with Viterbi and Posterior prediction models [0.4 prediction cutoff]) (Nguyen Ba et al., 2009); NLSdb (https://rostlab.org/services/nlsdb/) (Nair et al., 2003); and NLS Mapper cNLS (https://nls-mapper.iab.keio.ac.jp/cgi-bin/NLS_Mapper_form.cgi, using cut-off scores of 5.0, 4.0, and 3.0, Entire region) (Kosugi et al., 2009a; Kosugi et al., 2009b). Predicted NLSs were mapped against the AnkA protein sequence with and without mutated residues (**Figure 7**).

AnkA N-Terminal Ankyrin Repeat Structural Modeling

To predict impact of point mutations in the N-terminal region of AnkA, we modeled the first 300 amino acids to the top ranked model in a Phyre2 analysis. The model pdb file was then used to interrogate single mutants constructed for the *in vitro* studies using Missense 3D which allowed prediction of each potential residue substitution toward stability of protein structure and visualization of mutant residues on the top model's structure (Kelley et al., 2015; Ittisoponpisan et al., 2019). Additional analysis of the AnkA N-terminal 300 residue model was analyzed for the effects of structural changes with single residue alterations at every position using SuSPect (Yates et al., 2014).

Statistical Analysis

Two-tailed Student t-tests were performed by using Excel software (Microsoft, Redmond, WA). For multiple comparisons, one-way ANOVA with *post-hoc* Tukey HSD tests were performed, or for comparisons related to control only, Bonferroni corrections were performed (https://astatsa.com/OneWay_Anova_with_TukeyHSD/). Values of $p<0.05$ were considered significant.

DATA AVAILABILITY STATEMENT

The original contributions presented in the study are included in the article/**Supplementary Material**. Further inquiries can be directed to the corresponding author.

AUTHOR CONTRIBUTIONS

JD, YK and JW conceived and designed the study. YK, JW, and EC performed the experiments. YK and JD performed the statistical analysis. YK and JD wrote the paper. JW, EC, and DG participated in the drafting of the manuscript. All authors contributed to the preparation of the article and approved the submitted version.

FUNDING

This work was supported by grant R01-AI044102 from the National Institutes of Allergy and Infectious Diseases/National Institutes of Health to JD, and by grant PAT-74-3977 from the Uniformed Services University of the Health Sciences to JD.

ACKNOWLEDGMENTS

The authors would like to thank Ian Cadby, Ph.D. for helpful discussions, and acknowledge the participation of Valeria Pappas-Brown, Ph.D.

SUPPLEMENTARY MATERIAL

The Supplementary Material for this article can be found online at: https://www.frontiersin.org/articles/10.3389/fcimb.2022.828605/full#supplementary-material

Supplementary Figure 1 | Example of Fluorophore Colocalization analysis. A 2D field identified among HEK cells transfected with pEGFPC1-ankA (wild type) and imaged to visualize transfected cells (green) and all cell nuclei (blue) demonstrate a modest transfection efficiency (top panel). Representative fields that included eGFPexpression were selected for imaging. Among cells that display transfection, approximately 25 in the field shown here, colocalization of transfected shape by pixels was identified by designating 100-200 regions of interest (ROI) (bottom panel and insert). From these, the Pearson's correlation coefficient (r) was calculated to estimate the degree of overlap of the two signals. Values of r vary between -1 and +1, with clear colocalization indicated by positive r values closer to 1.

Supplementary Figure 2 | The AnkA N-terminal 300 residue structure was modeled by alignment using Phyre2 to identify the best match, 4RLV (ANK2). Using this model, the location and impact of changes in individual residues was assessed using Missense3D. The specific insertions are shown on the c4RLV models of AnkA ARs 1-4 by AnkA AR, and labeled with the specific residue change. Note that the model c4RLV model structure results in two non-contiguous templates resulting from a large gap in 4RLV compared to AnkA. AR1 and 2 are on one template; AR3 and 4 on a different template. No residue change was predicted to cause any structural damage.

Supplementary Figure 3 | Alignment of AnkA modeled by Phyre2 on 4RLV. ARs in AnkA are shown in yellow highlights, those in 4RLV are shown in green. Dashes indicate gaps in alignment. Note that AnkA AR2 spans a large gap in 4RLV. AnkA ARs 1-4 correspond to ARs 2, 5/20, 21, and 22 in 4RLV.

Supplementary Figure 4 | Detailed alignment of AnkA N-terminal 300 residues by Phyre2 to 4RLV showing predicted secondary structure for both AnkA and 4RLV templates. Yellow highlights show AnkA ARs.

REFERENCES

Adcox, H. E., Hatke, A. L., Andersen, S. E., Gupta, S., Otto, N. B., Weber, M. M., et al. (2021). *Orientia Tsutsugamushi* Nucleomodulin Ank13 Exploits the RaDAR Nuclear Import Pathway to Nodulate Host Cell Transcription. *mBio* 12, e0181621. doi: 10.1128/mBio.01816-21

Al-Khodor, S., Price, C. T., Kalia, A., and Abu Kwaik, Y. (2010). Functional Diversity of Ankyrin Repeats in Microbial Proteins. *Trends Microbiol.* 18, 132–139. doi: 10.1016/j.tim.2009.11.004

Bakken, J. S., and Dumler, J. S. (2015). Human Granulocytic Anaplasmosis. *Infect. Dis. Clin. North Am.* 29, 341–355. doi: 10.1016/j.idc.2015.02.007

Bierne, H., and Pourpre, R. (2020). Bacterial Factors Targeting the Nucleus: The Growing Family of Nucleomodulins. *Toxins (Basel)* 12, 220. doi: 10.3390/toxins12040220

Boersma, Y. L. (2018). Advances in the Application of Designed Ankyrin Repeat Proteins (DARPins) as Research Tools and Protein Therapeutics. *Methods Mol. Biol.* 1798, 307–327. doi: 10.1007/978-1-4939-7893-9_23

Casavan, W. G. Y., Parry-Hill, M. J., Claxton, N. S., and Davidson, M. W. (2021) *Fluorophore Colocalization* (Olympus Corporation). Available at: https://www.olympus-lifescience.com/en/microscope-resource/primer/java/colocalization/ (Accessed November 4, 2021).

Caturegli, P., Asanovich, K. M., Walls, J. J., Bakken, J. S., Madigan, J. E., Popov, V. L., et al. (2000). *Anka*: An *Ehrlichia Phagocytophila* Group Gene Encoding a Cytoplasmic Protein Antigen With Ankyrin Repeats. *Infect. Immun.* 68, 5277–5283. doi: 10.1128/IAI.68.9.5277-5283.2000

Cavazza, T., and Vernos, I. (2016). The RanGTP Pathway: From Nucleo-Cytoplasmic Transport to Spindle Assembly and Beyond. *Front. Cell. Devel. Biol.* 3, 1–12. doi: 10.3389/fcell.2015.00082

Dumler, J. S., Sinclair, S. H., Pappas-Brown, V., and Shetty, A. C. (2016). Genome-Wide *Anaplasma Phagocytophilum* AnkA-DNA Interactions are Enriched in Intergenic Regions and Gene Promoters and Correlate With Infection-Induced Differential Gene Expression. *Front. Cell. Infect. Microbiol.* 6, 97. doi: 10.3389/fcimb.2016.00097

Dumler, J. S., Sinclair, S. H., and Shetty, A. C. (2018). Alternative Splicing of Differentiated Myeloid Cell Transcripts After Infection by *Anaplasma Phagocytophilum* Impacts a Selective Group of Cellular Programs. *Front. Cell. Infect. Microbiol.* 8, 14. doi: 10.3389/fcimb.2018.00014

Evans, S. M., Rodino, K. G., Adcox, H. E., and Carlyon, J. A. (2018). *Orientia Tsutsugamushi* Uses Two Ank Effectors to Modulate NF-κb P65 Nuclear Transport and Inhibit NF-κb Transcriptional Activation. *PloS Pathog.* 14, e1007023. doi: 10.1371/journal.ppat.1007023

Garcia-Garcia, J. C., Barat, N. C., Trembley, S. J., and Dumler, J. S. (2009a). Epigenetic Silencing of Host Cell Defense Genes Enhances Intracellular Survival of the Rickettsial Pathogen *Anaplasma Phagocytophilum*. *PloS Pathog.* 5, e1000488. doi: 10.1371/journal.ppat.1000488

Garcia-Garcia, J. C., Milstone, A. M., and Dumler, J. S. (2007). *"Epigenetic Control of Host Cell Gene Expression by Anaplasma Phagocytophilum AnkA Protein"* (Toronto, Canda: 107th General Meeting of the American Society for Microbiology).

Garcia-Garcia, J. C., Rennoll-Bankert, K. E., Pelly, S., Milstone, A. M., and Dumler, J. S. (2009b). Silencing of Host Cell *CYBB* Gene Expression by the Nuclear Effector AnkA of the Intracellular Pathogen *Anaplasma Phagocytophilum*. *Infect. Immun.* 77, 2385–2391. doi: 10.1128/IAI.00023-09

Islam, Z., Nagampalli, R. S. K., Fatima, M. T., and Ashraf, G. M. (2018). New Paradigm in Ankyrin Repeats: Beyond Protein-Protein Interaction Module. *Int. J. Biol. Macromol.* 109, 1164–1173. doi: 10.1016/j.ijbiomac.2017.11.101

Ittisoponpisan, S., Islam, S. A., Khanna, T., Alhuzimi, E., David, A., and Sternberg, M. J. E. (2019). Can Predicted Protein 3D Structures Provide Reliable Insights Into Whether Missense Variants Are Disease Associated? *J. Mol. Biol.* 431, 2197–2212. doi: 10.1016/j.jmb.2019.04.009

Jernigan, K. K., and Bordenstein, S. R. (2014). Ankyrin Domains Across the Tree of Life. *PeerJ* 2, e264. doi: 10.7717/peerj.264

Kelley, L. A., Mezulis, S., Yates, C. M., Wass, M. N., and Sternberg, M. J. (2015). The Phyre2 Web Portal for Protein Modeling, Prediction and Analysis. *Nat. Protoc.* 10, 845–858. doi: 10.1038/nprot.2015.053

Kosugi, S., Hasebe, M., Matsumura, N., Takashima, H., Miyamoto-Sato, E., Tomita, M., et al. (2009a). Six Classes of Nuclear Localization Signals Specific to Different Binding Grooves of Importin Alpha. *J. Biol. Chem.* 284, 478–485. doi: 10.1074/jbc.M807017200

Kosugi, S., Hasebe, M., Tomita, M., and Yanagawa, H. (2009b). Systematic Identification of Cell Cycle-Dependent Yeast Nucleocytoplasmic Shuttling Proteins by Prediction of Composite Motifs. *Proc. Natl. Acad. Sci. U. S. A.* 106, 10171–10176. doi: 10.1073/pnas.0900604106

Lin, M., Den Dulk-Ras, A., Hooykaas, P. J., and Rikihisa, Y. (2007). *Anaplasma Phagocytophilum* AnkA Secreted by Type IV Secretion System is Tyrosine Phosphorylated by Abl-1 to Facilitate Infection. *Cell. Microbiol.* 9, 2644–2657. doi: 10.1111/j.1462-5822.2007.00985.x

Lin, J. R., and Hu, J. (2013). SeqNLS: Nuclear Localization Signal Prediction Based on Frequent Pattern Mining and Linear Motif Scoring. *PloS One* 8, e76864. doi: 10.1371/journal.pone.0076864

Lu, J., Wu, T., Zhang, B., Liu, S., Song, W., Qiao, J., et al. (2021). Types of Nuclear Localization Signals and Mechanisms of Protein Import Into the Nucleus. *Cell Commun. Signal.* 19, 60. doi: 10.1186/s12964-021-00741-y

Lu, M., Zak, J., Chen, S., Sanchez-Pulido, L., Severson, D. T., Endicott, J., et al. (2014). A Code for RanGDP Binding in Ankyrin Repeats Defines a Nuclear Import Pathway. *Cell* 157, 1130–1145. doi: 10.1016/j.cell.2014.05.006

Mittl, P. R., Ernst, P., and Plückthun, A. (2020). Chaperone-Assisted Structure Elucidation With DARPins. *Curr. Opin. Struct. Biol.* 60, 93–100. doi: 10.1016/j.sbi.2019.12.009

Nair, R., Carter, P., and Rost, B. (2003). NLSdb: Database of Nuclear Localization Signals. *Nucleic Acids Res.* 31, 397–399. doi: 10.1093/nar/gkg001

Nguyen Ba, A. N., Pogoutse, A., Provart, N., and Moses, A. M. (2009). NLStradamus: A Simple Hidden Markov Model for Nuclear Localization Signal Prediction. *BMC Bioinf.* 10, 202. doi: 10.1186/1471-2105-10-202

O'conor, M. C., Herron, M. J., Nelson, C. M., Barbet, A. F., Crosby, F. L., Burkhardt, N. Y., et al. (2021). Biostatistical Prediction of Genes Essential for Growth of *Anaplasma Phagocytophilum* in a Human Promyelocytic Cell

Line Using a Random Transposon Mutant Library. *Pathog. Dis.* 79, ftab029. doi: 10.1093/femspd/ftab029

Pan, X., Luhrmann, A., Satoh, A., Laskowski-Arce, M. A., and Roy, C. R. (2008). Ankyrin Repeat Proteins Comprise a Diverse Family of Bacterial Type IV Effectors. *Science* 320, 1651–1654. doi: 10.1126/science.1158160

Park, J., Kim, K. J., Choi, K. S., Grab, D. J., and Dumler, J. S. (2004). *Anaplasma Phagocytophilum* AnkA Binds to Granulocyte DNA and Nuclear Proteins. *Cell. Microbiol.* 6, 743–751. doi: 10.1111/j.1462-5822.2004.00400.x

Reller, M. E., and Dumler, J. S. (2020). Optimization and Evaluation of a Multiplex Quantitative PCR Assay for Detection of Nucleic Acids in Human Blood Samples From Patients With Spotted Fever Rickettsiosis, Typhus Rickettsiosis, Scrub Typhus, Monocytic Ehrlichiosis, and Granulocytic Anaplasmosis. *J. Clin. Microbiol.* 58, e01802. doi: 10.1128/JCM.01802-19

Rennoll-Bankert, K. E., Garcia-Garcia, J. C., Sinclair, S. H., and Dumler, J. S. (2015). Chromatin-Bound Bacterial Effector Ankyrin A Recruits Histone Deacetylase 1 and Modifies Host Gene Expression. *Cell. Microbiol.* 17, 1640–1652. doi: 10.1111/cmi.12461

Ribbeck, K., Lipowsky, G., Kent, H. M., Stewart, M., and Görlich, D. (1998). NTF2 Mediates Nuclear Import of Ran. *EMBO J.* 17, 6587–6598. doi: 10.1093/emboj/17.22.6587

Rikihisa, Y. (2017). Role and Function of the Type IV Secretion System in *Anaplasma* and *Ehrlichia* Species. *Curr. Top. Microbiol. Immunol.* 413, 297–321. doi: 10.1007/978-3-319-75241-9_12

Scharf, W., Schauer, S., Freyburger, F., Petrovec, M., Schaarschmidt-Kiener, D., Liebisch, G., et al. (2011). Distinct Host Species Correlate With *Anaplasma Phagocytophilum* ankA Gene Clusters. *J. Clin. Microbiol.* 49, 790–796. doi: 10.1128/JCM.02051-10

Sinclair, S. H., Rennoll-Bankert, K. E., and Dumler, J. S. (2014). Effector Bottleneck: Microbial Reprogramming of Parasitized Host Cell Transcription by Epigenetic Remodeling of Chromatin Structure. *Front. Genet.* 5, 274. doi: 10.3389/fgene.2014.00274

Sinclair, S. H., Yegnasubramanian, S., and Dumler, J. S. (2015). Global DNA Methylation Changes and Differential Gene Expression in *Anaplasma Phagocytophilum*-Infected Human Neutrophils. *Clin. Epigenet.* 7, 77. doi: 10.1186/s13148-015-0105-1

Soderholm, J. F., Bird, S. L., Kalab, P., Sampathkumar, Y., Hasegawa, K., Uehara-Bingen, M., et al. (2011). Importazole, A Small Molecule Inhibitor of the Transport Receptor Importin-β. *ACS Chem. Biol.* 6, 700–708. doi: 10.1021/cb2000296

Wang, C., Wei, Z., Chen, K., Ye, F., Yu, C., Bennett, V., et al. (2014). Structural Basis of Diverse Membrane Target Recognitions by Ankyrins. *Elife* 3, e04353. doi: 10.7554/eLife.04353.022

Yates, C. M., Filippis, I., Kelley, L. A., and Sternberg, M. J. (2014). SuSPect: Enhanced Prediction of Single Amino Acid Variant (SAV) Phenotype Using Network Features. *J. Mol. Biol.* 426, 2692–2701. doi: 10.1016/j.jmb.2014.04.026

Zhu, B., Nethery, K. A., Kuriakose, J. A., Wakeel, A., Zhang, X., and Mcbride, J. W. (2009). Nuclear Translocated *Ehrlichia Chaffeensis* Ankyrin Protein Iinteracts With the Mid A-Stretch of Host Promoter and Iintronic Alu Elements. *Infect. Immun.* 77, 4243–4255. doi: 10.1128/IAI.00376-09

Conflict of Interest: The authors declare that the research was conducted in the absence of any commercial or financial relationships that could be construed as a potential conflict of interest.

Publisher's Note: All claims expressed in this article are solely those of the authors and do not necessarily represent those of their affiliated organizations, or those of the publisher, the editors and the reviewers. Any product that may be evaluated in this article, or claim that may be made by its manufacturer, is not guaranteed or endorsed by the publisher.

frontiers | Frontiers in Cellular and Infection Microbiology

ORIGINAL RESEARCH
published: 09 June 2022
doi: 10.3389/fcimb.2022.867689

Coxiella burnetii Affects HIF1α Accumulation and HIF1α Target Gene Expression

Inaya Hayek, Manuela Szperlinski and Anja Lührmann *

Mikrobiologisches Institut – Klinische Mikrobiologie, Immunologie and Hygiene, Universitätsklinikum Erlangen, Friedrich-Alexander-Universität (FAU) Erlangen-Nürnberg, Erlangen, Germany

HIF1α is an important transcription factor regulating not only cellular responses to hypoxia, but also anti-infective defense responses. We recently showed that HIF1α hampers replication of the obligate intracellular pathogen *Coxiella burnetii* which causes the zoonotic disease Q fever. Prior to development of chronic Q fever, it is assumed that the bacteria enter a persistent state. As HIF1α and/or hypoxia might be involved in the induction of *C. burnetii* persistence, we analyzed the role of HIF1α and hypoxia in the interaction of macrophages with *C. burnetii* to understand how the bacteria manipulate HIF1α stability and activity. We demonstrate that a *C. burnetii*-infection initially induces HIF1α stabilization, which decreases then over the course of an infection. This reduction depends on bacterial viability and a functional type IV secretion system (T4SS). While neither the responsible T4SS effector protein(s) nor the molecular mechanism leading to this partial HIF1α destabilization have been identified, our results demonstrate that *C. burnetii* influences the expression of HIF1α target genes in multiple ways. Therefore, a *C. burnetii* infection promotes HIF1α-mediated upregulation of several metabolic target genes; affects apoptosis-regulators towards a more pro-apoptotic signature; and under hypoxic conditions, shifts the ratio of the inflammatory genes analyzed towards a pro-inflammatory profile. Taken together, *C. burnetii* modulates HIF1α in a still elusive manner and alters the expression of multiple HIF1α target genes.

Keywords: ***Coxiella burnetii*, HIF1α, T4SS, metabolism, apoptosis, inflammation**

OPEN ACCESS

Edited by:
Luís Jaime Mota, NOVA School of Science and Technology, Portugal

Reviewed by:
Anders Omsland, Washington State University, United States
Erin J Van Schaik, Texas A&M Health Science Center, United States

***Correspondence:**
Anja Lührmann
anja.luehrmann@uk-erlangen.de

Specialty section:
This article was submitted to Bacteria and Host, a section of the journal Frontiers in Cellular and Infection Microbiology

Received: *01 February 2022*
Accepted: *21 April 2022*
Published: *09 June 2022*

Citation:
Hayek I, Szperlinski M and Lührmann A (2022) Coxiella burnetii Affects HIF1α Accumulation and HIF1α Target Gene Expression. Front. Cell. Infect. Microbiol. 12:867689. doi: 10.3389/fcimb.2022.867689

INTRODUCTION

Hypoxia-inducible factor (HIF)-1 was first recognized as an essential regulator of cellular responses to limited oxygen availability (Majmundar et al., 2010). Recent research has shown that HIF1 activity is also critical for shifting cellular metabolism, regulating immune cell activity, and mounting anti-infective defense responses (Cramer et al., 2003; Knight and Stanley, 2019). HIF1 is a heterodimer, consisting of HIF1α and HIF1β (Wang et al., 1995). The activity of the complex is controlled by proteasomal degradation of the α-subunit. Thus, prolyl hydroxylases (PHDs) hydroxylate HIF1α, which mediates binding to the von Hippel-Lindau (VHL) E3 ubiquitin ligase and leads to proteasomal degradation of HIF1α (Maxwell et al., 1999; Ohh et al., 2000; Jaakkola et al., 2001). Importantly, PHDs require oxygen, Fe^{2+} and 2-oxoglutarate for HIF1α hydroxylation

[reviewed in: (Greer et al., 2012; Hayek et al., 2021)]. Therefore, in the absence of oxygen, its co-factors or co-substrates, HIF1α is stabilized. However, HIF1α stabilization can also occur under normoxic conditions (in the presence of oxygen) in response to increased levels of the TCA cycle intermediates succinate or fumarate, or in the presence of nitric oxide (NO) (Hewitson et al., 2007; Tannahill et al., 2013; Mills et al., 2016). In addition, bacterial, viral, fungal, and parasitic infections might also induce HIF1α stabilization (Devraj et al., 2017; Knight and Stanley, 2019). Once the heterodimer is formed, it attaches to the promoter region of genes containing the hypoxia response element (HRE) and induces their transcription. In addition, HIF1 interacts with other signaling pathways (including Notch, Wnt and Myc) in an HRE-independent manner (Koshiji et al., 2004; Gustafsson et al., 2005; Kaidi et al., 2007; Semenza, 2014; Strowitzki et al., 2019). Thereby, HIF1 regulates transcription of genes involved in metabolic reprogramming, immune responses, and anti-infectious activity (Obach et al., 2004; Kelly and O'Neill, 2015; Devraj et al., 2017).

Hypoxia, a state of insufficient oxygen availability, impairs several important antimicrobial defense mechanisms. To control bacterial infections under hypoxia, myeloid cells induce the production of anti-microbial peptides and pro-inflammatory cytokines, deplete essential metabolites, and modulate their phagocytic capacity and phagosome maturation (Hayek et al., 2021). Under these conditions, some bacteria are controlled under hypoxia and/or HIF1α, while other pathogens survive or even replicate.

We recently showed that in hypoxic murine macrophages, HIF1α or HIF1α -mediated signaling impedes *C. burnetii* replication (Hayek et al., 2019). This obligate intracellular bacterium is a zoonotic pathogen. Its primary reservoir are domestic ruminants such as cattle, sheep and goats (Maurin and Raoult, 1999). Although infected ruminants are mainly asymptomatic, in pregnant animals the infection might lead to abortion, premature delivery or stillbirth. Infected animals shed the pathogen through birthing products, feces or milk which are the main source for human infection (Van den Brom et al., 2015). Although often asymptomatic, Q fever may manifest in humans as an acute disease (mainly as a self-limited febrile illness, pneumonia, or hepatitis) or as a chronic disease (mainly endocarditis). Importantly, chronic Q fever develops several months or years after the primary infection (Anderson et al., 2013). A short-term treatment with doxycycline is still considered the mainstay of antibiotic therapy of acute Q fever, whereas chronic Q fever patients have to be treated with doxycycline in combination with hydroxyl chloroquine for at least 18 months. Thus, a more efficient therapy to treat chronic Q fever has to be developed. In addition, it is crucial to increase our knowledge of chronic Q fever development, especially since it develops months or years after the primary infection, during which the patient does not show any symptoms, suggesting a prolonged state of bacterial persistence (Harris et al., 2000; Sukocheva et al., 2016). Our previous results suggest that in macrophages, HIF1α is required for impeding *C. burnetii* replication by impairing STAT3 activation, which results in reduced levels of the TCA intermediate citrate (Hayek et al., 2019). Importantly, bacterial viability was maintained allowing bacterial persistence. Thus, HIF1α might play an important role in the induction of *C. burnetii* persistence, and consequently, the development of chronic Q fever. Therefore, we aim to analyze the roles of HIF1α and hypoxia for the interaction of macrophages with *C. burnetii* in more detail.

MATERIALS AND METHODS

Reagents and Cell Lines

Bone marrow derived macrophages from C57BL/6 "J" male mice (Charles River; Strain Code: 027) were prepared as described (Hayek et al., 2019). Briefly, bone marrow cells were extracted from femur and tibia of at least 6 weeks old mice and propagated in sterile Teflon bags (Angst+Pfister) containing DMEM + GlutaMax (Thermo Fisher), 10% Fetal Calf Serum (FCS) (Biochrom), 5% Horse Serum (Cell Concepts), 1% MEM Non-Essential Amino Acids Solution (Life Technologies), 0.5% HEPES (AppliChem) and 20% supernatant of L929 cells for 7-10 days at 37°C, 10% CO_2 and 21% O_2. Macrophages were cultured for infection experiments in CMoAB medium, consisting of RPMI 1640 medium (Thermo Fisher) supplemented with 10% FCS, 1% HEPES and 0.5% β-mercaptoethanol (Sigma Aldrich). Murine macrophages were seeded and left to adhere for 1 to 2 h at 37°C, 5% CO_2, 21% O_2 (normoxia) prior to infection.

C. burnetii Cultivation

All *C. burnetii* strains used in this study were inoculated at a concentration of 1 x 10^6 *C. burnetii*/ml in ACCM-2 (Sunrise Science Products, Cat#4700-300) medium and cultivated for 5 days at 37°C, 5% CO_2, and 2.5% O_2. The *C. burnetii* Nine Mile phase II (NMII) clone 4 (RSA439) served as wild type (wt) strain in this study. When growing *C. burnetii* Δ*dotA* (Schäfer et al., 2020) or the Δ*dotA C. burnetii* transposon mutant (kindly provided by Matteo Bonazzi (Martinez et al., 2014)), 3 μg/ml chloramphenicol was added to the axenic medium. *C. burnetii* NMII was heat-killed (Hk wt) at 70°C for 30 min under shaking at 500 rpm.

E. coli Cultivation

E. coli DH5α were plated on a Luria broth (LB) agar plate and placed overnight at 37°C. A single colony was picked to inoculate 3 ml LB medium, which was left to rotate for 5 h at 37°C. Then, 50 μl of the liquid culture were transferred into 3 ml of fresh LB medium and rotated overnight at 37°C.

Infection

To adjust *C. burnetii* infection concentrations, the optical density at OD_{600} was measured, with an OD_{600} of 1 equaling 1 x 10^9 *C. burnetii*/ml. To adjust *E. coli* infection concentrations, the optical density at OD_{600} was measured, where an OD_{600} of 1 equals 8 x 10^8 *E. coli*/ml. Unless otherwise mentioned, macrophages were infected with *C. burnetii* or *E. coli* at an MOI (multiplicity of

infection) of 10. After macrophage seeding, the cells were infected with the bacteria and placed under normoxia or 0.5% O_2 (hypoxia) for 4 h at 37°C, 5% CO_2. At the 4h time point, the cells were either harvested or the medium was discarded and replaced with fresh CMoAB for the later time points.

Treatment With LPS

The concentration of *E. coli* LPS (Sigma, L4391) was adjusted in CMoAB at 100 ng/ml. After macrophage seeding, the cells were treated with LPS and placed under normoxia or hypoxia. After 4 h, the medium was discarded and replaced with fresh CMoAB. Samples were harvested 24 h post-infection.

Treatment With Chemicals

Chloramphenicol (Roth) was adjusted to a concentration of 25 µg/ml in CMoAB and then applied to the infected macrophages to induce bacterial growth arrest along the course of infection.

Hypoxia

Hypoxic conditions were set to 0.5% O_2 and 5% CO_2 at 37°C in an InvivO2 hypoxic chamber (Baker Ruskinn). Media and buffers were equilibrated at least 4 h in the hypoxic chamber before starting an experiment.

Harvesting Protein Samples for Immunoblots

For HIF1α and actin immunoblot samples, uninfected, infected or LPS-treated macrophages were lysed with 10 mM Tris-HCl pH 6.8, 6.65 M Urea, 10% Glycerol, 1% SDS with freshly added 1 mM DTT and cOmplete Mini Protease Inhibitor Cocktail (Roche, Cat#04693124001). Hypoxic samples were harvested in the hypoxic chamber to prevent HIF1α destabilization. The samples were mixed for 30 s with the homogenizer unit (VWR) and corresponding pestles (VWR). Finally, 20 µL 4x Laemmli SDS buffer was added to the samples, which were then heated at 85°C for 8 min, shaking at 450 rpm.

Immunoblot

Proteins were separated by SDS-PAGE using 4-12% Bis-Tris Gels (Thermo Fischer Scientific) and transferred to a PVDF membrane (Merck Millipore). The membranes were probed with primary antibodies directed against HIF1α (Cayman 10006421/ Biomol) or actin (Sigma-Aldrich A2066). The proteins were visualized by using the secondary antibody α - Rabbit IgG (H+L)-HRP (Jackson ImmunoResearch Labs, Cat#111-035-045) and a chemiluminescence detection system (Thermo Fisher). Densitometric analysis was performed using ImageJ (NIH).

Immunofluorescence

The experimental steps of immunofluorescence staining were described in detail elsewhere (Hayek et al., 2019). Briefly, macrophages were seeded on 10 mm sterile coverslips in 24-well plates. After infection and incubation, the cells were fixed with 4% paraformaldehyde (PFA) and permeabilized with ice-cold methanol. The cells were then quenched with 50 mM NH_4Cl in PBS/5% goat serum (GS) followed by incubation with the primary antibody against *C. burnetii* NMII (Davids Biotechnology). Alexa Fluor 594 (Jackson ImmunoResearch Labs) was used as the secondary antibody. Finally, the slides were mounted with ProLong Diamond containing DAPI (Invitrogen). Immunofluorescent images were taken using the Carl Zeiss LSM 700 Laser Scan Confocal Microscope and the ZEN2009 software.

RNA

RNA samples were harvested with peqGOLD TriFast (Peqlab VWR, Cat#30-2010) or the RNeasy Plus Kit (Qiagen) and isolated according to manufacturer's protocol. Isolated RNA was treated with DNase and RDD buffer (QIAGEN, Cat#79254) for 10 min at 37°C, followed by DNase inactivation at 75°C for 5 min. The successful removal of any DNA contamination was confirmed by PCR analysis. Next, first strand cDNA was synthesized from the DNase-treated RNA with SuperScript II Reverse Transcriptase (Invitrogen by Life Technologies, Cat#18064-022) according to manufacturer's protocol. The resulting cDNA was diluted 5-fold (final concentration of about 100 ng) and served as template in qPCR using the QuantiFast SYBR Green PCR Kit (QIAGEN, Cat#204054), along with a final concentration of 100 nM of each primer in a final volume of 10 µL per reaction. Murine hypoxanthine guanine phosphoribosyl transferase (*mHprt1*) was the housekeeping gene. The sequence of the primer pairs used to investigate gene expression (*HIF1α*, *PHD1*, *PHD2*, *PHD3*, *VHL*, *IL1β*, *Nos2*, *IL10*, *IL6*, *PKM2*, *LDHA*, *Glut1*, *PDK1*, *Bcl2*, *Bax*, *Trp53*, *Becn1*, *Bnip3*, *Bnip3l*, *P300*, *FIH*, and *CBP*) are listed in **Table 1**. The expression levels of these genes were quantified by referencing to *mHPRT1* and normalizing to the uninfected or wt-infected normoxic sample. To calculate the fold change, the 2^-(ΔΔCT) method was applied.

Primers

The primers used are listed in **Table 1**.

Statistical Analysis

Using GraphPad Prism 5, statistical analysis of the presented data was performed. As mentioned in the individual figure legends, a one sample t-test or an unpaired two-tailed Student's t test was used. The one-sample t-test was used when comparing datasets to normalized values. A value of $p < 0.05$ was considered significant.

RESULTS

C. burnetii Infection Augments Hypoxia-Induced HIF1α Stabilization

Previous experiments suggested that *C. burnetii* increases the HIF1α protein level under hypoxic conditions (Hayek et al., 2019). As HIF1α accumulation is responsible for inhibiting *C. burnetii* replication, we aimed to determine whether *C. burnetii* is capable of modulating the HIF1α protein level. Thus, we infected bone marrow derived macrophages (BMDM) with *C. burnetii* at an MOI of 10 for 4 or 24 hours under normoxic

TABLE 1 | Primers used.

Name	Direction	5' to 3' sequence
HPRT1	forward	TCCTCCTCAGACCGCTTTT
HPRT1	reverse	CCTGGTTCATCATCGCTAATC
HIF1α	forward	CATCATCTCTCTGGATTTTGGCAGCG
HIF1α	reverse	GATGAAGGTAAAGGAGACATTGCCAGG
PHD2	forward	GCGGGAAGCTGGGCAACTAC
PHD2	reverse	CCATTTGGGTTATCAACGTGACGGAC
PHD3	forward	GGCCGCTGTATCACCTGTATCTACTAC
PHD3	reverse	CAGAAGTCTGTCAAAAATGGGCTCCAC
PHD1	forward	GTAATCCGCCACTGTGCAGGG
PHD1	reverse	CATCGCCGTGGGGATTGTCAAC
VHL	forward	GCCATCCCTCAATGTCGATGGAC
VHL	reverse	GACGATGTCCAGTCTCCTGTAGTTCTC
IL1β	forward	GTGCTGTCGGACCCATATGAGC
IL1β	reverse	CCCAAGGCCACAGGTATTTTGTCG
Nos2	forward	GACCAGAGGACCCAGAGACAAGC
Nos2	reverse	GCTTCCAGCCTGGCCAGATG
IL10	forward	TCAGCAGGGGCCAGTACAGC
IL10	reverse	GCAGTATGTTGTCCAGCTGGTCC
IL6	forward	AGACTTCCATCCAGTTGCCTTCTTGG
IL6	reverse	GTCTGTTGGGAGTGGTATCCTCTGTG
PKM2	forward	GACCTGAGATCCGGACTGGACTC
PKM2	reverse	GCAGATGTTCTTGTAGTCCAGCCAC
LDHA	forward	GGATCTCCAGCATGGCAGCC
LDHA	reverse	CTCTCCCCCTCTTGCTGACGG
Glut1	forward	GCTGTGGGAGGAGCAGTGC
Glut1	reverse	TGGATGGGATGGGCTCTCCG
PDK1	forward	CCTTAGAGGGCTACGGGACAGATG
PDK1	reverse	CACCAGTCGTCAGCCTCGTG
Bcl2	forward	TGACTGAGTACCTGAACCGGCATC
Bcl2	reverse	CCAGGCTGAGCAGGGTCTTCA
Bcl2	forward	GACAACATCGCCCTGTGGATGAC
Bcl2	reverse	TCAAACAGAGGTCGCATGCTGG
Bax	forward	GCCCCAGGATGCGTCCAC
Bax	reverse	GAGTCCGTGTCCACGTCAGC
Trp53	forward	CTGGGCTTCCTGCAGTCTGG
Trp53	reverse	ACCCACAACTGCACAGGGC
Becn1	forward	CTCGCCAGGATGGTGTCTCTCG
Becn1	reverse	GAGTCTCCGGCTGAGGTTCTCC
Bnip3	forward	GCCCAGCATGAATCTGGACGAAG
Bnip3	reverse	CTCGCCAAAGCTGTGGCTGTC
Bnip3l	forward	GCAGACTGGGTATCAGACTGGTCC
Bnip3l	reverse	GGCTCCACTCTTCCTCATGCTTAGAG
P300	forward	GCTTGCGGACTGCAGTCTATCATG
P300	reverse	CTGGGTGGACAGGCCCAGA
FIH	forward	GGGCAGCTGACCTCTAACCTGTT
FIH	reverse	AGGCACTCGAACTGATCCGGAG
CBP	forward	CACATGACACATTGTCAGGCTGGG
CBP	reverse	CAGGACAGTCATGTCGTGTGCAG

(21% O_2, 5% CO_2) or under reduced oxygen (0.5% O_2, 5% CO_2) conditions. In the following, we refer to this reduced oxygen condition as hypoxia. We analyzed the HIF1α protein level of the infected cells, kept under different oxygen conditions, by immunoblot analysis. Under normoxia, HIF1α is constantly degraded. However, the infection with *C. burnetii* for 4 h resulted in transient stabilization of HIF1α, which was almost absent at 24 h post-infection (**Figures 1A, B**). Under hypoxia, we observed HIF1α protein accumulation in uninfected cells at 4 and 24 h, which was further augmented by infection with *C. burnetii*. Importantly, lipopolysaccharide (LPS) stimulation also led to HIF1α stabilization under normoxia and, more pronounced, under hypoxia (**Figures 1C, D**). Thus, the *C. burnetii*-mediated HIF1α stabilization might be partially due to the recognition of LPS. However, we used LPS from *E. coli*. Thus, the comparison has to be taken with caution, as the lipid A of *C. burnetii* LPS differs significantly from enterobacterial lipid A and fails to signal via toll-like receptor (TLR) 2 and 4 (Zamboni et al., 2004; Abnave et al., 2017; Beare et al., 2018). The fact, that *C. burnetii* infection increased HIF1α stabilization, prompted us to analyze the impact of bacterial load on HIF1α stabilization. Therefore, we infected BMDM at an MOI of 10, 50 or 100 under hypoxia and analyzed the infection by immunofluorescence and the HIF1α protein level by immunoblot. As shown in **Figure 2A**, the increased MOI led to a higher bacterial load. Importantly, the increase in bacterial load did not result in increased HIF1α stabilization at 4 h post-infection (**Figure 2B**). However, at 24 h and 48 h post-infection, the increasing infection dose seemed to result in higher HIF1α protein levels (**Figures 2B, C**). Moreover, at an MOI of 10, HIF1α stabilization decreases during the course of the infection. Thus, not only the oxygen level influences HIF1α stabilization, but also the pathogen seems to modulate this important transcription factor. This hypothesis prompted us to determine whether bacterial viability is required for affecting HIF1α stabilization.

C. burnetii Curtails Infection-Induced HIF1α Stabilization

To analyze the role of *C. burnetii* in HIF1α stabilization, we infected BMDM at an MOI of 10 with either untreated *C. burnetii*, heat-killed *C. burnetii*, *C. burnetii* treated with chloramphenicol to inhibit bacterial protein synthesis or *E. coli* at an MOI of 10. In normoxic BMDM, *C. burnetii* led to HIF1α stabilization only at 4 h post-infection (**Figure 3A**). As this was observed regardless of the viability or physiological state of the pathogen, we assumed that this might be the reaction of the host cell to a pathogen associated molecular pattern (PAMP). This is in line with observations that microbial products, such as LPS, induce HIF1α accumulation also in the presence of O_2 (Blouin et al., 2004; Werth et al., 2010). The fact that HIF1α is degraded in infected normoxic macrophages at later time points of infection might be due to the intracellular lifestyle of *C. burnetii*, which hides in an intracellular vacuole (Pechstein et al., 2017). Importantly, under hypoxic conditions the infection with *E. coli* induced a higher HIF1α protein level at 4 and 24 h post-infection compared to the infection with viable *C. burnetii*, indicating that *C. burnetii* might be able to restrict HIF1α accumulation. Similarly, at 48 h post-infection, the HIF1α protein level was increased in hypoxic BMDM infected with heat-killed *C. burnetii* compared to BMDM infected with viable *C. burnetii* (**Figures 3A, B**). We hypothesized that *C. burnetii* might be able to actively curtail HIF1α accumulation under hypoxic conditions. The observation that hypoxic BMDM infected with chloramphenicol-treated bacteria showed an increased HIF1α level too, suggests that bacterial protein synthesis is important for *C. burnetii*-mediated restriction of HIF1α.

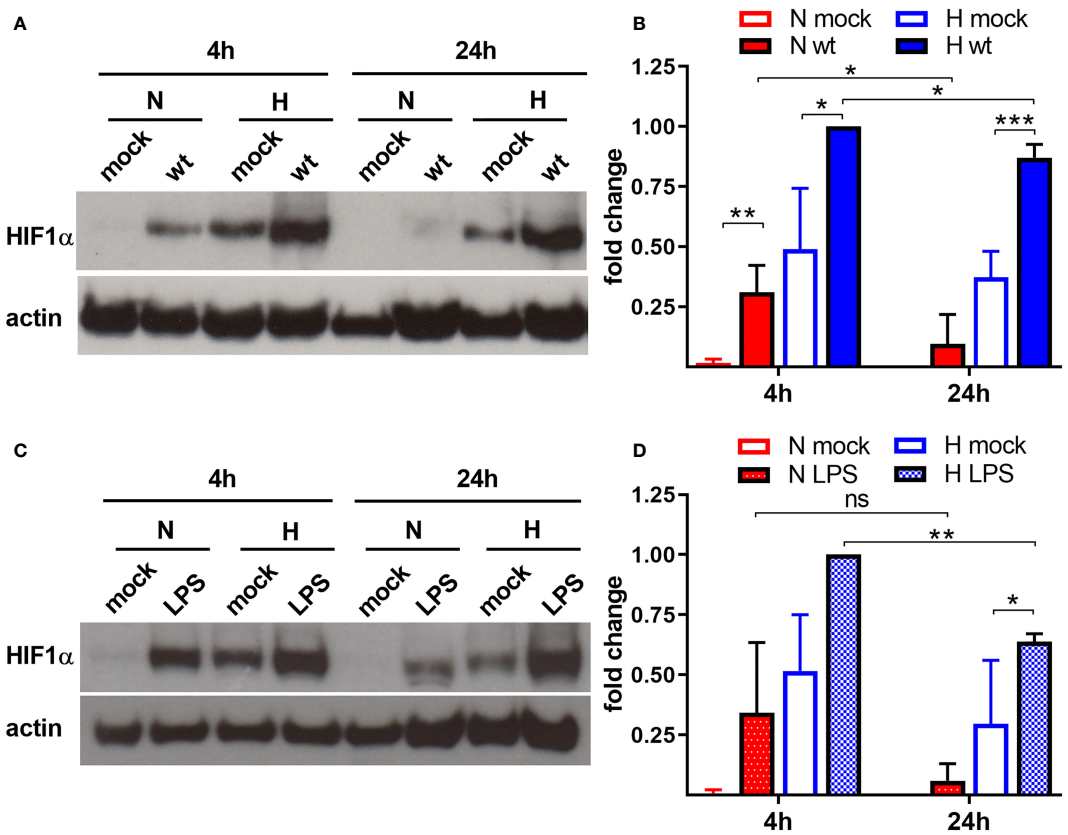

FIGURE 1 | *C. burnetii* and LPS boost HIF1α stabilization. **(A, B)** Murine BMDM either uninfected (mock) or infected with *C. burnetii* (wt) for 4 and 24 h under normoxia (N) or hypoxia (H) were analyzed by immunoblot analysis using antibodies against HIF1α and actin as loading control. **(A)** One representative experiment out of four independent experiments is shown. **(B)** Densitometric analysis of the HIF1α/actin ratio was performed using ImageJ. Fold changes are shown relative to cells infected for 4 hours under (H) Mean ± SD, n = 4, one-sample t test or t test. ***p < 0.001, **p < 0.01, *p < 0.05. **(C, D)** Murine BMDM either untreated (mock) or treated with LPS (100 ng/ml) for 4 and 24 h under N or H were analyzed by immunoblot analysis using antibodies against HIF1α and actin as loading control. **(C)** One representative experiment out of three independent experiments is shown. **(D)** Densitometric analysis of the HIF1α/actin ratio was performed using ImageJ. Fold changes are shown relative to cells treated with LPS for 4 hours under (H) Mean ± SD, n = 3, one-sample t test or t test. **p < 0.01, *p < 0.05, ns = non-significant.

C. burnetii Reduces HIF1α Accumulation in a T4SS-Dependent Manner

C. burnetii utilizes a type IV secretion system (T4SS) to inject bacterial effector proteins into the host cell to modify host cell pathways for the benefit of the pathogen (Lührmann et al., 2017). Bacteria lacking a functional T4SS are unable to replicate intracellularly, confirming that T4SS-driven modulation of host cell pathways is essential (Beare et al., 2011; Carey et al., 2011). Importantly, inhibition of bacterial protein synthesis by chloramphenicol-treatment also impairs T4SS function (Pan et al., 2008). Therefore, we asked whether the ability of *C. burnetii* to reduce HIF1α protein level under hypoxic conditions depends on the T4SS. We focused on hypoxic conditions, as, under normoxia, HIF1α is degraded starting at 24 h post-infection regardless of the pathogen viability (**Figure 3A**). Four hours of infection with the wild-type and the T4SS mutant (Δ*dotA*) similarly augmented hypoxia-induced HIF1α stabilization. Starting from 24 h post-infection, we detected increased HIF1α stabilization in hypoxic BMDM infected with the Δ*dotA* mutant (**Figures 4A, B**). Importantly, this was not mediated by differences in replication ability, as we did not observe any bacterial replication during the course of infection (**Figure 4C**). This is in line with our previous results, showing that *C. burnetii* is unable to replicate in hypoxic BMDM (Hayek et al., 2019). Taken together, our results suggest that *C. burnetii* infection results in HIF1α stabilization under hypoxia. However, viable *C. burnetii* are able to control HIF1α level in a T4SS-dependent manner.

The T4SS Is Dispensable for *C. burnetii*-Induced Transcriptional Modulation of *HIF1α* and *PHD1*

To determine how *C. burnetii* might be able to manipulate HIF1α stabilization, we first analyzed the mRNA levels of HIF1α, factors influencing HIF1α degradation and factors important for HIF1α transcription activation by qRT-PCR. The degradation of HIF1α is controlled by prolyl hydroxylases (PHDs), which hydroxylate HIF1α, leading to the recruitment of

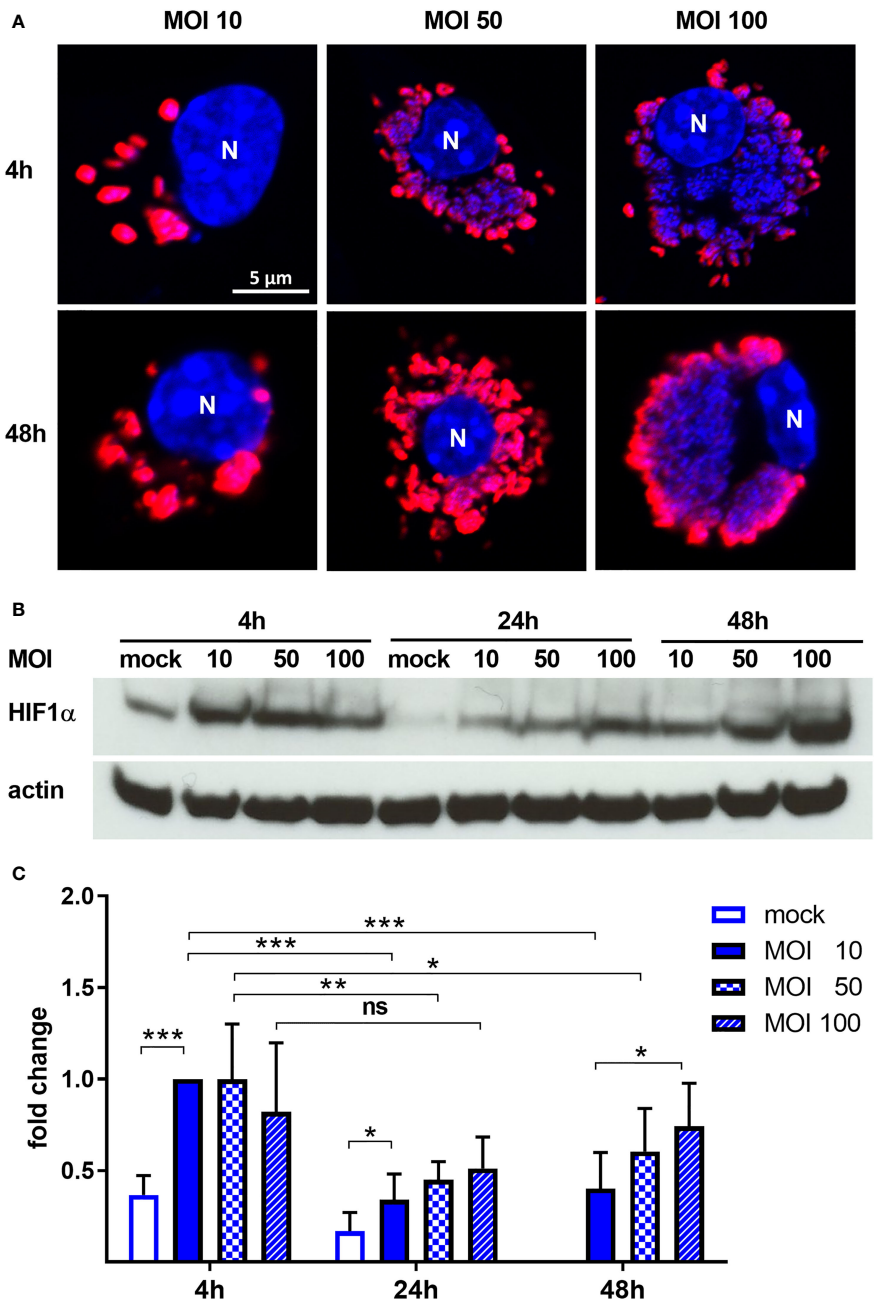

FIGURE 2 | *C. burnetii* intensifies HIF1α stabilization under hypoxia in a dose-dependent manner. **(A)** Representative immunofluorescence micrographs of murine BMDM infected with *C. burnetii* for 4 and 48 h under hypoxia at MOI 10, 50 or 100. The cells were fixed, permeabilized and stained with DAPI (blue) and anti-*C. burnetii* (red). N = nucleus. **(B, C)** BMDM infected with *C. burnetii* for 4, 24 and 48 h under hypoxia at MOI 10, 50 or 100 were analyzed by immunoblot using antibodies against HIF1α and actin as loading control. Importantly, uninfected BMDMs were only cultivated for 24 h under hypoxia, as cell viability was significantly reduced at later time points. **(B)** One representative immunoblot from 4 independent experiments is shown. **(C)** Densitometric analysis of the HIF1α/actin ratio was performed using ImageJ. Fold changes are shown relative to cells infected with MOI of 10 for 4 hours. Mean ± SD, n=6, one-sample t-test or t-test. ***$p < 0.001$, **$p < 0.01$, *$p < 0.05$, ns = $p > 0.05$.

the von Hippel-Lindau (VHL) E3 ubiquitin ligase, that ubiquitinates HIF1α targeting it for proteasomal degradation (Maxwell et al., 1999; Ohh et al., 2000; Jaakkola et al., 2001). Other factors influence HIF1α transcriptional activity: Factor Inhibiting HIF (FIH) hydroxylates HIF, preventing recruitment of p300 and CREB-binding protein (CBP) (Mahon et al., 2001), which are important for maximal transcriptional activation of HIF (Arany et al., 1996; Dyson and Wright, 2016; Pugh, 2016).

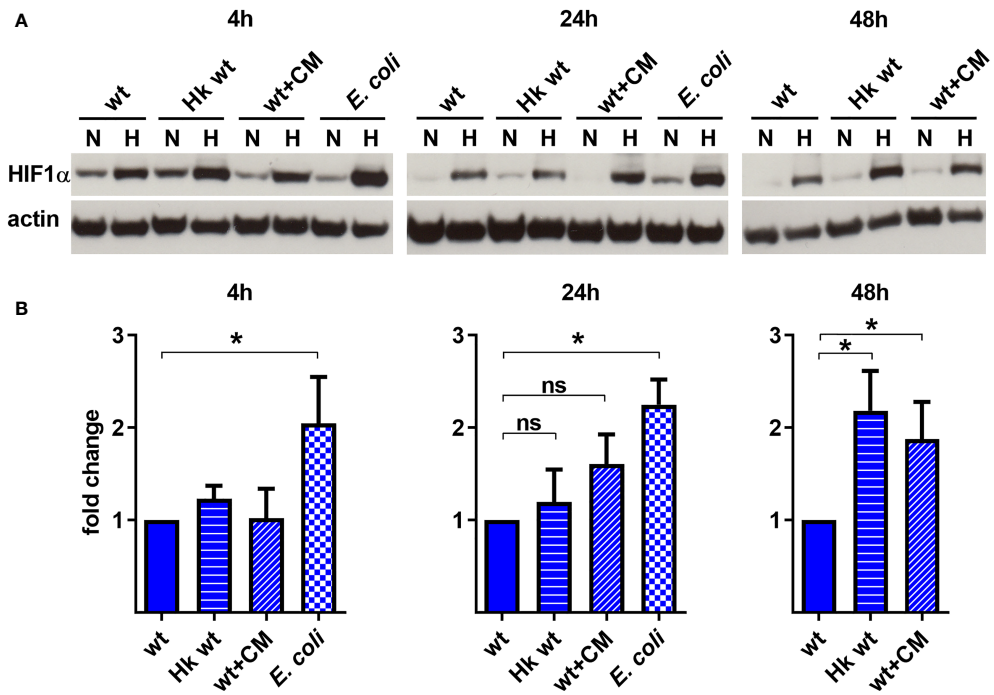

FIGURE 3 | *C. burnetii*-mediated reduction of infection-induced HIF1α depends on bacterial viability. **(A, B)** Murine BMDM infected with *C. burnetii* (wt), heat-killed *C. burnetii* (Hk), chloramphenicol-treated *C. burnetii* (CM, 25 µg/ml) or *E. coli* for 4, 24 and 48 h under normoxia (N) or hypoxia (H) were analyzed by immunoblot using antibodies against HIF1α and actin as loading control. Importantly, *E. coli* infected BMDMs were only cultivated for 24 h under hypoxia, as cell viability was significantly reduced at later time points. **(A)** One representative immunoblot from 4 independent experiments is shown. **(B)** Densitometric analysis of the HIF1α/actin ratio was performed using ImageJ. Fold changes under hypoxia (H) are shown relative to cells infected with viable bacteria. Mean ± SD, n=4, one-sample t-test. *p < 0.05, ns=p > 0.05.

A *C. burnetii* infection, but not LPS stimulation, led to upregulation of *HIF1α* expression under hypoxia regardless of the pathogen´s genotype (wild-type or Δ*dotA*) (**Figure 5**). The expression of the *PHDs* was affected differently by hypoxia. While the *PHD1* expression level was slightly increased by hypoxia, the levels of *PHD2* and *PHD3* were strongly increased, with a particularly striking induction of *PHD3*. These results are in line with previous publications (Appelhoff et al., 2004; Marxsen et al., 2004). Importantly, the infection with wild-type or Δ*dotA C. burnetii* did not alter the *PHD2* and *PHD3* expression level. The infection with both *C. burnetii* strains, but not LPS, resulted in *PHD1* upregulation under normoxic conditions (**Figure 5**). The mRNA level of *VHL* was increased by hypoxia, which was augmented by LPS and by infection with wild-type or Δ*dotA C. burnetii*. While neither the oxygen level nor the infection state influenced *FIH* and *p300* expression, we observed that LPS resulted in reduced expression of *FIH* under normoxia and hypoxia and of *p300* under normoxia (**Figure 5**). In addition, *CBP* expression was reduced in hypoxic conditions and under normoxia when infected with Δ*dotA C. burnetii* (**Figure 5**). These data demonstrate that a *C. burnetii* infection influenced *HIF1α* (H) and *PHD1* (N) mRNA levels, regardless of the T4SS and in a different manner than LPS. Furthermore, under normoxia, the infection with Δ*dotA C. burnetii*, but not with the wild-type, reduces *CBP* expression.

C. burnetii Infection Supports the Switch to Glycolysis in Macrophages

HIF1α is an important transcription factor critical for cellular metabolism, for regulation of apoptosis and autophagy and for immune responses (Cramer et al., 2003; Corcoran and O'Neill, 2016; Knight and Stanley, 2019). Therefore, we analyzed the role of oxygen availability in combination with a *C. burnetii* infection or with LPS stimulation as a control on HIF1α target gene expression. First, we concentrated on metabolic genes. As shown in **Figure 6**, oxygen limitation resulted in upregulation of *PKM2*, *LDHA*, *Glut1* and *PDK1*. These factors are involved in glucose uptake (Glut1), generation of pyruvate (PKM2), conversion of pyruvate to lactate (LDHA), and inhibition of the conversion of pyruvate to acetyl-CoA (PDK1), which indirectly increases the conversion of pyruvate to lactate. These data are in line with previous findings showing that HIF1α is essential for the switch to glycolysis in macrophages (Cramer et al., 2003). The infection with wild-type and Δ*dotA C. burnetii* increases the expression of *PKM2* and *LDHA* in normoxic and hypoxic BMDM, and the expression of *Glut1* and *PDK1* only in normoxic BMDM (**Figure 6**). Importantly, treatment with LPS resulted in a similar modulation of the expression of the metabolic genes analyzed. There were only two exceptions: 1) the infection with *C. burnetii* induced a significantly higher expression of PKM2 under hypoxia than LPS; 2) the infection with *C. burnetii*

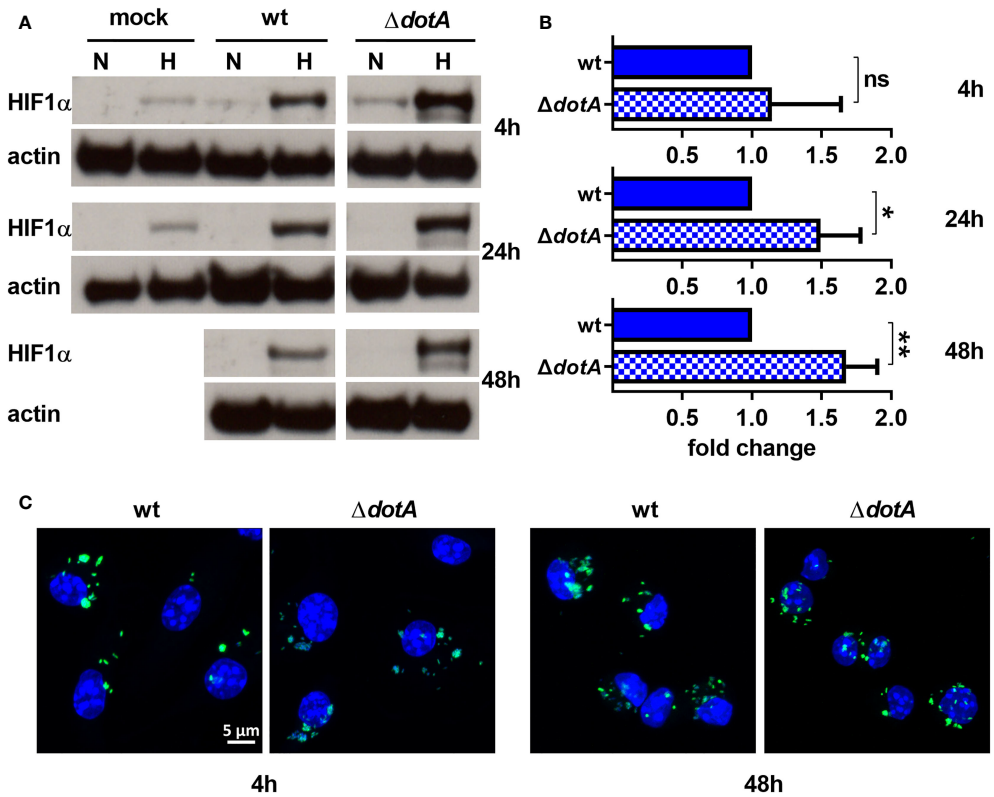

FIGURE 4 | *C. burnetii* reduces HIF1α levels in a T4SS-dependent manner. **(A, B)** Murine BMDM either uninfected (mock) or infected with *C. burnetii* (wt) or *C. burnetii* lacking a functional T4SS (Δ*dotA*) for 4, 24 and 48 h under normoxia (N) or hypoxia (H) were analyzed by immunoblot using antibodies against HIF1α and actin as loading control. Importantly, uninfected BMDMs were only cultivated for 24 h under hypoxia, as cell viability was significantly reduced at later time points. **(A)** One representative Western blot from 4 independent experiments is shown. **(B)** Densitometric analysis of the HIF1α/actin ratio was performed using ImageJ. Fold changes under hypoxia (H) are shown relative to cells infected with wt. Mean ± SD, n=4, one-sample t-test. $^{**}p < 0.01$, $^{*}p < 0.05$, ns=$p > 0.05$. **(C)** Representative immunofluorescence micrographs of murine BMDM infected with *C. burnetii* (wt) (green) or the T4SS transposon mutant (Δ*dotA*) (green) for 4 and 48 h under hypoxia are shown. The cells were fixed, permeabilized and stained with DAPI (blue).

induced a significantly higher expression of PDK1 under normoxia than LPS. These data suggest that an infection partially promotes upregulation of the metabolic target genes analyzed. How *C. burnetii* supports the switch to glycolysis mechanistically is unknown. LPS might play a role in this shift (**Figure 6**), which is in line with previous reports (Rodriguez-Prados et al., 2010).

C. burnetii Infection and Hypoxia Independently Result in a More Pro-Apoptotic Signature

Next, we analyzed HIF1α target genes involved in regulating apoptotic and autophagic cell death. We then analyzed the mRNA levels of anti-apoptotic Bcl-2, pro-apoptotic Bax and p53, which regulates ~500 target genes, thereby influencing DNA repair, cell cycle arrest, metabolism and cell death (Aubrey et al., 2018). While hypoxia decreased the expression of anti-apoptotic *Bcl-2*, it increased the expression of *Bax*. The infection with wild-type *C. burnetii* did not alter the transcription levels of *Bcl-2* and *Bax* under hypoxia. However, infection with Δ*dotA C. burnetii* resulted in down-regulation of Bcl-2 and upregulation of Bax under hypoxia. Under normoxia, the infection resulted in down-regulation of *Bcl-2* and up-regulation of *Bax* regardless of the genotype of the pathogen (**Figure 7**). This result was unexpected, as *C. burnetii* displays anti-apoptotic activity, and no influence on Bcl-2 and Bax protein levels was determined (Lührmann and Roy, 2007; Voth et al., 2007; Cordsmeier et al., 2019). However, this might be due to different cell types, primary versus cell lines, used.

Hypoxia and HIF1α regulate p53 in several ways and *vice versa* (Zhang et al., 2021). We did not find an influence of hypoxia on *p53* transcription level, but the infection under hypoxia resulted in an increased *p53* expression (**Figure 7**). Importantly, cells infected with the Δ*dotA* mutant showed a significant higher expression of *p53* compared to cells infected with wild-type *C. burnetii* (**Figure 7**).

This might be due to an increased HIF1α level in cells infected with the Δ*dotA* mutant (**Figures 4A, B**), but independent of LPS signaling, as LPS resulted in downregulation of *p53* expression under normoxia and hypoxia.

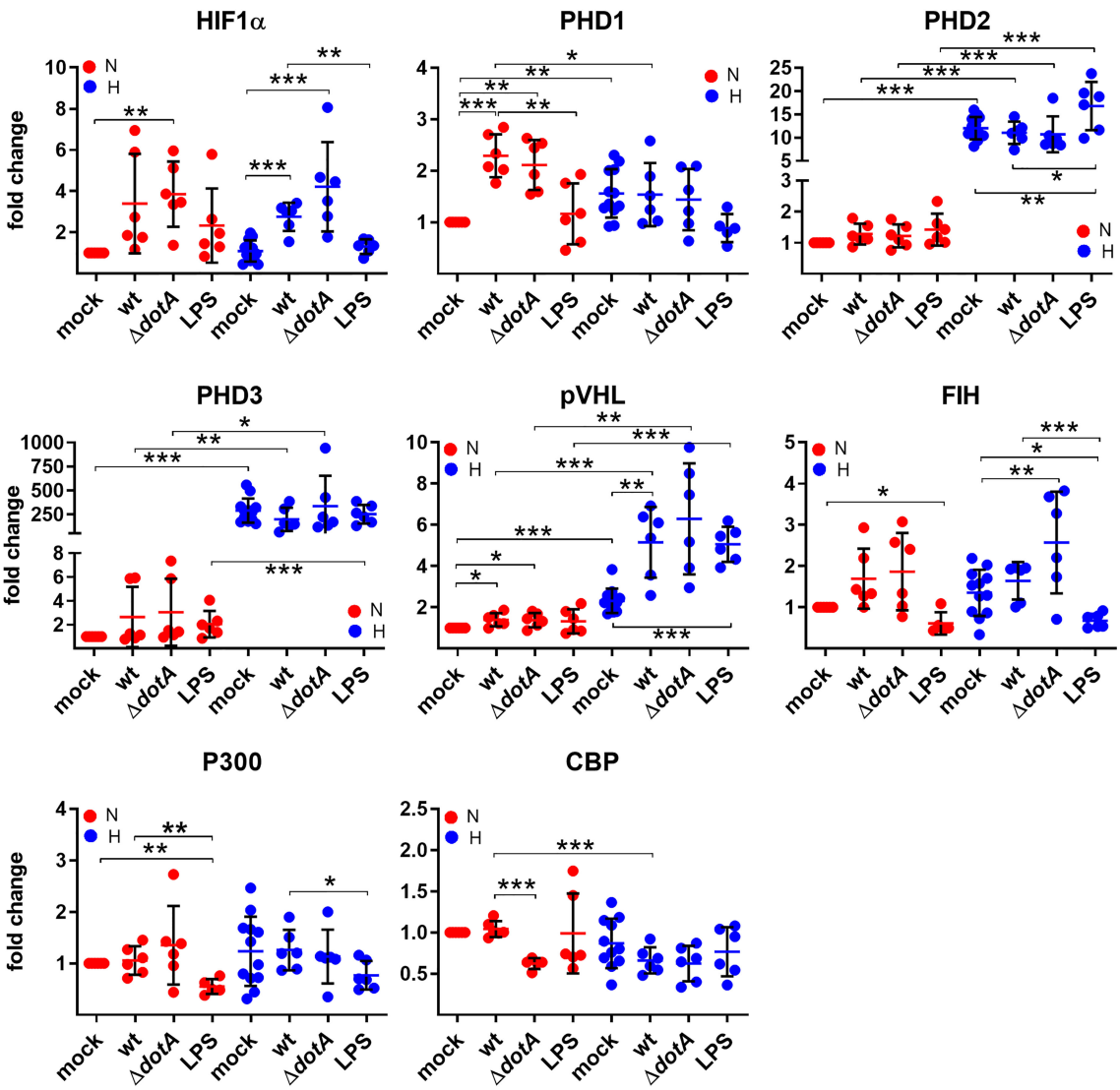

FIGURE 5 | *C. burnetii* only marginally influences the expression of genes regulating HIF1α stability. BMDM were either uninfected (mock), infected with *C. burnetii* (wt), the T4SS transposon mutant (Δ*dotA*), or treated with LPS (100 ng/ml) for 24 h under normoxia (N) and hypoxia (H). Using qRT-PCR, the gene expression of murine *HIF1α*, *PHD1*, *PHD2*, *PHD3*, *VHL*, *FIH*, *p300* and *CBP* was analyzed. The data are displayed as Mean ± SD of 2^-ΔΔCT values (using murine *HPRT1* as a calibrator). Fold changes are shown relative to uninfected cells under N. The data shown for each of the *C. burnetii* (wt and Δ*dotA*) infection experiment and the LPS treatment experiment represent 3 independent experiments with biological duplicates. One sample t test or t test, n=5-6. ***p < 0.001, **p < 0.01, *p < 0.05.

While analyzing genes involved in autophagic cell death induction, we observed an upregulation of *Beclin 1*, *Bnip3* and *Bnip3l* by hypoxia. The infection influenced the expression level of *Beclin 1*, both under normoxia and hypoxia, similarly as did LPS.

Bnip3 expression was only upregulated by a *C. burnetii* infection under normoxia, but not under hypoxia, while *Bnip3l* expression was not modulated by the infection at all. Importantly, LPS treatment resulted in significant upregulation of *Bnip3* and *Bnip3l* under hypoxia, demonstrating that *C. burnetii*-induced expression modulation of the genes analyzed was partially independent of LPS signaling (**Figure 7**). These data suggest that hypoxia and the infection with *C. burnetii* affect the apoptosis-regulators analyzed independently towards a more pro-apoptotic signature.

C. burnetii Infection Induces an Upregulation of Inflammatory Genes, Which is Shifted Under Hypoxia Towards a Pro-Inflammatory Signature

Next, we analyzed the role of hypoxia and/or a *C. burnetii* infection on the transcription of inflammatory genes. We analyzed the pro-inflammatory HIF1α target genes *IL1β*, *IL6*, *Nos2* and the anti-inflammatory gene *IL10*. In the absence of

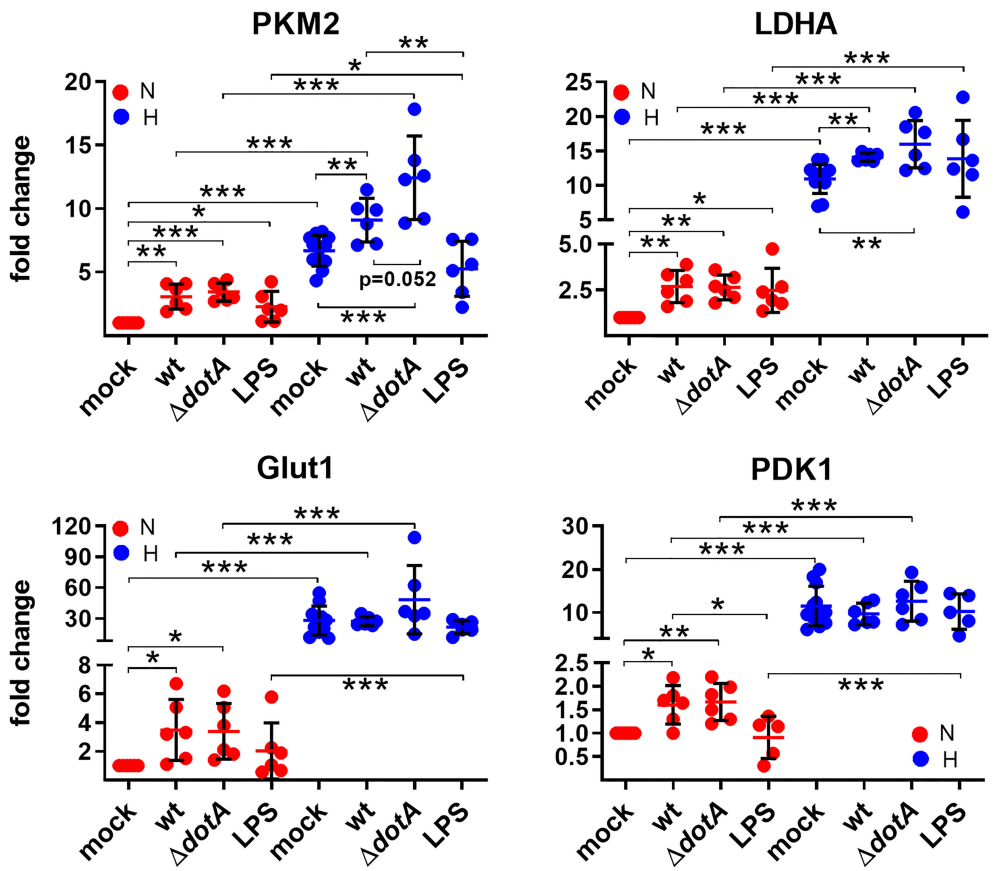

FIGURE 6 | *C. burnetii*-infected macrophages reveal a shift to glycolysis. BMDM were either uninfected (mock), infected with *C. burnetii* (wt), the T4SS transposon mutant (Δ*dotA*), or treated with LPS (100 ng/ml) for 24 h under normoxia (N) and hypoxia (H). Using qRT-PCR, the gene expression of murine *PKM2*, *LDHA*, *Glut1*, and *PDK1* was analyzed. The data are shown as Mean ± SD of 2^-ΔΔCT values (using murine *HPRT* as a calibrator). Fold changes are shown relative to uninfected cells under N. The data shown for each of the *C. burnetii* (wt and Δ*dotA*) infection experiments and the LPS treatment experiment represent 3 independent experiments with biological duplicates. One sample t test or t test, n=5-6. ***p < 0.001, **p < 0.01, *p < 0.05.

infection, we detected an increase of *IL1β* and a decrease in *IL10*, when comparing normoxia versus hypoxia (**Figure 8**), which is in line with the observation that the HIF pathway regulates cytokine production in multiple cell types (Malkov et al., 2021). In contrast, the infection increased the expression of all genes analyzed. While the expression of the pro-inflammatory genes was increased under hypoxia compared to under normoxia, this was the opposite for the anti-inflammatory gene *IL10* (**Figure 8**). Importantly, the *C. burnetii* infection resulted in significantly stronger induction of *IL10* under normoxia than the LPS treatment. In contrast, the combination of hypoxia and LPS treatment resulted in an upregulation of *IL6* expression by ~9 fold, while the combination of hypoxia and *C. burnetii* infection only led to a ~3 fold upregulation. However, we did not detect a difference between BMDM infected with the wild-type or the T4SS mutant, indicating that the effect of *C. burnetii* on inflammatory HIF1α-target genes is independent of the T4SS. Thus, our data indicates that the *C. burnetii* infection results in upregulation of pro- and anti-inflammatory genes. Importantly, under hypoxia, the expression profile of the genes analyzed shifts towards a pronounced pro-inflammatory signature.

DISCUSSION

While HIF1α was first identified as an essential regulator of hypoxia (Majmundar et al., 2010), it is now clear that this transcription factor is also activated by several human pathogens even under normoxia (Werth et al., 2010). As HIF1α regulates cellular metabolism, immune cell activity, and inflammatory responses (Knight and Stanley, 2019), it is a central player during host-pathogen interaction.

Thus, it is not surprising that several pathogens have evolved proteins that modulate HIF1α activity (Knight and Stanley, 2019). For example, the *Salmonella enterica* siderophore Sal activates HIF1 (Hartmann et al., 2008), as does BadA from *Bartonella henselae* (Riess et al., 2004). In contrast, the AQ signaling molecule from *Pseudomonas aeruginosa* leads to

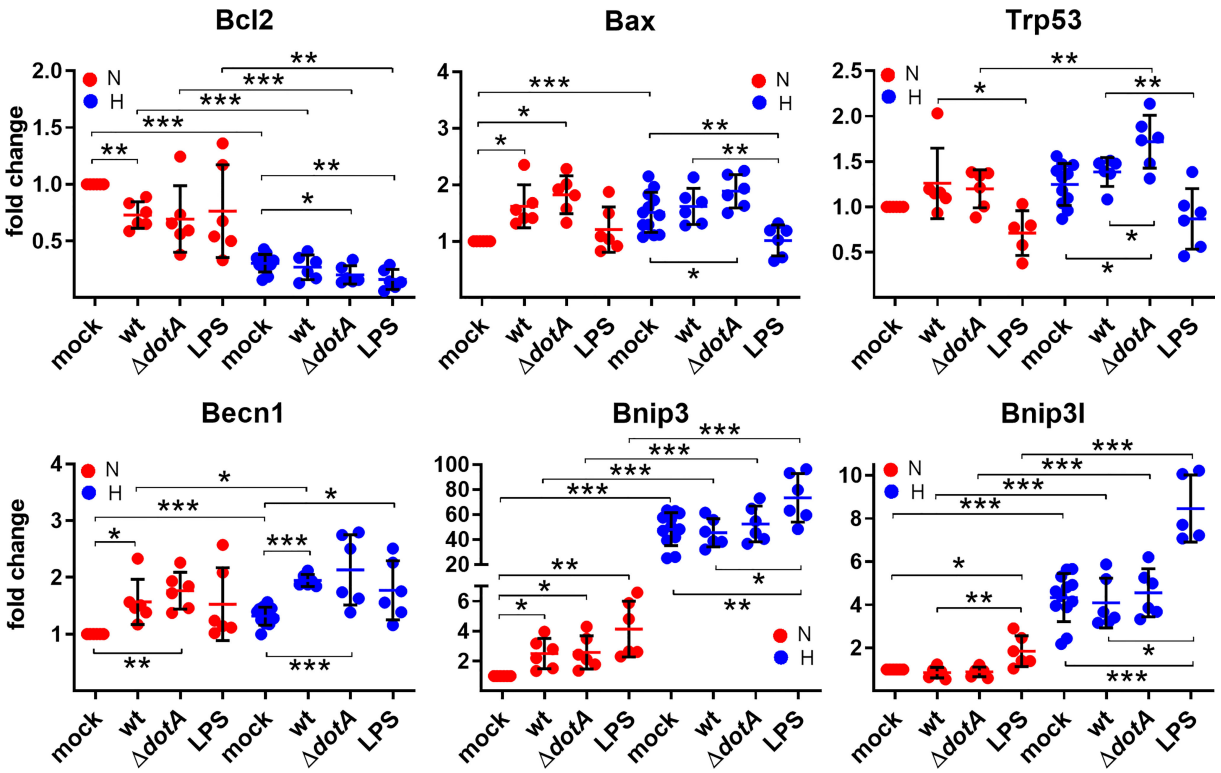

FIGURE 7 | A pro-apoptotic expression signature is more prominent in *C. burnetii*-infected or hypoxic macrophages. BMDM were either uninfected (mock), infected with *C. burnetii* (wt), the T4SS transposon mutant (Δ*dotA*), or treated with LPS (100 ng/ml) for 24 h under normoxia (N) and hypoxia (H). Using qRT-PCR, the gene expression of murine *Bcl2*, *Bax*, *Trp53*, *Becn1*, *Bnip3*, and *Bnip3l* was analyzed. The data are depicted as Mean ± SD of 2^-ΔΔCT values (using murine *HPRT* as a calibrator). Fold changes are shown relative to uninfected cells under N. The data shown for each of the *C. burnetii* (wt and Δ*dotA*) infection experiments and the LPS treatment experiment represent 3 independent experiments with biological duplicates. One sample t test or t test, n=5-6. ***p < 0.001, **p < 0.01, *p < 0.05.

proteasomal degradation of HIF1 (Legendre et al., 2012). These examples demonstrate that dependent on the nature and requirements of the respective pathogen, the ability to interfere with HIF1 is distinct.

We recently showed that HIF1α is responsible for controlling *C. burnetii* infection in an *in vitro* infection model using primary murine and human macrophages (Hayek et al., 2019). However, although HIF1α was proven beneficial for limiting bacterial replication (Hayek et al., 2021), it did not affect the cell´s ability to clear *C. burnetii* (Hayek et al., 2019). This is in line with previous observations that hypoxia and/or HIF1α induce a state of bacterial persistence and dormancy, which might impair bacterial clearance and allow the emergence of reoccurring or chronic infections (Sershen et al., 2016; Hayek et al., 2019; Hayek et al., 2021).

Here, we show that *C. burnetii* is able to curtail HIF1α, which depends on bacterial viability and protein synthesis (**Figures 3A, B**). The data suggests that the T4SS is involved (**Figures 4A, B**) indicating that a bacterial factor is required for this activity. The T4SS, an essential virulence factor of *C. burnetii*, injects over 150 effector proteins into the host cell to manipulate several host cell pathways enabling the pathogen to survive and replicate intracellularly (Lührmann et al., 2017). Only a few of these effector proteins have been functionally characterized. They interfere with host cell transcription, apoptosis, pyroptosis, ER stress, autophagy, and vesicular trafficking (Cordsmeier et al., 2019; Burette and Bonazzi, 2020b; Thomas et al., 2020; Dragan and Voth, 2020). The effector protein(s) involved in destabilizing HIF1α is currently unknown. The reason why increasing infection rates, which most likely result in increased numbers of secreted effector proteins, did not result in increased HIF1α degradation (**Figures 2B, C**), is currently unknown. It might be the balance between activation by PAMPs and dampening by effector proteins. As we could not show the biological consequence of the T4SS-dependent HIF1α destabilization (**Figures 5 – 8**), we hypothesize that HIF1α destabilization might be a side effect and not the primary function of a so far unknown effector protein. Thus, an effector protein interfering with the NF-κB signaling pathway might be involved, as NF-κB regulates HIF1α (Rius et al., 2008). Importantly, NF-κB modulation by the *C. burnetii* T4SS has been described (Mahapatra et al., 2016) and recently the *C. burnetii* T4SS effector protein NopA was identified to perturb NF-κB activation (Burette et al., 2020a). Thus, it can be speculated that NopA or a so far unknown effector protein might be indirectly involved in HIF1α activation. The increased level of

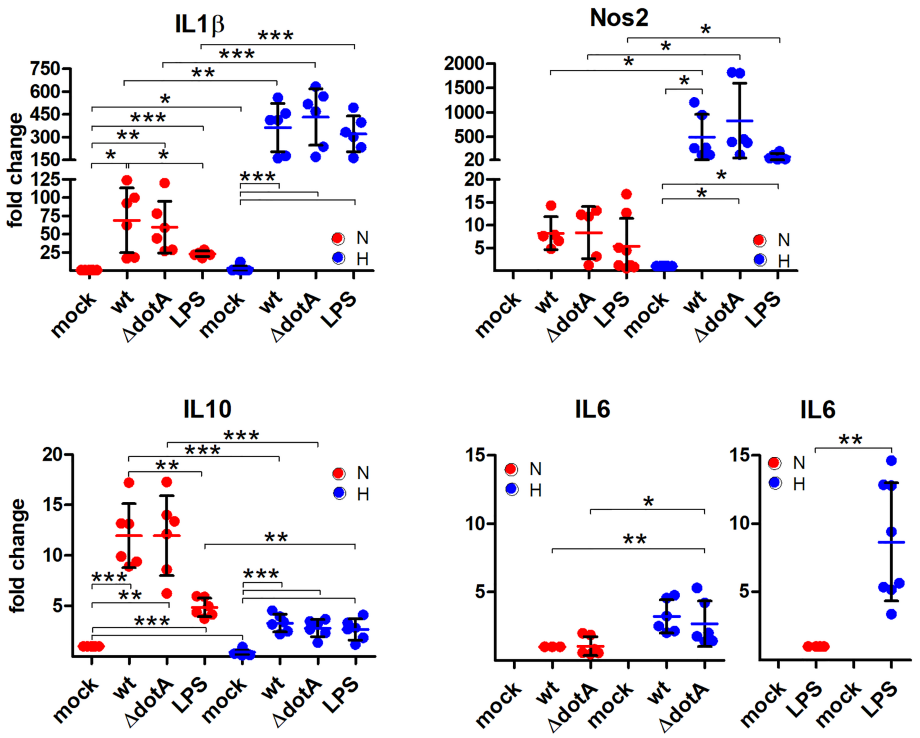

FIGURE 8 | A pro-inflammatory profile is observed through *C. burnetii* infection under hypoxia. BMDM were either uninfected (mock), infected with *C. burnetii* (wt), the T4SS transposon mutant (Δ*dotA*), or treated with LPS (100 ng/ml) for 24 h under normoxia (N) and hypoxia (H). Using qRT-PCR, the gene expression of murine *IL1β*, *Nos2*, *IL10*, and *IL6* was analyzed. The data are plotted as Mean ± SD of 2^-ΔΔCT values (using murine *HPRT* as a calibrator). In case of *IL1β* and *IL10*, fold changes are shown relative to uninfected cells under N, while for *Nos2* they are represented relative to uninfected cells under H. For *IL6*, fold changes are shown relative to wt-infected cells or LPS-treated cells under N. The data shown for each of the *C. burnetii* (wt and Δ*dotA*) infection experiments and the LPS treatment experiment represent 3 independent experiments with biological duplicates. One sample t test or t test, n=5-6. ***p < 0.001, **p < 0.01, *p < 0.05.

HIF1α in cells infected with the T4SS mutant (Δ*dotA*) in comparison to cells infected with wild-type *C. burnetii* did not correlate with differences in the expression levels of HIF1α modulators (**Figure 5**), suggesting that a so far unknown effector protein might not interfere with the expression of HIF1α modulators. It might be possible that the effector protein interferes with the enzymatic activity of the PHDs or the availability of PHD co-factors (Siegert et al., 2015). Further research will be necessary to determine the molecular mechanisms leading to T4SS-dependent reduction of *C. burnetii*-induced HIF1α stabilization.

Nevertheless, we did not detect a difference in the expression of most of the HIF1α target genes analyzed in BMDM infected with either wild-type *C. burnetii* or the Δ*dotA* mutant (**Figures 6** – **8**), suggesting that the HIF1α protein level does not correlate with the level of HIF1α target gene expression. This was an unexpected finding, as correlation between HIF1α protein level and HIF1α target gene expression has been reported (Lee and Thorgeirsson, 2004; Lv et al., 2021). However, those reports analyzed the role of HIF1α in cancer or in cell lines, while we analyzed the role of HIF1α in primary cells during infection. Infected tissue is commonly found to be hypoxic, which triggers HIF1α stabilization (Jantsch and Schödel, 2015), and pathogens or their products are known to trigger HIF1α accumulation also under normoxia. In addition, bacterial products also activate transcription factors that might act synergistically or antagonistically with HIF1α (Hayek et al., 2021). Importantly, our data clearly demonstrates that the *C. burnetii* infection under hypoxia leads to upregulation of the pro-inflammatory genes *IL1β*, *IL6* and *Nos2*, and to downregulation of the anti-inflammatory gene *IL10* (**Figure 8**). This is in line with reports that HIF1α is required for mounting a pro-inflammatory response to bacterial and fungal pathogens (Peyssonnaux et al., 2005; Tannahill et al., 2013; Mills et al., 2016; Li et al., 2018). Especially the increased expression of *Nos2* and *IL1β* might be of biological consequence for the *C. burnetii* infection. The homodimeric enzyme NOS2 converts L-arginine and oxygen into L-citrulline and nitric oxide (NO) (Bogdan, 2015). The latter is important for controlling bacterial infections (Nathan and Shiloh, 2000), including a *C. burnetii* infection (Howe et al., 2002; Zamboni and Rabinovitch, 2003; Brennan et al., 2004). IL1β is produced as an inactive pro-form, which has to be cleaved to its active form following inflammasome activation (Dinarello, 2018). *C. burnetii* avoids activation of the inflammasome, and thus, pyroptosis (Cunha et al., 2015; Delaney et al., 2021). However, whether *C. burnetii* is able to prevent IL1β

secretion induced by potent inflammasome stimuli has to be clarified, as conflicting reports exist (Cunha et al., 2015; Delaney et al., 2021). Of note, NO was found to inhibit the NLRP3 inflammasome-dependent processing of IL1β (Mishra et al., 2013). Thus, it will be of importance to analyze whether not only the expression of IL1β is increased, but also its secretion. In addition, we have to elucidate whether the increased levels of NO in hypoxic *C. burnetii* infected BMDM might inhibit IL1β processing and secretion.

In summary, our data demonstrate that *C. burnetii* influences HIF1α stability and activity. As HIF1α is important for mounting anti-bacterial responses, this might have consequences for the host-pathogen interaction and, thus, disease outcome.

DATA AVAILABILITY STATEMENT

The original contributions presented in the study are included in the article. Further inquiries can be directed to the corresponding author.

AUTHOR CONTRIBUTIONS

IH and MS performed the experiments and analyzed the data. AL and IH conceived the study. AL obtained funding, supervised the study and drafted the manuscript. All authors contributed to the writing of the manuscript.

FUNDING

This work was supported by the Deutsche Forschungsgemeinschaft (DFG) through the Collaborative Research Initiative 1181 (CRC1181) project A06 to AL. IH was partially funded by the Bavarian Equal Opportunities Sponsorship – Realisierung von Chancengleichheit von Frauen in Forschung und Lehre (FFL) – Realization Equal Opportunities for Women in Research and Teaching.

ACKNOWLEDGMENTS

This work was supported by the Deutsche Forschungsgemeinschaft (DFG) through the Collaborative Research Initiative 1181 (CRC1181) project A06 to AL. We thank all members of the Lührmann, Soulat and Petter labs for discussions, Christian Berens for critically reading the manuscript, Matteo Bonazzi (IRIM, CNRS, Université de Montpellier, France) for providing *C. burnetii* transposon mutants, and Philipp Tripal (Optical Imaging Center Erlangen (OICE)) for support with confocal microscopy.

REFERENCES

Abnave, P., Muracciole, X., and Ghigo, E. (2017). *Coxiella burnetii* Lipopolysaccharide: What Do We Know? *Int. J. Mol. Sci.* 18, 2509. doi: 10.3390/ijms18122509

Anderson, A., Bijlmer, H., Fournier, P. E., Graves, S., Hartzell, J., Kersh, G. J., et al. (2013).). Diagnosis and Management of Q Fever–United States 2013: Recommendations From CDC and the Q Fever Working Group. *MMWR. Recommend. Rep.* 62, 1–30.

Appelhoff, R. J., Tian, Y. M., Raval, R. R., Turley, H., Harris, A. L., Pugh, C. W., et al. (2004). Differential Function of the Prolyl Hydroxylases PHD1, PHD2, and PHD3 in the Regulation of Hypoxia-Inducible Factor. *J. Biol. Chem.* 279, 38458–38465. doi: 10.1074/jbc.M406026200

Arany, Z., Huang, L. E., Eckner, R., Bhattacharya, S., Jiang, C., Goldberg, M. A., et al. (1996). An Essential Role for P300/CBP in the Cellular Response to Hypoxia. *Proc. Natl. Acad. Sci. U. S. A.* 93, 12969–12973. doi: 10.1073/pnas.93.23.12969

Aubrey, B. J., Kelly, G. L., Janic, A., Herold, M. J., and Strasser, A. (2018). How Does P53 Induce Apoptosis and How Does This Relate to P53-Mediated Tumour Suppression? *Cell Death Differ.* 25, 104–113. doi: 10.1038/cdd.2017.169

Beare, P. A., Gilk, S. D., Larson, C. L., Hill, J., Stead, C. M., Omsland, A., et al. (2011). Dot/Icm Type IVB Secretion System Requirements for Coxiella Burnetii Growth in Human Macrophages. *MBio* 2, e00175–e00111. doi: 10.1128/mBio.00175-11

Beare, P. A., Jeffrey, B. M., Long, C. M., Martens, C. M., and Heinzen, R. A. (2018). Genetic Mechanisms of *Coxiella burnetii* Lipopolysaccharide Phase Variation. *PLoS Pathog.* 14, e1006922. doi: 10.1371/journal.ppat.1006922

Blouin, C. C., Page, E. L., Soucy, G. M., and Richard, D. E. (2004). Hypoxic Gene Activation by Lipopolysaccharide in Macrophages: Implication of Hypoxia-Inducible Factor 1alpha. *Blood* 103, 1124–1130. doi: 10.1182/blood-2003-07-2427

Bogdan, C. (2015). Nitric Oxide Synthase in Innate and Adaptive Immunity: An Update. *Trends Immunol.* 36, 161–178. doi: 10.1016/j.it.2015.01.003

Brennan, R. E., Russell, K., Zhang, G., and Samuel, J. E. (2004). Both Inducible Nitric Oxide Synthase and NADPH Oxidase Contribute to the Control of Virulent Phase I Coxiella Burnetii Infections. *Infect. Immun.* 72, 6666–6675. doi: 10.1128/IAI.72.11.6666-6675.2004

Burette, M., Allombert, J., Lambou, K., Maarifi, G., Nisole, S., Di Russo Case, E., et al. (2020a). Modulation of Innate Immune Signaling by a Coxiella Burnetii Eukaryotic-Like Effector Protein. *Proc. Natl. Acad. Sci. U. S. A.* 117, 13708–13718. doi: 10.1073/pnas.1914892117

Burette, M., and Bonazzi, M. (2020b). From Neglected to Dissected: How Technological Advances are Leading the Way to the Study of Coxiella Burnetii Pathogenesis. *Cell Microbiol.* 22, e13180. doi: 10.1111/cmi.13180

Carey, K. L., Newton, H. J., Lührmann, A., and Roy, C. R. (2011). The Coxiella Burnetii Dot/Icm System Delivers a Unique Repertoire of Type IV Effectors Into Host Cells and is Required for Intracellular Replication. *PLoS Pathog.* 7, e1002056. doi: 10.1371/journal.ppat.1002056

Corcoran, S. E., and O'Neill, L. A. (2016). HIF1alpha and Metabolic Reprogramming in Inflammation. *J. Clin. Invest.* 126, 3699–3707. doi: 10.1172/JCI84431

Cordsmeier, A., Wagner, N., Lührmann, A., and Berens, C. (2019). Defying Death - How Coxiella Burnetii Copes With Intentional Host Cell Suicide. *Yale J. Biol. Med.* 92, 619–628. doi: 10.1038/cdd.2017.169

Cramer, T., Yamanishi, Y., Clausen, B. E., Forster, I., Pawlinski, R., Mackman, N., et al. (2003). HIF-1alpha is Essential for Myeloid Cell-Mediated Inflammation. *Cell* 112, 645–657. doi: 10.1016/S0092-8674(03)00154-5

Cunha, L. D., Ribeiro, J. M., Fernandes, T. D., Massis, L. M., Khoo, C. A., Moffatt, J. H., et al. (2015). Inhibition of Inflammasome Activation by Coxiella Burnetii Type IV Secretion System Effector IcaA. *Nat. Commun.* 6, 10205. doi: 10.1038/ncomms10205

Delaney, M. A., Hartigh, A. D., Carpentier, S. J., Birkland, T. P., Knowles, D. P., Cookson, B. T., et al. (2021). Avoidance of the NLRP3 Inflammasome by the Stealth Pathogen, Coxiella Burnetii. *Vet. Pathol.* 58, 624–642. doi: 10.1177/0300985820981369

Devraj, G., Beerlage, C., Brune, B., and Kempf, V. A. (2017). Hypoxia and HIF-1 Activation in Bacterial Infections. *Microbes Infect.* 19, 144–156. doi: 10.1016/j.micinf.2016.11.003

Dinarello, C. A. (2018). Overview of the IL-1 Family in Innate Inflammation and Acquired Immunity. *Immunol. Rev.* 281, 8–27. doi: 10.1111/imr.12621

Dragan, A. L., and Voth, D. E. (2020). Coxiella Burnetii: International Pathogen of Mystery. *Microbes Infect.* 22, 100–110. doi: 10.1016/j.micinf.2019.09.001

Dyson, H. J., and Wright, P. E. (2016). Role of Intrinsic Protein Disorder in the Function and Interactions of the Transcriptional Coactivators CREB-Binding Protein (CBP) and P300. *J. Biol. Chem.* 291, 6714–6722. doi: 10.1074/jbc.R115.692020

Greer, S. N., Metcalf, J. L., Wang, Y., and Ohh, M. (2012). The Updated Biology of Hypoxia-Inducible Factor. *EMBO J.* 31, 2448–2460. doi: 10.1038/emboj.2012.125

Gustafsson, M. V., Zheng, X., Pereira, T., Gradin, K., Jin, S., Lundkvist, J., et al. (2005). Hypoxia Requires Notch Signaling to Maintain the Undifferentiated Cell State. *Dev. Cell* 9, 617–628. doi: 10.1016/j.devcel.2005.09.010

Harris, R. J., Storm, P. A., Lloyd, A., Arens, M., and Marmion, B. P. (2000). Long-Term Persistence of Coxiella Burnetii in the Host After Primary Q Fever. *Epidemiol. Infect.* 124, 543–549. doi: 10.1017/S0950268899003763

Hartmann, H., Eltzschig, H. K., Wurz, H., Hantke, K., Rakin, A., Yazdi, A. S., et al. (2008). Hypoxia-Independent Activation of HIF-1 by Enterobacteriaceae and Their Siderophores. *Gastroenterology* 134, 756–767. doi: 10.1053/j.gastro.2007.12.008

Hayek, I., Fischer, F., Schulze-Luehrmann, J., Dettmer, K., Sobotta, K., Schatz, V., et al. (2019). Limitation of TCA Cycle Intermediates Represents an Oxygen-Independent Nutritional Antibacterial Effector Mechanism of Macrophages. *Cell Rep.* 26, 3502–3510, e3506. doi: 10.1016/j.celrep.2019.02.103

Hayek, I., Schatz, V., Bogdan, C., Jantsch, J., and Lührmann, A. (2021). Mechanisms Controlling Bacterial Infection in Myeloid Cells Under Hypoxic Conditions. *Cell Mol. Life Sci.* 78, 1887–1907. doi: 10.1007/s00018-020-03684-8

Hewitson, K. S., Lienard, B. M., McDonough, M. A., Clifton, I. J., Butler, D., Soares, A. S., et al. (2007). Structural and Mechanistic Studies on the Inhibition of the Hypoxia-Inducible Transcription Factor Hydroxylases by Tricarboxylic Acid Cycle Intermediates. *J. Biol. Chem.* 282, 3293–3301. doi: 10.1074/jbc.M608337200

Howe, D., Barrows, L. F., Lindstrom, N. M., and Heinzen, R. A. (2002). Nitric Oxide Inhibits Coxiella Burnetii Replication and Parasitophorous Vacuole Maturation. *Infect. Immun.* 70, 5140–5147. doi: 10.1128/IAI.70.9.5140-5147.2002

Jaakkola, P., Mole, D. R., Tian, Y. M., Wilson, M. I., Gielbert, J., Gaskell, S. J., et al. (2001). Targeting of HIF-Alpha to the Von Hippel-Lindau Ubiquitylation Complex by O2-Regulated Prolyl Hydroxylation. *Science* 292, 468–472. doi: 10.1126/science.1059796

Jantsch, J., and Schödel, J. (2015). Hypoxia and Hypoxia-Inducible Factors in Myeloid Cell-Driven Host Defense and Tissue Homeostasis. *Immunobiology* 220, 305–314. doi: 10.1016/j.imbio.2014.09.009

Kaidi, A., Williams, A. C., and Paraskeva, C. (2007). Interaction Between Beta-Catenin and HIF-1 Promotes Cellular Adaptation to Hypoxia. *Nat. Cell Biol.* 9, 210–217. doi: 10.1038/ncb1534

Kelly, B., and O'Neill, L. A. J. (2015). Metabolic Reprogramming in Macrophages and Dendritic Cells in Innate Immunity. *Cell Res.* 25, 771–784. doi: 10.1038/cr.2015.68

Knight, M., and Stanley, S. (2019). HIF-1alpha as a Central Mediator of Cellular Resistance to Intracellular Pathogens. *Curr. Opin. Immunol.* 60, 111–116. doi: 10.1016/j.coi.2019.05.005

Koshiji, M., Kageyama, Y., Pete, E. A., Horikawa, I., Barrett, J. C., and Huang, L. E. (2004). HIF-1alpha Induces Cell Cycle Arrest by Functionally Counteracting Myc. *EMBO J.* 23, 1949–1956. doi: 10.1038/sj.emboj.7600196

Lee, J. S., and Thorgeirsson, S. S. (2004). Genome-Scale Profiling of Gene Expression in Hepatocellular Carcinoma: Classification, Survival Prediction, and Identification of Therapeutic Targets. *Gastroenterology* 127, S51–S55. doi: 10.1053/j.gastro.2004.09.015

Legendre, C., Reen, F. J., Mooij, M. J., McGlacken, G. P., Adams, C., and O'Gara, F. (2012). Pseudomonas Aeruginosa Alkyl Quinolones Repress Hypoxia-Inducible Factor 1 (HIF-1) Signaling Through HIF-1alpha Degradation. *Infect. Immun.* 80, 3985–3992. doi: 10.1128/IAI.00554-12

Li, C., Wang, Y., Li, Y., Yu, Q., Jin, X., Wang, X., et al. (2018). HIF1alpha-Dependent Glycolysis Promotes Macrophage Functional Activities in Protecting Against Bacterial and Fungal Infection. *Sci. Rep.* 8, 3603. doi: 10.1038/s41598-018-22039-9

Lührmann, A., Newton, H. J., and Bonazzi, M. (2017). Beginning to Understand the Role of the Type IV Secretion System Effector Proteins in Coxiella Burnetii Pathogenesis. *Curr. topic. Microbiol. Immunol.* 413, 243–268. doi: 10.1007/978-3-319-75241-9_10

Lührmann, A., and Roy, C. R. (2007). Coxiella Burnetii Inhibits Activation of Host Cell Apoptosis Through a Mechanism That Involves Preventing Cytochrome C Release From Mitochondria. *Infect. Immun.* 75, 5282–5289. doi: 10.1128/IAI.00863-07

Lv, C., Wang, S., Lin, L., Wang, C., Zeng, K., Meng, Y., et al. (2021). USP14 Maintains HIF1-Alpha Stabilization *via* its Deubiquitination Activity in Hepatocellular Carcinoma. *Cell Death Dis.* 12, 803. doi: 10.1038/s41419-021-04089-6

Mahapatra, S., Gallaher, B., Smith, S. C., Graham, J. G., Voth, D. E., and Shaw, E. I. (2016). Coxiella Burnetii Employs the Dot/Icm Type IV Secretion System to Modulate Host NF-Kappab/RelA Activation. *Front. Cell Infect. Microbiol.* 6, 188. doi: 10.3389/fcimb.2016.00188

Mahon, P. C., Hirota, K., and Semenza, G. L. (2001). FIH-1: A Novel Protein That Interacts With HIF-1alpha and VHL to Mediate Repression of HIF-1 Transcriptional Activity. *Genes Dev.* 15, 2675–2686. doi: 10.1101/gad.924501

Majmundar, A. J., Wong, W. J., and Simon, M. C. (2010). Hypoxia-Inducible Factors and the Response to Hypoxic Stress. *Mol. Cell* 40, 294–309. doi: 10.1016/j.molcel.2010.09.022

Malkov, M. I., Lee, C. T., and Taylor, C. T. (2021). Regulation of the Hypoxia-Inducible Factor (HIF) by Pro-Inflammatory Cytokines. *Cells* 10, 2340. doi: 10.3390/cells10092340

Martinez, E., Cantet, F., Fava, L., Norville, I., and Bonazzi, M. (2014). Identification of OmpA, a Coxiella Burnetii Protein Involved in Host Cell Invasion, by Multi-Phenotypic High-Content Screening. *PLoS Pathog.* 10, e1004013. doi: 10.1371/journal.ppat.1004013

Marxsen, J. H., Stengel, P., Doege, K., Heikkinen, P., Jokilehto, T., Wagner, T., et al. (2004). Hypoxia-Inducible Factor-1 (HIF-1) Promotes its Degradation by Induction of HIF-Alpha-Prolyl-4-Hydroxylases. *Biochem. J.* 381, 761–767. doi: 10.1042/BJ20040620

Maurin, M., and Raoult, D. (1999). Q Fever. *Clin. Microbiol. Rev.* 12, 518–553. doi: 10.1128/CMR.12.4.518

Maxwell, P. H., Wiesener, M. S., Chang, G. W., Clifford, S. C., Vaux, E. C., Cockman, M. E., et al. (1999). The Tumour Suppressor Protein VHL Targets Hypoxia-Inducible Factors for Oxygen-Dependent Proteolysis. *Nature* 399, 271–275. doi: 10.1038/20459

Mills, E. L., Kelly, B., Logan, A., Costa, A. S. H., Varma, M., Bryant, C. E., et al. (2016). Succinate Dehydrogenase Supports Metabolic Repurposing of Mitochondria to Drive Inflammatory Macrophages. *Cell* 167, 457–470.e413. doi: 10.1016/j.cell.2016.08.064

Mishra, B. B., Rathinam, V. A., Martens, G. W., Martinot, A. J., Kornfeld, H., Fitzgerald, K. A., et al. (2013). Nitric Oxide Controls the Immunopathology of Tuberculosis by Inhibiting NLRP3 Inflammasome-Dependent Processing of IL-1beta. *Nat. Immunol.* 14, 52–60. doi: 10.1038/ni.2474

Nathan, C., and Shiloh, M. U. (2000). Reactive Oxygen and Nitrogen Intermediates in the Relationship Between Mammalian Hosts and Microbial Pathogens. *Proc. Natl. Acad. Sci. U. S. A.* 97, 8841–8848. doi: 10.1073/pnas.97.16.8841

Obach, M., Navarro-Sabate, A., Caro, J., Kong, X., Duran, J., Gomez, M., et al. (2004). 6-Phosphofructo-2-Kinase (Pfkfb3) Gene Promoter Contains Hypoxia-Inducible Factor-1 Binding Sites Necessary for Transactivation in Response to Hypoxia. *J. Biol. Chem.* 279, 53562–53570. doi: 10.1074/jbc.M406096200

Ohh, M., Park, C. W., Ivan, M., Hoffman, M. A., Kim, T. Y., Huang, L. E., et al. (2000). Ubiquitination of Hypoxia-Inducible Factor Requires Direct Binding to the Beta-Domain of the Von Hippel-Lindau Protein. *Nat. Cell Biol.* 2, 423–427. doi: 10.1038/35017054

Pan, X., Lührmann, A., Satoh, A., Laskowski-Arce, M. A., and Roy, C. R. (2008). Ankyrin Repeat Proteins Comprise a Diverse Family of Bacterial Type IV Effectors. *Science* 320, 1651–1654. doi: 10.1126/science.1158160

Pechstein, J., Schulze-Luehrmann, J., and Lührmann, A. (2017). Coxiella Burnetii as a Useful Tool to Investigate Bacteria-Friendly Host Cell Compartments. *Int. J. Med. Microbiol.* 308, 77–83. doi: 10.1016/j.ijmm.2017.09.010

Peyssonnaux, C., Datta, V., Cramer, T., Doedens, A., Theodorakis, E. A., Gallo, R. L., et al. (2005). HIF-1alpha Expression Regulates the Bactericidal Capacity of Phagocytes. *J. Clin. Invest.* 115, 1806–1815. doi: 10.1172/JCI23865

Pugh, C. W. (2016). Modulation of the Hypoxic Response. *Adv. Exp. Med. Biol.* 903, 259–271. doi: 10.1007/978-1-4899-7678-9_18

Riess, T., Andersson, S. G., Lupas, A., Schaller, M., Schafer, A., Kyme, P., et al. (2004). Bartonella Adhesin a Mediates a Proangiogenic Host Cell Response. *J. Exp. Med.* 200, 1267–1278. doi: 10.1084/jem.20040500

Rius, J., Guma, M., Schachtrup, C., Akassoglou, K., Zinkernagel, A. S., Nizet, V., et al. (2008). NF-kappaB Links Innate Immunity to the Hypoxic Response Through Transcriptional Regulation of HIF-1alpha. *Nature* 453, 807–811. doi: 10.1038/nature06905

Rodriguez-Prados, J. C., Traves, P. G., Cuenca, J., Rico, D., Aragones, J., Martin-Sanz, P., et al. (2010). Substrate Fate in Activated Macrophages: A Comparison Between Innate, Classic, and Alternative Activation. *J. Immunol.* 185, 605–614. doi: 10.4049/jimmunol.0901698

Schäfer, W., Schmidt, T., Cordsmeier, A., Borges, V., Beare, P. A., Pechstein, J., et al. (2020). The Anti-Apoptotic Coxiella Burnetii Effector Protein AnkG is a Strain Specific Virulence Factor. *Sci. Rep.* 10, 15396. doi: 10.1038/s41598-020-72340-9

Semenza, G. L. (2014). Oxygen Sensing, Hypoxia-Inducible Factors, and Disease Pathophysiology. *Annu. Rev. Pathol.* 9, 47–71. doi: 10.1146/annurev-pathol-012513-104720

Sershen, C. L., Plimpton, S. J., and May, E. E. (2016). Oxygen Modulates the Effectiveness of Granuloma Mediated Host Response to Mycobacterium Tuberculosis: A Multiscale Computational Biology Approach. *Front. Cell Infect. Microbiol.* 6, 6. doi: 10.3389/fcimb.2016.00006

Siegert, I., Schodel, J., Nairz, M., Schatz, V., Dettmer, K., Dick, C., et al. (2015). Ferritin-Mediated Iron Sequestration Stabilizes Hypoxia-Inducible Factor-1alpha Upon LPS Activation in the Presence of Ample Oxygen. *Cell Rep.* 13, 2048–2055. doi: 10.1016/j.celrep.2015.11.005

Strowitzki, M. J., Cummins, E. P., and Taylor, C. T. (2019). Protein Hydroxylation by Hypoxia-Inducible Factor (HIF) Hydroxylases: Unique or Ubiquitous? *Cells* 8, 384. doi: 10.3390/cells8050384

Sukocheva, O. A., Manavis, J., Kok, T. W., Turra, M., Izzo, A., Blumbergs, P., et al. (2016). Coxiella Burnetii Dormancy in a Fatal Ten-Year Multisystem Dysfunctional Illness: Case Report. *BMC Infect. Dis.* 16, 165. doi: 10.1186/s12879-016-1497-z

Tannahill, G. M., Curtis, A. M., Adamik, J., Palsson-McDermott, E. M., McGettrick, A. F., Goel, G., et al. (2013). Succinate is an Inflammatory Signal That Induces IL-1beta Through HIF-1alpha. *Nature* 496, 238–242. doi: 10.1038/nature11986

Thomas, D. R., Newton, P., Lau, N., and Newton, H. J. (2020). Interfering With Autophagy: The Opposing Strategies Deployed by Legionella Pneumophila and Coxiella Burnetii Effector Proteins. *Front. Cell Infect. Microbiol.* 10, 599762. doi: 10.3389/fcimb.2020.599762

Van den Brom, R., van Engelen, E., Roest, H. I., van der Hoek, W., and Vellema, P. (2015). Coxiella Burnetii Infections in Sheep or Goats: An Opinionated Review. *Vet. Microbiol.* 181, 119–129. doi: 10.1016/j.vetmic.2015.07.011

Voth, D. E., Howe, D., and Heinzen, R. A. (2007). Coxiella Burnetii Inhibits Apoptosis in Human THP-1 Cells and Monkey Primary Alveolar Macrophages. *Infect. Immun.* 75, 4263–4271. doi: 10.1128/IAI.00594-07

Wang, G. L., Jiang, B. H., Rue, E. A., and Semenza, G. L. (1995). Hypoxia-Inducible Factor 1 is a Basic-Helix-Loop-Helix-PAS Heterodimer Regulated by Cellular O2 Tension. *Proc. Natl. Acad. Sci. U. S. A.* 92, 5510–5514. doi: 10.1073/pnas.92.12.5510

Werth, N., Beerlage, C., Rosenberger, C., Yazdi, A. S., Edelmann, M., Amr, A., et al. (2010). Activation of Hypoxia Inducible Factor 1 is a General Phenomenon in Infections With Human Pathogens. *PLoS One* 5, e11576. doi: 10.1371/journal.pone.0011576

Zamboni, D. S., and Rabinovitch, M. (2003). Nitric Oxide Partially Controls Coxiella Burnetii Phase II Infection in Mouse Primary Macrophages. *Infect. Immun.* 71, 1225–1233. doi: 10.1128/IAI.71.3.1225-1233.2003

Zamboni, D. S., Campos, M. A., Torrecilhas, A. C., Kiss, K., Samuel, J. E., Golenbock, D. T., et al. (2004). Stimulation of Toll-Like Receptor 2 By *Coxiella burnetii* Is Required for Macrophage Production of Pro-Inflammatory Cytokines and Resistance to Infection. *J. Biol. Chem.* 279, 54405–54415. doi: 10.1074/jbc.M410340200

Zhang, C., Liu, J., Wang, J., Zhang, T., Xu, D., Hu, W., et al. (2021). The Interplay Between Tumor Suppressor P53 and Hypoxia Signaling Pathways in Cancer. *Front. Cell Dev. Biol.* 9, 648808. doi: 10.3389/fcell.2021.648808

Conflict of Interest: The authors declare that the research was conducted in the absence of any commercial or financial relationships that could be construed as a potential conflict of interest.

Publisher's Note: All claims expressed in this article are solely those of the authors and do not necessarily represent those of their affiliated organizations, or those of the publisher, the editors and the reviewers. Any product that may be evaluated in this article, or claim that may be made by its manufacturer, is not guaranteed or endorsed by the publisher.

Advantages of publishing in Frontiers

OPEN ACCESS
Articles are free to read for greatest visibility and readership

FAST PUBLICATION
Around 90 days from submission to decision

HIGH QUALITY PEER-REVIEW
Rigorous, collaborative, and constructive peer-review

TRANSPARENT PEER-REVIEW
Editors and reviewers acknowledged by name on published articles

Frontiers
Avenue du Tribunal-Fédéral 34
1005 Lausanne | Switzerland

Visit us: www.frontiersin.org
Contact us: frontiersin.org/about/contact

REPRODUCIBILITY OF RESEARCH
Support open data and methods to enhance research reproducibility

DIGITAL PUBLISHING
Articles designed for optimal readership across devices

FOLLOW US
@frontiersin

IMPACT METRICS
Advanced article metrics track visibility across digital media

EXTENSIVE PROMOTION
Marketing and promotion of impactful research

LOOP RESEARCH NETWORK
Our network increases your article's readership